



ΠΑΝΕΠΙΣΤΗΜΙΟ ΚΡΗΤΗΣ  
ΙΑΤΡΙΚΗ ΣΧΟΛΗ



ΙΔΡΥΜΑ ΤΕΧΝΟΛΟΓΙΑΣ ΚΑΙ ΕΡΕΥΝΑΣ  
ΙΝΣΤΙΤΟΥΤΟ ΜΟΡΙΑΚΗΣ ΒΙΟΛΟΓΙΑΣ ΚΑΙ ΒΙΟΤΕΧΝΟΛΟΓΙΑΣ

## ΔΙΔΑΚΤΟΡΙΚΗ ΔΙΑΤΡΙΒΗ

“Μελέτη της ανάπτυξης του τραχειακού συστήματος  
της *Drosophila melanogaster*”

Γεωργία Τσικαλά

Ιανουάριος 2015



UNIVERSITY OF CRETE  
SCHOOL OF MEDICINE



FOUNDATION OF RESEARCH AND TECHNOLOGY  
INSTITUTE OF MOLECULAR BIOLOGY AND BIOTECHNOLOGY

## PhD THESIS

“Study of the development of the trachea system of  
*Drosophila melanogaster*”

Georgia Tsikala

January 2015

«Η παρούσα έρευνα έχει συγχρηματοδοτηθεί από την Ευρωπαϊκή Ένωση (Ευρωπαϊκό Κοινωνικό Ταμείο - ΕΚΤ) και από εθνικούς πόρους μέσω του Επιχειρησιακού Προγράμματος «Εκπαίδευση και Δια Βίου Μάθηση» του Εθνικού Στρατηγικού Πλαισίου Αναφοράς (ΕΣΠΑ) – Ερευνητικό Χρηματοδοτούμενο Έργο: Ηράκλειτος ΙΙ . Επένδυση στην κοινωνία της γνώσης μέσω του Ευρωπαϊκού Κοινωνικού Ταμείου».



**European Union**  
European Social Fund



MINISTRY OF EDUCATION & RELIGIOUS AFFAIRS, CULTURE & SPORTS  
MANAGING AUTHORITY

**Co-financed by Greece and the European Union**



**Επιβλέπων:**

Δόμνα Καραγωγέως, Καθηγήτρια, Ιατρική Σχολή Πανεπιστημίου Κρήτης

**Τριμελής Επιτροπή:**

Δόμνα Καραγωγέως, Καθηγήτρια, Ιατρική Σχολή Πανεπιστημίου Κρήτης

Χρήστος Δελιδάκης, Καθηγητής, Τμήμα Βιολογίας Πανεπιστημίου Κρήτης

Χρήστος Ζέρβας, Ερευνητής, Ίδρυμα Ιατροβιολογικών Ερευνών Ακαδημίας Αθηνών

**Επταμελής Επιτροπή:**

Δόμνα Καραγωγέως, Καθηγήτρια, Ιατρική Σχολή Πανεπιστημίου Κρήτης

Χρήστος Δελιδάκης, Καθηγητής, Τμήμα Βιολογίας Πανεπιστημίου Κρήτης

Χρήστος Ζέρβας, Ερευνητής, Ίδρυμα Ιατροβιολογικών Ερευνών Ακαδημίας Αθηνών

Γιώργος Μαυροθαλασσίτης, Καθηγητής, Ιατρική Σχολή Πανεπιστημίου Κρήτης

Νεκτάριος Ταβερναράκης, Καθηγητής, Ιατρική Σχολή Πανεπιστημίου Κρήτης

Δέσποινα Αλεξανδράκη, Αναπλ. Καθηγήτρια, Τμήμα Βιολογίας Πανεπιστημίου Κρήτης

Ιωάννης Βόντας, Αναπλ. Καθηγητής, Τμήμα Βιολογίας Πανεπιστημίου Κρήτης



*Στους γονείς και τα αδέρφια μου*

*Ένα μεγάλο ευχαριστώ...*

*Ολοκληρώνοντας τη διδακτορική μου διατριβή, θα ήθελα να ευχαριστήσω όλους εκείνους που στάθηκαν στο πλευρό μου αυτά τα χρόνια, τόσο σε επαγγελματικό, όσο και σε προσωπικό επίπεδο.*

*Θα ήθελα αρχικά να ευχαριστήσω την καθηγήτρια μου Δόμνα Καραγωγέως για τη συνεργασία που είχαμε όλα αυτά τα χρόνια. Την ευχαριστώ για την εμπιστοσύνη που μου έδειξε και για τη βοήθειά της σε οποιαδήποτε δυσκολία και αν αντιμετώπισα.*

*Στη συνέχεια θα ήθελα να ευχαριστήσω τα μέλη της τριμελούς επιτροπής Χρήστο Δελιδάκη και Χρήστο Ζέρβα, που ήταν πάντοτε πρόθυμοι να συζητήσουν μαζί μου την εξέλιξη της παρούσας εργασίας και βοήθησαν σημαντικά στην εξέλιξη της, καθώς και τους: Γιώργο Μαυροθαλασσίτη, Νεκτάριος Ταβερναράκης, Δέσποινα Αλεξανδράκη και Ιωάννη Βόντα που αποδέχθηκαν αμέσως να συμμετάσχουν στην Επταμελή Επιτροπή Αξιολόγησης της παρούσας μελέτης.*

*Οφείλω ένα τεράστιο ευχαριστώ στη Maura Strigini, τον άνθρωπο που έδωσε το έναυσμα της συγκεκριμένης εργασίας και υπήρξε σημαντικός για την εξέλιξη και την ολοκλήρωση της. Η Maura αποτελεί υπόδειγμα και σπουδαία δασκάλα για μένα, όχι μόνο για της γνώσεις που απέκτησα δουλεύοντας μαζί της, αλλά και για τον τρόπο που προσεγγίζει την επιστήμη και την έρευνα, αλλά και την εργαστηριακή ζωή. Υπήρξε όλα αυτά τα χρόνια σύμβουλος και πηγή λογικής και ψυχραιμίας σε περιόδους υψηλού στρες και πάνω από όλα ένας πολύ ευχάριστος και αισιόδοξος άνθρωπος. Την ευχαριστώ πολύ!*

*Θα ήθελα ακόμα να ευχαριστήσω τα μέλη του εργαστηρίου Καραγωγέως: Κώστα Θεοδωράκη, Μαρία Σαββάκη, Αήδα Ζούπη, Simona Tivodar, Μαριλένα Καστρίτη, Γιώργο Μπαστάκη, Κατερίνα Καλεμάκη, Ζουζάνα Κούνουπα, τα παλαιότερα μέλη Μαρίνα Βιδάκη και Μαρκέλλα Κατίδου, καθώς και πολλά άλλα άτομα που πέρασαν από το εργαστήριο όλα αυτά τα χρόνια, για το ευχάριστο κλίμα και την όμορφη συνεργασία.*

*Παράλληλα ένα μεγάλο ευχαριστώ στους Χρήστο Δελιδάκη και Μιχάλη Αβέρωφ που με φιλοξένησαν στο εργαστηριακό τους περιβάλλον....., καθώς και τους: Μαριάνθη Κηπαράκη, Pawel Piwko, Srivathsa Magadi, Kristina Kux, Εύα Ζαχαριουδάκη, Κωνσταντίνα Καλοδήμου, Ιωάννα Κολτσάκη, Βάσω Θεοδώρου, Βασίλη Μπαούση, Ζαχαρία Κονταράκη, Μαργαρίτα Σταπούντζη, Ana Pinheiro, Anna Gilles, Johannes Schinko, Claudia Roedel, Meriem Takarli, Andres Sarazin, Andrew Peel, Έλπη Καλογεροπούλου και Νίκο Κωνσταντινίδη καθώς και τη Μαρία Μοναστηριώτη και Γιάννη Λειβαδάρα.*

*Ιδιαίτερα ευχαριστώ τον κ. Δελιδάκη για την φιλοξενία του στο εργαστήριο τον τελευταίο χρόνο και τη δυνατότητα που μου έδωσε να ασχοληθώ με ένα διαφορετικό σύστημα και να αποκτήσω επιπλέον γνώσεις, αλλά και τις Αντωνία Κανδαράκη, Λίντα Γρηγοράκη και Ουρανία Γαλανοπούλου με τις οποίες συνεργάστηκα.*

*Όμως η παρούσα εργασία δε θα ήταν δυνατό να πραγματοποιηθεί αν δεν είχα κοντά μου τους φίλους και την οικογένεια μου. Θέλω λοιπόν να ευχαριστήσω τους: Γιωργία, Ελένη, Τέτα, Άννα, Μαρία, Ειρήνη, Ρίτσα, Ιάκωβο, Ισμήνη, Ιωάννα, Νίκο, Αριάδνη, Πολύδωρο, Matthias και Ρένα για τις όμορφες στιγμές που περάσαμε μαζί αλλά και το Νίκο που βρίσκεται στο πλευρό μου και κάνει τις στιγμές μοναδικές.*

*Τέλος ένα τεράστιο ευχαριστώ στην οικογένεια μου, τους γονείς μου Στέλλα και Μπάμπη και τα αδέρφια μου Γιάννη και Ρούσσα. Τους αγαπώ πολύ και είμαι πολύ τυχερή που έχω την αγάπη και τη στήριξή τους σε όλες μου τις επιλογές και τα βήματα.*

---

## ΠΕΡΙΛΗΨΗ

---

Τα επιθήλια αποτελούν σημαντικές δομικές αλλά και λειτουργικές μονάδες πολυάριθμων ιστών. Συμμετέχουν στο σχηματισμό των περισσότερων, αν όχι όλων των οργάνων και είναι σημαντικά για τη αλληλεπίδραση τους με τους γειτονικούς ιστούς και το περιβάλλον. Εμπλέκονται σε διάφορες φυσιολογικές διεργασίες όπως την πρόσληψη θρεπτικών συστατικών και το φιλτράρισμα του αίματος. Παράλληλα, προστατεύουν τον οργανισμό από τη εισβολή εξωγενών παθογόνων και λειτουργούν ως φραγμοί διαπερατότητας περιορίζοντας την ελεύθερη διάχυση νερού και διαλυτών.

Το αναπνευστικό σύστημα των εντόμων αποτελείται από ένα περίπλοκο δίκτυο επιθηλιακών αγωγών (την τραχεία και τα αναπνευστικά στόμια) που μεταφέρουν οξυγόνο μέσω του αέρα σε όλα τα επιμέρους όργανα. Αναπτύσσεται κατά την εμβρυογένεση και γίνεται λειτουργικό κατά την εκκόλαση της προνύμφης. Οι αεραγωγοί και τα αναπνευστικά στόμια της *Drosophila melanogaster* έχουν μελετηθεί εκτενώς καθώς αποτελούν αντιπροσωπευτικό μοντέλο για την κατανόηση της ανάπτυξης, της ωρίμανσης και της λειτουργίας των επιθηλιακών σωληνοειδών οργάνων.

Σε μια προσπάθεια εντοπισμού νέων γονιδίων που εμπλέκονται στην ανάπτυξη και την ωρίμανση του αναπνευστικού συστήματος της *Drosophila* και ειδικότερα στο σχηματισμό του φραγμού διαπερατότητας του τραχειακού επιθηλίου, πραγματοποιήθηκε γενετική διαλογή διαφόρων μεταλλαγμένων στελεχών. Η συγκεκριμένη προσέγγιση οδήγησε στην ταυτοποίηση του γονιδίου *Btk29A* ως σημαντικό για τη μορφογένεση των οπίσθιων αναπνευστικών στομίων, τη λειτουργία του τραχειακού φραγμού διαπερατότητας και την ωρίμανση του τραχειακού συστήματος. Το γονίδιο *Btk29A* κωδικοποιεί για μια κινάση τυροσίνης, της οικογένειας των Tec κινασών, η οποία είναι συντηρημένη τόσο στα σπονδυλωτά, όσο και στα ασπόνδυλα.

Στόχος της παρούσας μελέτης είναι η αποσαφήνιση του ρόλου του *Btk29A* στην ανάπτυξη του αναπνευστικού συστήματος της *Drosophila*.

Ανάλυση του προτύπου έκφρασης του γονιδίου *Btk29A* με πειράματα *in situ* υβριδοποίησης και ανοσοϊστοχημικές χρώσεις, με χρήση νέου πολυκλωνικού αντισώματος για την πρωτεΐνη *Btk29A*, που αναπτύχθηκε στο εργαστήριο στα πλαίσια της παρούσας μελέτης, αποκάλυψε πως το γονίδιο εκφράζεται στα κύτταρα του τραχειακού συστήματος και των οπίσθιων αναπνευστικών στομίων. Η έκφραση του *Btk29A* στους συγκεκριμένους ιστούς ξεκινά στο εμβρυικό στάδιο 11 και διατηρείται μέχρι και το τέλος της εμβρυογένεσης. Παράλληλα αποκαλύφθηκε πως μονάχα η μια από τις δυο ισομορφές της πρωτεΐνης *Btk29A*, η Τύπου 1 (ή Κοντή) ισομορφή, εκφράζεται από τα κύτταρα του αναπνευστικού συστήματος, ενώ η Τύπου 2 (ή Μακριά) ισομορφή εντοπίζεται μονάχα στα κύτταρα του κεντρικού νευρικού συστήματος.

---

Τα οπίσθια αναπνευστικά στόμια της *Drosophila* συνδέουν το τραχειακό σύστημα με το περιβάλλον. Αποτελούνται εσωτερικά από τον αναπνευστικό θάλαμο (spiracular chamber), ένα σωληνοειδή ιστό, συνεχή του τραχειακού σωλήνα, και εξωτερικά από το στιγματοφόρο (stigmatorphore), μια εκτενή επιδερμική δομή που περιβάλλει τον αναπνευστικό θάλαμο. Ο ιστός αναπτύσσεται από μια ομάδα επιθηλιακών κυττάρων εκτοδερμικής προέλευσης μέσα από ποικίλες μορφογενετικές αλλαγές. Στο τέλος της εμβρυογένεσης, τα συγκεκριμένα κύτταρα ολοκληρώνουν τοπολογικές αναδιατάξεις σχηματίζοντας τα τρισδιάστατα οπίσθια αναπνευστικά στόμια. Τόσο τα κύτταρα του αναπνευστικού θαλάμου, όσο και τα κύτταρα του στιγματοφόρου εκφράζουν Btk29A. Σε ομόζυγα μεταλλαγμένα έμβρυα για το *Btk29A*, τα οπίσθια αναπνευστικά στόμια είναι κοντότερα από αυτά των αγρίου τύπου εμβρύων και εμφανίζουν μη φυσιολογικό σχήμα.

Παρατήρηση της ανάπτυξης των οπίσθιων αναπνευστικών στομίων ζωντανών εμβρύων, με *in vivo* μικροσκοπία, αποκάλυψε πως τα κύτταρα του αναπνευστικού θαλάμου δεν ολοκληρώνουν τη διαδικασία εγκόλπωσης που είναι αναγκαία για τη μορφογένεσή του ιστού, με τα πιο οπίσθια αυτών να παραμένουν στην επιφάνεια. Για την καλύτερη ανάλυση του φαινοτύπου, εξετάστηκαν παράμετροι που εμπλέκονται στη ρύθμιση της εγκόλπωσης των κυττάρων του αναπνευστικού θαλάμου, όπως: η διαδικασία σύσφιξης της κορυφαίας μεμβράνης (apical constriction), οι αλλαγές στο σχήμα των κυττάρων, η οργάνωση του κυτταροσκελετικού δικτύου της ακτίνης και της μυοσίνης και η ενεργότητα της Rho1 GTPase. Καμία από τις παραπάνω παραμέτρους δεν επηρεάζεται σε ομόζυγα μεταλλαγμένα έμβρυα για το *Btk29A*. Παράλληλα, πραγματοποιήθηκαν πειράματα διάσωσης φαινοτύπου βασισμένα στην ιστοειδική έκφραση του γονιδίου *Btk29A* με χρήση του συστήματος UAS-GAL4. Τα συγκεκριμένα πειράματα έδειξαν πως η επαναφορά της έκφρασης της Btk29A στα κύτταρα του αναπνευστικού θαλάμου δε διασώζει την ανώμαλη μορφογένεση των οπίσθιων αναπνευστικών στομίων. Ιδιαίτερο ενδιαφέρον παρουσιάζει το γεγονός πως ο φαινότυπος διασώζεται με επαναφορά της έκφρασης της Btk29A στα κύτταρα του στιγματοφόρου. Τα παραπάνω αποτελέσματα προτείνουν πως η εγκόλπωση των κυττάρων του αναπνευστικού θαλάμου είναι πιθανό να ρυθμίζεται μέσω κυτταρικά μη αυτόνομης (non-cell autonomous) δράσης της Btk29A στα κύτταρα του στιγματοφόρου.

Παρατήρηση των μορφογενετικών κινήσεων των κυττάρων του στιγματοφόρου ζωντανών εμβρύων, με *in vivo* μικροσκοπία, αποκάλυψε πως η Btk29A είναι σημαντική για τις τοπολογικές ανακατατάξεις των κυττάρων του στιγματοφόρου. Επιπρόσθετα, αποκάλυψε πως η σωστή ρύθμιση αυτών των ανακατατάξεων είναι σημαντική για τη φυσιολογική τοποθέτηση των γειτονικών κυττάρων του αναπνευστικού θαλάμου και την ολοκλήρωση της εγκόλπωσης τους.

Συνολικά, η παρούσα μελέτη προτείνει πως η κινάση τυροσίνης Btk29A, της οποίας η έκφραση στα οπίσθια αναπνευστικά στόμια ρυθμίζεται από το μεταγραφικό παράγοντα Abdominal-B, επηρεάζει τη μορφογένεση του συγκεκριμένου ιστού με δύο διακριτούς τρόπους. Πρωτίστως,

---

ρυθμίζει τις τοπολογικές ανακατατάξεις των κυττάρων του στιγματοφόρου δρώντας κυτταρικά αυτόνομα (cell autonomously) στα κύτταρα αυτά. Δευτερευόντως, η *Btk29A* εξασφαλίζει, δρώντας κυτταρικά μη αυτόνομα (non-cell autonomously), την αποτελεσματική εγκόλπωση των κυττάρων του αναπνευστικού θαλάμου.

Πέραν του μη φυσιολογικού σχηματισμού των οπίσθιων αναπνευστικών στομιών, το αναπνευστικό σύστημα των ομόζυγα μεταλλαγμένων *Btk29A* στελεχών χαρακτηρίζεται και από διατάραξη του φραγμού διαπερατότητας του τραχειακού επιθηλίου και μη ολοκλήρωση της ωρίμανσης του κατά το τέλος της εμβρυογένεσης. Η συνολική μορφολογία της τραχείας δεν επηρεάζεται: οι αεραγωγοί εμφανίζουν φυσιολογικό μέγεθος, σχηματισμό των διακλαδώσεων και η χιτίνη εναποτίθεται φυσιολογικά στο εσωτερικό του τραχειακού αυλού. Για την κατανόηση της εμπλοκής της *Btk29A* στη διατάραξη του επιθηλιακού φραγμού διαπερατότητας της τραχείας εξετάσθηκε η δομή και η μοριακή σύσταση συγκεκριμένων διακυτταρικών συνδέσεων, των Διαφραγματικών Συνδέσεων (septate junctions, SJs), που είναι σημαντικές για το σχηματισμό και τη διατήρηση των επιθηλιακών φραγμών διαπερατότητας στη *Drosophila*. Ανάλυση των διαφραγματικών συνδέσεων που αναπτύσσονται μεταξύ των κυττάρων της τραχείας δεν αποκάλυψε ανωμαλία στη δομή και τον εντοπισμό των πρωτεϊνικών μορίων που τις συνιστούν. Κατά συνέπεια, η διατάραξη του επιθηλιακού φραγμού διαπερατότητας δεν είναι αποτέλεσμα μη φυσιολογικού σχηματισμού ή διατήρησης των Διαφραγματικών Συνδέσεων.

Συνοψίζοντας, η παρούσα μελέτη προσφέρει νέες πληροφορίες για τη δράση της κινάσης *Btk29A* στην ανάπτυξη και ωρίμανση του αναπνευστικού συστήματος της *Drosophila melanogaster*. Ειδικότερα, επισημαίνει τη σημασία των πολύπλοκων αλληλεπιδράσεων που αναπτύσσονται μεταξύ των οργάνων κατά τη μορφογένεση για τη σωστή ανάπτυξη και λειτουργία των οργάνων.

---

## ABSTRACT

---

Epithelia are key building blocks of many organs. They play important roles from both a structural and functional point of view. Epithelia line most if not all organs and they can play important roles in the interactions with the surrounding environment and nearby tissues. Transport properties of epithelia are key to many physiological functions in a multicellular organism, like nutrient uptake and blood filtering. Epithelia also protect the body from the invasion of external pathogens. Finally, they work as permeability barriers and limit the free diffusion of water and solutes, allowing the establishment and maintenance of specific intra-organ and luminal milieu across the two sides of the epithelium.

The respiratory system of insects is a vital organ primarily consisting of a complex network of epithelial tubes (the trachea and spiracles) that deliver air-borne oxygen to all organs. It develops in the embryo and becomes functional as the embryo hatches to become a crawling larva. In particular the airways and spiracles of *Drosophila melanogaster* have long been studied as a tractable model to understand the development, maturation and function of epithelial tubular organs.

A genetic screen had been conducted in our laboratory to identify new candidate genes involved in the development and maturation of the fly respiratory system, and in particular the establishment of the permeability barrier of the tracheal epithelium. This screen led to the identification of *Btk29A* as a gene essential for spiracle morphogenesis, tracheal barrier function and airways maturation. *Btk29A* encodes for a non-receptor tyrosine kinase, a member of the Tec family of tyrosine kinases, conserved across vertebrates and invertebrates.

The aim of this study was to unravel the role of *Btk29A* in the formation of the respiratory system.

Analysis of *Btk29A* expression pattern with *in situ* hybridization and antibody staining (using a newly developed polyclonal Btk29A antibody) enabled the documentation of the expression in the trachea and posterior spiracles. *Btk29A* expression is detected in both tissues from embryonic stage 11 till late embryogenesis. Interestingly, in the embryo only one of the two Btk29A isoforms, the Short (or Type 1) isoform, is expressed by the cells of the respiratory system, while the Long (or Type 2) isoform appears solely in the cells of the central nervous system.

The posterior spiracles of *Drosophila* connect the tracheal tubes to the environment. They consist internally of the spiracular chamber, an invaginated tube with filtering properties that is continuous to the trachea and externally of the stigmatophore, an extensible epidermal structure that covers the spiracular chamber. The tissue develops from a two-dimensional group of ectoderm-

---

derived epithelial cells and involves multiple morphogenetic steps. In the end of embryogenesis the cells have rearranged their positions to form three-dimensional tubular structures. Both of the posterior spiracle compartments express Btk29A. The spiracles of *Btk29A* mutant embryos are shorter and display abnormal shape.

*In vivo* imaging of the posterior spiracle morphogenesis in *Btk29A* mutants revealed that although the invagination process is not completely abolished, the most distal of the spiracular chamber cells fail to invaginate. In order to explain the phenotype, several parameters known to affect the fine-tuning of spiracular chamber invagination were examined: apical constriction, cell shape changes, organization of actin-myosin network and activation of the Rho1 GTPase. None of these parameters seems impaired in *Btk29A* mutants. In parallel, phenotypic rescue experiments, using different tissue specific GAL4 drivers, showed that recovery of Btk29A expression by the spiracular chamber cells is not sufficient to rescue the invagination phenotype. Interestingly the recovery of the kinase in the stigmatophore cells led to normally shaped posterior spiracles. The above suggests that Btk29A might regulate spiracular chamber cell invagination through stigmatophore cells in a non-cell autonomous manner.

*In vivo* imaging of the morphogenetic movements of the stigmatophore cells further showed that Btk29A is indeed important for the regulation of the spatial rearrangements of the stigmatophore cells. Additionally, it revealed that the positioning of the spiracular chamber cells and the execution of their invagination program is highly dependent on the extent of stigmatophore cell rearrangements.

Overall, it seems that Btk29A, acting downstream of the spiracle master regulator Abdominal-B, affects spiracle morphogenesis in two distinct ways: first it cell-autonomously controls the convergent extension of stigmatophore cells; second, Btk29A ensures, non-cell autonomously, the efficient invagination of spiracular chamber cells.

The respiratory system of *Btk29A* mutant embryos is additionally characterised by a leaky tracheal permeability barrier and a failure to fill with air at the end of embryogenesis. The overall trachea morphology is not affected: the airways have normal size, branch patterning and chitin deposition in the tracheal lumen. In order to understand the cause of the permeability barrier defect, specific intercellular junctions, the Septate Junctions (SJs) were examined. These junctions are crucial for the establishment of the epithelial permeability barriers in *Drosophila*. The ultrastructure of the SJs, as well as the subcellular localization of the SJ proteins, is not impaired in the tracheal cells of *Btk29A* mutants. It is thus likely that the permeability phenotype is not due to gross impairment in SJ formation or maintenance.



---

In conclusion the work undertaken during my doctoral studies offers insights into the role of Btk29A kinase in the development and maturation of the *Drosophila* respiratory system. In particular my work has highlighted the complex physical interactions that take place among organ components during morphogenesis, which contribute to their final form and function.

---

## Table of Contents

<b>ΠΕΡΙΛΗΨΗ</b> .....	1
<b>ABSTRACT</b> .....	4
<b>A. INTRODUCTION</b> .....	11
A.1. Respiratory system of <i>Drosophila melanogaster</i> .....	12
A.2. Posterior spiracles.....	13
A.2.A. Posterior spiracles.....	13
A.2.B. Posterior spiracle morphogenesis.....	15
A.2.B.1. Spiracular chamber formation.....	16
A.2.B.2. Stigmatophore formation.....	18
A.2.B.3. AbdB masters the gene network driving posterior spiracle specification and morphogenesis .....	21
A.2.B.3.a. <i>Abdominal-B</i> and the specification of posterior spiracle primordia.....	21
A.2.B.3.b. Patterning of the posterior spiracle primordia – AbdB primary target genes.....	22
A.2.B.3.c. Secondary targets.....	24
A.2.B.3.d. Realisator genes.....	26
A.3. Tracheal system.....	30
A.3.A. Tracheal system development.....	30
A.3.A.1. Specification of tracheal cells and early tracheal development.....	30
A.3.A.2. Tracheal branch morphogenesis – Formation of the tubular network.....	32
A.3.A.3. Chitin deposition and tracheal tube elongation.....	34
A.3.A.4. Tracheal maturation.....	35
A.3.B. Trachea as a model system to study epithelial integrity.....	38
A.4. Btk29A in the respiratory system.....	42
A.4.A. Genetic screen and <i>Btk29A</i> .....	42
A.4.B. Btk29A in the respiratory system.....	44
A.5. Btk29A.....	46
A.5.A. <i>Btk29A</i> expression pattern.....	49

---

A.5.B. <i>Btk29A</i> functions.....	52
- In embryonic development .....	52
- In the embryonic trachea system.....	53
- In later stages .....	54
Aim of this study.....	56
<b>B. MATERIALS AND METHODS</b> .....	57
B.1. Mutant Fly Strains .....	58
B.2. Transgenic Fly Strains .....	58
B.3. Molecular biology and transgenic lines.....	59
B.4. Btk29A polyclonal antibody.....	60
B.5. Embryo fixation and immunohistochemistry .....	61
B.6. In situ hybridization.....	63
B.7. Live imaging.....	63
B.8. Dye penetration assay .....	63
B.9. Ultrastructural analysis .....	64
B.10. Protein extraction from <i>Drosophila</i> embryos and Western blot analysis.....	64
<b>C. RESULTS</b> .....	65
C.1. <i>Btk29A</i> expression pattern .....	66
C.1.A. Btk29A expression pattern in wild type embryos.....	66
C.1.A.1. Btk29A mRNA expression .....	66
C.1.A.1a. Expression of All <i>Btk29A</i> transcripts (All Isoforms).....	67
C.1.A.1b. Expression pattern of different Btk29A transcripts .....	70
C.1.A.2. Btk29A protein expression .....	72
C.1.A.3. Subcellular localization of Btk29A protein .....	75
C.1.B. Btk29A expression in mutant alleles .....	76
C.2. Btk29A in tissue morphogenesis .....	80
C.2.A. Genetic control of spiracle morphogenesis.....	81
C.2.A.1. Btk29A expression in different sets of posterior spiracle cells .....	81

---

---

C.2.A.2. AbdB regulates the expression of <i>Btk29A</i> in the posterior spiracles .....	83
C.2.B. Morphogenesis of the posterior spiracles .....	86
C.2.B.1. Posterior spiracle morphology in <i>Btk29A</i> mutants.....	86
C.2.B.1a. Number of spiracular chamber cells .....	88
C.2.B.1b. Spatial distribution of spiracular chamber cells.....	88
C.2.B.1c. Secondary effect of a trachea phenotype.....	88
C.2.B.2. Live imaging of posterior spiracle invagination .....	89
C2.B.3. Phenotypic characterization of the spiracular chamber cells.....	90
C.2.B.3a. Epithelial cell polarity .....	91
C.2.B.3b. Apical constriction and cell shape changes .....	92
C.2.B.3c. Actin-Myosin organization .....	93
C.2.B.3d. RhoGTPase activity .....	94
C.2.B.3e. Endoreplication .....	95
C.2.C. Rescue experiments .....	97
C.2.D. Stigmatophore cell rearrangements .....	104
C.2.D.1. Defective cell rearrangements during stigmatophore morphogenesis in <i>Btk29A</i> mutants .....	104
C.2.D.2. Btk-dependent cell rearrangements in the stigmatophore contribute to the invagination of the spiracular chamber .....	108
C.2.D.3. Grain affects the stigmatophore cell rearrangements .....	108
C.2.E. <i>Btk29A</i> in convergent extension-like movements .....	111
C.3. <i>Btk29A</i> in tracheal system development and function.....	115
C.3.A. Tracheal morphogenesis .....	116
C.3.A.1. Tracheal morphology.....	116
C.3.A.2. Tracheal length .....	117
C.3.B. Dye penetration phenotype .....	119
C.3.B.1. Septate junctions .....	119
C.3.B.2. Gliotactin and the Tricellular Septate Junctions .....	122
C.3.B.3. Chitin deposition and organization .....	125

---

---

C.3.B.4. Dye permeability and posterior spiracle morphogenesis .....	127
C.3.B.4a. Is dye penetration phenotype “posterior spiracle-dependent”?.....	127
C.3.B.4b. Phenotypic rescue of the dye penetration phenotype.....	129
C.3.B.5. Permeability in time and space .....	130
<b>D. DISCUSSION</b> .....	131
D.1. <i>Btk29A</i> expression pattern .....	132
D.2. Posterior Spiracle morphogenesis .....	134
D.2.A. Btk-dependent epithelial cell rearrangements contribute to the invagination of nearby tubular structures in the posterior spiracles of <i>Drosophila</i> .....	134
D.2.B. Convergent extension of stigmatophore cells.....	135
D.2.C. Spiracular chamber invagination .....	136
D.2.D. Contribution of convergent extension to invagination .....	137
D.2.E. Btk29A as a “member” of the AbdB regulatory cascade.....	139
D.2. F. Conclusion and perspectives .....	140
D.3.Trachea system .....	141
D.3.A. Is the Btk29A kinase a regulator of tissue insulation? .....	142
D.3.B. The “yet unknown” cellular basis for Btk29A function in the tracheal system .....	143
<b>CONCLUSION</b> .....	144
<b>REFERENCES</b> .....	145

---

# **A. INTRODUCTION**

---

## A.1. Respiratory system of *Drosophila melanogaster*

---

*Drosophila melanogaster* is a well-established model system for studying developmental processes which are necessary for building multicellular organisms *in vivo*. The ample information concerning its genetics, its relatively easy manipulation and the existence of various genetic tools render *Drosophila* a leading model in experimental science.

The respiratory system of *Drosophila* consists of two morphologically distinct compartments: the trachea system and the spiracles. These structures are established during *Drosophila* embryonic development. The proper formation of both trachea and spiracles and the connection of the two structures ensures the functionality of the system.

The tracheal system of *Drosophila* is a bilaterally symmetrical epithelial network that spans the body of the fly and supplies all tissues with oxygen (Ghabrial et al., 2003). It consists of one network of numerous interconnected tubular branches - primary, secondary and terminal branches, characterized by different tube size and properties (Figure 1).

The network develops during embryogenesis, but it becomes functional just before the embryo hatches. The tracheal branches reach all internal organs and facilitate the supply of oxygen throughout the body of the newly hatched 1<sup>st</sup> instar larva. The trachea undergoes further remodeling during metamorphosis to the pupal and adult stages. In the larva, pupa and adult, ambient air flows into the network through the spiracles (see Paragraph A.2), it passes into the tracheal tubes and reaches the target tissues, where air-born oxygen can diffuse (Manning and Krasnow, 1993).

The developmental processes that underline the formation of the embryonic respiratory system compartments: the posterior spiracles and the trachea system, will be described in the following Paragraphs (Paragraph A.2 and A.3 respectively).

---

## A.2. Posterior spiracles

---

### A.2.A. Posterior spiracles

The spiracles are external openings of the respiratory system of the insects, which facilitate air (and thus oxygen) supply from the environment to the tissues. In *Drosophila*, they connect to the spiracular branches of the tracheal metameres (Tr1-Tr10): the lumens of trachea and spiracles are thus continuous and air flows through the spiracles to the airways. Spiracles are of ectodermal origin and they grow an elaborate cuticular structure. Their specialized complex morphology enables air supply, limits water loss and prevents foreign bodies from entering the trachea system (Manning and Krasnow, 1993).

Posterior spiracles are the only functional spiracles in the early larval life of *Drosophila*. They develop during embryogenesis in the embryonic segment A8 (adjacent to the Tr10 spiracular branch) and become functional just before hatching of the first instar larva (Figure 1A and B). The anterior spiracles (Figure 1A), which are formed during embryogenesis in the first thoracic segment T1, are occluded in the first two larval instars and become functional only later in larval life (in third instar) (Figure 1A). The lumen of the spiracular tracheal branches of segment T2 to A7 collapse in all larval stages and no functional spiracles develop at their openings. During pupal development, the limited oxygen needs of the pupa are met solely by the supply through the Anterior Spiracles. After metamorphosis, the adult fly has nine fully functional pairs of spiracles located in anterior T2, in posterior T3, and in the middle of each abdominal segment A1-A7 (Figure 1) (Manning and Krasnow, 1993). In the current study, we will focus on the embryonic development of the posterior spiracles of *Drosophila*.

As mentioned above, posterior spiracles are ectoderm-derived epithelial structures. They consist of two distinct structures: the *spiracular chamber* and the *stigmatophore* (Figure 2). The spiracular chamber is an internal multicellular tube continuous to the tracheal dorsal trunk. In the larva this tube acts as a cuticular refractile filter, the *filzkörper* (Figure 2). The opening of the spiracular chamber, the stigma, is surrounded by four sensory organs: the spiracular hairs (Figure 2).

The external part of the posterior spiracles, the stigmatophore, is a protruding structure that surrounds and supports the inner spiracular chamber. The stigmatophore enables the projection of the larval spiracle outside of the semi-liquid medium where the larva feeds, so that breathing while feeding is possible. Although they eventually form together the respiratory system, the posterior spiracles and the trachea (Paragraph A.3.) develop through different morphogenetic programmes (Hu and Castelli-Gair, 1999).



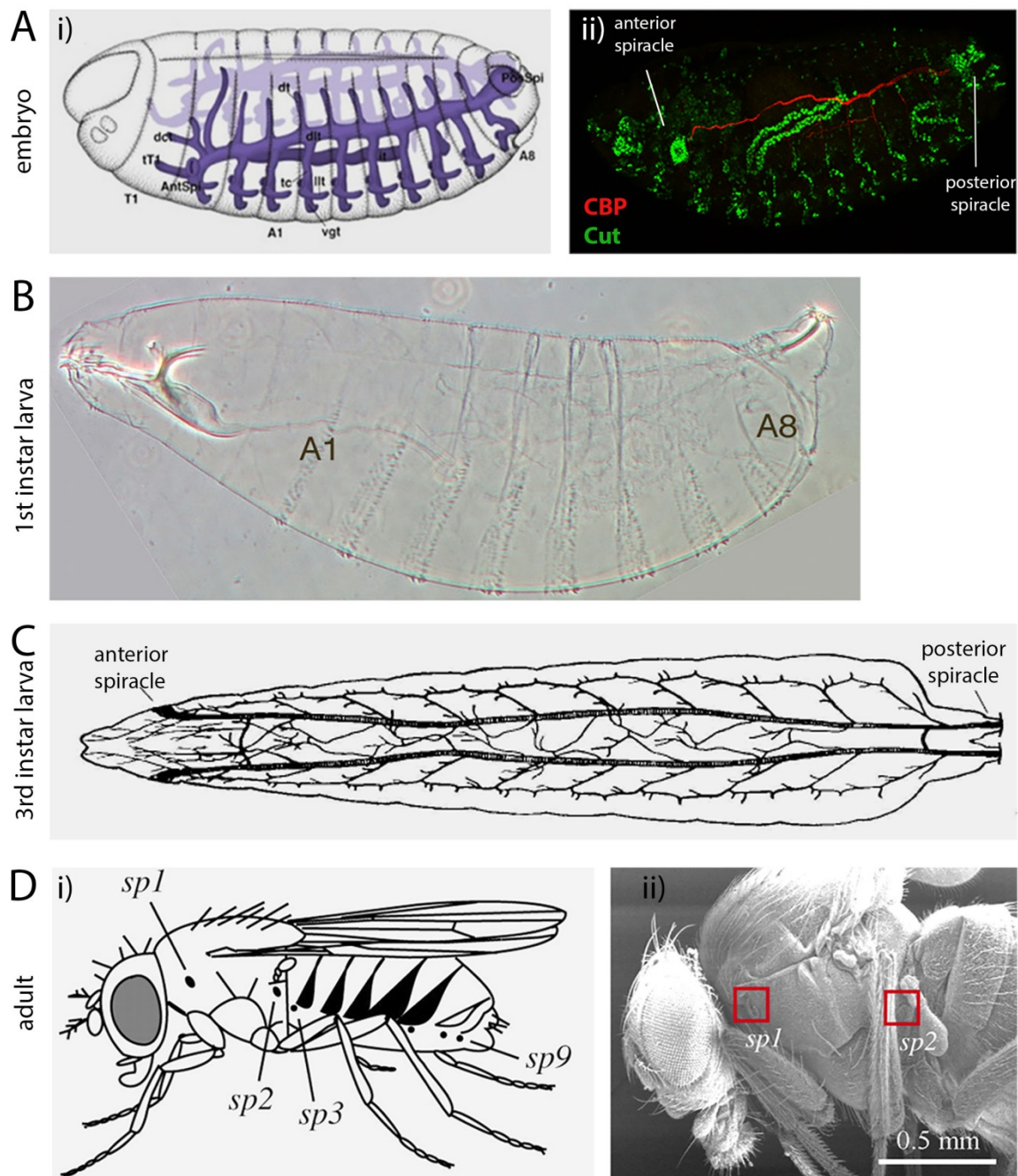


Figure 1: Spiracles in *Drosophila melanogaster*

A. The anterior and posterior spiracles of *Drosophila* develop during embryogenesis at the first thoracic (T1) and eighth abdominal (A8) embryonic segment. The tissues become functional only during larval stages. i) Schematic representation of the tracheal network and spiracles in embryonic stage 15. ii) Antibody staining for the trachea luminal marker CBP (Chitin Binding Probe - red) and Cut (which is expressed by both anterior and posterior spiracle cells - green) showing the localization of the tissues (panel i is original from Atlas of *Drosophila* development by V. Hartenstein (<http://www.sdbonline.org/sites/fly/atlas/2021.htm>)). B. After hatching the 1st instar larva posterior spiracle enable air exchange (original from Castelli-Gair Hombría et al. (2009), Figure 1A). C. During 3rd instar, anterior

spiracle becomes functional. D. Adult flies display 9 spiracles located in anterior T2, in posterior T3, and in the middle of each abdominal segment A1-A7. i) Schematic representation of the adult fly. ii) Scanning electron microscopic image of *Drosophila* shows the position of sp1 and sp2 adult spiracles (panels i and ii are original from Heymann and Lehmann (2006), Figure 1A and B respectively).

### A.2.B. Posterior spiracle morphogenesis

The morphogenesis of posterior spiracles depends on a developmental program orchestrated by the Hox gene *Abdominal-B* (*AbdB*) (Hu and Castelli-Gair, 1999). It starts at embryonic stage 11 and it involves a group of epithelial cells located adjacent to the most abdominal tracheal pit (Tr10, see Figure 3B and area indicated by arrowhead in Figure 6A). The process involves multiple steps, from the initial specification of the spiracular cell primordia, to the final acquisition of the three dimensional tissue morphology.

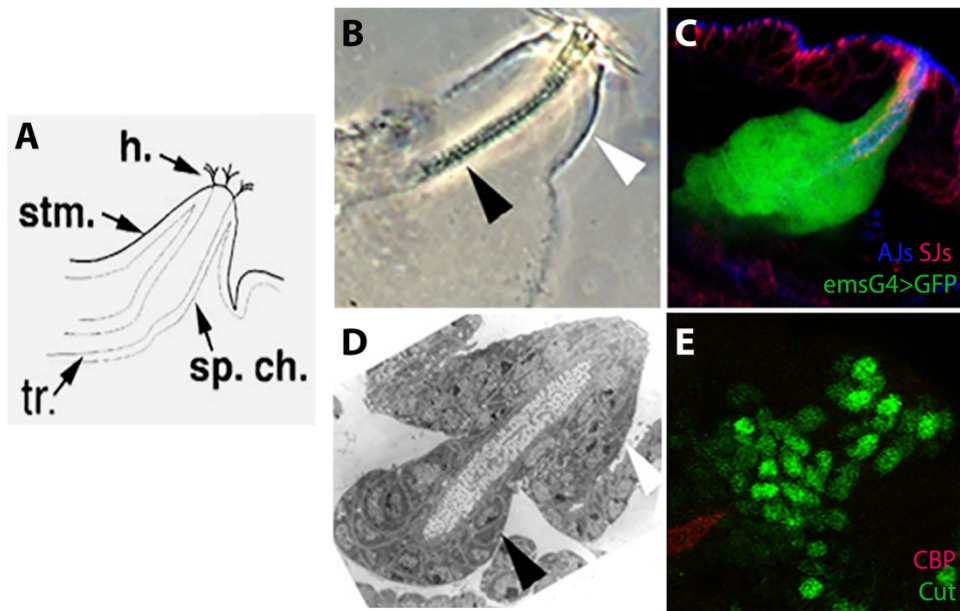


Figure 2: Posterior spiracles

Posterior spiracles consist of the outer stigmatophore (white arrowhead in B and D) and the inner spiracular chamber (black arrowhead in B and D). The filzkörper, a refractile filter, is deposited inside the trachea lumen and 4 sensory organs (spiracular hair) are located at the tip of the tissue. A) Schematic representation of the posterior spiracle compartments. B) Brightfield image of the posterior spiracles. (filzkörper and spiracular hair are obvious), C) Posterior spiracle cell polarity and basolateral elongation observed with antibody staining for AJ (blue), SJ (red) markers and GFP expressed by the cells (green) under the emsGAL4. D) Transmission electron microscope micrograph showing the ultrastructural arrangements of the spiracular cells. E) Arrangement of the spiracular chamber nuclei in correlation with the trachea lumen (zoom of Figure 1Aii, CBP – red and Cut – green). Figures B, C and D from Castelli-Gair.

---

### A.2.B.1. Spiracular chamber formation

As previously mentioned, the spiracular chamber is the inner part of the posterior spiracles that is continuous to the trachea lumen and connects the airways to the environment.

The development of the tissue starts at embryonic stage 11, soon after the specification of the posterior spiracle primordia (see Paragraph A.2.B.3), from a group of 70 epithelial cells located posterior to the most abdominal tracheal pit (Tr10) (Figure 3B and area indicated by arrowhead in Figure 6A). At this initial stage the cells are undistinguishable from the rest of the epidermis of the fully elongated embryo. They can only be discerned by the expression of the primary target protein Cut (marking all the spiracular chamber cells, see also Figure 20) and Ems (marking a subgroup of the cells) (Hu and Castelli-Gair, 1999).

As the germ band retraction of the embryo starts, the Cut<sup>+</sup> cells undergo apical constriction, rearrange their position around the adjacent tracheal opening (Tr10) and start to invaginate (shortly after the completion of the invagination of the Tr10 tracheal cells) (Hu and Castelli-Gair, 1999) (Figure 3). The invagination process is spatially and temporally controlled, as the cells that lay adjacent to the trachea invaginate first and the more posterior cells follow (Simões et al., 2006). During this process, the invaginating cells undergo cell shape changes and elongate their basolateral membrane, acquiring a bottle-shape morphology. By stage 13 (end of germ band retraction), all the spiracular chamber cells have invaginated, forming a tube continuous to the trachea (Simões et al., 2006). Further elongation of the basolateral membrane of the cells leads to the formation of the three dimensional spiracular chamber with the bottle-shaped Cut<sup>+</sup> cells enseathing the spiracular lumen (Simões et al., 2006). After stage 16, the spiracular chamber morphogenesis is terminated by the secretion of the filzkörper inside the spiracular lumen. Filzkörper is a refractile cuticular structure important for air filtering during the upcoming larval stages (Hu and Castelli-Gair, 1999).

Spiracular chamber morphogenesis requires proper execution and coordination of the necessary cell shape changes (apical constriction and basolateral elongation) and invagination of the cells. All these processes depend on the fine tuning of the cell polarity, adhesion and cytoskeletal organization, which in the case of posterior spiracles are regulated (directly or indirectly) by the so called realisator genes that lay downstream of AbdB morphogenetic cascade (Paragraph A.2.B.3.d).



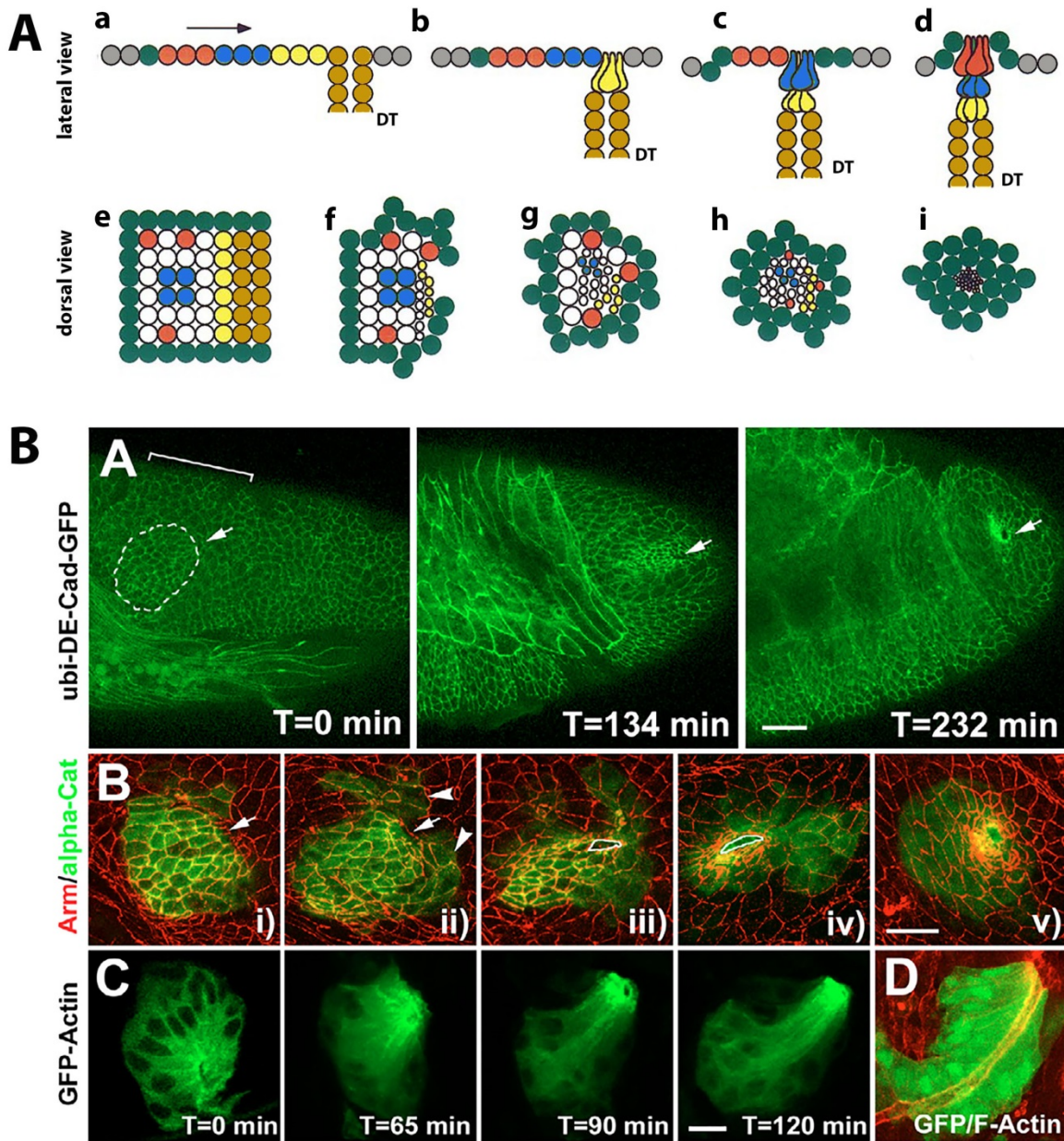


Figure 3: Model for posterior spiracle morphogenesis

A. Schematic representation of the cells of the posterior spiracle at different stages of development. In stage 11 (a and e) the posterior spiracle primordia are specified, adjacent to the invaginated tracheal cells (dark yellow) and they are indistinguishable from one another and the adjacent epidermal cells. Gradually, the spiracular chamber cells undergo apical constriction and invagination, with the more proximal to the trachea spiracular chamber cells (expressing *Ems*, in yellow) invaginating first (b and f) and the more distal ones (in blue and red) following them (c, d and g - i). By stage 13, all the spiracular chamber cells have undergone invagination and are no longer visible at the cell surface (d and i). The cells will further elongate their basolateral membrane to acquire bottle-shape morphology. Parallel to the spiracular chamber morphogenetic changes, the stigmatophore cells (dark green) rearrange their positions around the spiracular chamber cells filling the space previously occupied by them (e-i). The cell rearrangement in the stigmatophore results in its elevation/protrusion over the surrounding ectoderm (d and i). a-d are lateral/side and e-i dorsal views of the posterior

---

spiracles. (tracheal cells in orange; stigmatophore cells in green; spiracular chamber cells in yellow, blue, red and white) Scheme adapted from Hu and Castelli-Gair, 1999, Figure 10.

B. A) Apical constriction and invagination of posterior spiracles: At stage 11 ( $t=0$  minutes), spiracular chamber cells (dashed line) are superficial and localize posteriorly to the A8 tracheal pit (Tr10) (arrow), they gradually undergo apical constriction and inward cell movement to form a lumen (arrow). DE-Cadh-GFP in green. B) Expression of Catenin-GFP (green), using the spiracle specific *ems-GAL4* driver, shows that: (i,ii) Initial lumen formation (stage 11) involves rearrangement of the most anterior cells (arrowheads) around the tracheal opening (arrow). (iii) The more posterior cells (left from white outline) constrict apically and invaginate later (iv), to form the complete chamber (v). Armadillo is in red. C) Stills of a live embryo expressing GFP-Actin in the spiracle invaginating cells.  $t=0$  minutes corresponds to end of stage 12. Notice apical enrichment of GFP-Actin and elongation of the basolateral cell domain, with the cell nuclei (black) remaining basally localised. Phalloidin staining (red) in the spiracular chamber cells expressing GFP (green). Notice the accumulation of F-Actin at the apical/luminal side of the spiracular chamber cells (lateral view). Panels A-D are original from Simões et al., 2006.

### A.2.B.2. Stigmatophore formation

The specification of the stigmatophore depends on AbdB and is performed at stage 11 along with that of the spiracular chamber. The newly specified cells start expressing the stigmatophore-specific AbdB primary target *sal* (see Paragraph A.2.B.3) and are located in the dorsal part of the A8 embryonic segment adjacent to the spiracular chamber primordia (Hu and Castelli-Gair, 1999). The morphology of the *Sal*<sup>+</sup> cells is initially indistinguishable from the rest of the epidermis (just like the stigmatophore cells).

Previous studies have revealed that accurate morphogenesis of the tissue depends on spatial rearrangements of the stigmatophore cells (Brown and Castelli-Gair Hombria, 2000; Hu and Castelli-Gair, 1999). Specifically, following their specification the *Sal*<sup>+</sup> cells rearrange their positions and encircle the spiracular chamber primordia. By stage 12, the “stigmatophore circle” has a width of 2-3 cell and a circumference of approximately 25 cells. As the spiracular chamber cells invaginate, the circle undergoes drastic changes, acquiring a broader width (about 10 cell wide at stage 15) and smaller circumference (around 10 cells at stage 15) (Figure 3A and 4) (Hu and Castelli-Gair, 1999). Moreover, *in vivo* observation of the stigmatophore movements revealed that the cell rearrangements occur discontinuously and at a non-uniform speed (Brown and Castelli-Gair Hombria, 2000). At the end of embryogenesis the stigmatophore cells have completed their spatial arrangements, ensuring the sufficient closure of the spiracle area (after the invagination of the spiracular chamber cells) and the elongation of the stigmatophore.

*Sal* is a the zinc finger transcription factor involved in several developmental processes, among which, the specification of the terminal pattern elements (head and tail) in early embryogenesis (Kuhnlein et al., 1994) and the trachea development (Kuhnlein and Schuh, 1996). Its role in the

---

posterior spiracle development is restricted to the stigmatophore development, as spiracular chamber is not dramatically affected in *sal* mutants (see Paragraph A.2.B.3). In the stigmatophore *Sal* is important for the activation of the transcription factors *grn* and *en*, which fall into the category of AbdB secondary targets (see Paragraph A.2.B.3.c).

Mutants for these genes form defective posterior spiracles with non-protruding stigmatophore (*grn* mutants show defective spiracular chamber as well) (described also in Paragraph A.2.B.3.c). Interestingly, the stigmatophore phenotype observed in *grn* mutants is not related to defective patterning of the tissue, but rather to impairment of the stigmatophore cell rearrangements (Brown and Castelli-Gair Hombria, 2000). In detail, the width and circumference of the “stigmatophore circle” remains more or less constant in *grn* mutants (around 2-3 and 25 cells respectively) (Brown and Castelli-Gair Hombria, 2000).

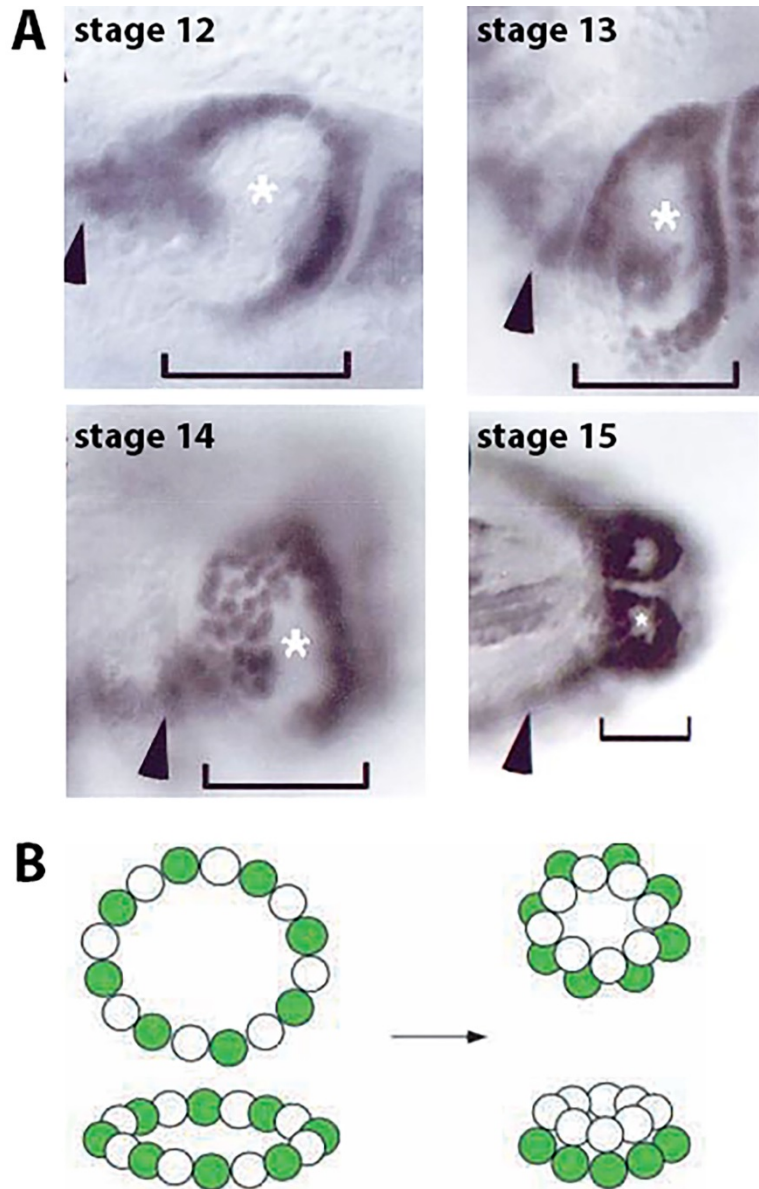


Figure 4: Morphogenetic movements of the stigmatophore cells

A. The stigmatophore cells (marked with anti-Sal) undergo spatial rearrangements. As a result, the 2- to 3-cell-wide “stigmatophore circle” at stage 13 becomes 4 to 5 cells wide at stage 14 and about 10 cells wide at stage 15. Simultaneously the spiracular area (marked with asterisk) decreases. Magnification in stage 15 is half of the other stages. The position of A8 is indicated by a bracket. Arrowheads point to the trachea.

B. Schematic representation of the stigmatophore cell rearrangements. Convergent extension-like movements of the stigmatophore cells lead to spiracle opening closure and increases in the number of stigmatophore cell tiers. Adapted from Brown and Castelli-Gair Hombria, 2000.



---

### A.2.B.3. AbdB masters the gene network driving posterior spiracle specification and morphogenesis

#### A.2.B.3.a. Abdominal-B and the specification of posterior spiracle primordia

*Abdominal-B* (*AbdB*) is a homeotic gene involved in the patterning of the posterior abdominal segments of *Drosophila* embryo. It is expressed throughout segments A8 to A11 and is the only Hox gene required for spiracle specification. Two different isoforms of the AbdB protein have been characterized: the long AbdBm (morphogenetic) and the short AbdBr (regulatory) isoform (Casanova et al., 1986). Although both isoforms have the capacity to repress transcription of more anterior Hox genes, a common feature of Hox *Drosophila* proteins (Struhl and White, 1985), it seems that only AbdBm is capable of inducing posterior spiracle formation (Castelli-Gair Hombría et al., 2009). Mutants for AbdBm do not develop posterior spiracles (Hu and Castelli-Gair, 1999; Sanchez-Herrero et al., 1985), while ectopic expression of the protein in more anterior segments leads to ectopic spiracle formation (Castelli-Gair et al., 1994; Lamka et al., 1992). In agreement to this, AbdBm is expressed in A8 embryonic segment, while AbdBr in the A9 segment that does not form spiracles (Boulet et al., 1991).

The formation of the spiracles requires the correct spatial (segment A8) but also temporal activation of *AbdB* before germ-band retraction (Castelli-Gair Hombría et al., 2009). Consistently, ectopic expression of *AbdB* can only induce the formation of posterior spiracles in the first 5 hours of development (Castelli-Gair, 1998), suggesting that cells are capable to acquire posterior spiracle characteristics only if instructed to do so within a limited time window.

Little is known about the upstream transcriptional regulators of *AbdB* in A8. Although several components required for the early patterning of the embryo (gap, pair-rule and terminal genes) affect the expression of the gene, no direct correlation of these genes to AbdB function in posterior spiracle formation has been made (Castelli-Gair Hombría et al., 2009). A protein known to modulate AbdB activity is Lines (Lin), but Lin does so without affecting AbdB expression (Castelli-Gair, 1998). AbdB requires Lin for the activation of all of its known targets, but not for the repression of the anterior Hox genes (Castelli-Gair, 1998).

AbdB is expressed throughout segments A8 to A11, yet the posterior spiracle primordia are specified, at early stage 11 of *Drosophila* embryogenesis, only in a dorsal-anterior region of the A8 abdominal segment (see arrowhead in Figure 6A). The commitment of these (dorsal-anterior) cells to the spiracular fate is regulated by additional cues (Hu and Castelli-Gair, 1999). For example, the dorsally expressed Decapentaplegic (Dpp) signalling is likely to participate in the activation of posterior spiracle specific genes in the dorsal part of A8 (Castelli-Gair Hombría et al., 2009).



---

#### A.2.B.3.b. Patterning of the posterior spiracle primordia – AbdB primary target genes

The newly specified spiracular cells are initially indistinguishable from the adjacent epidermal cells. The very first sign of spiracle specification is the expression of a small set of genes (primarily transcription factors: *cut* (*ct*), *empty spiracles* (*ems*), *unpaired* (*upd*) and *spalt* (*sal*)) induced by AbdB in the presumptive tracheal placode. (Hu and Castelli-Gair, 1999; Lovegrove et al., 2006). These genes are essential for the patterning of posterior spiracles and are known as AbdB primary targets (Figure 5).

*AbdB* mutants lack expression of primary genes, while on the opposite, ectopic expression of *AbdB* leads to primary target gene expression and ectopic spiracle formation (Lovegrove et al., 2006). Furthermore, with the exception of *Sal* (which is likely to be transcriptionally repressed by *Cut*, see below and Figure 5), the expression of primary genes is not interdependent (Hu and Castelli-Gair, 1999). Taken together, these observations suggest that AbdB directly regulates the aforementioned genes. Till today, direct activation by AbdB has only been described for *ems* (Jones and McGinnis, 1993; Rivas et al., 2013).

The transcription factors *Cut* and *Ems* and the JAK/STAT ligand *Upd* are expressed by the spiracular chamber precursors in partially overlapping patterns, while *Sal* is expressed by the presumptive stigmatophore cells, in a pattern complementary to *Cut*. This complementary expression results from the repression of *sal* transcription by *Cut* and might be one of the principal mechanisms subdividing the spiracular primordium in spiracular chamber and stigmatophore cells (Castelli-Gair Hombría et al., 2009). The expression of *upd* and *ems* persists till stage 13, while *cut* and *sal* are expressed throughout embryogenesis.

Mutations in the primary target genes have different effects on the posterior spiracles (Hu and Castelli-Gair, 1999). In *ems* mutants the spiracular chamber completely lacks a filzkörper and is not connected to the trachea. Thus, the continuity between the trachea and the spiracles is lost and the trachea does not reach the surface of the embryo. The spiracular hair and the stigmatophore are not affected. In *cut* mutants, although the filzkörper is almost completely missing in late embryos, a remnant of the spiracular chamber still develops: the trachea keeps the connection to the spiracular chamber. The stigmatophore is not affected, but the spiracular hair are missing.

Mutations affecting the JAK/STAT pathway (the transcription factor *STAT*, the *Upd* ligands or the receptor *Dome*), cause a lack of spiracular cell elongation (see Paragraph A.2.B.1 and Lovegrove et al., 2006) and stigmatophore cell misplacement. Hence, the stigmatophore phenotype seems either secondary to the spiracular chamber defect, or to be caused by a specific requirement of the JAK/STAT signalling in the stigmatophore cells.

Mutants for the stigmatophore specific *sal* gene fail to form the stigmatophore. This results in the formation of a normal spiracular chamber that does not protrude.

Simultaneous elimination of the four primary target genes: *cut*, *sal*, *ems* and *dome*, leads to complete absence of posterior spiracles, similarly to the *AbdB* mutant embryos. Moreover, simultaneous ectopic expression of Cut, Upd, Ems and Grain (Grn), a secondary target of AbdB developmental project regulated by Sal (see following Paragraph), induces the expression of downstream targets in the ectopic spiracles. These observations once again suggest that *cut*, *sal*, *ems* and JAK/STAT pathway) are the main AbdB primary target genes (Lovegrove et al., 2006). It should be noted that more genes, like *klumpfuss* and *nubbin*, are considered putative AbdB primary targets in the spiracles. However, their mutations do not affect posterior spiracle development (Castelli-Gair Hombría et al., 2009; Hu and Castelli-Gair, 1999).

Following their expression in the posterior spiracle primordia, the primary targets will activate downstream transcription factors and signalling molecules that will further pattern the tissue and ensure its accurate morphogenesis, the so called AbdB secondary targets.

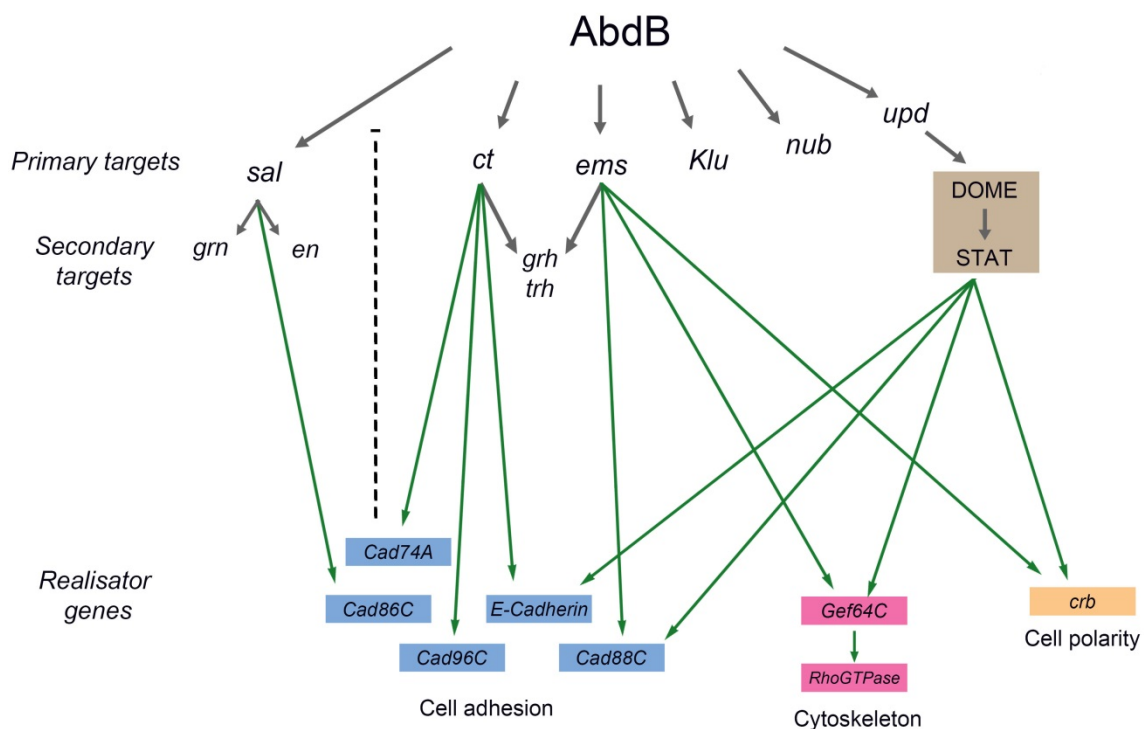


Figure 5: AbdB genetic cascade in posterior spiracle morphogenesis

Summary of genetic interactions that are controlled downstream of AbdB during posterior spiracle organogenesis. AbdB, in combination with intrasegmental cues (possibly Dpp signaling and others) activates early-transcription factors and signaling molecules (*sal*, *cut*, *ems*, and *upd*) in the primordium of the posterior spiracle. These activate directly or indirectly the expression of cell adhesion (blue), cell polarity (orange) and cytoskeleton regulators (pink) that locally confer unique cell behaviors leading to spiracle morphogenesis. The orange box groups JAK/STAT pathway elements not directly regulated by AbdB. Adapted from Lovegrove et al., 2006, Figure 7M)

---

### A.2.B.3.c. Secondary targets

The secondary target gene expression initiates at stage 11 after the activation of the primary targets. They include transcription factors and signalling molecules that will ensure the transformation of the two dimensional primordium to a three dimensional posterior spiracle by the end of embryogenesis. Usually, one or more primary genes cooperatively regulate the spiracular expression of secondary genes, thus secondary gene expression appears in different subsets of posterior spiracle cells (Castelli-Gair Hombría et al., 2009). While loss of AbdB obviously leads to loss of secondary target expression, direct activation of secondary target genes by AbdB is not very likely, since the primary targets are able to induce ectopic spiracles even in the absence of AbdB (Lovegrove et al., 2006).

Only a few secondary target genes have been identified (Figure 5). Among them, the transcription factors *grainy head* (*grh*), *tracheiless* (*trh*) and *DmOAZ* are involved in the patterning of the spiracular chamber, while *engrailed* (*en*) and *grain* (*grn*) are implicated in the stigmatophore formation (Figure 5). Some signalling molecules are also secondary targets of the cascade (Castelli-Gair Hombría et al., 2009).

#### - Spiracular chamber specific secondary targets

During embryogenesis, *grh* (Bray and Kafatos, 1991) is expressed in the epidermis and tracheal system. In the posterior spiracle it is detected in a subgroup of the posterior spiracle primordia. Different enhancers of the gene ensure its proper expression in different tissues, with *grh*-D4 enhancer specifically driving posterior spiracle expression (Hu and Castelli-Gair, 1999).

Marking the cells with a *grh* spiracular enhancer trap (*grh*-D4-lacZ) revealed that they acquire extremely elongated shapes at the end of spiracular morphogenesis (Hu and Castelli-Gair, 1999). The function of the gene in the spiracles is not determined, as mutants for *grh* do not display abnormal morphology of the spiracles (unpublished observations). The expression of *grh* is regulated by Ems and Cut, since mutants for those primary targets fail to express *grh*-D4-lacZ (Hu and Castelli-Gair, 1999).

As described in Paragraph A.3.A.1 the transcription factor *trh* is important for tracheal development (Isaac and Andrew, 1996). Similar to *grh*, the spiracular expression of *trh* is regulated by Ems and Cut through specific enhancers (Hu and Castelli-Gair, 1999; Isaac and Andrew, 1996). In *trh* mutants the tracheal system does not form and the posterior spiracles develop shorter filzkörper (Hu and Castelli-Gair, 1999; Isaac and Andrew, 1996). The spiracular phenotype is

---

likely to be due to a direct function of Trh in the spiracles, since other mutations affecting trachea development (like *vvl*) do not affect posterior spiracle morphogenesis (de Celis et al., 1995).

Another secondary target that lays downstream of Ems and Cut is the *Drosophila melanogaster* homologue of the OAZ zinc finger protein family, DmOAZ. High levels of DmOAZ expression are detected throughout spiracular development. Mutants for this gene display filzkörpers with abnormal morphology and fail to completely fill their trachea with air (Krattinger et al., 2007).

It should be noted here that mutants for any of the above secondary targets (*grh*, *trh* and *DmOAZ*) do not affect the expression of the other two. This suggests that the three factors act independently of each other to ensure proper posterior spiracle development (Hu and Castelli-Gair, 1999; Krattinger et al., 2007).

### - *Stigmatophore-specific secondary targets*

As previously described, Sal is the only stigmatophore-specific primary target of AbdB. The main secondary targets regulated by Sal in the stigmatophore are the transcription factor *Grain/GATAc* (*Grn*) and the homeobox gene *engrailed* (*en*) (Castelli-Gair Hombría et al., 2009).

Grn is expressed both in the stigmatophore and spiracular chamber cells. In the spiracular chamber, its expression is regulated by the JAK/STAT pathway (Upd) (Lovegrove et al., 2006). In the stigmatophore, it has been described to regulate stigmatophore cell rearrangements important for the morphogenesis of the tissue (Brown and Castelli-Gair Hombría (2000) and Paragraph A.2.B.2). *Grn* mutants display irregular stigmatophore and shorter spiracular chamber. Although this second phenotype is likely due to the absence of Grn in the spiracular chamber cells, the possibility of an indirect action of the stigmatophore rearrangements cannot be excluded (Brown and Castelli-Gair Hombría, 2000; Castelli-Gair Hombría et al., 2009).

The homeodomain transcription factor *engrailed* (*en*) acts as a segment-polarity gene in early embryonic development. It is expressed in a stripy pattern from between embryonic stage 8 and 12 (14 bands of cells along the antero-posterior axis), localized at the anterior compartment of each embryonic parasegment (Sanson, 2001). After stage 12, En acquires a differential A8 expression pattern: at the dorsal part of the stripe it is expressed by a circle of Sal-expressing stigmatophore cells while the ventral expression is lost (Merabet et al., 2005). This differential expression is regulated by Sal (Castelli-Gair Hombría et al., 2009; Hu and Castelli-Gair, 1999). Moreover, *en* mutants display abnormal stigmatophore formation, but the spiracular chamber and filzkörper formation is not affected (Merabet et al., 2005).

---

### - *Intersegmental patterning genes as Secondary targets*

During early *Drosophila* embryogenesis, the segment polarity genes *wingless* (*wg*), *rhomboid* (*rho*) and *en*, involved in the WNT, EGFR and Hedgehog (Hh) signalling respectively, regulate the antero-posterior (A-P) patterning of the embryo (Sansom, 2001). These molecules constitute an important class of ABD-B secondary targets.

Although all three of the aforementioned genes are expressed in a segmental pattern in early embryonic stages, by stage 11 their expression changes in A8, in response to AbdB activation. More specifically, the stripe of expression of the WNT ligand *wg* disappears and it is substituted by only two A8 *wg* expressing cells, while the expression of the protease Rho persists and one extra patch of Rho expressing cells appears. *En* expression is induced at the dorsal part (see also previous Paragraph) and Hh acquires an *En*-independent expression in the dorsal ectoderm of A8 (Merabet et al., 2005). All of these expression changes in A8 are regulated by AbdB. Interestingly for the regulation of *wg* and *rho* expression, *Lin* and Hh activity is required (Merabet et al., 2005).

Mutants for *wg*, *hh*, *Egfr* fail to develop posterior spiracles. Additionally, inhibition of the function of these signalling pathways in A8 during spiracular morphogenesis causes severe spiracle defects. Thus, the phenotypes: i) are not related to an early loss of segmental polarity, ii) are not due to failure of posterior spiracle primordia specification but iii) rather they seem to be related to later functions of these signalling pathways (after stage 12) (Merabet et al., 2005).

Further analysis of the function of these signalling pathways reveals that they control multiple cellular events during posterior spiracle organogenesis, including cell survival, maintenance of cell polarity and adhesion required for tissue integrity (Maurel-Zaffran et al., 2010).

#### **A.2.B.3.d. Realisator genes**

Hox genes are known to implement their function as fate-determining regulators (“master regulatory functions”) through the activation of so-called realisator genes: target genes responsible for determining local cell behaviours, like cell shape, cell adhesion, etc (Garcia-Bellido, 1975). In the posterior spiracle these factors are divided in three distinct groups according to their function: cell adhesion proteins, cytoskeletal regulators and cell polarity proteins (Figure 5). Examples of realisator genes belonging to each of the three categories will be presented below.

---

### - Cell adhesion proteins (e.g. Cadherins)

Cadherins are calcium-dependent cell adhesion proteins. They are divided in two different groups: the classical and the non-classical Cadherins depending on the presence of a conserved catenin-binding domain. Three classical: Shotgun (Shg)/ *Drosophila* Epithelial-Cadherin (DE-Cad), *Drosophila* Neuronal Cadherin (DN-Cad) and Cadherin N2 (CadN2) and fourteen non-classical Cadherins have been identified in *Drosophila* (Fung et al., 2008; Hill et al., 2001). The posterior spiracle cells show expression of the classical DE-Cadherin, as well as several non-classic Cadherins (*cad86C*, *cad74A*, *cad88C* and *cad96C*) (Lovegrove et al., 2006).

Spiracular expression of DE-Cadherin is exceptionally high compared to the levels of the protein in the epidermis. This expression is regulated by the primary target Cut and the JAK/STAT pathway (Figure 5). *cad86C*, *cad74A*, *cad88C* and *cad96C* show a mosaic distribution on different groups of spiracular cells (Lovegrove et al., 2006): *cad86C* is expressed in the distal cells of the stigmatophore, *cad74A* in the distal cells of the spiracular chamber, and *cad88C* and *cad96C* are co-expressed in the most internal spiracular chamber cells. Activation of the non-canonical Cadherins depends on Cut, Ems and the JAK/STAT pathway (Figure 5) (Lovegrove et al., 2006).

When DE-Cadherin is absent from the posterior spiracle the spiracular chamber is affected, as the cells only partially complete the invagination process necessary for the morphogenesis of the tissue (see Paragraph A.2.B.1). The non-invaginated cells remain on the surface where they elongate and differentiate, in an abnormal superficial position, the refractile filzkörper (Lovegrove et al., 2006). Contrary to this, absence of one (or two) non-classical Cadherins does not affect the morphogenesis of the spiracles, suggesting that the non-classical Cadherins have minor role in posterior spiracle development (Simões et al., 2006).

### - Cell polarity proteins (e.g. Crumbs)

Cell polarity is a characteristic feature of epithelial cells, whose plasma membrane is not uniform in protein and lipid composition. The plasma membrane of epithelial and polarised cells shows clearly distinct domains, usually separated by cell-cell junctions, as in the examples of epithelial tissues. Typically one side of the membrane faces the outside environment or the internal lumen of internal organs (the apical membrane), while the other domain (the basolateral membrane) faces the internal body space. This characteristic is dependent on the differential membrane localization of several proteins, such as junctional proteins, transporters, pumps and receptors for signalling molecules etc. Acquisition and maintenance of the correct cell polarity is important for tissue integrity and physiology and, during development, proper tissue morphogenesis. The

---

epithelial cells of the posterior spiracles undergo a series of shape changes in order to facilitate proper tissue formation.

Several polarity markers are known to be upregulated in the posterior spiracles (Lovegrove et al., 2006). The transmembrane protein Crumbs (Crb) is one of the best characterized. Crb localizes at the subapical region of the epithelial cells (apically to the Adherens Junctions) (Figure 9A) and is necessary for the maintenance of the cell polarity (Grawe et al., 1996; Klebes and Knust, 2000). Previous studies have shown that the protein is expressed at very high levels in the posterior spiracle primordia where it persists till the end of the tissue morphogenesis. This expression is indirectly regulated by AbdB through the JAK/STAT pathway (Lovegrove et al., 2006).

*crb* mutants display short spiracles and elongation defects reminiscent to that of the JAK/STAT mutants. Thus, although the means of action of Crb in posterior spiracle morphogenesis are not understood, it is possible that the protein is involved in the maintenance of the apical membrane at a stage when the basolateral membrane is elongating. Alternatively, increased Crb levels may help the subcellular relocalisation of the RhoGEFs cytoskeleton regulators (see below) and other proteins to the apical membrane (Castelli-Gair Hombría et al., 2009; Lovegrove et al., 2006).

### - Cytoskeletal regulators

In posterior spiracles, proper actin and myosin organization is important for spiracular chamber formation (Simões et al., 2006). Mutants for the Myosin II regulatory light chain (MRLC, encoded by the *spaghetti squash* gene) fail to complete the spiracular chamber invagination. Moreover, Actin and Myosin II (light and heavy chain) localize at the apical region of the spiracular chamber cells. Impairment of this preferential subcellular localization leads to invagination defects (Simões et al., 2006).

RhoGTPases are main regulators of cytoskeletal organization. Their function is based on their molecular switch from an active GTP to an inactive GDP bound form, which is regulated by the GTPase regulators: RhoGEFs (Rho Guanine Exchange Factors) and RhoGAPs (Rho GTPase Activating Proteins). More specifically, RhoGEFs activate the GTPases by displacing the GDP molecule allowing Rho to bind the excess of GTP present in the cytoplasm, while RhoGAPs repress by binding to RhoGTP and enhancing its GTPase activity.

*Drosophila* RhoGTPase Rho1 is highly expressed in the spiracular chamber cells and affects their morphogenesis: *rho1* loss of function leads to irregular filzkörper and invagination defects, together with an abnormal cortical actin organization and non-uniform Myosin II distribution. The



---

distribution of cell adhesion molecules (Armadillo) is affected but the basolateral elongation is normally performed (Simões et al., 2006).

Despite its ubiquitous localization, the protein seems to have a preferential apical distribution. Use of a probe that binds to the active form of Rho1 showed that by the end of stage 11, the protein gets highly activated on the apical side in a pattern consistent with the actin accumulation on that side of the cells. This apical activation of Rho (as well as the apical accumulation of actin and myosin) persists till the completion of spiracular chamber morphogenesis (Simões et al., 2006). The above suggests an involvement of Rho1 in the organization of the spiracular chamber actomyosin network. Although the GTPase is not activated by AbdB, its regulators (see below) are putting Rho1 indirectly in the AbdB morphogenetic programme (Castelli-Gair Hombría et al., 2009).

Rho1 activity in the posterior spiracle is regulated by at least two RhoGEFs: RhoGEF64C and RhoGEF2 and one RhoGAP: Crossveinless-c (*Cv-c*). Activation of *RhoGEF64C* in the posterior spiracles is regulated by AbdB through Ems and JAK/STAT (Lovegrove et al., 2006). Additionally, upregulation of *cv-c* in the tracheal pit of A8 (the rest of the tracheal pits express lower levels of *cv-c*) depends on AbdB (Lovegrove et al., 2006). Although AbdB does not regulate the expression of RhoGEF2 in the posterior spiracle cells, it is important for the shift of the protein from basal to apical side of the cell (Castelli-Gair Hombría et al., 2009). Interestingly these proteins acquire a characteristic subcellular localization in the spiracular chamber cells: GEFs are localised on the apical region of the cells, while *Cv-c* on the basolateral. This differential localisation is crucial for spiracular chamber morphogenesis. Mutations in any of the GTPase regulating factors show impaired spiracular chamber formation: the accumulation of the actin on the apical region is affected, the invagination process of the cells remains incomplete and the filzkörper is abnormally formed (Simões et al., 2006).

From the above, one could conclude that the posterior spiracle morphogenetic requires the combinatorial function of transcription factors and signalling molecules, downstream of AbdB. These factors will enable the proper regulation of cell adhesion, cell polarity and cytoskeletal regulation and effectuate the cell shape changes, invagination process and cell rearrangements necessary for the establishment of functional posterior spiracles.



---

## A.3. Tracheal system

---

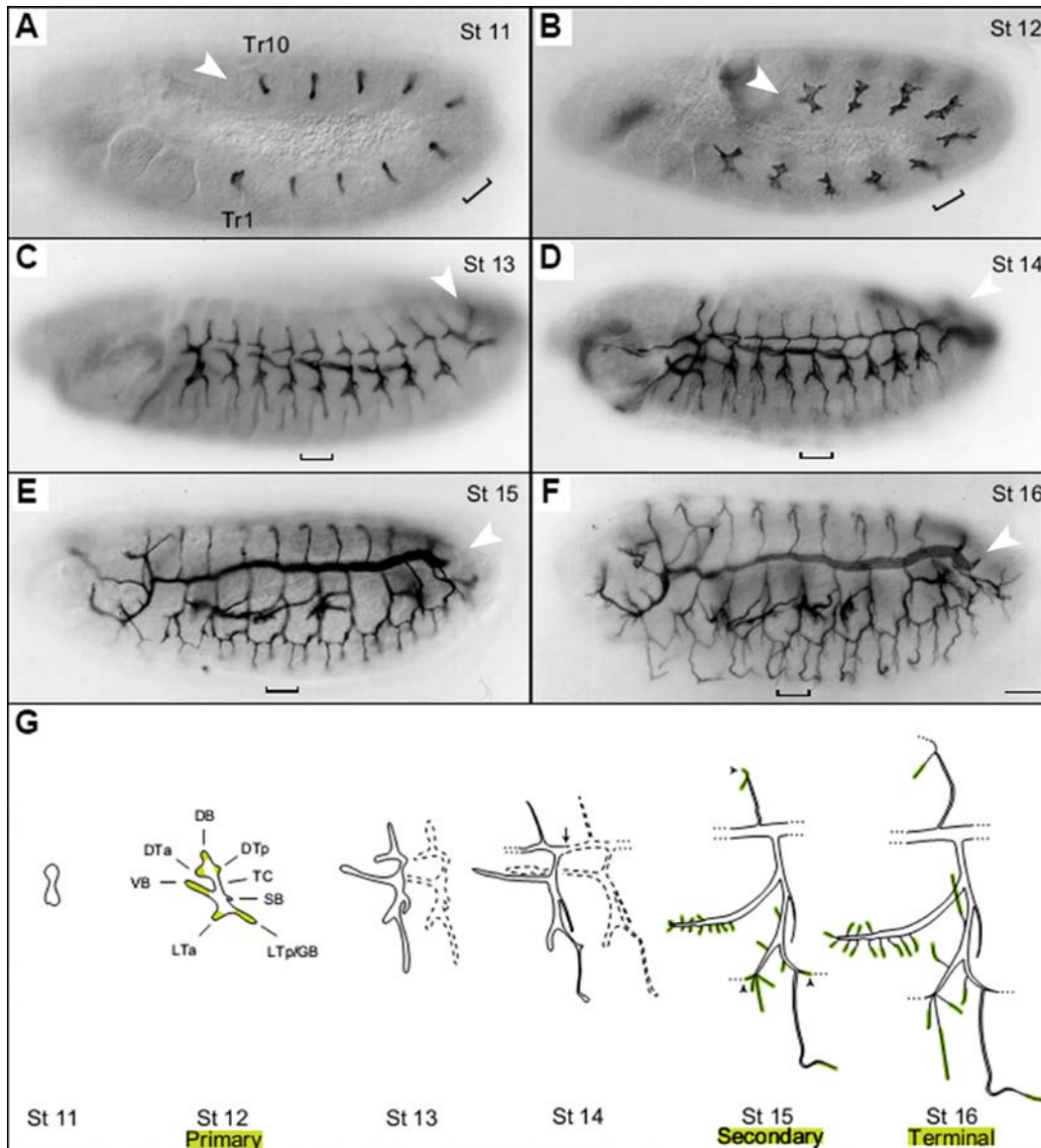
### A.3.A. Tracheal system development

The embryonic development of the tracheal system starts around stage 10 from 20 groups of ectoderm-derived epidermal cells, the tracheal placodes: 10 placodes for each side of the embryo from thoracic segment 2 (T2) to abdominal segment 8 (A8) and 2 for each segment (right and left) (Kerman et al., 2006) (Figure 6A). After their specification, the tracheal cells undergo multiple series of events to finally form the functional tracheal network just before embryo hatching. The basic aspects of this process will be described in the following Paragraphs (A.3.A.1 – A.3.A.4).

#### A.3.A.1. Specification of tracheal cells and early tracheal development

The specification of tracheal primordia depends on the combinatorial action of early patterning genes: the zinc finger transcription factor Spalt (Sal), expressed in the anterior and posterior regions of the early embryo, restricts tracheal development to the segments from T2 to A8 (Kuhnlein and Schuh, 1996), Decapentaplegic (Dpp) signaling sets the dorsal limit (Isaac and Andrew, 1996; Wilk et al., 1996) and the segment polarity gene Wingless (Wg) the lateral boundary (Wilk et al., 1996) of the placodes. Moreover, JAK-STAT signaling induces tracheal formation by activating the expression of the early tracheal genes *tracheiless* (*trh*) (Brown et al., 2001; Isaac and Andrew, 1996; Wilk et al., 1996) and *ventral veinless* (*vvl*) (de Celis et al., 1995; Sotillos et al., 2010). These genes (together with *knirps* (*kni*) and *knirps-related* (*knrl*) (Chen et al., 1998)) are known to induce early trachea development.

Trh, a basic helix-loop-helix (bHLH)-PAS transcription factor, is considered to be the master regulator of tracheal development. *trh* mutants fail to form a trachea system, while the overexpression of the gene leads to formation of ectopic tracheal metameres (Isaac and Andrew, 1996; Wilk et al., 1996). Trh regulates the expression of most of the known trachea-related genes (Chung et al., 2011).



**Figure 6: Development of the tracheal network**

A-F. Tracheal development is performed from embryonic stage 11 to 16 and involves several morphogenetic processes: invagination, migration, branching, fusion, elongation. The embryos are stained with TL-1 (A-D) and 2A12 (E-F). Anterior is left and dorsal is up in all figures. Square bracket indicates the fifth tracheal hemisegment (Tr5) and white arrowheads indicate the region where the posterior spiracle cells are laying. Scale bar: 25  $\mu$ m.

I. Development of Tr5. The six primary branches (dorsal branch, DB; dorsal trunk anterior, DTa; dorsal trunk posterior, DTp; visceral branch, VB; lateral trunk anterior, LTa; lateral trunk posterior/ganglionic branch, LTp/GB) are highlighted at stage 12. Secondary branches are highlighted at stage 15. At stage 16, single terminal branches (highlighted) begin to sprout from the end of each secondary branch (except the three fusion branches which are indicated by arrowheads at stage 15). In the late embryo and larva many more terminal branches form at these positions. The points of transition from secondary to terminal branches are approximate. (Solid lines, lumen of Tr5; dashed lines, adjacent tracheal hemisegments; arrow, Tr5-Tr6 dorsal trunk fusion point; TC, transverse connective; SB, spiracular branch) Arrowheads point to the region where the posterior spiracle cells are located. Adapted from Samakovlis et al., 1996a.

---

The tracheal placodes are specified in the plane of the epidermis, while the mature airways are a complex internal organ. *Trh* expression in the tracheal primordia at stage 10 triggers the morphogenetic movements that lead to the formation of the complex tracheal network. Each of the tracheal placodes initially consists of 40 epithelial cells. The cells undergo apical constriction and invagination to form small epithelial sacs, the tracheal pits (Figure 6A). The process is regulated by Rhomboid and EGFR signaling (Brodu and Casanova, 2006; Llimargas, 1999), possibly through the spatial and temporal coordination of the invagination activities of the cells (Nishimura et al., 2007). At this point, tracheal cells complete one final round of mitotic division to double their number (thus reaching approximately 80 cells per tracheal placode) (Kondo and Hayashi, 2013; Nishimura et al., 2007).

### **A.3.A.2. Tracheal branch morphogenesis – Formation of the tubular network**

After their internalization, many of the tracheal cells start to migrate and rearrange in a stereotypic pattern (reviewed in (Ghabrial et al., 2003). Tracheal migration is regulated by *breathless (btl)*, one of the two *Drosophila* Fibroblast Growth Factor (FGF) receptors (Klämbt et al., 1992) and its ligand Branchless (Bnl) (Sutherland et al., 1996). More specifically, one or two Btl-expressing tracheal cells start migrating towards nearby tissues expressing Bnl. FGF signaling in these cells (which are acting as leading cells) is sufficient to confer migratory capacity to more tracheal cells (trailing cells) (Lebreton and Casanova, 2014; Sutherland et al., 1996). Specific cells in all branches (or the cells of specific branches) are known to rely on additional mechanisms for their migration (Epidermal Growth Factor/ EGF signaling, integrin and Robo/Slit) (Gallio et al., 2004; Lundström et al., 2004).

Initially the migrating cells rearrange to form the *primary branches* of the system: the Dorsal and Lateral Trunk (DT and LT respectively), the Transverse Connectives (TC) and the Dorsal, Visceral, Ganglionic and Spiracular Branches) (DB, VB, GB and SB respectively) (Figure 6G and Samakovlis et al., 1996). Primary branches are lined by more than one tracheal cells. These cells together form a tubular epithelial structure with their apical surfaces on the luminal side of the tube and the basolateral sides towards the hemolymph and the internal body space (Figure 7A). The formation of the two main trunks of the system (the thicker DT and the finer LTs) (Figure 6E and F) requires the fusion of different metameric parts (anastomosis) (Caviglia and Luschnig, 2014; Chandran et al., 2014; Lee and Kolodziej, 2002; Samakovlis et al., 1996b). The primary branch cells are connected with intercellular junctions and (in the finer primary branches) with intercellular and autocellular junctions (Figure 7A).

---

Finer branches, the so called *secondary branches*, branch out from the primary ones (except from the DT). These tubes are usually formed by elongation and intercalation of adjacent tracheal cells (Figure 6G and Samakovlis et al., 1996). More specifically, the secondary branch cells, that are initially facing each other, undergo substantial cell shape changes and junctional remodeling (from intercellular to autocellular junctions) and they are repositioned in a single row around the lumen (Ribeiro et al., 2004; Uv et al., 2003 for example). They appear at the tip and in fewer cases at inner positions of the primary branches.

The finest branches of the trachea, the *terminal branches* are formed as cytoplasmic extensions of subsets of secondary branch cells (Figure 6G and Samakovlis et al., 1996). These cells develop elongated subcellular lumens that are continuous with the rest of the trachea lumen (Gervais and Casanova, 2010). The completion of the main events in branching morphogenesis takes almost 10 hours, while terminal branches formation continues and takes place during the larval stages where it is not stereotypic and genetically determined but it is regulated by the oxygen needs of the target tissues (Centanin et al., 2008; Centanin et al., 2010; Samakovlis et al., 1996a).

Tracheal tubes vary in their size and morphology. Their diameters range from the largest ones of 4-5micron to the finest ones of less than half micron (Figure intro3.2). As summarized below, cell migration, planar cell rearrangements, the formation and elaboration of specialized cell junctions and the growth of specialized cytoplasmic and membrane protrusions all contribute to branch morphogenesis.

By stage 14, the DT of the system has formed (completion of the fusion of all the tracheal metameres) (Figure 6D). The rest of the branches undergo further rearrangements, they elongate and acquire their final shape (Figure 6F).

During this period of tracheal development the size of the network has to be properly established. The regulation of the tracheal size is not based on the number, size or overall shape of the tracheal cells, but is rather linked to the apical surface organization and the branch identity (Beitel and Krasnow, 2000). Several genes have been shown to be involved in the establishment of the correct tracheal size, through different mechanisms (see following Paragraph). By stage 16 the complex tracheal network has formed.

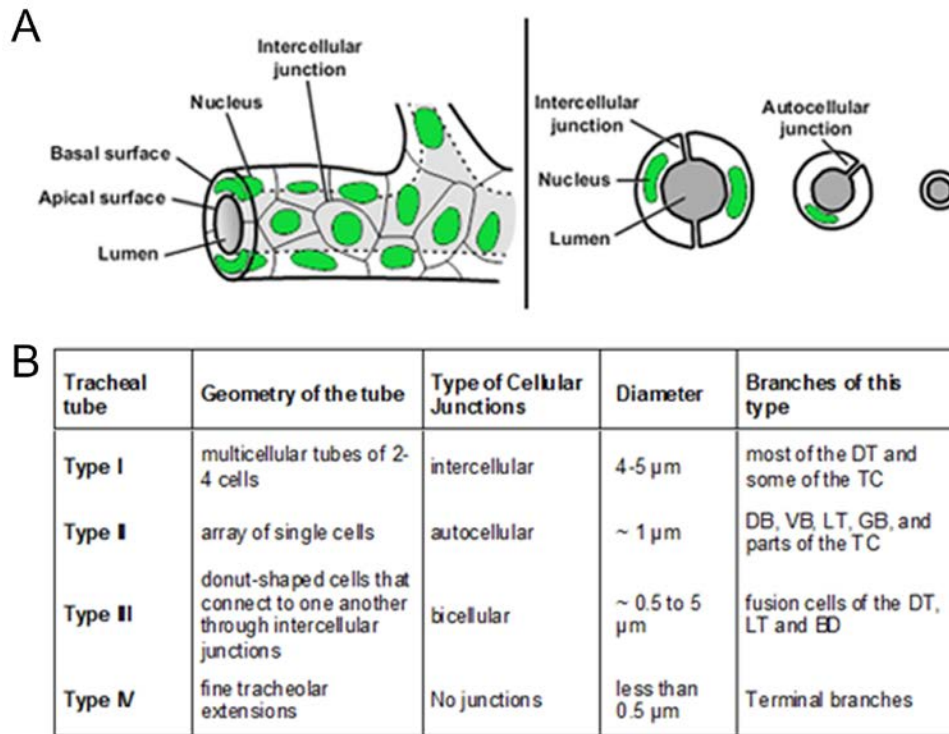


Figure 7: Features of the tracheal tubes

A. Schematic representation of a main tracheal tube and a branch point (left panel) and schematic representation of the different types of tracheal tubes (right panel): multicellular primary branch with two intercellular junctions, a unicellular secondary branch with an autocellular junction and a subcellular terminal branch with no junctions. Adapted from Samakovlis et al., 1996. B. Features of different types of tracheal tubes.

### A.3.A.3. Chitin deposition and tracheal tube elongation

Chitin is a fibrous polysaccharide substance, secreted in the trachea lumen throughout the DT growth. Its accumulation and efficient organization is known to be involved in the coordination and stabilization of tube elongation and, later, luminal expansion (see next Paragraph A.3.A.4) (Araújo et al., 2005; Devine et al., 2005; Tonning et al., 2005; Tsarouhas et al., 2007). Luminal chitin depends on specialized molecules that ensure the synthesis (chitin synthase Krotzkopf verkehrt (Kkv) (Moussian, 2010; Moussian et al., 2005a)) and the proper modification of chitin (mediated by Knickkopf (Knk) (Moussian et al., 2006), Retroactive (Rtv) (Moussian et al., 2005b; Moussian et al., 2006), Vermiform (Verm) (Luschnig et al., 2006; Wang et al., 2006), Serpentine (Serp) (Luschnig et al., 2006; Wang et al., 2006), Convoluted (conv) (Swanson et al., 2009) and possibly other molecules). Mutants for the aforementioned genes display irregular tracheal size (Luschnig et al., 2006; Moussian, 2010; Moussian et al., 2005a; Moussian et al., 2005b; Moussian et al., 2006;

---

Swanson et al., 2009; Wu et al., 2007). Interestingly, while genes encoding proteins involved in the chitin synthesis and secretion regulate the uniform expansion of the lumen (luminal width and length), genes encoding chitin modification proteins specifically control lumen length (Xu et al., 2012).

Important molecules affecting the chitin-dependent tracheal size regulation include Septate Junction (SJ) components. The SJs are intercellular junctions that interconnect the epithelial cells and ensure the formation of a diffusion barrier (see Paragraph A.3.B). Mutants for several SJ components affect tracheal tube length and diameter (Beitel and Krasnow, 2000; Llimargas et al., 2004; Paul et al., 2003; Wu et al., 2004). Previous studies have shown that SJs regulate tracheal size through multiple mechanisms, with the most prominent being the regulation of the secretion of Chitin modifying molecules (Verm and Serp) (Luschnig et al., 2006; Wang et al., 2006). Additionally, the SJ components Discs Large (Dlg), Yurt (Yrt) and Scribble (Scrib) regulate the tracheal size in a chitin-independent manner (Laprise et al., 2010). It has been shown that the FERM protein Yurt controls tracheal lumen length by antagonizing the apical determinant protein, Crumbs (Laprise et al., 2010). Other molecules like Serrano, which is involved in planar cell polarity (Chung et al., 2009), and Convuluted/dALS (Swanson et al., 2009) are involved in the trachea size regulation, in a chitin independent manner.

Finally, recent studies revealed that the non-receptor tyrosine kinase Src42A participates in the regulation of tracheal tube size. Src42 mediates the anisotropic growth of the apical surface of the tracheal cells (Forster and Luschnig, 2012; Nelson et al., 2012). *Src42A* mutants develop shortened tracheal tubes, while overexpression of the gene leads to tube elongation (Forster and Luschnig, 2012; Nelson et al., 2012).

#### **A.3.A.4. Tracheal maturation**

The crawling larva absolutely requires oxygen, delivered through the airways, for its survival. After the first developmental steps that establish the tracheal network with all its branches, the trachea has to undergo further maturation events in order to become functional by the time the embryo hatches. Failure of any of such events eventually leads to failure to fill the tracheal system with air, and therefore to a major decrease in oxygenation of internal organs. In particular, the final steps of the trachea development involve a series of three sequential developmental transitions: i) tube enlargement driven by a secretion burst that deposits proteins inside the trachea lumen, ii) the rapid clearance of solutes and macromolecules from the tracheal lumen and iii) clearance of the liquid filling the embryonic tracheal lumen which will enable the air filling of the airways. Live

---

imaging and mutant analysis by Tsarouhas et al., 2007, has shed light into the cellular and molecular mechanisms that underlie the regulation of these three steps.

#### ***- Secretory burst and tracheal size regulation***

The secretory burst is initiated around stage 13 and facilitates the deposition of large amounts of solid material, including chitin, inside the trachea lumen (Figure 8). This step requires the activity of Sara1, Sec13, Sec23 and Sec24, COPI and COPII, components of the membrane trafficking and ER-Golgi secretory machine (Förster et al., 2010; Jayaram et al., 2008; Tsarouhas et al., 2007). It also depends on Rho-Diaphanous-MyosinV-dependent transport (Massarwa et al., 2009). Apical secretion is tightly linked to the regulation of the tracheal tube size, both through the secretion of chitin and chitin modifying molecules, and by contributing to the apical membrane growth.

#### ***- Luminal clearance***

At the end of embryogenesis, the material inside the trachea lumen is removed through an endocytic pulse (Tsarouhas et al., 2007). The small GTPases Rab5, Dynamin and Clathrin have been shown to affect the endocytic pulse and luminal protein clearance (Tsarouhas et al., 2007). It is unclear whether receptor-dependent endocytosis or an unspecific uptake of solutes from the lumen is driving clearance of luminal macromolecules.

#### ***- Liquid clearance***

Finally, just before embryo hatching, a liquid clearance step ensures the air-filling of the tracheal tubes (Tsarouhas et al., 2007). Very little is known about this process. Distinct cellular mechanisms (e.g. pinocytosis) are likely to be involved.



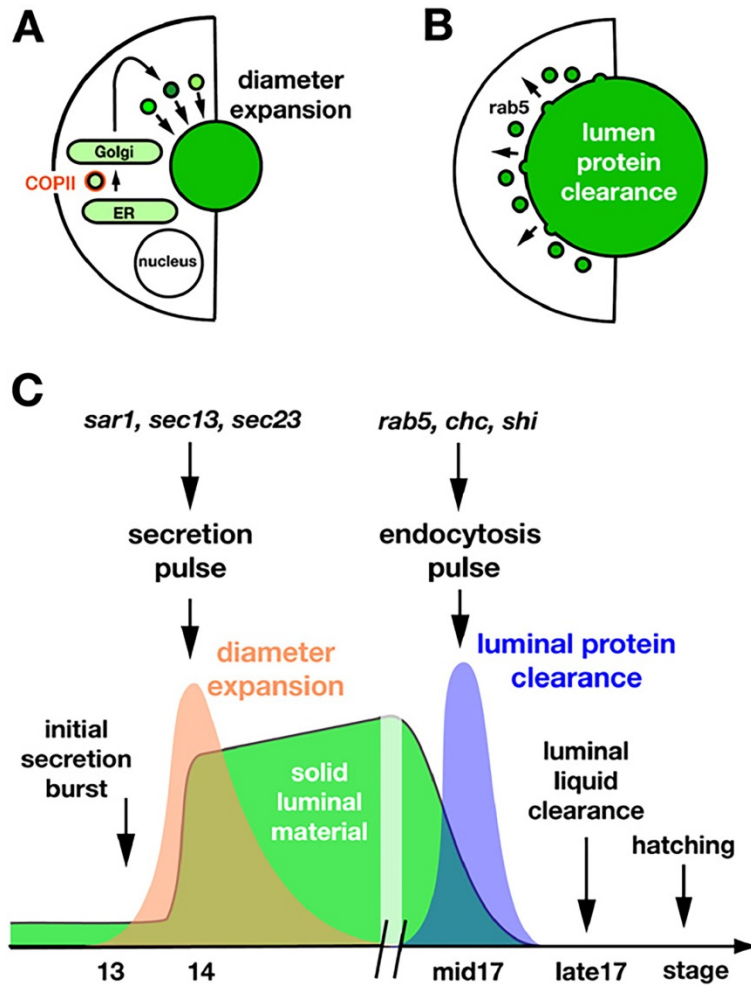


Figure 8: Tracheal maturation involves distinct pulses of secretion and endocytosis.

A-B. Schematic representation of a cross section of the tracheal system. A) In stage 14, a pulse of luminal secretion that mediates diameter expansion. During this process, the ER, Golgi and post-Golgi vesicles carry luminal proteins (green) into the lumen. COPII vesicles are important for this step. B) Subsequently, around mid-stage 17, Rab-5-dependent endocytosis ensures the removal of solid contents (green) from the tracheal lumen.

C. Schematic model of airway maturation based on live imaging and mutant analysis. COPII-dependent secretion pulse is essential for luminal matrix assembly and tube diameter expansion. At early stage 17, the tracheal epithelium activates an endocytic pulse that requires Rab5, Clathrin, and Dynamin, to internalize and remove solid contents from the lumen. Solid luminal material is indicated in green, the secretion pulse in orange, the endocytic pulse in blue. Adapted from Tsarouhas et al., 2007.



### A.3.B. Trachea as a model system to study epithelial integrity

In *Drosophila* the tracheal cells arrange next to each other to form the tubular structures (Figure 7). They align their apical domain on the luminal side of the tube, the lateral domain to contact the neighboring cells of the epithelial layer, and the basal domain to face the neighboring tissues. Distinct junctional complexes between the cells ensure tissue polarity and integrity (Figure 9 and reviewed in Tepass et al., 2001).

Four types of junctions have been characterized in *Drosophila* epithelia (Figure 9): the Adherens, the Septate, the Gap and the Hemiadherens Junctions (also referred to as Focal Contacts) (Tepass et al., 2001). In the current study we will focus on the Septate Junctions (SJs), since they are the ones responsible for the establishment of the epithelial permeability barrier.

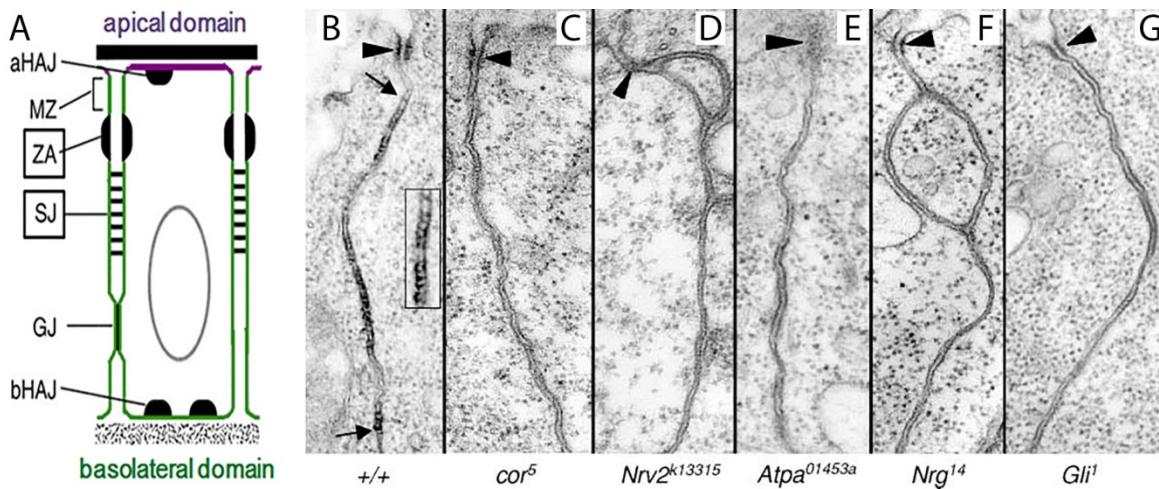


Figure 9: Polarized epithelial cells display different types of cellular junctions

A. Schematic representation of an epithelial cell of *Drosophila melanogaster*. The cell membrane is divided in the apical and the basolateral region. The cellular junctions are indicated to the left: aHAJ, apical hemi adherens junction; bHAJ, basal HAJ; DE-cad, DE-cadherin; ECM, extracellular matrix; GJ, gap junction; MZ, marginal zone; SJ, septate junction; ZA, zonula adherens. Adapted from Tepass et al., 2001.

B. Wild-type embryos have distinct junctional structures in the apical-lateral domain of polarized epithelial cells, including the Adherens Junctions (AJ) (arrowhead in B) and the SJ (arrow in B). The inset in B demonstrates the alignment of septae between uniformly spaced membranes of adjacent cells (inset corresponds to region basal to the upper arrow).

C-G. In mutants for the SJ components Coracle (C), Nervana (D), Na/K ATPalpha (E), Neuroglian (F) and Gliotactin (G) the AJs (arrowheads) remain intact, however the SJs are disrupted (the transverse septae, arrow in B) are fewer or completely missing. Adapted from Genova and Fehon, 2003.

---

The SJs are localized at the apical region of the basolateral membrane, basally to the Adherens Junctions (AJs) (referred to as ZA in Figure 9). They appear midway through to embryogenesis after cellularization is completed, epithelial polarity has been established, and the Zonula Adherens (AZ) has formed (Tepass et al., 2001). The SJ molecules are initially (stage 12) highly mobile on the lateral membrane, but in stage 13 they form a stable core complex (that consists of Na/K ATPase subunit (ATP $\alpha$ ), Coracle (Cora), Megatrachea (Mega), Neuroglian (Nrg) , Nervana 2 (Nrv2) , Neurexin IV (Nrx IV), Sinuous (Sinu) and Varicose (Vari)) (see also below) (Figure 10) (Oshima and Fehon, 2011). Loss of any of these SJ components affects the mobility and/or stability of the complex. Some other proteins (e.g. Lys-6 family proteins) do not localize at the SJ region but affect SJs assembly and/or maintenance (Nilton et al., 2010).

Two different kinds of SJs have been described in *Drosophila*: the smooth SJs and the pleated SJs. Among them, the pleated SJs are detected in the ectoderm-derived tissues (such as epidermis, tracheal cells, salivary glands) and the glial cells that form the blood brain barrier (Stork et al., 2008), while smooth SJs have only been detected in the midgut (Tepass et al., 2001). Observation of the pleated SJ at the electron microscope revealed parallel rows of electron dense material (septa), between and perpendicular to the membranes of the epithelial cells, leading to a characteristic ladder like morphology of the SJs (Tepass et al., 2001) (Figure 9). The distance between the cellular membranes is about 15nm.

SJ formation is based on several protein molecules that localise at the specific region of the basolateral membrane of the epithelial cells and interact with each other, referred to as SJ components. The molecular composition of the SJs has been widely analysed in the past. One of the most extensively studied components of the SJs is the transmembrane protein Neurexin IV (Nrx IV) (Baumgartner et al., 1996). Nrx IV is a core SJs molecule: it forms heterophilic interactions with the transmembrane molecules DContactin (DCont) (*in cis*) (Faivre-Sarrailh et al., 2004) and Neuroglian (Nrg) (*in trans*) (Genova and Fehon, 2003) forming a tripartite complex. This complex is crucial for the integrity of the epithelial permeability barrier. Moreover, Nrx IV interacts with the cytoplasmic proteins Coracle (Cora) and Varicose (Vari). The localization of the Four-point-one, Ezrin, Radixin, Moesin (FERM) family protein Cora at the SJs is dependent on Nrx IV, since in Nrx IV mutants, Cora is cytoplasmic (Fehon et al., 1994; Lamb et al., 1998; Ward et al., 1998). Varicose is a Membrane-Associated Guanylate Kinase homologues (MAGUKs) family protein important for the formation but not the maintenance of the SJs (Bachmann et al., 2008; Wu et al., 2007). It is likely that Cora and Vari act as scaffolding molecules that interconnect Nrx IV/Cont/ Nrg complexes (Laval et al., 2008). Recruitment of three more proteins: the Claudins Megatrachea (Mega) (Behr et

al., 2003) and Sinous (Sinus) (Wu et al., 2004) and the alpha subunit of the Na/K ATPase (Paul et al., 2007; Paul et al., 2003) lead to the core complex formation (Oshima and Fehon, 2011).

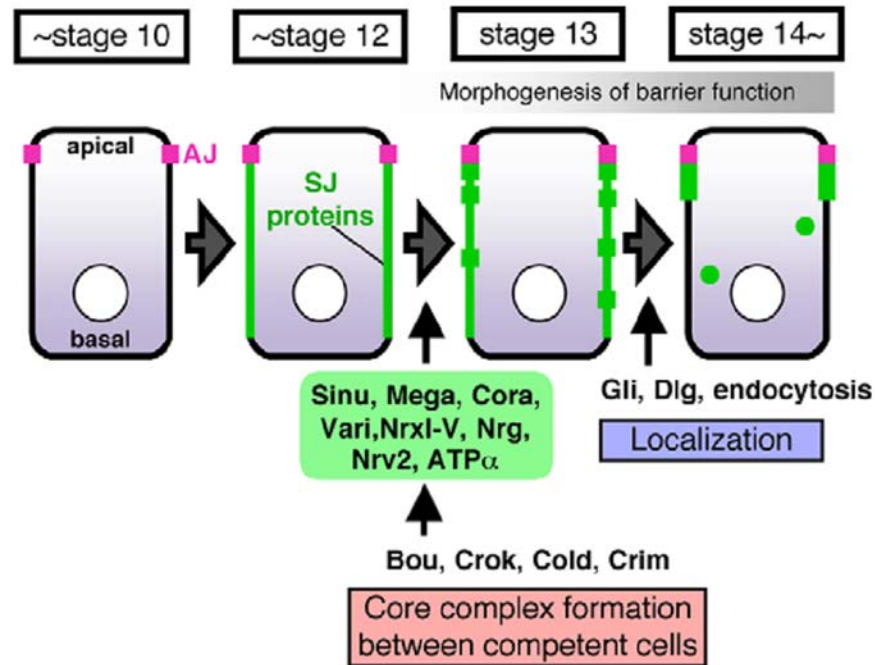


Figure 10: SJ maturation during embryogenesis

Schematic model of SJ maturation during embryogenesis. SJ proteins are initially highly mobile on the lateral membrane (stage 12), but in stage 13, Sinu, Mega, Cora, Vari, Nrxi-V, Nrg, Nrv2 and ATP $\alpha$  begin to form a stable SJ core complex just basal to the AJ. Four Ly6-like proteins (Bou, Crok, Cold and Crim) are necessary for this process. In addition, proper localization of the core complex requires Dlg, Gli and endocytosis. Adapted from Oshima and Fehon 2011.

Scribble (Scrib) and Discs large (Dlg) are two more proteins known to interact with Nrxi IV (Woods et al., 1996). These proteins together with Lethal giant larvae (Lgl), form the Lgl/Dlg/Scrib complex which has an early role in the establishment of apicobasal polarity (Tepass et al., 2001). Other SJs components identified, like Gliotactin (Gli) (Padash-Barmchi et al., 2010; Schulte et al., 2003) and Lachesin (Lac) (Llimargas et al., 2004; Strigini et al., 2006) are also crucial for the SJ formation and the permeability barrier establishment. Additional proteins, (e.g. the lipid phosphate phosphatases (LPPs) Wunen (Wun) and Wunen2 (Wun2) (Ile et al., 2012), do not localize at the SJ region, but affect SJ integrity and the trans-epithelial barrier.

---

In summary, mutations for SJ components lead to the mislocalization of other SJs components, disruption of the characteristic septa (Figure 9) and impairment of the epithelial permeability barrier (Behr et al., 2003; Faivre-Sarrailh et al., 2004; Genova and Fehon, 2003; Llimargas et al., 2004; Paul et al., 2003; Schulte et al., 2003; Wu et al., 2004; Wu et al., 2007). Additionally, they affect the tracheal size (Llimargas et al., 2004; Paul et al., 2003; Wu et al., 2004; Wu and Beitel, 2004) and regulate the apical secretion of chitin deacetylases (Verm and Serp, see also previous Paragraph).

Insect SJs display functional similarity to the vertebrate Tight Junctions (TJs). TJs also form a diffusion barrier that prevents water and solute exchange across epithelia (Tepass et al., 2001; Tsukita et al., 2001), but localize apical to the AJs. Furthermore, the two types of junctions display morphological and molecular differences (Anderson, 2001; Tepass et al., 2001). Interestingly though, they both include Claudin molecules (in *Drosophila* Sinu and Mega) (Behr et al., 2003; Wu et al., 2004), suggesting they might have a common evolutionary origin.

---

## A.4. Btk29A in the respiratory system

---

### A.4.A. Genetic screen and *Btk29A*

In an attempt to identify new molecules involved in the development of the respiratory system of *Drosophila*, our lab had selected mutant alleles for a group of candidate genes and screened: a) for the impairment of the epithelial integrity and function of the trachea system and, in a second round, b) for abnormalities in the morphology of the trachea and the posterior spiracles.

A well-established method for testing the permeability barrier of the tracheal epithelium and the tracheal integrity, known as dye penetration assay (Lamb et al., 1998) (Figure 11) was used for the first part of the analysis.. This method is based on the injection of stage 16 homozygous mutant embryos with fluorescently tagged dextran (rhodamine-dextran 10kD) (see Materials and Methods). The dye fills the hemocoel, so it can diffuse freely and quickly in the hemolymph in which all organs are bathed. In wild type embryos, with functional permeability barrier, the dye will be excluded from the trachea lumen, while in the case of mutants affecting the trachea permeability, the lumen will be filled with the dye. The injected embryos were observed under the microscope for permeability barrier integrity defects.

For the second part of the analysis, homozygous mutant embryos for the selected mutant alleles were collected and observed under the microscope for morphological defects of the trachea and the posterior spiracles.

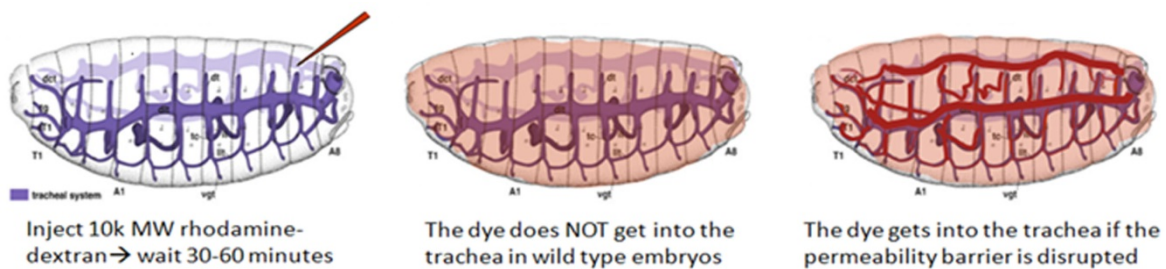


Figure 11: Dye penetration assay

Stage 16 *Drosophila* embryos are selected and aligned on a microscope slide. Fluorescently labelled dextran is injected in the hemocoel of the embryos. The embryos are observed under the microscope 30-60min after the injection. The dye penetrates the trachea lumen only in the case that the permeability barrier of the trachea epithelium is impaired.

---

One of the mutations identified in this screen was *stmA*<sup>18.2</sup> (*rbo*<sup>3</sup>). This stock carries a point mutation in the *stambha A* (*rolling-blackout*) locus (Kumar et al., 2001). *Stambha A* is an integral plasma membrane lipase known to be involved in phototransduction and synaptic neurotransmission (Huang et al., 2004; Huang et al., 2006). *stmA*<sup>18.2</sup> homozygous mutant embryos display defective permeability barrier and lack of tracheal gas-filling at the end of the embryogenesis. Additionally, they have short and abnormally formed posterior spiracles (Figure 12). They die before the end of embryogenesis.

Study of different alleles of the gene did not confirm the involvement of *stambha A* in the respiratory system development: homozygous mutants for *stmA*<sup>rev499</sup> (*rbo*<sup>2</sup>) (Faulkner et al., 1998) which is a complete null allele and *stmA*<sup>rev499</sup>/*stmA*<sup>18.2</sup> transheterozygotes, didn't show the permeability and air filling defects and developed intact posterior spiracles. This together with the fact that the *stmA*<sup>18.2</sup> mutant stock was developed through gamma ray mutagenesis (Kumar et al., 2001) led us to the hypothesis that a second hit mutation on the second chromosome of the stock was responsible for the respiratory system phenotypes.

In order to identify and map the mutation, I and other team members crossed *stmA*<sup>18.2</sup> to the stocks of the deficiency kit for the second chromosome from the Bloomington *Drosophila* Stock Center (BDSC). We primarily looked for non-complementation of the lethal phenotype and subsequently for non-complementation of the characteristic phenotypes in the trachea system and the posterior spiracles.

Lethality was not complemented by eight stocks of the kit (BL179, BL1888, BL2583, BL3079, BL3138, BL4960, BL6999 and BL8836), while only 2 of them (BL179 and BL8836), uncovering the 29A region of the second chromosome, failed to complement the airway phenotypes.

A smaller deficiency (*Df(2L)BSC235* (BL9710)) and mutant alleles for 4 genes mapped in and around the 29A chromosomal region (see Materials and Methods) were acquired from Bloomington Stock Center and tested for non-complementation with the *stmA*<sup>18.2</sup> stock. *Df(2L)BSC235* and *Btk29A*<sup>k00206</sup> (BL10469) stocks were the only ones that did not complement, suggesting that the second hit mutation of *stmA*<sup>18.2</sup> stock is on the *Btk29A* locus.

The non-complementation of the lethality with the other six stocks of the deficiency kit mentioned above suggested the presence of one or more additional lethal mutations in *stmA*<sup>18.2</sup> stock. According to Roegiers et al., 2009, several of the second chromosome stocks from the Bloomington Stock Center carry mutations in the *lgl* locus. It is thus likely that the mutations are mapped in that locus, which we indeed confirmed.

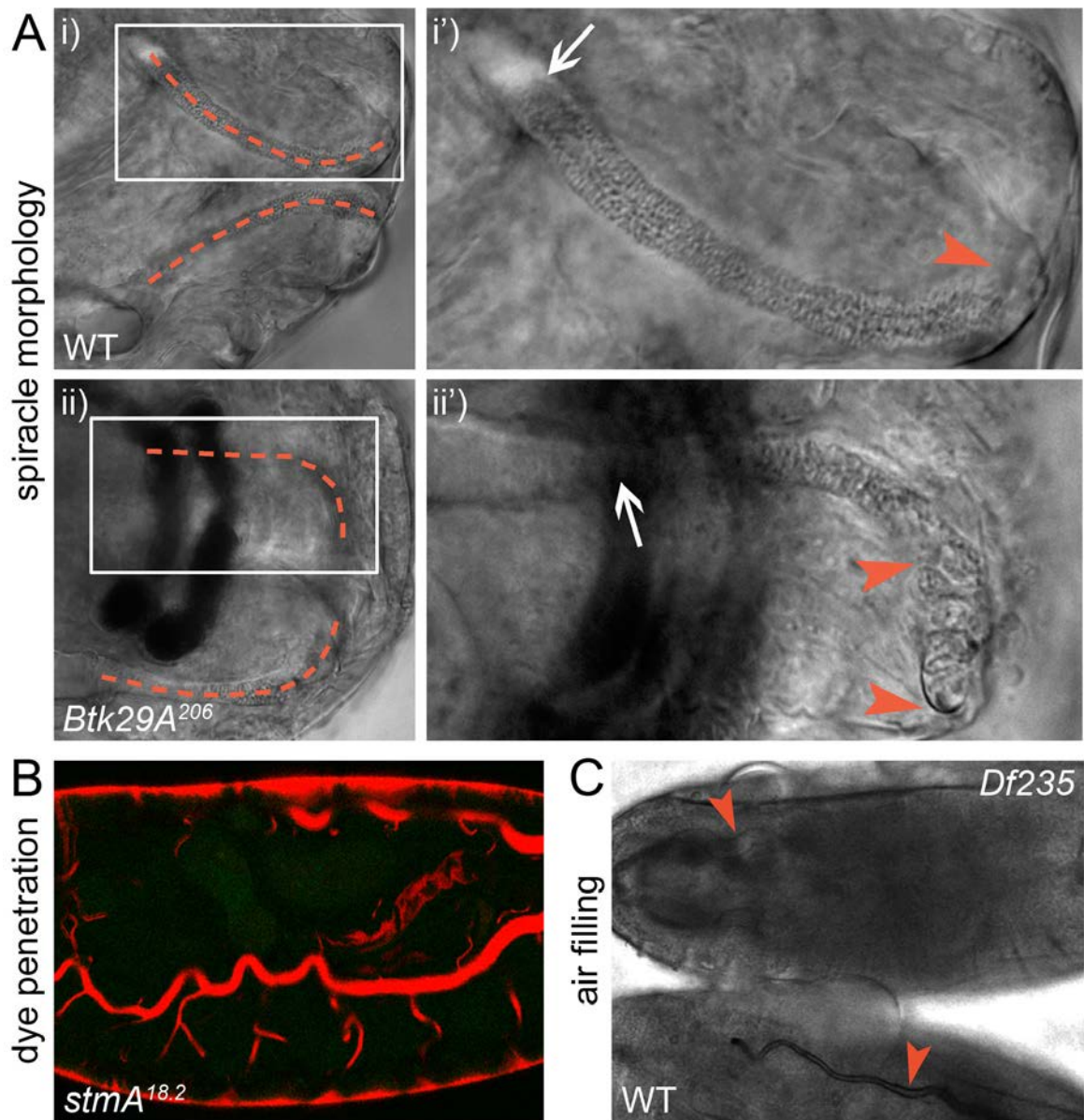


---

#### A.4.B. Btk29A in the respiratory system

Different *Btk29A* alleles were obtained and tested for the respiratory system phenotypes: *Btk29A*<sup>EP2167</sup> (BL17235) from Bloomington Stock Center and *Btk29A*<sup>k05610</sup> (DGRC102398) from *Drosophila* Genetic Resource Center. These alleles carry P-element insertions in intronic regions of *Btk29A* locus (Figure 13). Homozygous mutant embryos for the above alleles (will be referred to as *Btk29A*<sup>206</sup>, *Btk29A*<sup>EP</sup> and *Btk29A*<sup>5610</sup>) and their trans-heterozygous combinations show trachea and posterior spiracle phenotypes similar to *stmA*<sup>18.2</sup> stock. More specifically, all the alleles have a dye penetration phenotype and they cannot complete trachea air filling at the end of the trachea maturation. We therefore decided to continue the characterization of the novel respiratory system phenotypes with these alleles and not the initial *stmA*<sup>18.2</sup>.

Additionally, we examined the respiratory system of homozygous mutant embryos for *Df(2L)BSC235* (BL9710) stock, carrying a small chromosomal deletion (28F1-29A3), which removes 23 known and predicted genes around *Btk29A* locus. Homozygous mutant embryos for this deficiency (will be referred to as *Df235*) have permeability barrier defects and they do not complete the gas-filling of the trachea in the end of the embryogenesis. They also show a posterior spiracle phenotype undistinguishable from the *Btk29A*<sup>206</sup> homozygous mutants (Figure 12).



**Figure 12: Defective respiratory system development in *Btk29A* mutants**

A. Morphology of the posterior spiracles in stage 16 WT and *Btk29A*<sup>206</sup> mutant embryos. The overall shape of the spiracles is impaired in mutant embryos (i and ii): the filzkörper appears shorter (i' and ii') and the distal-most part (area between arrowheads in ii') has an irregular arrangement. Arrows point to the region where trachea and spiracle meet. Similar phenotype is observed in *Btk29A*<sup>5610</sup>, *Btk29A*<sup>EP</sup> and *Df235* homozygous mutant embryos (data not shown).

B. Impaired epithelial permeability barrier of the trachea system in *stmA*<sup>18.2</sup> homozygous mutant embryos uncovered by dye penetration assay. The injected 10kDa Rhodamine-dextran is accumulating in the trachea lumen of stage 16 *stmA*<sup>18.2</sup> homozygous mutants. The same phenotype is observed in *Btk29A*<sup>206</sup>, *Btk29A*<sup>5610</sup>, *Btk29A*<sup>EP</sup> and *Df235* homozygous mutants. (Rhodamine-dextran in red)

C. Trachea gas-filling in WT and *Df235* homozygous mutant embryos. *Df235* as well as all *Btk29A* alleles (data not shown) fail to fill their trachea with air in the end of embryogenesis. Arrowheads point to the trachea of the embryos.



---

## A.5. Btk29A

---

Non-receptor tyrosine kinases are cytoplasmic molecules responsible for the phosphorylation of substrate molecules in conserved tyrosine residues. They are involved in many cellular processes: cell growth, differentiation, adhesion, migration (Superti-Furga and Courtneidge, 1995). Non receptor tyrosine kinases are divided in distinct subclasses, among which the well-studied Src family (see Inglay, 2008; Parson and Parson, 2004 for recent reviews) and the related Tec family.

The gene at the centre of the present work, *Btk29A* (also known as Tec29A, Dsrc29A, Dsrc28C and Fickle), is the only *Drosophila* member of the Tec family of tyrosine kinases. Tec kinases contain the Src homology domains 2 and 3 (SH2 and SH3) and a kinase domain (all of which are also present in Src kinases). Additionally they display a Plekstrin homology (PH) domain and a characteristic Tec homology (TH) at the amino-terminus. They play a role in multiple processes including proliferation, cell survival, differentiation and cytoskeletal regulation (Smith et al., 2001). Five Tec kinases have been characterised in vertebrates: Tec, Btk, Itk/Emt/Tsk, Bmx and Txk/Rlk. These molecules are shown to be abundantly expressed in the hematopoietic tissues where they function in growth and differentiation of the blood cells (Mano, 1999).

Due to the high similarity of the SH2 and SH3 domains of Btk29A to those of Src proteins and the presence of a characteristic kinase domain, the protein was initially identified as a member of the Src family of non-receptor tyrosine kinases (Gregory et al., 1987; Wadsworth et al., 1985). Subsequent identification of the complete cDNAs for its long isoforms (see below), featuring additionally a PH domain and a Tec domain, clearly defined the protein as a Tec family member.

*Btk29A* is mapped on the left arm of the second chromosome of *Drosophila* (2L:8258755..8301079) (cytological region: 29A1-29A3). It consists of 24 exons (Table 1) and 22 introns. Alternative splicing leads to different transcripts of the gene (8 annotated in Flybase: <http://flybase.org/reports/FBgn0003502.html>, Figure 13 and Table 1) and subsequently to the expression of differential protein isoforms: the Short or Type 1 and Long or Type 2 isoform. Both isoforms contain the SH3, SH2 and kinase domains, but differ in the presence of the PH domain, which is only present in the Type 2 protein. Additionally, they have a TH domain (partial in Short and full length in Long Isoform) (Figure 13).

The structural differences of the two isoforms lead to their differential assignment in different tyrosine kinases families: the Short isoform to the Src family and the Long isoform to the Tec family (Baba et al., 1999) .

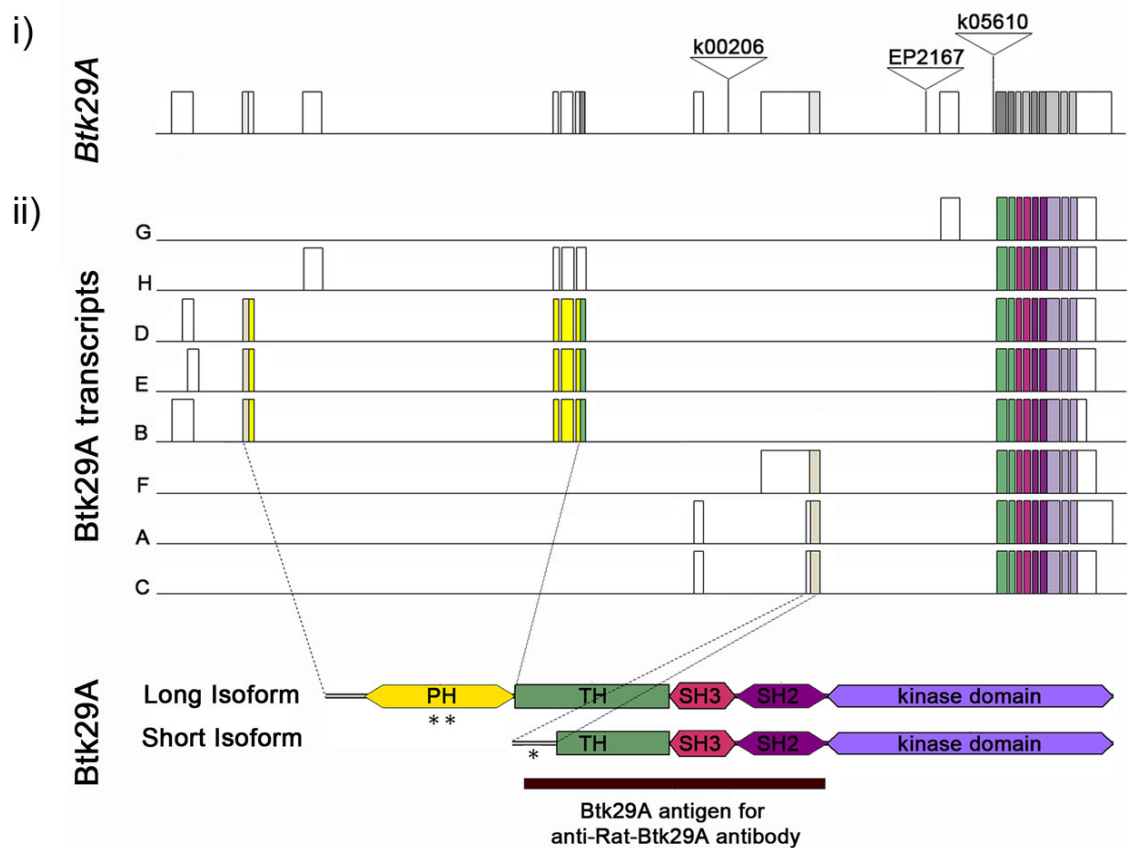


Figure 13: Schematic representation of the gene locus of *Btk29A*, the eight different transcripts and two protein isoforms.

i) *Btk29A* gene (<http://flybase.org/reports/FBgn0003502.html>) is located on the second chromosome (2L: 8258755..8301079). It consists of 23 exons and 22 introns. The mutant stocks used for the current study derive from insertional mutagenesis with P-element constructs in intronic regions of *Btk29A*: K00206 (2L: 8277179..8277186), EP2167 (2L:8266138) and K05610 (2L:8262681..8271935).

ii) 8 transcripts and 8 polypeptides (4 of them unique) are annotated for *Btk29A*. Translation of transcripts B, D and E will give rise to the Long Isoform protein, while transcripts F, A and C will encode for the Short Isoform. The two isoforms differ in the N-terminal region: the Long Isoform has a PH domain that is not present in the Short. Transcript G encodes for a predicted smaller polypeptide (565 amino acids) that lacks 38 amino acids at the N-terminus compared to the short isoform. Transcript H encodes for a predicted 464 amino acid long protein that lacks most of the TH domain. The protein domains and the exons corresponding to them are marked with different colors. The cDNA sequences that correspond to the protein regions marked with asterisks were used for the development of the RNA probes: \* for the Short Transcript Probe and \*\* for the Long Transcript Probe. The whole cDNA for transcript B was used for the All Transcript probe development (see Materials and Methods). The black line outlines the protein fragment used for the development of the rat polyclonal antibody.

Table 1: *Btk29A* transcripts

TRANSCRIPTS	EXONS																								Transcript Length	Protein length	
	1	2	3	4	5	6	7	8	9	10	11	12	13	14	15	16	17	18	19	20	21	22	23	24			
<b>A</b>	√			√	√	√	√	√	√	√		√			√											4026	603
<b>B</b>			√	√	√	√	√	√	√	√						√	√	√		√		√				3420	786
<b>C</b>		√		√	√	√	√	√	√	√			√		√											3279	603
<b>D</b>		√		√	√	√	√	√	√	√						√	√	√		√				√		3674	786
<b>E</b>		√		√	√	√	√	√	√	√						√	√	√		√	√		√			4785	786
<b>F</b>		√		√	√	√	√	√	√	√				√												4992	603
<b>G</b>		√		√	√	√	√	√	√	√	√	√														3302	565
<b>H</b>		√		√	√	√	√	√	√	√						√	√	√	√							3826	464

Color coding used in the table corresponds to the one used in Figure 13 and refers to the different protein domains. Non coding regions of the transcripts are marked in white. Grey boxes indicate the absence of the exon. The transcript length (nucleotides) and protein length (amino acids) are indicated (as predicted in Flybase).

---

### A.5.A. *Btk29A* expression pattern

*Btk29A* expression has been assessed several times in the past, both at the mRNA and protein level, giving sometimes discordant results (Gregory et al., 1987; Katzen et al., 1990; Vincent et al., 1989). More definitive descriptions of the gene structure, transcripts (predicted and experimentally confirmed), protein products and their expression patterns have accumulated recently (Chandrasekaran and Beckendorf, 2005; Hamada-Kawaguchi et al., 2014; this work).

*Btk29A* is expressed throughout the life of *Drosophila*, from early embryogenesis, till the adult stage. The embryonic expression of the gene is detected soon after the fertilization of the embryo, in a uniformly distributed pattern (stages 1-4), that corresponds to maternally supplied gene transcripts. Gradually, while the cellular blastoderm is forming, *Btk29A* starts being zygotically expressed in the newly formed cells (stage 5). The expression persists mostly in the dorsal region of the embryo during gastrulation (stage 6-7), and after stage 8 it is observed in a distinctive and reproducible stripy pattern. In the rest of the embryogenesis, transient *Btk29A* expression is detected in many of the developing tissues: salivary glands, gut epithelium, tracheal epithelium, posterior spiracles, dorsal vessel etc (Katzen et al., 1990; Wadsworth et al., 1990). The cells of the central nervous system express *Btk29A* more constantly, from embryogenesis (stage 12) till the adult fly (in low levels) (Katzen et al., 1990). I confirmed these observations in the embryo and provided a more detailed description of *Btk29A* expression in the respiratory system (see Paragraph C.1).

During larval life, *Btk29A* expression is detected in several tissues: the developing imaginal discs, the gonads (and especially the ovaries in the females), the cells of the lymph glands and the dorsal vessel and discrete regions of the central nervous system. The expression persists in most of these tissues during pupal and adult stages. In the adults, the ovarian expression is prominent; blood cells also express *Btk29A* at high levels, while in the central nervous system expression is low (Katzen et al., 1990).

The early studies dealing with the expression of the *Btk29A* protein had identified two main protein isoforms: p66 and p55 (with molecular weight of 66 and 55kDa respectively). The two protein isoforms were described to differ in 125 amino acids in the amino-terminal region, present only in the p66. Both proteins have an SH2, SH3 and a kinase domain, they are characterized by basic pI and although they retain a characteristic poly-glycine rich domain near the amino-terminus (Gregory et al., 1987; Vincent et al., 1989), they lack the usual amino-terminal myristylation signal observed in src kinases (Theroux and Wadsworth, 1992).

Comparative analysis of the expression of the two proteins isoforms revealed that they display differential subcellular distribution. More specifically, p66 protein localises at the cell membrane,

while p55 is cytoplasmic (Gregory et al., 1987). Both isoforms are expressed during embryogenesis: p66 in earlier stages (4-12 hours of embryonic development) and p55 from the middle till the end of embryogenesis (8-20hours). Among the two, p55 is expressed in the nervous system, tracheal cells, dorsal vessel, etc. (Gregory et al., 1987; Wadsworth et al., 1990), while p66 is expressed in the cellular blastoderm and salivary glands (Wadsworth et al., 1990).

Functional *in vitro* analysis revealed that although both proteins display a kinase domain, only p66 is able to phosphorylate conserved tyrosine residues in the substrate molecules tested. This could suggest that the 125 amino acids missing from p55 are necessary for the kinase activity of the protein. Another possibility is that the kinase activity of p55 is enabled only in certain cell types (central nervous system cells) and could not be reproduced with the *in vitro* assay used (Theroux and Wadsworth, 1992).

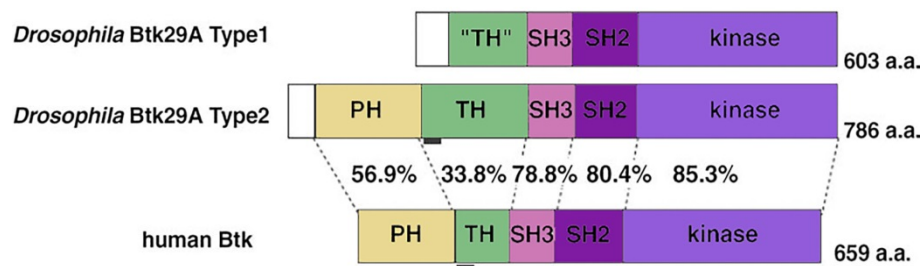


Figure 14: Structural comparison of *Drosophila* and human Btk orthologues

Two types of *Drosophila* Btk29A are compared with human Btk. The Type 2 isoform is closely related to the human Btk while Type 1 lacks the PH and displays a slightly different TH domain. Overall, the percent similarity between the *Drosophila* type 2 protein and its mammalian counterpart is 67.7%. Comparison by domain verifies the high conservation: 56.9% (PH), 33.8% (TH), 78.8% (SH3), 80.4% (SH2), and 85.3% (kinase). The low value for the TH domain is due to the polyglycine stretch present in the *Drosophila* sequence (which is not present in the mammalian TH) and increases to 76.9% if only the Btk motif in the TH domain is considered for comparison (Baba et al., 1999). Scheme adapted from Hamada et al., 2005 and color coding similar to Figure 13.

---

A third, 95kDa Btk29A form (p95) has also been described (Vincent et al., 1989). Although this protein was identified in expression analysis performed in the early *Btk29A* papers (western blot analysis from embryonic (Vincent et al., 1989) and ovarian protein extracts (Guarnieri et al., 1998) a long time passed before its role was unveiled. It was only in 1999, when Baba et al., isolated the genetic variant *fickle<sup>P</sup>* (*fic<sup>P</sup>*) in a screen for mutations affecting mating behaviour, that this isoform was characterised. *fickle<sup>P</sup>* is a P-element induced intronic mutation located in the *Btk29A* locus. Thorough analysis of the genomic region surrounding the insertion led to the identification of two isoform of *Btk29A*: i) one 603amino acids long that displayed high similarity (but is slightly smaller) to the previously described Btk29A p66 isoform (Gregory et al., 1987) and ii) a second isoform of higher molecular weight (Baba et al., 1999). Both isoforms, referred to as Type 1 (Short) and Type 2 (Long) proteins are expressed in the central nervous system and imaginal discs (Baba et al., 1999). Analysis of the expression of the two isoforms in the embryo revealed that Type 1 isoform is expressed in the epidermis and in the salivary gland cells, while Type 2 isoform is expressed only by the cells of the central nervous system (Chandrasekaran and Beckendorf, 2005; this work). Furthermore, additional studies have described Type 2 protein expression in the ovaries (Guarnieri et al., 1998; Roulier et al., 1998).

The above mentioned observations, together with the transcript information available from Flybase: <http://flybase.org/reports/FBgn0003502.html>, form the current picture of the *Btk29A* expression. In summary, alternative splicing leads to differential forms of Btk29A protein: the Short Type 1 (around 66kDa), the Long Type 2 (around 95kDa) and a third smaller one (around 55kDa). All of these molecules display similar carboxy-terminal, but differential amino-terminal region (Figure 13).

All *Btk29A* isoforms are described to be expressed in embryonic stages. It should be noted though, that the comparison of the expression analysis of *Btk29A* in the “older” (before the genome sequencing) versus the “more recent” studies are somehow confusing. More explicitly, the older studies state that: i) p55 (that possibly lacks kinase activity (Theroux and Wadsworth, 1992)) is the most abundant embryonic isoform in central nervous system, trachea, etc., ii) p66 is expressed only in the salivary glands and iii) they lack information about the long isoform expression (Gregory et al., 1987; Katzen et al., 1990; Vincent et al., 1989; Wadsworth et al., 1990). Opposing to this, the more recent studies focusing on p66/ Short isoform and 95kDa Long isoform (Baba et al., 1999; Chandrasekaran and Beckendorf, 2005), show that the Long isoform is central nervous system-specific while the Short is expressed in the salivary glands (and other tissues, like epidermis) (Chandrasekaran and Beckendorf, 2005). Are both p55 and long isoform expressed in the central nervous system? Is p66 expressed solely in salivary glands? A simultaneous analysis of the expression of all three isoforms would clarify the picture.

---

### A.5.B. *Btk29A* functions

The broad expression of *Btk29A* in all of the developmental stages of *Drosophila*, suggests that *Btk29A* is involved in several developmental processes. Many studies have tried to assess the role of the *Btk29A* in different tissues. Most of the bibliography, focuses on the embryonic stages (Beckett and Baylies, 2006; Chandrasekaran and Beckendorf, 2005; Li et al., 2000; Matusek et al., 2006; Tateno et al., 2000; Thomas and Wieschaus, 2004), with only few studies describing the role of the gene in adult tissues (Baba et al., 1999; Guarnieri et al., 1998; Hamada-Kawaguchi et al., 2014; Hamada et al., 2005; Lu et al., 2004; Roulier et al., 1998).

#### - In embryonic development

In the embryonic stages, *Btk29A* plays a role in anterior-posterior patterning (Beckett and Baylies, 2006), cellularization (Thomas and Wieschaus, 2004), salivary gland morphogenesis (Chandrasekaran and Beckendorf, 2005), dorsal closure (Tateno et al., 2000) and tracheal cuticle patterning (Matusek et al., 2006).

In early embryogenesis, *Btk29A* affects the early antero-posterior patterning of *Drosophila* embryo. *Btk29A* activity in this context is regulated by *Parcas* (*Prc*), the *Drosophila* homologue of the mammalian protein Sab (SH3domain binding protein that preferentially associates with Btk), which is known to inhibit the activation of Btk in mammals (Beckett and Baylies, 2006; Sinka et al., 2002).

Additionally, *Btk29A* is involved in the formation of the cellular blastoderm (cellularization). Cellularization is based on the formation of membrane infoldings, known as furrow canals that will gradually grow inwards and form the membranes of the new cells. Actin and myosin at the base of the furrow canals creates microfilament rings important for providing the contractile pulling forces that helps the inward invagination of the membranes (Schejter and Wieschaus, 1993; Thomas and Wieschaus, 2004). In *Btk29A* mutants, the microfilament rings are not constricted and although the furrow canals are forming, they have abnormal arrangements and fail to complete the basal closure (Thomas and Wieschaus, 2004). It should be noted that a similar phenotype is observed in mutants for *Src64B*, a member of the closely related Src kinase family.



---

Later on in embryonic development, Btk29A has been shown to interact with the Src kinase Src42A in the regulation of Basket (Bsk), the *Drosophila* homologue of the Jun amino-terminal kinase (JNK), in the process of epidermal closure at the dorsal region of the embryo (Tateno et al., 2000). Double mutants for *Btk29A* and *Src42* display a dorsal opening phenotype and die before the end of embryogenesis. Additionally, the leading edge cells of these mutants (which are facilitating the dorsal closure) contain decreased quantities of filamentous actin and phosphotyrosine (Tateno et al., 2000).

A recent study revealed that Btk29A together with the Src kinases Src42A and Src64B participate in the wound healing response mediated by the receptor tyrosine kinase Stitich (Stit). These non-receptor tyrosine kinases were shown to bind to phosphorylated Stit and collectively act in the establishment and maintenance of actin ring at the perimeter of the wound (Tsarouhas et al., 2014). Additionally, Src42, but not Btk29A or Src64B, regulates the Stit-mediated transcriptional activation of wound response genes upon epithelial wounding (Tsarouhas et al., 2014).

Another role of *Btk29A* involves the regulation of the actin cytoskeleton organization and cell cycle during salivary gland formation. Salivary gland formation starts at embryonic stage 10 from two groups of post-mitotic epithelial cells in the ventral region of the second parasegment of *Drosophila* embryo. These cells undergo apical constriction and invaginate in order to form the tubular salivary glands. After the completion of invagination, the cells go through an endoreplication cycle (from G to S phase without cell division) to become polyploid. Btk29A has been described to affect both actin cytoskeleton regulation and endoreplication. More specifically, it ensures the proper equilibrium between the filamentous and monomeric actin during invagination and regulates the proper timing of the endoreplication (after the completion of invagination) (Chandrasekaran and Beckendorf, 2005).

### - In the embryonic trachea system

Limited information is available about the role of Btk29A in the respiratory system. Btk29A has been described to function, together with Src42A, to properly pattern the cuticle deposited inside the tracheal lumen in late embryonic stages, in parallel bundles called taenidial folds (Matusek et al., 2006). *Btk29A* (and *Src42A*) mutants display a disorganized cuticular pattern, accompanied with irregular arrangement of the actin cytoskeleton at the apical region of the tracheal cells, phenotypes similar to the ones observed in mutants for the formin DAAM (Dishevelled associated activator of morphogenesis). Epistatic analysis revealed that the two kinases act



---

downstream of or in parallel to DAAM (which is regulated by RhoA) in the regulation of the actin organization and cuticular patterning (Matusek et al., 2006).

Involvement of Btk29A in the permeability barrier of the trachea system has not been previously described (Paragraph A.4). Additionally, although *Btk29A* mutants have been described to acquire shorter filzkörper (Li et al., 2000), no further analysis of the spiracular phenotypes has been performed.

### - In later stages

In the adult, *Btk29A* has been shown to affect the male and female genitalia formation and/ or function (Baba et al., 1999; Hamada-Kawaguchi et al., 2014), the olfactory system sensitization (olfactory jump reflex) (Asztalos et al., 2007) and the survival of the flies (Baba et al., 1999).

In the male flies, selective loss of the Type 2 transcript (in *fic<sup>P</sup>* mutants) reduces the life span in the adult and leads to malformation of the male genitalia (Baba et al., 1999). Both phenotypes can be partially rescued by the human homolog of the gene Btk that displays high similarity with the Type 2 Btk29A isoform (Figure 14) (Hamada et al., 2005).

During oogenesis, Btk29A is localized at the ring canals of the oocytes of the female flies where it mediates the organization of the actin cytoskeleton (Guarnieri et al., 1998; Lu et al., 2004; Roulier et al., 1998). The Btk29A localization in the ring canals is dependent on Src64B kinase (Guarnieri et al., 1998; Roulier et al., 1998). More explicitly, Src64B phosphorylates Y677 within the kinase domain of Btk29A and activates it. Upon activation, Type 2 Btk29A phosphorylates target proteins and localises in the ring canals via its SH2 and SH3 domains. Furthermore, it generates additional docking sites for more Btk29A molecules (Lu et al., 2004). Moreover, the PH domain has a significant role in Btk29A ring canal localization, as it enhances or suppresses Btk29A membrane targeting in the presence or absence of Src64B respectively (Lu et al., 2004). Although Btk29A Long isoform is more abundant, Short isoform is also expressed in the ovaries. This form constitutively localises at the ring canals, but requires Src64B for its full activation (Lu et al., 2004).

Finally, a recent study revealed that the Type 2 isoform of Btk29A appears to act downstream of Wnt4 in the niche, phosphorylating Armadillo/ $\beta$ -catenin and thus up-regulating its transcriptional activity in somatic escort cells; this in turn terminates proliferation of the germ cells (Hamada-Kawaguchi et al., 2014).

---

From the above it becomes clear that Btk29A is involved in several processes during *Drosophila* lifetime. The common feature in most of the cases is the function of the protein in the organization of the actin cytoskeleton (salivary glands, ring canals, trachea cuticle deposition, etc) (Chandrasekaran and Beckendorf, 2005; Guarnieri et al., 1998; Matusek et al., 2006; Roulier et al., 1998). Additionally it should be noted that Btk29A executes many of its functions in cooperation with other Src kinases (Src42A, Src64B) (Guarnieri et al., 1998; Matusek et al., 2006; Roulier et al., 1998; Tateno et al., 2000).

---

## Aim of this study

---

A genetic screen previously conducted in the lab led to the identification of the non-receptor tyrosine kinase *Btk29A* as an important player for the development and maturation of the respiratory system of *Drosophila melanogaster*. In this study, I performed a series of experiments in order to:

- Thoroughly describe the expression pattern of *Btk29A* in the *Drosophila* embryo and more specifically in the respiratory system in wild type and *Btk29A* mutant embryos (Chapter C.1 )
- Characterize the *Btk29A* mutant phenotypes in the posterior spiracles and unravel the mechanism through which *Btk29A* regulates posterior spiracle morphogenesis (Chapter C.2)
- Characterize the tracheal phenotypes of *Btk29A* mutants and make an attempt to understand the role of the protein in the trachea development and function (Chapter C.3)

---

## **B. MATERIALS AND METHODS**

---

## B.1. Mutant Fly Strains

For the needs of the current study, several *Btk29A* alleles were acquired:

*Btk29A*<sup>k00206</sup> (BL10469), *Btk29A*<sup>EP2167</sup> (BL17235) and *Df(2L)BSC23* (BL9710) carrying a small deletion at the *Btk29A* locus (28F1-29A3) from *Drosophila* Bloomington Stock Center (DBSC) and *Btk29A*<sup>k05610</sup> (DGRC102398) from the *Drosophila* Genetic Resource Center (Figure 13).

For the gene mapping we acquired: the Second Chromosome Deficiency kit from DBSC and mutant alleles for the genes: *Pvr*<sup>c02195</sup> (BL10856), *Bsg*<sup>k13638</sup> (BL11096), *emb*<sup>k16715</sup> (BL11195) and *Btk29A*<sup>206</sup> (see above), mapped on the in and around the 29A chromosomal region of the second chromosome. The initial *rbo*<sup>3</sup> (Huang et al., 2004) was kindly donated by Kendal Brodie).

Other mutant stocks used in this work: *Abdb*<sup>M1</sup> (Casanova et al., 1986); *Df(2L)5sal salr* (de Celis et al., 1996); *ems*<sup>9H</sup> (Dalton et al., 1989); *grn*<sup>7L</sup> (Brown and Castelli-Gair Hombria, 2000); *grh*<sup>B37</sup> (Bray and Kafatos, 1991); *cut*<sup>145</sup> (Johnson and Judd, 1979); *Df(1)os1A* (Brown et al., 2003) (Brown et al., 2003); *trh*<sup>1</sup>, *trh*<sup>2</sup>, *trh*<sup>8</sup> (Isaac and Andrew, 1996) (Isaac and Andrew, 1996).

## B.2. Transgenic Fly Strains

*yw*; *ubi-DE-Cad-GFP* (Oda and Tsukita, 2001), *Sqh*<sup>AX3</sup>; *ubi-Sqh-GFP* (Royou et al., 2002), *UAS-PKNG58AeGFP* (Simões et al., 2006), *grhD4-lacZ* (described in Hu and Castelli-Gair, 1999), *UAS-actin*<sup>5C</sup>*mRFP* (BL24779) (Liu et al., 2008), *yw* ; *UAS-EGFP-6xMyc-nlsGo3 / TM6B* (*UAS-GFP-NLS*) (Wang and Struhl, 2005), *AbdB-GAL4* (de Navas et al., 2006), *69B-GAL4* (Brand and Perrimon, 1993), *sal-GAL4* (alias 459.2GAL4 as described in Brown and Castelli-Gair Hombria, 2000) , *ems-GAL4* (Merabet et al., 2002), *btl-GAL4* (Shiga et al., 1996)

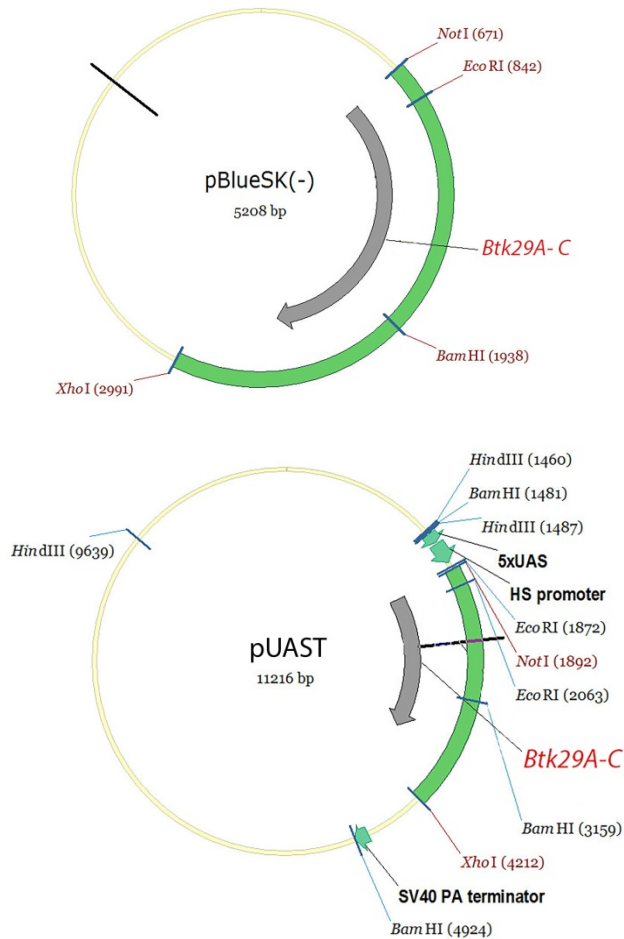
For our rescue experiments we used *UAS-Btk29A-C* (short isoform; see Paragraph C.2.C); we also generated a *UAS-Btk29A-B* construct (long isoform).

### B.3. Molecular biology and transgenic lines

To generate the cDNA sequence of the Btk29A-C (Figure 13), we purchased the cDNA for *Btk29A-RB* from *Drosophila* Genomics Resource Center (LD16208, <https://dgrc.cgb.indiana.edu/product/View?product=5076>) and replaced 713bp at the 5' end with the sequence:

g c g g c c c c a a c a t g a t t c c c t g c g t g a g t t t g g c c g a a c g a g c g t c a t t g g c a a c a t g a a g g a g c g g g t c a a g g a a t g a a g g t g t t c g g e t g c c g a c t c a a c t t c t g g a a c c a t t g g t c a c a g c c t g a c c a g t t c c a a a a c c a a g a a g g c a a c g g c a g t t c c a g c c c a g a a t t c (182bp, synthesized by Biomatik).

The synthetic sequence was inserted as a NotI/EcoRI fragment in the pBS SK-. The synthetic Btk29A-RC cDNA was then cloned into the NotI/XhoI sites of pUAST (Map1 and 2). The Btk29A-B cDNA from the original DGRC plasmid was cloned into the NotI/XhoI sites of pUAST. Transgenic flies were generated using standard procedures.



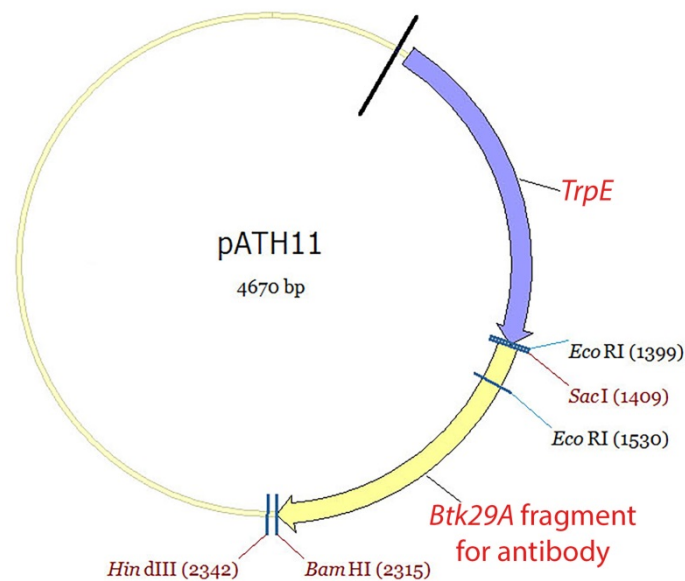
---

#### B.4. Btk29A polyclonal antibody

To generate Btk29A polyclonal antibody, we cloned a selected fragment of the Btk29A-RB coding sequence (<http://flybase.org/reports/FBtr0079616.html>) into the expression vector pATH11 (Koerner et al., 1991) in frame with the TrpE gene (Map 3). The selected fragment encodes for part of the TH, the SH3 and the SH2 domains of the Btk29A protein (Figure 13) and is thus common to both long and short isoforms.

Selected Btk29A protein fragment:

```
NGSSPAQNSTRSISPNSSTTNSQFSLQHNSSGSLGGGVGGGLGGGSLGLGGGGGGGG  
SCTPTSLQPQSSLTTFKQSPTLLNGNGTLLDANMPGGIPTPGTPNSKAKDNSHFVKLVVALY  
PFKAIEGGDLSLEKNAEYEVIDDSQEHWWKVKDALGNVGYIPSNYVKPKALLGLERYEWY  
VGDMRQRAESLLKQGDKEGCFVVRKSSTKGLYTLSSLHTKVPQSHVKHYHIKQNARCEY  
YLSEKHCCETIPDLINYHRHNSGGLACRL.
```



#### Map3:

*Btk29A* gene fragment was cloned into the *SacI*/ *BamHI* sites of pATH11 expression vector, and in frame with the TrpE gene.

The polypeptide was purified from bacterial inclusion bodies according to a protocol developed by N. Patel (U.C.Berkeley) and used for rat immunization. Two, one-month old female rats were kindly provided from Kiki Thermou (Pharmacology lab, Medical School, University of Crete). Initially the rats were injected with a mixture of the antigen with Complete Freund's adjuvant (1:1) in order to induce the primary immune response. After 20 days (and after this, every 30 days for a total

---

9month period) the rats were subjected to antigen injection (1:1, antigen to Incomplete Freund's adjuvant. 11-15 days after the injection, blood was isolated (from the tail). After 9months, the rats were sacrificed with heart puncture. The blood samples were incubated at 37°C for 1 hr, the serum was isolated, aliquoted and stored at -20°C.

The specificity of the antibody was tested with Western blot analysis and staining of *Df235* homozygous embryos (Figure 18). Pre-immune serum did not give any specific staining. The antibody detects both Btk29A isoforms. The working concentration of Btk29A rat polyclonal antibody is 1:400 for immunostaining and 1:4000 for WB.

### **B.5. Embryo fixation and immunohistochemistry**

**Fixation:** For embryo fixation, embryos were dechorionated in 50% bleach solution, fixed in a 1:1 mix of 4% formaldehyde in 1 x PBS (1x Phosphate Buffer Saline) : heptane, in a 5ml glass vial, for 20 minutes, at room temperature, with vigorous shaking and devitellinized with methanol. The embryos were then stored at -20°C or rehydrated in 1x PBS - 0.1% Triton-X-100 and stained (see below). For phalloidin staining hand-devitellinization was performed to avoid the use of methanol.

**Hand devitellinization (fixation without methanol):** The embryos were dechorionated in 50% bleach solution, collected in a 5ml glass vial and fixed in a 1:1 mix of 4% formaldehyde in 1 x PBS : heptane solution, for 4 minutes, at room temperature. The embryos were then transferred with a pasteur pipette, on a Whatman paper to allow heptane evaporation. The Whatman paper was inverted and the embryos were transferred (and stuck) on a double sticky tape, positioned at the bottom of a small Petri dish (35x10mm) lid and immediately covered with 1 x PBS. The vitelline membrane was removed manually under a dissecting stereoscope using 23-gauge needle mounted on a 3ml syringe. The devitellinized embryos were transferred in 1.5ml tube in PBS and immediately stained (with phalloidin or antibody).

For antibody staining, the fixed embryos were rinsed 3 times with PBT (1x PBS - 0.1% Triton-X-100), washed 3 times (10 minutes each) in PBT. They were incubated in blocking solution (1x PBT with 0.5w/v BSA) for 30 minutes, in room temperature and in the primary antibody mix overnight at 4°C. The next day the antibody mix was removed, the embryos were subjected to 3 rinses followed by 3 washes (15 minutes each) with PBT and incubated in blocking solution for 30 minutes. They were incubated for 2 hours with the secondary antibody mix in room temperature and



---

washed extensively (3 rinses and 3 washes for 20 minutes each, in PBT). The stained embryos were kept in 80% glycerol-nPG at 4°C till mounting.

The following primary antibodies were used:

- rat polyclonal anti-Btk29A 1:400 (this work)
- mouse monoclonal anti-Btk29A 1:100 (Chandrasekaran and Beckendorf, 2005)
- rabbit anti-Spalt 1:200 (de Celis et al., 1999)
- mouse anti-CyclinE (8B10) 1:20 (Richardson et al., 1995)
- mouse anti-Megatrachea (1:50)
- rabbit anti-Grain 1:400 and rat anti-Grain 1:400 (Garces and Thor, 2006)
- rabbit anti-GFP 1:10000 (purchased from Minotech)
- rabbit anti-beta-galactosidase 1:5000 (purchased from Cappel)
- rabbit anti-NeurexinIV 1:1000 (Baumgartner et al., 1996)
- mouse anti-Gliotactin 1:100 (Auld et al., 1995)
- rabbit anti-Serpentine (1:300)
- rabbit anti-Myosin Heavy Chain (Zipper) 1:1000 (Jordan and Karess, 1997)
- rat anti-Trh 1:1000 (Bradley and Andrew, 2001)
- rabbit anti-Trh 1:10 (Brodu and Casanova, 2006)
- guine pig anti-Gasp (1:1000)
- guine pig anti-Vermiform (1:50)
- From the Developmental Studies Hybridoma Bank:
  - mouse anti-Coracle (C615.16) 1:100
  - mouse anti-Discs-large (4F3) 1:50
  - mouse anti-Cut (2B10) 1:100
  - mouse anti-Crumbs (Cq4) 1:5
  - mouse anti-alpha-Spectrin (3A9, 1:50)
  - mouse anti-Armadillo (N2 7A1, 1:50)
  - mouse anti-2A12
  - rat anti-DE-Cadherin (DCAD2, 1:20)

Rhodamine phalloidin (purchased from Invitrogen) was used to highlight actin filaments at 1:500, following the manufacturer's instructions.

---

The following secondary antibodies were used:

anti-rat Alexa-555, anti-rat Alexa-633, anti-mouse Alexa-405, anti-mouse Alexa-488, anti-mouse Alexa-555, anti-mouse Alexa-647, anti-rabbit Alexa-488, anti-rabbit CF405M Biotium.

*Leica TCS SP8* or *SP2* confocal microscopes were used for the imaging.

## B.6. In situ hybridization

Whole-embryo *in situ* hybridization was carried out using standard methods (Lehmann and Tautz, 1994). Three different antisense digoxigenin-labelled RNA probes (Figure 13) were generated by transcription of the reverse strands of:

- i) the whole cDNA Btk29A-B (All probe),
- ii) 1105bp of the 5' end of Btk29A-B cDNA (containing 719bp of the CDS) corresponding to part of the N-terminus of the Long Isoform (Long probe)
- iii) 170bp at the 5' end of Btk29A-C CDS corresponding to part of the N-terminus of the Short Isoform (Short probe).

We also generated the corresponding three sense control probes.

## B.7. Live imaging

Embryos expressing DE-CadherinGFP ubiquitously (ubi-DE-CadGFP) or GFP-NLS in the stigmatophore (sal-GAL4 driving UAS-GFP-NLS) were hand dechorionated and stuck on a coverslip with heptane-glue, or properly oriented in a MatTek petri dish. The embryos were monitored for up to 11 hours with time intervals of 2-4 minutes using the *Leica TCS SP8* or *BioRad Radiance 2100* confocal microscopes.

## B.8. Dye penetration assay

Embryos of the desired genotype were aged for 13-15 hours and then dechorionated in 50% bleach solution. The embryos were arrayed on apple juice plates, transferred to double-stick tape on glass coverslips, and desiccated in a closed container containing Drierite (W. A. Hammond Drierite Company, Xenia, OH) for 5min. The embryos were then covered with halocarbon oil

---

(Halocarbon, North Augusta, SC). Rhodamine-labeled dextran (Mr, 10,000; Molecular Probes, Eugene, OR) in injection buffer (Rubin and Spradling, 1982) was then injected into the hemocoel using a micromanipulator under a microscope, and the embryos were examined under the microscope.

### **B.9. Ultrastructural analysis**

The embryos were dechorionated and placed in a vial containing 250  $\mu$ l 50% glutaraldehyde, 250  $\mu$ l 0.1 M Phosphate buffer pH 7.2 and 500  $\mu$ l Heptane. They were incubated in this buffer for 20 minutes, shaking. The embryos were hand devitellinized (as described in B.xxx) in 0.1 M phosphate buffer pH=7.2 and fixed for 30 minutes in 1% osmium/2% glutaraldehyde solution. After fixation, the embryos were rinsed in phosphate buffer pH=7.2 and fixed (second fixation) with 2% osmium for 60 minutes on ice in the dark. The embryos were washed with dH<sub>2</sub>O and incubated in 2% uranylacetate in dH<sub>2</sub>O for 30-60 minutes at room temperature in the dark. Gradual dehydration 50% /70% /90% /96% ethanol for 5 min each on ice, incubation in 100% ethanol 10 minutes twice, 2 washes with propylene oxide at room temperature and the final incubation of the samples with DURCUPAN in embedding molds, overnight at 65°C in order to polymerise.

### **B.10. Protein extraction from *Drosophila* embryos and Western blot analysis**

The embryos were dechorionated with 50% bleach, washed and transferred on an apple-juice plate. Embryos of the desired genotype were selected under the microscope, transferred (with a brush) in an ice-cold 200 ml tube and immediately homogenized using a “smoothened” yellow tip. SDS-containing loading buffer (100mM Tris HCl pH=6.8, 4% SDS, 0.2% bromophenol blue, 20% glycerol, 200mM  $\beta$ -mercaptoethanol) was added to the homogenate (2  $\mu$ l of buffer for each embryo). The mix was heated at 100°C for 5 minutes, cooled briefly on ice and centrifuged at maximum speed for 5 minutes. The samples were then stored at -20, or loaded into the acrylamide gel.

The WB analysis was performed according to standard protocols. Polyclonal anti-Btk29A was used at a final concentration of 1:4000 and mouse anti-alpha-tubulin (Molecular probes, 1:200) was used as a loading control.

---

## **C. RESULTS**

---

## C.1. *Btk29A* expression pattern

---

In order to understand the role of *Btk29A* in the respiratory system of *Drosophila*, we decided to re-examine the mRNA and protein expression of the gene throughout embryogenesis, focusing on the trachea and posterior spiracle cells.

As described in Paragraph A.5.A, *Btk29A* expression was assessed at both the mRNA and protein level in early studies (Gregory et al., 1987; Katzen et al., 1990; Vincent et al., 1989). Due to the fact that initially only part of the total gene was cloned, essentially corresponding to the short isoform, the data regarding the expression of the different isoforms of *Btk29A* gave confusing and controversial results (see Paragraph A.5.A). Today, the available tools, the exact genome sequence and the clear annotations enable a more efficient analysis.

### C.1.A. *Btk29A* expression pattern in wild type embryos

#### C.1.A.1. *Btk29A* mRNA expression

*Btk29A* mRNA expression throughout embryogenesis was examined with whole mount embryo *in situ* hybridization. Three different antisense digoxigenin-labelled RNA probes (as well as their corresponding sense probes) were generated:

- i) *All transcript probe*: obtained from the transcription of the reverse strand of the whole *Btk29A*-RB cDNA (3420bp long) that consists of 13 exons (Figure 13 and Table 1) and encodes for the Long *Btk29A* Isoform. It is expected to hybridize with all the transcripts of *Btk29A*.
- ii) *Long transcript probe*: obtained from the transcription of the reverse strand of the 719bp of the 5' end of *Btk29A*-RB CDS, which includes exons 16, 17, 18 and 20 and corresponds to the amino-terminal part of the Long Isoform (Figure 13 and Table 1). This probe is expected to hybridize only with the Long transcripts B, D and E and thus to monitor the expression of the Long Isoform of the gene. This probe also reacts with transcript H (Figure 13 and Table 1)
- iii) *Short transcript probe*: obtained from the transcription of the reverse strand of the 170bp at the 5' end of *Btk29A*-RC CDS that includes a region common in exon 12 (of transcript A), 13 (of transcript C) and 14 (of transcript F) and corresponds to the amino-terminal part of the Short Isoform (Figure 13 and Table 1). It is expected to hybridize only with the Short transcripts A, C and F and thus to reflect the expression of the Short Isoform of the gene.

---

G transcript comprises of the exons 2 and 4-10 (Table 1) that are common to all transcripts. Thus it cannot hybridize with the *Short nor Long Transcript probes*. The expression of G transcript can be indirectly deduced by the comparison of all three expression patterns: it will be any expression observed by the All transcript, but not the Long or Short transcript probe. Of course the possibility that this transcript is expressed together with one or more others cannot be excluded.

Initially, we tried to assess the overall *Btk29A* mRNA expression with the *All transcript probe*, and subsequently to clarify which of the gene transcripts are expressed in the tissues of interest, by using the *Long* and *Short transcript probes*.

#### C.1.A.1a. Expression of All *Btk29A* transcripts (All Isoforms)

*In situ* hybridization with the All transcript probe reveals that *Btk29A* is expressed in multiple tissues during embryogenesis. Table 2: Embryonic expression of *Btk29A* Table 2 summarizes the overall embryonic expression of *Btk29A* from early stages till the end of embryogenesis.

##### Embryonic expression

*Btk29A* mRNA, which is maternally supplied to the oocyte, can be detected throughout the syncytium of the fertilized embryo (stage 1-3, data not shown). Gradually, while the nuclei move to the embryo periphery to form the first cells of the embryo, the mRNA is detected close to the newly formed cell membranes (cellularization, stages 4-5) (see Table 2, also expression analysis from Berkeley *Drosophila* Genome Project (BDGP): <http://insitu.fruitfly.org/cgi-bin/ex/report.pl?ftype=3&ftext=RE17878>). This is likely to correspond to the first zygotic expression.

During gastrulation (stages 6-7), *Btk29A* mRNA can be detected in cells of all three germ layers. However, the levels of *Btk29A* mRNA seem to be low in the ventral furrow cells (mesoderm) and higher in the endodermal cells and the ectoderm. The highest mRNA levels are detected at the anterior area of the embryo (anterior region till the anterior midgut primordium) and the posterior midgut precursor and proctodeal region.

After the completion of gastrulation, the germ band starts elongating. During these stages of embryogenesis, high levels of *Btk29A* expression are detected in the posterior midgut and proctodeal primordium, the anterior midgut primordium, cephalic furrow region and in distinct regions of the head. Lower levels are detected in the amnioserosa, some mesodermal cells and

---

neuroblasts. The epidermal cells show a moderate uniform level of *Btk29A* expression over which a characteristic stripy metameric pattern is superimposed with higher levels (see also Paragraph A.5.A).

By stage 10, the germ band of the embryo is fully elongated. The tracheal primordia first appear during this stage (Manning and Krasnow, 1993). By stages 11-12, while the germ band of the embryo retracts, *Btk29A* expression is detected in the tracheal and posterior spiracle primordia and in other ectoderm-derived tissues: epidermis, salivary glands, amniorerosa, central nervous system and peripheral nervous system. The expression of the gene in the trachea, the posterior spiracle primordia and the salivary glands during these stages is very high.

After the completion of the germ band retraction at stage 13 and for the rest of the embryogenesis (stages 14-17), *Btk29A* expression persists in the epidermis of the embryo, the amnioserosa, the CNS and the PNS. Expression of the gene is also detected in the developing malpighian tubules (stage 13-17), the gonads (stage 15-17) the hindgut (stage 13-17), the dorsal vessel cells (stage 13-17), the leading edge cells during dorsal closure (stage 13-16) and the cells of the anterior spiracles (stage 13-17). High levels of expression are also detected in regions of the head.

#### Tracheal system

According to the above observations, *Btk29A* mRNA is expressed at high levels by the tracheal cells at the beginning of the tracheal development: stage 11-12. Tracheal *Btk29A* expression is very difficult to visualize at stages 13-17 because of the expression of the gene in more superficial tissues like the epidermis and the PNS. It seems though that the expression persists till stage 13-14, but then it lowers below detection levels.

#### Posterior spiracle cells

Posterior spiracle cells seem to express *Btk29A* mRNA throughout their development. Interestingly, the epidermal cells of the posterior-most abdominal segment A8 of the embryo have higher levels of expression compared to the more anterior ones (from stage 11 till the end of embryogenesis). These are the cells that form the outer part of the posterior spiracle, the stigmatophore.



Table 2: Embryonic expression of *Btk29A*

Stage 4-5		<p><b>Cellularization</b></p> <p>1. Newly formed cells, 2. Yolk, 3. Pole cells</p>
Stage 6-8		<p><b>Gastrulation</b></p> <p>1. Anterior epidermal region, 2. Anterior midgut primordium, 3. Cephalic furrow, 4. Anterior transversal fold, 5. Posterior transversal fold, 6. Proctodeal primordium and posterior midgut precursor cells, 7. Ventral furrow</p>
Stage 9-10		<p><b>Germ band elongation</b></p> <p>1. Stomodeum and Anterior midgut primordium, 2. Cephalic furrow, 3. Mesodermal cells and neuroblasts, 4. Epidermal stripes, 5. Proctodeal primordium and posterior midgut precursor cells, 6. Amnioserosa, 7. Head region and optic lobes of CNS</p>
Stage 11		<p><b>Fully elongated germ band</b></p> <p>1. Stomodeum, 2. Salivary glands, 3. Tracheal pits, 4. Epidermal stripes, 5. Posterior spiracle primordium, 6. Amnioserosa, 7. Head region and optic lobes of CNS, 8. Proctodeum</p>
Stage 12		<p><b>Germ band retraction</b></p> <p>1. Stomodeum, 2. Salivary glands, 3. Tracheal branches, 4. Peripheral nervous system cells, 5. Posterior spiracle primordium, 6. Amnioserosa, 7. Head region and optic lobes of CNS, 8. Ventral nerve cord of CNS</p>
Stage 13		<p><b>End of germ band retraction</b></p> <p>1. Salivary glands, 2. Anterior spiracle primordium, 3. Central nervous system, 4. Peripheral nervous system, 5. Abdominal segment 8 and Posterior spiracles, 6. Amnioserosa, 7. Malpighian tubules, 8. Hindgut</p>
Stage 15		<p><b>Dorsal closure</b></p> <p>1. Central nervous system, 2. Posterior spiracles, 3. Gonads, 4. Dorsal vessel, 5. Amnioserosa and leading edge cells, 6. Head region</p>
Stage 16-17		<p><b>End of embryogenesis</b></p> <p>1. Central nervous system, 2. Anterior spiracle, 3. Malpighian tubules, 4. Peripheral nervous system, 5. Gonads, 6. Posterior spiracles, 7. Amnioserosa and leading edge cells, 8. Head region</p>

Different focal planes of antisense; images corresponding to the sense probe are lacking any signal.

---

The inner spiracular chamber cells of the spiracle, which have already invaginated by stage 13, show even higher levels of *Btk29A* expression throughout the morphogenesis of the tissue (stage 11 till stage 16). Close to the end of the embryogenesis (stage 17), the expression of the gene in the posterior spiracles decreases significantly and gets restricted to only a few cells at the tip of the spiracular chamber (sensory cells).

### C.1.A.1b. Expression pattern of different *Btk29A* transcripts




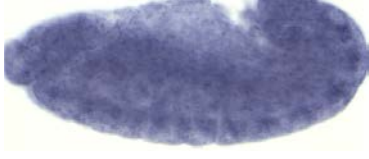

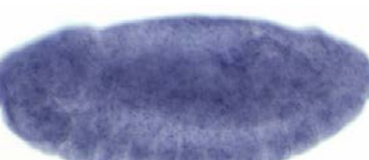
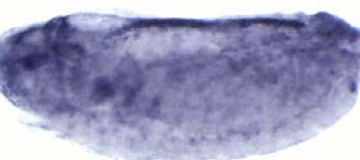
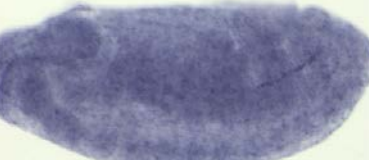

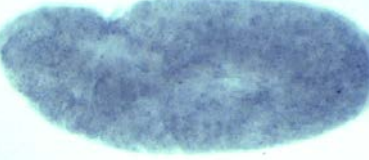
As described above, *Btk29A* mRNA is quite abundant in the *Drosophila* embryo. But into which of the protein isoforms would the transcripts be translated in each one of the embryonic tissues?

Due to the lack of isoform-specific antibodies, in an attempt to answer the above question, we used an indirect approach: we performed *in situ* hybridization using two different RNA probes for *Btk29A* (see Paragraph C.1.A). These probes, the *Short* and *Long transcript probes*, will specifically hybridize to transcripts encoding the Short and the Long isoforms respectively and will thus unravel their expression pattern.

Table 3 summarizes the expression of *Btk29A* transcripts during the development of the respiratory system (stage 11-17). It is clear that the Short transcripts are the ones expressed in most of the embryonic tissues (among which the trachea and the posterior spiracles), while the Long transcripts are only detected in the cells of the central nervous system in low levels.

The Long isoform expression could be the result of the translation of one, some or all four transcripts: B, D, E (Long isoform transcripts) or H. Since the predicted molecular weight of transcript H is around 52.9kDa (Flybase), it is likely that this transcript is the one encoding for the previously described p55 (Vincent et al., 1989; Wadsworth et al., 1990). Unfortunately, the sequence similarities of this transcript to the Long isoform transcripts, do not allow the discrimination of its expression from the expression of the rest. It is thus likely that only one or both Long and p55 isoforms are expressed in the central nervous system.

Table 3: Expression of the different Transcripts of Btk29A

	Short transcripts	Long transcripts
Stage 11		
Stage 12		
Stage 13		
Stage 15-17		
Sense probes (st11)		
Expressing Tissues	<p><i>Stomodeum, Salivary gland, Tracheal cells, Posterior spiracle cells, Epidermis, Head region, Proctodeum, Anterior spiracle, Malphigian tubule, Gonads, PNS, leading edge cells, dorsal vessel</i></p>	
		CNS

---

### C.1.A.2. Btk29A protein expression

Btk29A protein expression, which was previously described by Vincent et al., 1989, was reassessed in the current study, focusing on the respiratory system. For the needs of the study small amount of the published mouse monoclonal anti-Btk29A antibody (Vincent et al., 1989) was obtained as a kind gift of Vidya Chandrasekaran. Additionally, a new polyclonal anti-Btk29A antibody was generated by rat immunization (see Materials and Methods). The antibody was raised against a Btk29A fragment that contains the TH, SH3 and SH2 domains which are common to all *Btk29A* isoforms. Thus it can be used to assess the expression of all of the gene products. (Figure 13).

The efficiency of the newly developed antibody to detect Btk29A expression was tested with western blot analysis. Three bands are detected in protein extracts from wild type embryos: an intense 66kDa and two fainter 95kDa and 55kDa bands (Figure 15). These sizes are consistent with the ones observed in previous studies (Vincent et al., 1989) and the predicted ones (Flybase), and correspond to the Short/ Type 1, the Long/Type 2 and a smaller isoform referred to as p55 in older studies (Vincent et al., 1989; Wadsworth et al., 1990). Protein extracts from *Df235* homozygous mutants that are null for *Btk29A* (see Paragraph A.4.B), do not show any signal, verifying the specificity of the protein.

Additionally, wild type and *Df235* homozygous mutant embryos were stained with anti-Btk29A. Although wild type embryos showed wide Btk29A expression (see Figure 16), *Df235* homozygotes did not show any signal (data not shown). The antibody also detects the protein in the expected patterns upon ectopic/over-expression (see for example Figure 29, 31) as well as by Western blot.

Overall, the above prove that the antibody is highly specific and able to detect the two isoforms of Btk29A protein in whole embryo protein extracts.

#### Embryonic expression

Wild type embryos were collected and immunostained with anti-Btk29A. Figure 16 summarizes the expression of the protein in three representative stages. Throughout embryogenesis, Btk29A expression is observed in ectoderally derived tissues: salivary glands, central nervous system, peripheral nervous system, anterior and posterior spiracles, amnioserosa, malphigian tubules, hindgut, etc. These data are consistent with the mRNA expression analysis (Paragraph C.1.A.1) and previous studies (Vincent et al., 1989).

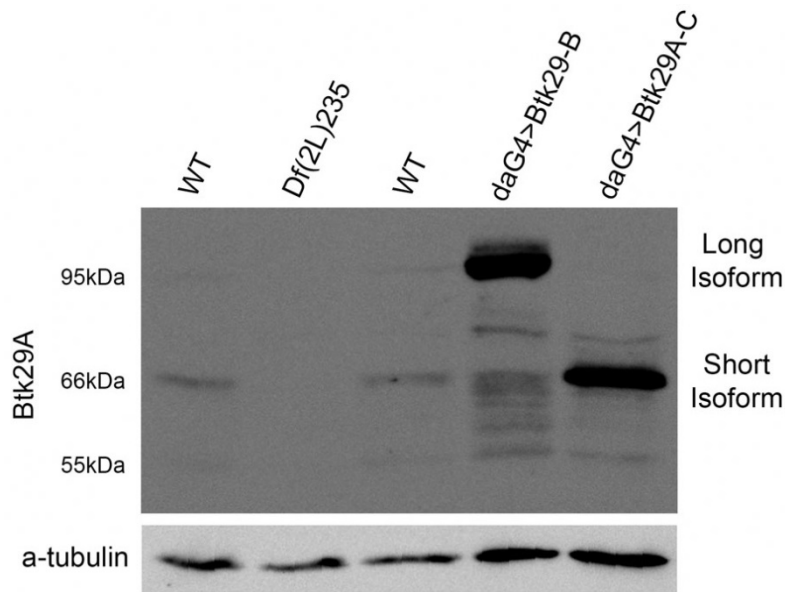


Figure 15: Embryonic expression of Btk29A protein.

Protein extracts from wild type embryos (WT), embryos null for *Btk29A* (homozygous *Df(2L)235* referred to as *Df235*) and embryos overexpressing *Btk29A* under the ubiquitous daughterless-GAL4 driver (*da-GAL4>Btk29A*) were subjected to SDS-PAGE electrophoresis and immunoblotting with the newly developed rat polyclonal anti-Btk29A antibody. Three different bands were detected corresponding to the Long Isoform (95kDa), the Short Isoform (66kDa) and a faster running band (55kDa).

These bands are not present in the *Df235* extract (null mutants) confirming the specificity of the protein. The sizes of the Long and the Short Isoform bands in the WT lanes are consistent with the thick bands observed in samples *da-GAL4>Btk29A-B* and *da-GAL4>Btk29A-C*, which correspond to overexpression of the Long and Short Isoform respectively. Fifty embryos (stg. 0-17) were used per sample. Monoclonal mouse anti-alpha-tubulin antibody was used as a loading control.

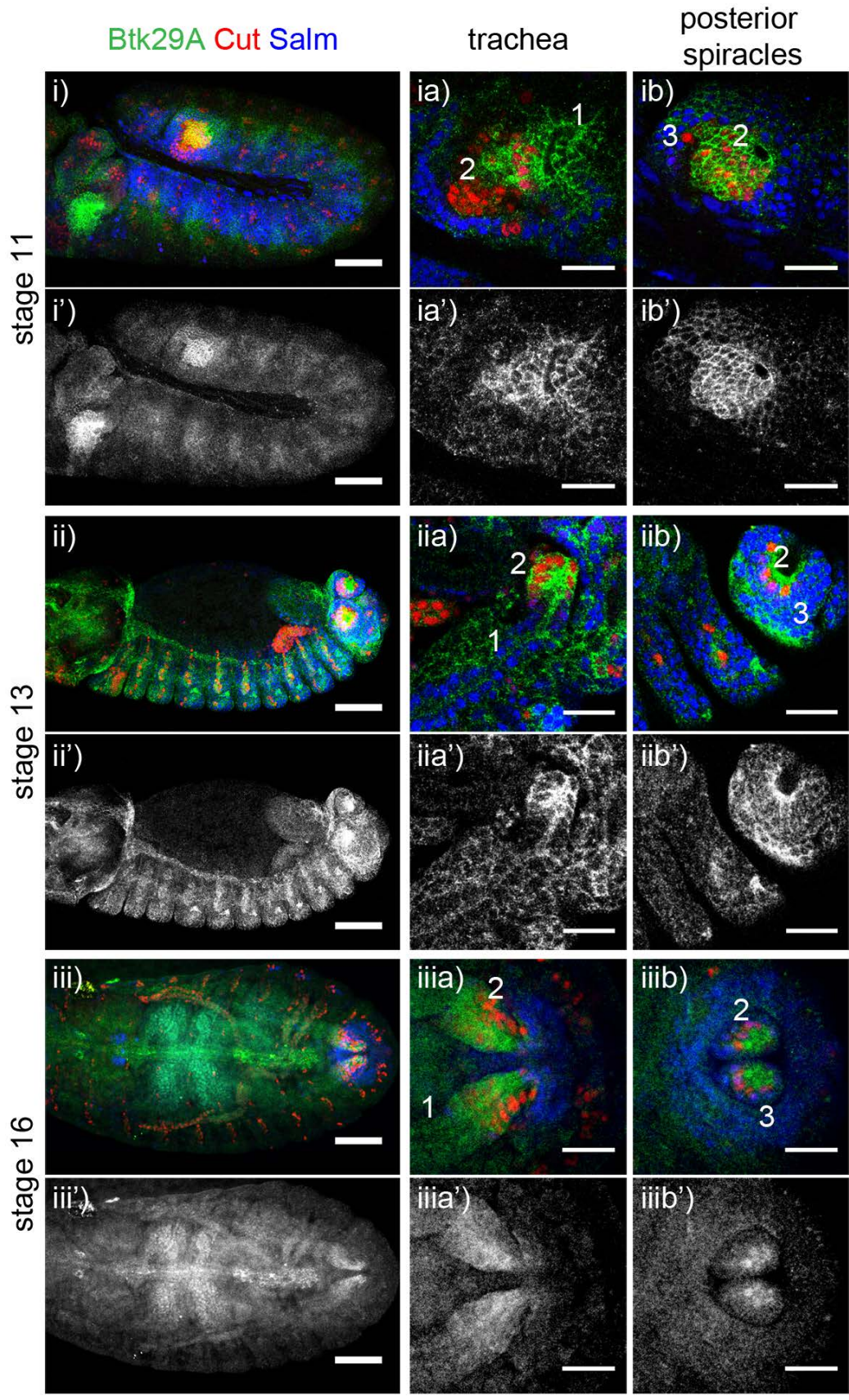
### Tracheal system

In the trachea, Btk29A expression is observed in all the tracheal pit cells (both *sal+* and *sal-*) (Figure 16) by stage 11 of embryogenesis. Its expression persists at stage 12 while the tracheal cells are migrating, elongating and fusing in order to form the tracheal network by stage 13-14. During stage 15-16, the expression seems significantly decreased (below detection levels). These data are consistent with the mRNA expression analysis (Paragraph C.1.A.1).

### Posterior spiracle cells

During early posterior spiracle development (stage 11), Btk29A protein is detected in both spiracular chamber (*Cut+* cells, high levels of expression) and stigmatophore cells (*Sal+* cells, moderate levels of expression) (Figure 16). The expression persists till the end of embryogenesis showing a significant decrease at stage 17.





### Figure 16: Btk29A protein expression during embryogenesis

Expression of Btk29A in: i) stage 11, ii) stage 13-14 and iii) stage 15-16 of embryogenesis. Antibodies for the transcription factors Cut and Sal (which mark subgroups of tracheal and posterior spiracle cells) (Hu and Castelli-Gair, 1999) were used for tissue identification. Btk29A is marked in green. (z-projections of 20microscope slices, scale: 50um)

ia-iiia') Btk29A expression in the trachea is initially detected by stage 11 of embryogenesis. The expression persists till stage 14 of and then it decreases significantly. In stage 16, trachea Btk29A expression is below detection levels.

ib-iiib') Btk29A expression in posterior spiracle begins at stage 11 of embryogenesis. Both groups of spiracle cells express Btk29A, from stage 11 till the end of embryogenesis: spiracular chamber in very high levels and stigmatophore in moderate levels. (iia-iiia': stages 13-14 and iiia-iiia': stages 15-16). By stage 17, the expression is significantly lower in both tissues.

1: tracheal cells, 2: spiracular chamber cells, 3: stigmatophore cells.

All posterior spiracle and trachea figures are single z-axis slices. (Scale bar: 20 µm)

### C.1.A.3. Subcellular localization of Btk29A protein

Previous studies have shown that Btk29A kinase is localized in the apical region of the salivary gland epithelial cells (Chandrasekaran and Beckendorf, 2005). The above antibody staining (Figure 16) suggests that this could be the case for the epidermal, the tracheal and the posterior spiracle cells.

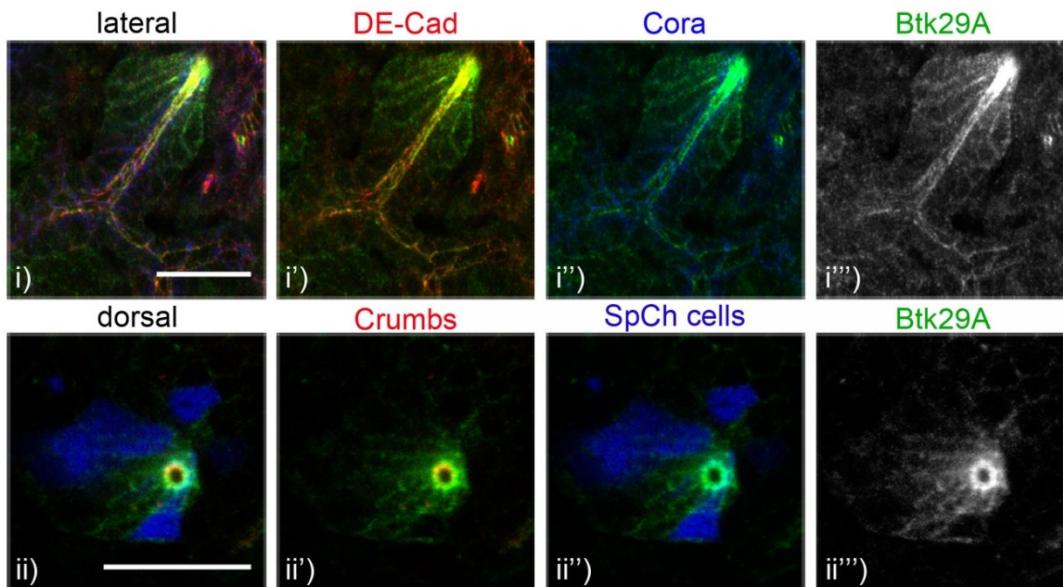


Figure 17: Subcellular localization of Btk29A.

Btk29A is localized at the cell periphery, and mostly at the apical side of epithelial cells: apical to the Septate Junction region (Coracle), colocalizing with DE-Cadherin (i-i''') and Crumbs (ii-ii'''); SpCh (blue) is *ems-GAL4>GFP* (Scale bar: 20 µm)



---

For the analysis of the subcellular localization of Btk29A in the trachea and posterior spiracles, antibody staining was performed (Figure 17). Antibodies for different polarity markers: the apical polarity marker Crumbs (Crb) (Knust et al., 1987; Tepass et al., 1990), the Adherens Junction (AJ) protein DE-Cadherin (DE-Cad) (Oda et al., 1994) and the Septate Junction (SJ) protein Coracle (Cora) (Fehon et al., 1994; Lamb et al., 1998; Ward et al., 1998) were used.

Btk29A is observed at the cell periphery of the epithelial cells of the trachea and the posterior spiracles with preferential high accumulation in the apical region. It co-localizes with DE-Cad and Crb, but not with Cora.

### C.1.B. Btk29A expression in mutant alleles

Four basic *Btk29A* mutant alleles are used in this study: *Btk29A*<sup>206</sup> (Chandrasekaran and Beckendorf, 2005) (Matussek et al., 2006; Tateno et al., 2000), *Btk29A*<sup>EP</sup> (Maybeck and Roper, 2009), *Btk29A*<sup>5610</sup> (Chandrasekaran and Beckendorf, 2005; Lu et al., 2004; Tateno et al., 2000) and *Df235* a deletion of the 29A region of the second chromosome encompassing 23 genes around the *Btk29A* locus. All of them display defective tracheal epithelial permeability barrier and do not complete the trachea air filling by the end of embryogenesis. Additionally, they form posterior spiracles with impaired morphology. Both phenotypes are equally severe in all of the alleles and occur with the same penetrance (see also Paragraph A.4.B). The expression of the *Btk29A* mRNA and protein in homozygous mutant embryos of the above four alleles was examined with *in situ* hybridization and antibody staining.

Initially, the newly developed antibody was used in order to examine Btk29A protein expression in the P-element alleles: *Btk29A*<sup>206</sup> and as well as in the homozygous deficiency (*Df235*) and in combinations of them (Figure 18). All the alleles have been reported to be embryonic null (Chandrasekaran and Beckendorf, 2005).

Surprisingly, in all homozygous P-element mutants, as well as in their trans-heterozygous combinations, residual antibody staining could be detected in the spiracular chamber and tracheal cells. Interestingly, the subcellular localization of the protein seems to be disrupted: it is not localised close to the cell membranes and apical region of the tracheal and spiracular cells, like in wild type, but it appears more cytoplasmic. This might suggest that the protein detected in the mutants is truncated, lacking a fragment important for its localization at the cell periphery and

preferentially the apical region of the cells. This potentially truncated form should not be functional, since the phenotypes observed in the different alleles (*Btk29A*<sup>206</sup>, *Btk29A*<sup>5610</sup>) are undistinguishable from those of the deficiency removing the *Btk29A* locus (*Df235*).

Finally, the hypothesis that the phenotypes observed in the respiratory system of homozygous embryos of these stocks are due to loss of function of the *Btk29A* gene and not of another gene was tested with an attempt to rescue such phenotype by expression of *Btk29A*. Indeed, we rescue the defects in the airways and spiracles (see Paragraph C.2.C).

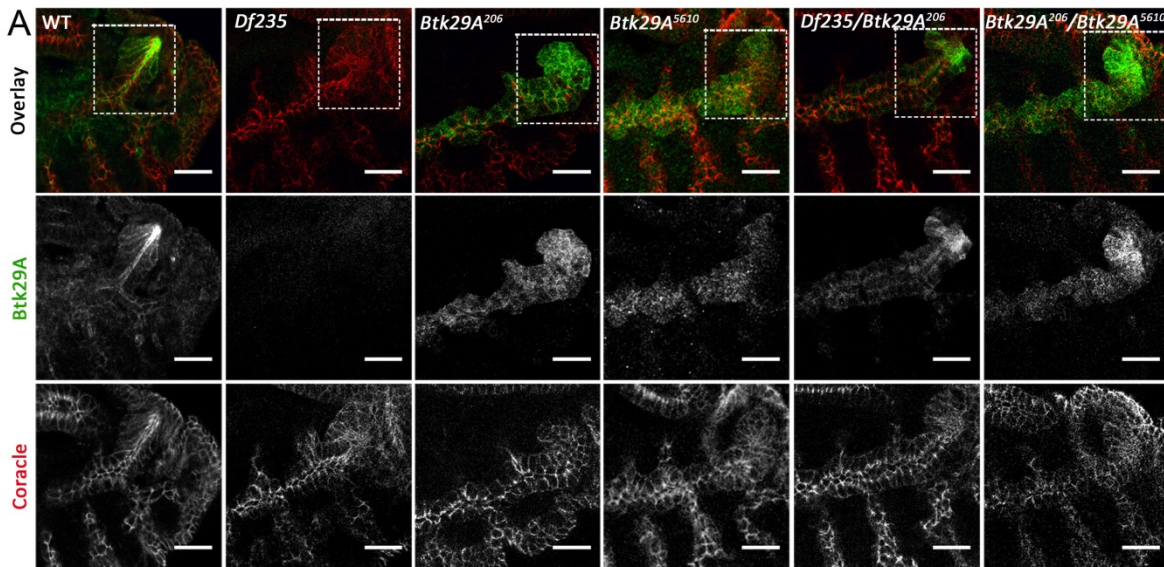


Figure 18: *Btk29A* expression in different alleles of *Btk29A*.

Homozygous mutant embryos for *Df235* are protein null, while the alleles *Btk29A*<sup>206</sup> and *Btk29A*<sup>5610</sup>, as well as their trans-heterozygous combinations are not: they still retain some residual expression. Importantly, the *Df235* and all the *Btk29A* mutant embryos (homozygous, trans-heterozygous and trans-heterozygous with the deficiency) have disrupted spiracle morphogenesis to the same degree. Spiracular chamber cells outlined with dotted lines. (Scale bar: 20  $\mu$ m)

Subsequently to the *Btk29A* protein expression analysis, the three probes described in Paragraph C.1.A (see also Materials and Methods) were used for the analysis of the *Btk29A* mRNA expression in the mutant alleles. The expression was examined in all the tissues throughout embryogenesis focusing on the respiratory system.

Figure 19 summarizes the expression of *Btk29A* mRNA in *Btk29A*<sup>206</sup> homozygous mutant embryos. As previously mentioned (Paragraph C.1.A.1), only the Short Isoform transcripts are expressed by the tracheal and posterior spiracle cells (Table 3 and Figure 16) in wild type embryos.

These transcripts are quite abundant in most of the embryonic tissues, while the Long Isoform transcripts are detected only in the Central Nervous System.

*In situ* hybridization analysis (Figure 19) revealed that the expression of both Short and Long Isoform transcripts is significantly decreased throughout the embryogenesis in almost all the embryonic tissues in *Btk29A*<sup>206</sup> homozygous mutants. But these mutants are not null: the expression of both transcripts, is not eliminated in the respiratory system: *Btk29A* mRNA expression is observed in the spiracular chamber and tracheal cells of the *Btk29A*<sup>206</sup> homozygous mutants. The same is observed for *Btk29A*<sup>EP</sup> and *Btk29A*<sup>5610</sup> but not *Df235* homozygous mutant embryos (data not shown).

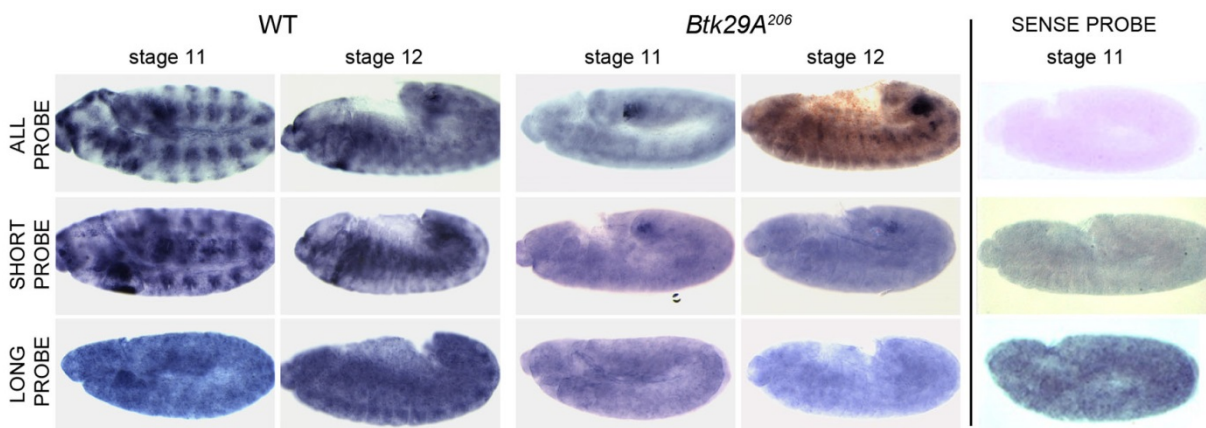


Figure 19: Expression of *Btk29A* mRNA in mutant alleles.

In situ hybridization with All, Short and Long Transcript *Btk29A* probes, suggests that the *Btk29A*<sup>206</sup> allele is not a complete null. The mRNA expression is absent or below detection levels in most of the tissues in the mutants, except from the respiratory system where a signal can be detected. The same was observed for *Btk29A*<sup>5610</sup> and *Btk29A*<sup>EP</sup> (data not shown). *Df235* homozygous mutants do not show any *Btk29A* mRNA expression in the whole embryo, as expected (data not shown).

The above results are in accordance to the antibody staining (Figure 18) and reveal that the P-element alleles used in the current study are not molecular null. They lack *Btk29* expression in most of the tissues, but retain some residual expression in the respiratory system. All three P-elements are inserted in intronic regions of the *Btk29A* locus. Taking into account: i) the region of each P-element insertion in each allele, ii) the epitope recognized by the polyclonal antibody used and iii) the observation that only the Short isoform (maybe also transcript G) are expressed in the cells of the trachea and spiracles, we tried to understand the origin of this residual expression.

In *Btk29A*<sup>206</sup> allele, the P-element is inserted in the intronic region before the “ATG-bearing” exon (exon 12, 13, 14 for A, C, F Short transcripts respectively). Thus it is likely that this exon is

---

affected and the translation of the produced mRNA initiates from another downstream ATG. Depending on the location of the ATG, the produced protein could be lacking one or more of the Btk29A characteristic domains (TH, SH3, SH2 and kinase domain). We already know that: i) the smaller transcripts of Btk29A G and H have a different (downstream) ATG compare to the A, C and F transcripts and ii) the p55 protein isoform (which is likely to be encoded by transcript H) is cytoplasmic (Gregory et al., 1987). Thus, it is not unlikely that the “mutated protein” observed in the tracheal cells of *Btk29A*<sup>206</sup> homozygous mutants is a truncated version of Btk29A, similar to p55. The fact that in vitro functional analysis of p55 had shown that the protein is kinase dead (Theroux and Wadsworth, 1992), further strengthens this possibility. In summary, it is likely that the *Btk29A*<sup>206</sup> P-element insertion disrupts the original ATG leading to a shorter Btk29A protein similar to p55, which is known to be cytoplasmic and to lack a kinase activity. The same is possible for *Btk29A*<sup>5610</sup>. It should be noted that in all cases, the “mutated transcripts” should retain at least part of the “ATG-bearing” exon, since the residual expression can be detected with the Short transcript probe.

Interestingly, the above mentioned P-element alleles (*Btk29A*<sup>206</sup> and *Btk29A*<sup>5610</sup>) carry a lac-Z enhancer reporter construct in the *Btk29A* locus. Indeed beta-Gal expression can be detected in these embryos, and the expression of the reporter indeed reflects *Btk29A* expression. This argues that transcription is occurring at this locus from the two transgenes.

---

## C.2. Btk29A in tissue morphogenesis

---

The posterior spiracles are epithelial structures located posterior to the tracheal tubes of *Drosophila* embryo. They consist of two different groups of cells: the inner, spiracular chamber and the outer, stigmatophore cells. *Btk29A* is expressed in both groups of posterior spiracle cells, with the spiracular chamber cells (Cut+) showing exceptionally high levels of Btk29A (Paragraph C.1.A, Figure 16). In *Btk29A* mutant embryos the spiracles appear to have an abnormal morphology (Figure 12 and Paragraph A.4.B).

In an attempt to understand the role of Btk29A in posterior spiracle development, we tried to:

1. examine if Btk29A is part of the genetic cascade that controls posterior spiracle morphogenesis downstream of Abdominal B (Paragraph C.2.A),
2. characterize the posterior spiracle phenotypes observed in *Btk29A* mutants (Paragraph C.2.B),
3. examine if tissue-specific expression of Btk29A can rescue the spiracular phenotypes in *Btk29A* mutants (Paragraph C.2.C)
4. understand the mechanism through which Btk29A regulates posterior spiracle morphogenesis (Paragraph C.2.D - 2.E)

---

## C.2.A. Genetic control of spiracle morphogenesis

Previous studies on posterior spiracle morphogenesis placed Abdominal B on top of the gene cascade that patterns the posterior spiracles (Hu and Castelli-Gair, 1999; Lovegrove et al., 2006) (described in Paragraph A.2.B.1). AbdB activates the expression of “early” transcription factors (*cut*, *empty spiracles*, *nubbin*, *klumpfuss*, and *spalt*) and signalling molecules (*upd*), which will in turn regulate (directly or indirectly) the activation of other transcription factors (secondary targets) and “realizator” genes. The realizators contribute to the correct morphogenesis of posterior spiracles through the fine-tuning of cell adhesion, cell polarity and cytoskeletal organization of the spiracular cells (Figure 5).

Btk29A is expressed at exceptionally high levels in the posterior spiracles throughout their development (Paragraph C.1.A). This suggests that *Btk29A* could be part of the “Abdominal B genetic cascade” that regulates posterior spiracle morphogenesis. In order to examine this possibility, we conducted a more thorough spatial analysis of *Btk29A* spiracular expression in wild type embryos (Paragraph C.2.A.1) and tested the effect of mutations for AbdB and other factors of the cascade (Primary and Secondary - see Paragraph A.2.B.3) on *Btk29A* expression.

### C.2.A.1. Btk29A expression in different sets of posterior spiracle cells

For the analysis of the regulation of *Btk29A* expression in posterior spiracles, we initially compared Btk29A expression to that of previously identified spiracular markers (anti-Cut and anti-Spalt antibodies, *ems-GAL4>UAS-GFP* and *grhD4-lacZ*) (Maurel-Zaffran et al., 2010). Cut and Spalt mark the spiracular chamber and the stigmatophore, respectively; the *grhD4-lacZ* reporter reflects the spiracular expression of *grh* and is expressed in a subset of around 15 cells at the proximal part of the spiracular chamber (it will be referred to as *grhD4*); Green Fluorescent Protein (GFP) under the *ems-GAL4* driver reports the spiracular expression of *ems* and it will be referred to as *emsGFP* (described in Maurel-Zaffran et al., 2010)

Stainings with anti-Btk29A and combinations of the above markers show that high Btk29A expression overlaps with the Cut positive cells (as well as *grhD4-lacZ* positive cells). The spiracular chamber *ems-GAL4>UAS-GFP* positive cells display high levels of Btk29A while the tracheal ones (*emsGFP* +, Cut -) have significantly reduced Btk29A expression (Figure 20).



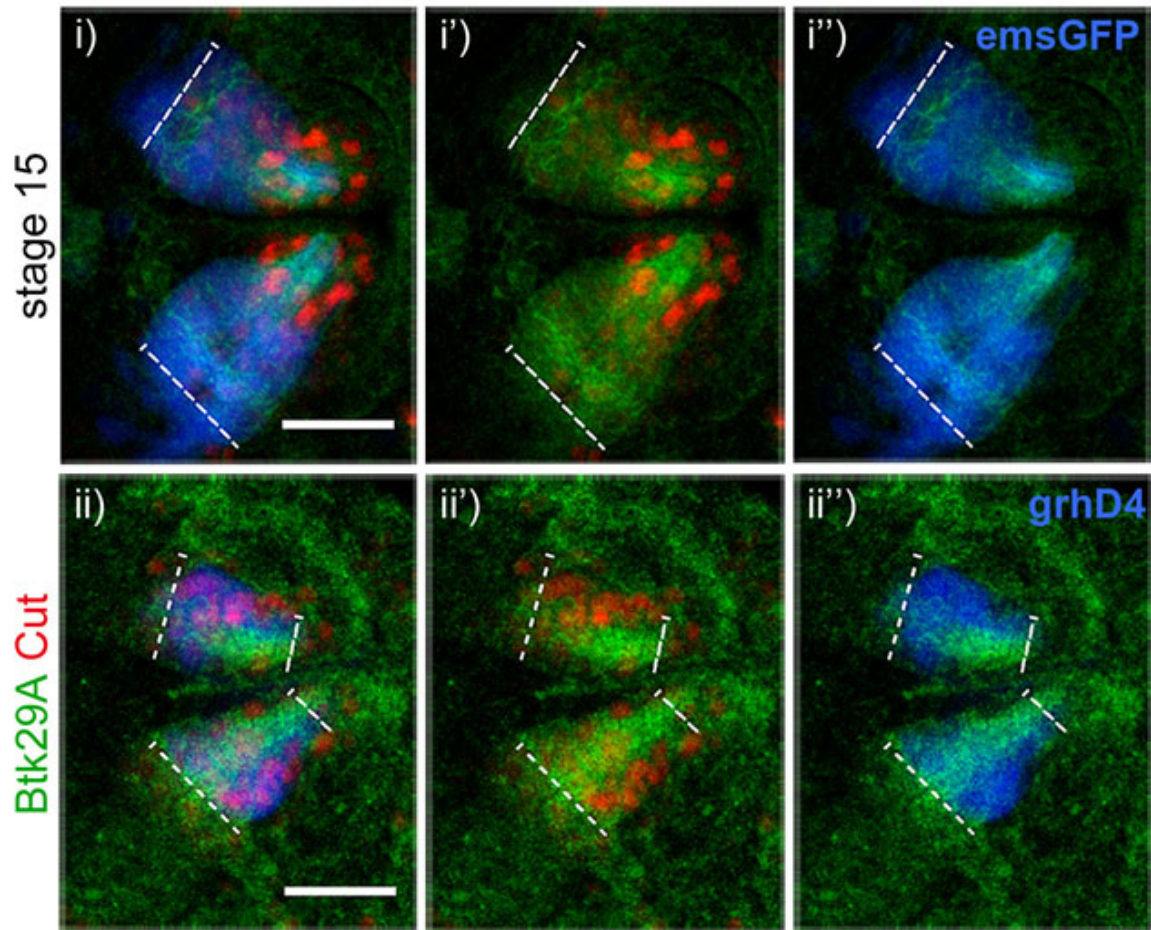


Figure 20 :Btk29A protein expression in different groups of spiracular chamber cells

High levels of Btk29A expression (green) are detected in all the Cut+ cells (red) and the emsGFP + (blue) cells of the spiracle, while the tracheal emsGFP +,Cut - cells (few blue cells on the left side from the dashed lines in i-i'') have lower levels of Btk29A. All grhD4 + cells (blue) express Btk29A. (Dashed lines in ii-ii'' indicate the grhD4 + cells) (Scale bar: 20  $\mu$ m)



### C.2.A.2. AbdB regulates the expression of *Btk29A* in the posterior spiracles

AbdB is necessary and sufficient to induce posterior spiracle formation (Hu and Castelli-Gair (1999), see also Paragraph A.2.B.3). In *AbdB-M1* mutants the posterior spiracles do not form and no spiracle-specific genes are expressed at the A8 segment of the embryo (Lovegrove et al., 2006). Additionally, ectopic expression of AbdB under the ectodermal 69B-GAL4 driver leads to induction of ectopic spiracles in the more anterior segments (Castelli-Gair et al., 1994; Lovegrove et al., 2006). These spiracles express the AbdB direct targets (*cut*, *spalt* (Figure 21), *ems*, *upd*), secondary targets (e.g. *grainyhead*) and realisers (*Neurotactin*, *DE-Cadherin* and others) similarly to the WT ones (Castelli-Gair Hombría et al., 2009; Lovegrove et al., 2006).

In order to examine if *AbdB* regulates the expression of *Btk29A* in posterior spiracles, *AbdB-M1* homozygous mutant embryos were collected and stained with anti-Btk29A (Figure 22ii). The posterior spiracles are not specified in the *AbdB-M1* mutants (Hu and Castelli-Gair, 1999) and the dorsal epidermis in A8 expresses low levels of Btk29A, similar to those detected in the equivalent regions of the more anterior segments of the embryo.

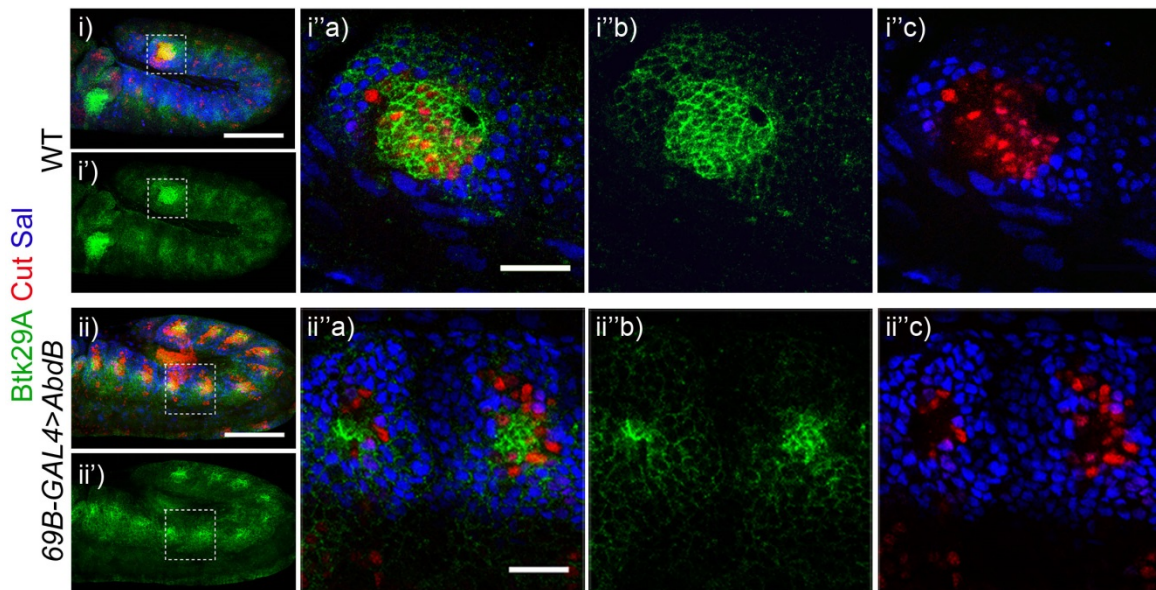


Figure 21: AbdB-induced anterior ectopic spiracles show increased levels of Btk29A

Antibody staining of WT (i – i'c) and embryos overexpressing AbdB under 69B-GAL4 driver (stage 11) (ii – ii'c). AbdB overexpression induces the formation of ectopic spiracles that consist of distinct spiracular chamber (Cut+, red) and stigmatophore (Spalt+, blue) cells. Both cell populations show higher levels of Btk29A expression (green) (compared to the neighboring epidermal cells), with Cut+ cells having exceptionally high and Spalt+ moderately high Btk29A levels (similar to the WT posterior spiracles). (Scale bar: 20  $\mu$ m)

---

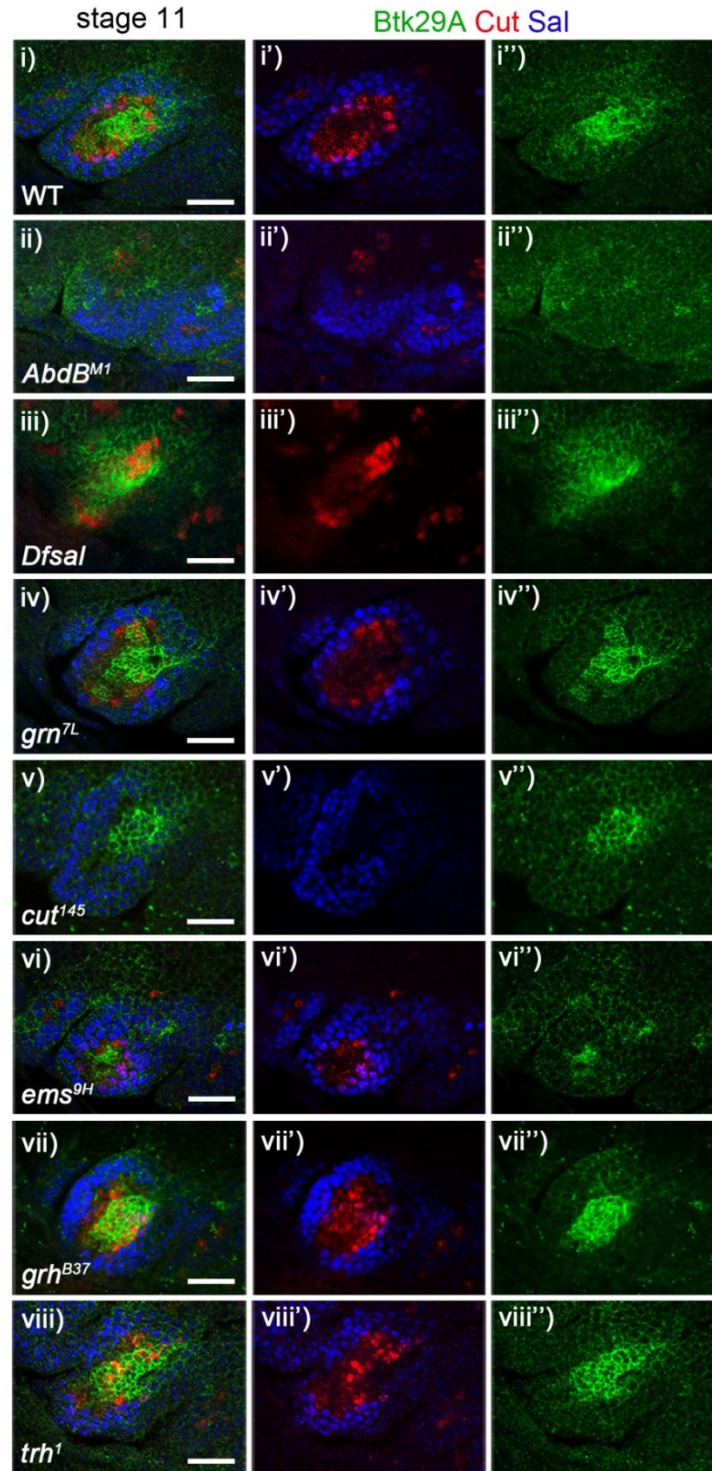
Additionally, Btk29A expression was examined in the ectopic spiracles of embryos overexpressing AbdB under 69B-GAL4 (Figure 21). *Btk29A* is upregulated in the ectopic spiracles in a pattern similar to the WT posterior spiracles: the ectopic Cut+ spiracular chamber cells express exceptionally high levels of Btk29A, while the Spalt+ stigmatophore cells acquire moderate Btk29A levels.

The above observations suggest that *Btk29A* expression is directly regulated by AbdB in posterior spiracles. This could be achieved either directly or indirectly through the primary targets of AbdB.

We examined Btk29A expression in mutant alleles for several transcription factors that act downstream of AbdB in posterior spiracles (Paragraph intro A.2.B.3). Stage 11 homozygous mutant embryos for the transcription factors *spalt*, *grain*, *cut*, *empty spiracles*, *grainyhead* and *trachealess* were stained with anti-Btk29A. The posterior spiracle cells were examined for impairment of Btk29A expression in both the stigmatophore (Spalt+) and the spiracular chamber cells (Cut+).

As shown in Figure 22, Btk29A high spiracular chamber expression does not seem to be affected in any of the mutant alleles studied (Figure 22iii-viii). The same is observed for the intermediate levels of Btk29A expression at the stigmatophore.

These observations suggest that *Btk29A* spiracular expression could be directly activated by AbdB. Another possibility is that Btk29A is regulated by more than one of the transcription factors examined. Regulation of *Btk29A* expression by the putative AbdB primary target genes *nubbin* and/or *klumpfuss* (which were not examined) is not likely, since mutants for these genes do not show phenotypes similar to Btk29A/do not show posterior spiracle phenotypes.



**Figure 22: Btk29A protein expression during embryogenesis**

Expression of Btk29A in mutants for different transcription factors downstream of AbdB: *Df(sal)*, *grn<sup>7L</sup>*, *cut<sup>145</sup>*, *ems<sup>9H</sup>*, *grh<sup>B37</sup>* and *trh<sup>1</sup>*. Stage 11 homozygous mutant embryos were stained with anti-Cut (red), anti-Spalt (blue) and anti-Btk29A (green). The expression of Btk29A is affected only in the *AbdB<sup>M1</sup>* mutants (ii-ii''), while the rest maintain high and moderate levels of Btk29A in the spiracular chamber and stigmatophore cells respectively (iii-viii) (Scale bar: 20  $\mu$ m)

---

## C.2.B. Morphogenesis of the posterior spiracles

### C.2.B.1. Posterior spiracle morphology in *Btk29A* mutants

In order to better understand the posterior spiracle morphological defect in *Btk29A* mutants, we decided to perform antibody staining in late (stage 16) *Drosophila* embryos, expected to have completed the morphogenesis of the tissue. Heterozygous and homozygous *Btk29A*<sup>206</sup> mutants were stained with antibodies for the membrane protein DE-Cadherin and the transcription factor Cut (Figure 23).

DE-Cadherin is expressed and subcellularly localized at the apical region of all epithelial cells (Simões et al., 2006), nicely marking the spiracular cell profiles and outlining the spiracular lumen morphology. In the case of *Btk29A*<sup>206</sup> homozygous mutant embryos, the spiracular lumen is shorter compared to the wild type (Figure 23

Bi' and ii'). Moreover, it is continuous to the trachea and the luminal part proximal to the trachea which forms normally, but the distal part develops an abnormal morphology (see also Figure intro 5.1). Additionally, the two mutant spiracles do not get as close to each other as in wild type embryos (double-headed arrows in Figure 23B

i' and ii'). The latter phenotype might be a secondary effect of the impaired dorsal closure observed in *Btk29A* mutants (Tateno et al., 2000).

But what is the cause of the phenotype in the posterior spiracles? The decrease in the length of the spiracular lumen in *Btk29A* mutants could be either due to reduction of the number of the cells that are building the lumen, or impairment of their spatial arrangements. Another possibility is that the posterior spiracle phenotype is a secondary effect of altered tracheal length/size in *Btk29A* mutants. Previous studies have shown that mutations in tyrosine kinases Src42 and Src64, which are closely related to Btk29A, affect tracheal development and result in a shorter Dorsal Trunk (DT) (Forster and Luschnig, 2012; Nelson et al., 2012) (see also Paragraph A.3.A). Is the same phenotype observed in *Btk29A* mutants, and if so, does it affect the posterior spiracle length? We decided to test these hypotheses.



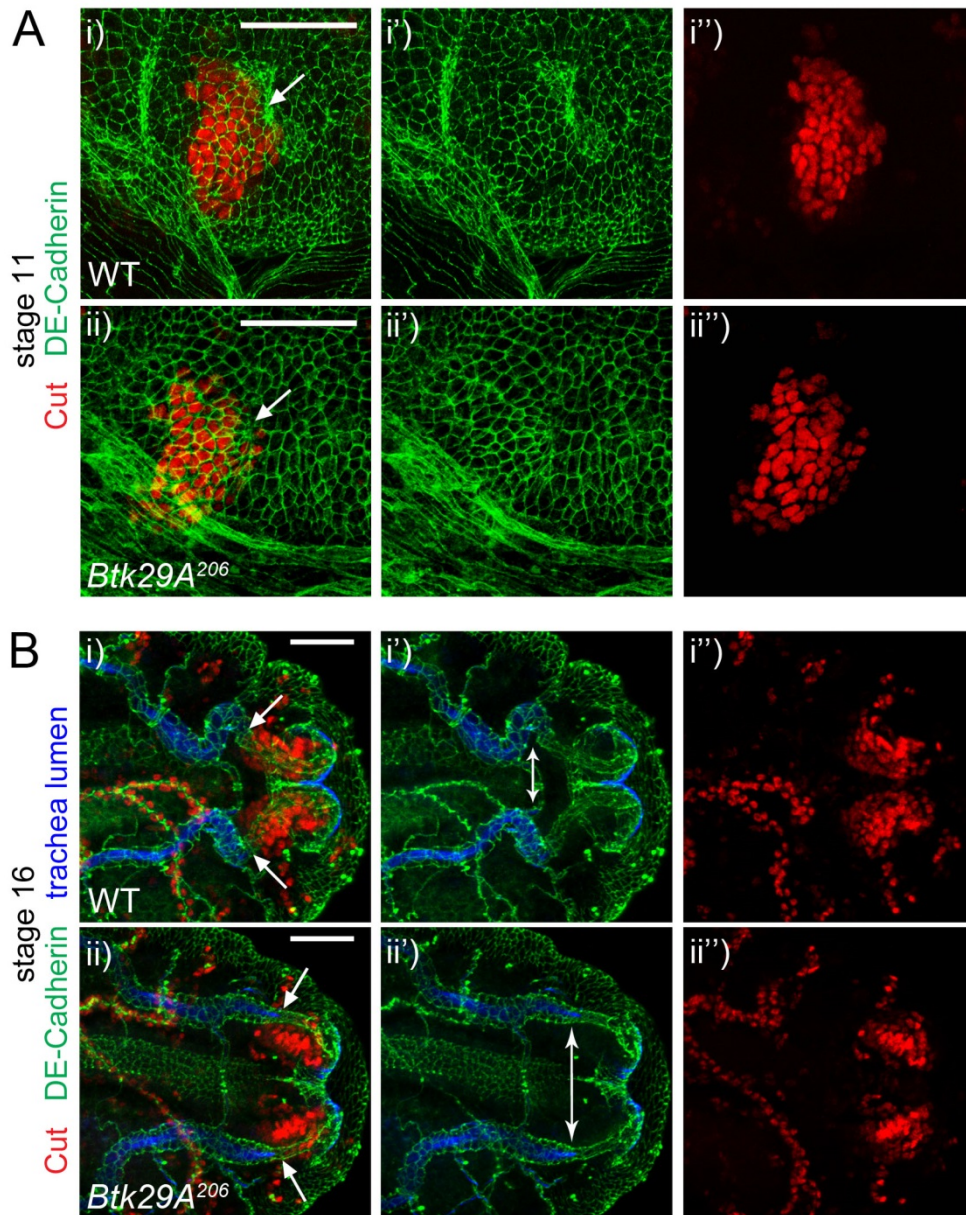


Figure 23: Posterior spiracle morphogenesis in *Btk29A* mutants is abnormal.

Antibody staining of WT and *Btk29A*<sup>206</sup> mutant embryos for the transcription factor Cut (red) and the membrane marker DE-Cadherin (green).

A: The spiracular chamber precursors have already been specified by stage 11 of embryogenesis. They are located adjacent and posterior to the posterior-most tracheal pit and they start expressing Cut+ (red). The number of the Cut+ cells is not affected in *Btk29A*<sup>206</sup> mutants compared to WT.

B: Comparison of WT and *Btk29A*<sup>206</sup> mutants at the end of embryogenesis (stage 16) reveals abnormalities in spiracular morphogenesis. (i'-ii') The length of the spiracular lumen in *Btk29A*<sup>206</sup> mutants is shorter compared to the WT, while the distance between the two spiracles seems increased (double-headed arrows). (i''-ii'') In WT spiracles, the Cut+ nuclei surround the spiracular chamber lumen. In *Btk29A*<sup>206</sup> homozygous mutants the Cut+ cells fail to arrange properly and they are mostly located on the inner side of the spiracular chamber lumen. The above phenotypes are observed with all different *Btk29A* mutant alleles and *Df235*. The tracheal lumen is depicted in blue. Arrows point at the region where trachea and spiracle meet. (Scale bar: 30  $\mu$ m)

---

### C.2.B.1a. Number of spiracular chamber cells

In order to test whether the number of the spiracular chamber cells is decreased in *Btk29A* mutants, we performed antibody staining for Cut and counted the number of the spiracular Cut+ nuclei. We selected stage 11 embryos for the analysis, since the spiracular chamber cells (that are already defined by this stage), have not started invaginating yet and thus are easier to count (Figure 23). Wild type embryos have around 70 Cut+ cells in each one of their spiracles. Approximately, the same number was counted in *Btk29A* mutant spiracles. We conclude that the spiracular chamber cells are normally specified by stage 11 of embryogenesis and that their number is not altered in *Btk29A* mutants.

### C.2.B.1b. Spatial distribution of spiracular chamber cells

What about the spatial distribution of the spiracular chamber cells? As shown in Figure 23A the spiracular chamber cells are specified posterior to the most abdominal tracheal placode (Tr 10) both in WT and *Btk29A* mutants. In wild type embryos, these cells will undergo morphogenetic processes and they will acquire their final position by the end of embryogenesis (stage 16): the Cut+ nuclei will uniformly surround the spiracular lumen (Figure 23Bi-i’). This is not the case for the *Btk29A*<sup>206</sup> mutants: the spiracular Cut+ nuclei are mostly observed at the inner side of the spiracular lumen, concentrated towards the medial axis of the embryo (compare Figure 23Bi’ and ii’).

### C.2.B.1c. Secondary effect of a trachea phenotype

Measurements of the tracheal dorsal trunk (DT) length of stage 16 WT and *Btk29A* mutant embryos revealed that lack of *Btk29A* does not affect tracheal length (reported in Paragraph A.3.A). This suggests that the defective posterior spiracle morphogenesis is not a secondary result arising from the defect in tracheal length.

In conclusion, the above observations suggest that the irregular morphology of the posterior spiracles in *Btk29A* homozygous mutants is not a secondary effect of impaired tracheal development, nor is it linked to a decrease of the spiracular chamber cell number. Rather the spiracular defects correlate with the abnormal positioning of the cells of the spiracular chamber. Invagination is the key morphogenetic program undertaken by spiracular chamber cells that contributes to their final position (Simões et al., 2006). I next investigated if and how chamber invagination is altered in *Btk29A* mutants.

### C.2.B.2. Live imaging of posterior spiracle invagination

In order to follow “live” the invagination process of the spiracular chamber cells, we took advantage of *Drosophila* strains that ubiquitously express DE-Cadherin fused with GFP (Oda and Tsukita, 2001). *Btk29A* recombinants with the ubi-DE-Cadherin.GFP were developed and used for live imaging experiments. Cadherin.GFP enables the observation of the apical membrane of the spiracular chamber cells.

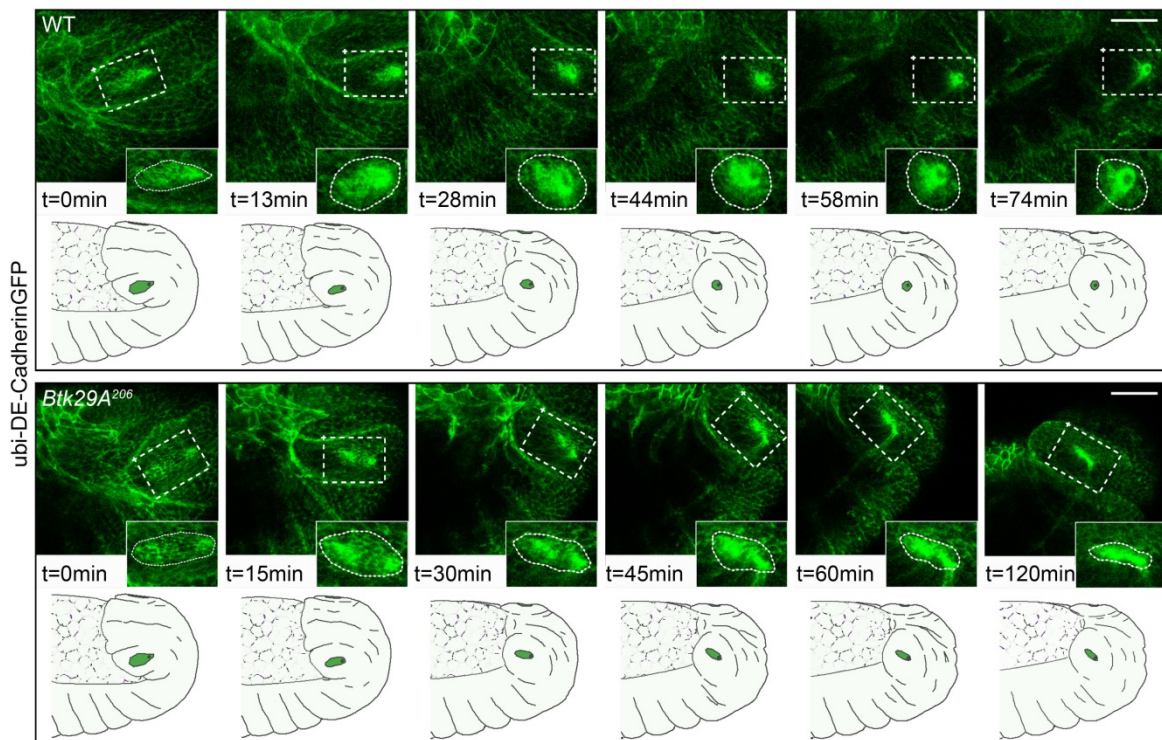


Figure 24: Invagination of the spiracular chamber cells is impaired in *Btk29A* mutants.

Stills of movies showing the posterior region of WT and *Btk29A*<sup>206</sup> mutant embryos expressing DE-Cadherin-GFP. The embryos were monitored from middle stage 12 (8h 30min after egg laying) till stage 13 (for approximately 2 hours). At stage 12, the WT spiracular chamber cells undergo apical constriction and invaginate in a temporally and spatially controlled manner. The cells that are adjacent to the trachea are the first to invaginate and the more distal cells follow. In WT the invagination process was completed 70 min after the beginning of the imaging. In the *Btk29A* mutant, the process is impaired, as the more distal cells do not complete invagination even after 120 min from the beginning of imaging. A higher magnification of the spiracular chamber area is shown for each still (area marked with dashed lines in the stills). Dotted lines in higher magnification panels outline the spiracular chamber cells undergoing apical constriction (stronger DE-Cad expression). Each still is accompanied by a schematic drawing of the posterior half of the embryo showing the position and shape of the invaginating spiracular chamber (corresponding to the strong DE-Cad expression on the embryo surface) (Scale bar: 30  $\mu$ m)



---

According to Simões et al. (2006) spiracle cell invagination starts at embryonic stage 11. It occurs in a spatially and temporally controlled manner and involves spatial rearrangements and apical constriction of the spiracular chamber cells. The process continues throughout stage 12 and is completed by the end of embryonic stage 13.

We selected stage 12 (8hrs 30min after egg laying) wild type and mutant embryos and monitored them for up to 2 hours (Figure 24) by live confocal microscopy. We can clearly identify cells of the spiracular chamber primordium while they undergo apical constriction in both genotypes and follow them through to stage 13. This time interval (mid stage 12 to 13) spans the process of germband retraction. Interestingly, in *Btk29A* mutants, not all of the apically constricted spiracular chamber cells complete the invagination process: the ones proximal to the trachea (the first ones to invaginate) invaginate successfully, while the more distal ones fail to invaginate and remain at the epidermal surface (even 2 hours after the initiation of the imaging) (Figure 24).

The above data suggest that the impaired posterior spiracle morphology in *Btk29A* mutants is the result of incomplete invagination of the spiracular chamber cells. But how is *Btk29A* affecting the invagination of these cells? In order to answer this question, several parameters that affect tissue invagination were examined (following Paragraph).

### **C2.B.3. Phenotypic characterization of the spiracular chamber cells**

Invagination is one of the key morphogenetic processes that contribute to the tissue and organ formation, as it enables the transformation of epithelial cell monolayers to three-dimensional structures. Posterior spiracle cell invagination relies on apical constriction, which in turn depends on the proper tuning of the acto-myosin contraction (Hu and Castelli-Gair, 1999; Simões et al., 2006).

In order to understand the role of *Btk29A* in the spiracular chamber cell invagination during posterior spiracle morphogenesis, we examined a number of features known to be related to the fine tuning of the process. More specifically, we examined the epithelial polarity of the spiracular chamber cells as well as apical constriction, cell shape changes, organization of the acto-myosin network and RhoGTPase activity. Additionally, since *Btk29A* has been shown to influence the invagination of the salivary gland by regulating the actin organization and the endoreplication of the cells (Chandrasekaran and Beckendorf, 2005) (see Paragraph intro A.5.B), we examined if the posterior spiracle cells undergo endoreplication.

### C.2.B.3a. Epithelial cell polarity

Apical constriction and cell-shape changes depend on membrane dynamics that in turn rely on the correct specification of the cell apical-basal polarity. For this reason, the polarity of the spiracular chamber cells was examined. Wild type and *Btk29A* mutants were stained for the polarity markers alpha-Spectrin (a-Spec), Coracle (Cora), Discs-large (Dlg), NeurexinIV (NrxIV), Gliotactin (Gli), DE-Cadherin (DE-Cad), Armadillo (Arm) and Crumbs (Crb). As shown in Figure 25 (also data not shown), the polarity of the invaginating as well as of the non-invaginating spiracular chamber cells (arrowheads in Figure 25Aii-ii'' and Bii-ii'') is similar to wild type.

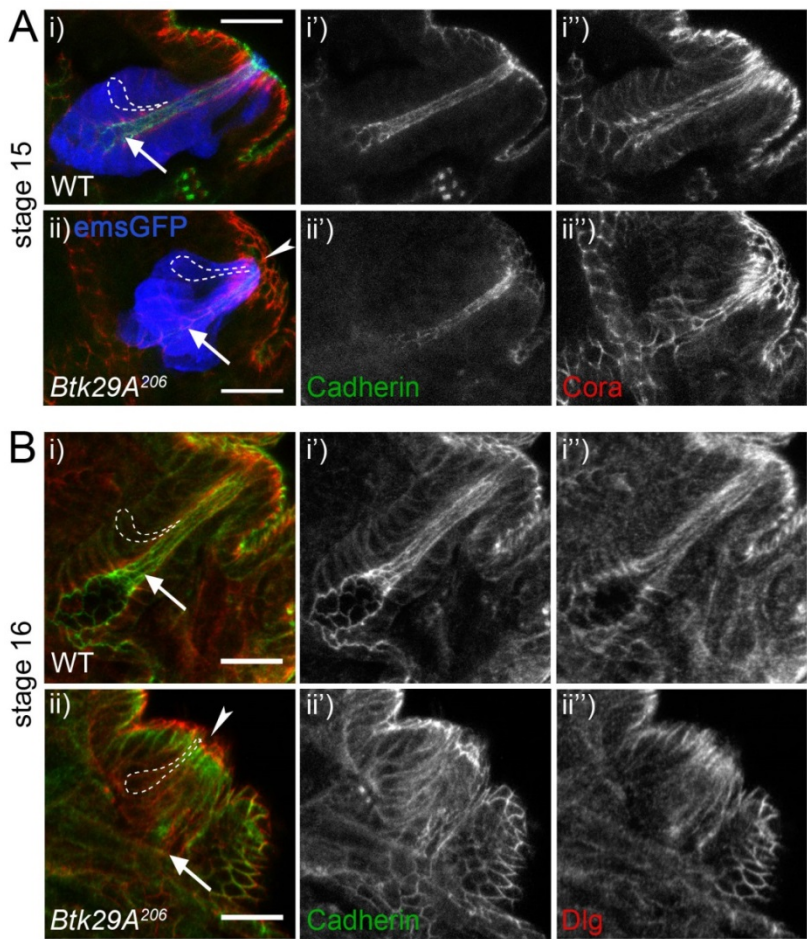


Figure 25: The non-invaginating spiracular chamber cells of *Btk29A* mutants display normal cell polarity.

Antibody staining with the polarity markers Cadherin (green) and Coracle (red) (A) and Discs large (red) (B), reveals that the subcellular distribution of the proteins is not affected in non-invaginating cells of the spiracular chamber in *Btk29A* homozygous mutants (Cadherin apically and Coracle, Dlg apico-laterally). The latter acquire a bottle shape comparable to that of the invaginated WT spiracular chamber cells. Dashed lines outline the periphery of single spiracular chamber cells. *ems*-GAL4>GFP (blue) was used for the identification of the spiracular chamber cells. Arrows point at the region where trachea and spiracle meet and arrowhead at the non-invaginating spiracular chamber cells. (Scale bar: 15  $\mu$ m)

---

### C.2.B.3b. Apical constriction and cell shape changes

Apical constriction is a critical step for epithelial invagination (Llimargas and Casanova, 2010). The spiracular chamber cells start constricting their apical membrane from stage 11, at the initiation of the invagination process (Simões et al., 2006). It is likely that impaired apical constriction of these cells would lead to invagination defects.

The time lapse analysis described in Figure 24 revealed that both the invaginating and non-invaginating cells are constricting their apical surface in *Btk29A* mutants. The same result was observed with antibody staining for the apical markers Crb and DE-Cadherin (data not shown).

Moreover, it has been shown that spiracular chamber cell invagination is accompanied by cell shape changes of these cells. In particular, the cells elongate their basolateral membrane and they acquire characteristic bottle-shape morphology (see also Paragraph A.2.B.1). Antibody staining with the polarity markers: DE-Cad, Cora, Dlg (Figure 25) and a-Spec (data not shown) revealed that the non-invaginating mutant cells attain an elongated bottle-shape similar to the controls. Strikingly, these cells remain on the surface of the epidermis, with their apical side aligning with that of the surrounding epidermal cells, instead of lining the spiracular lumen.

The above observations indicate that the invagination defect observed in *Btk29A* mutants is not due to failure of the cells to perform the necessary shape changes: apical constriction and basolateral elongation.

### C.2.B.3c. Actin-Myosin organization

The acto-myosin network has been shown to be critical for the establishment of the contractile forces necessary for the apical constriction and invagination of several tissues (Martin et al., 2010), among which the spiracular chamber cells (Simões et al., 2006). More specifically, actin preferentially accumulates at the apical side of the cells where it remains at high levels till the end of the invagination process. In a similar fashion, Myosin II, that is initially (stage 11) distributed along the lateral membrane, is gradually enriched apically, colocalizing with actin (Simões et al., 2006). Moreover, previous work from Chandrasekaran and Beckendorf, 2005, has revealed that *Btk29A* influences the balance between monomeric and filamentous actin during the invagination of the salivary gland primordia.

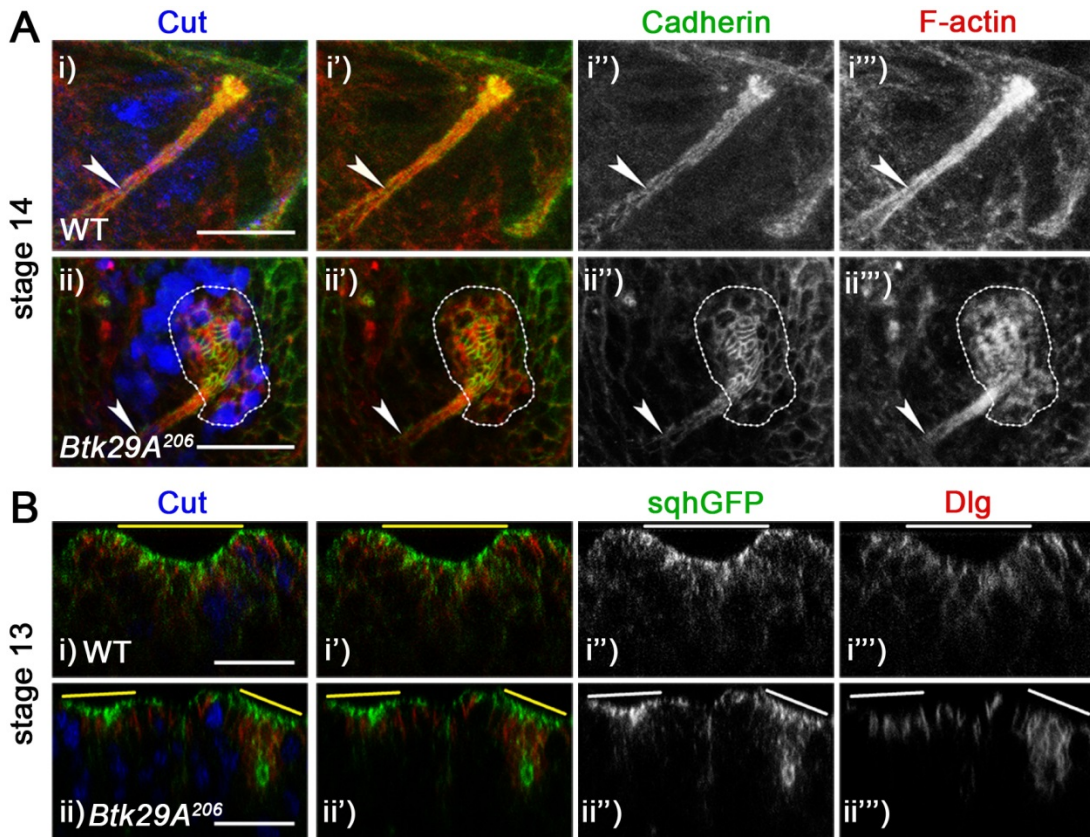


Figure 26: Actin and Myosin organization is not affected in *Btk29A* mutants.

A. Actin (red) accumulates at high levels at the apical side of the non-invaginating spiracular chamber cells in *Btk29A* mutants (outlined by the dotted line in ii), colocalizing with the DE-Cadherin (green). Arrowhead indicates the meeting point of the trachea and spiracle. Cut (blue) marks the cells of spiracular chamber.

B: Myosin II localization is not impaired in *Btk29A* mutants at stage 13 compared to WT, as observed by SqhGFP (Myosin II light regulatory chain fused to GFP) localization relative to Dlg (red) (for the WT, see also Simões et al., 2006). The images are acquired in an xzy mode and the straight yellow lines mark the Cut+ spiracular chamber cells (blue). One spiracle is visible in the view of the WT embryo, two spiracles in the mutant. (Scale bar: 15  $\mu$ m)



We therefore examined the apical acto-myosin cytoskeleton in the spiracular chamber cells of *Btk29* mutant and control embryos. Initially we examined the distribution of actin-RFP (data not shown) and monitored filamentous actin accumulation with phalloidin staining. As shown in Figure 26A, we could not detect any difference between mutant and control embryos. Next, we used the myosin light chain *spaghetti-squash* (*sqh*) GFP fusion (*sqh*-GFP) in order to examine the myosin organization in *Btk29A* mutants. *Sqh*-GFP was localised in a region apical to the SJ marker *Dlg* in *Btk29A* mutants, like in wild type embryos (Figure 26B). It is thus likely that the invagination defect observed in *Btk29A* mutants is not due to impaired acto-myosin organization.

### C.2.B.3d. RhoGTPase activity

Modulation of Rho GTPase activity has been shown to affect spiracular chamber cell invagination (reviewed in Castelli-Gair Hombría et al. (2009)). Specifically, activation of the Rho1 GTPase at the apical region of the spiracular chamber cells is essential for proper invagination of the cells. We therefore wondered whether *Btk29A* modulates spiracular invagination through the regulation of Rho1 spatial activation.

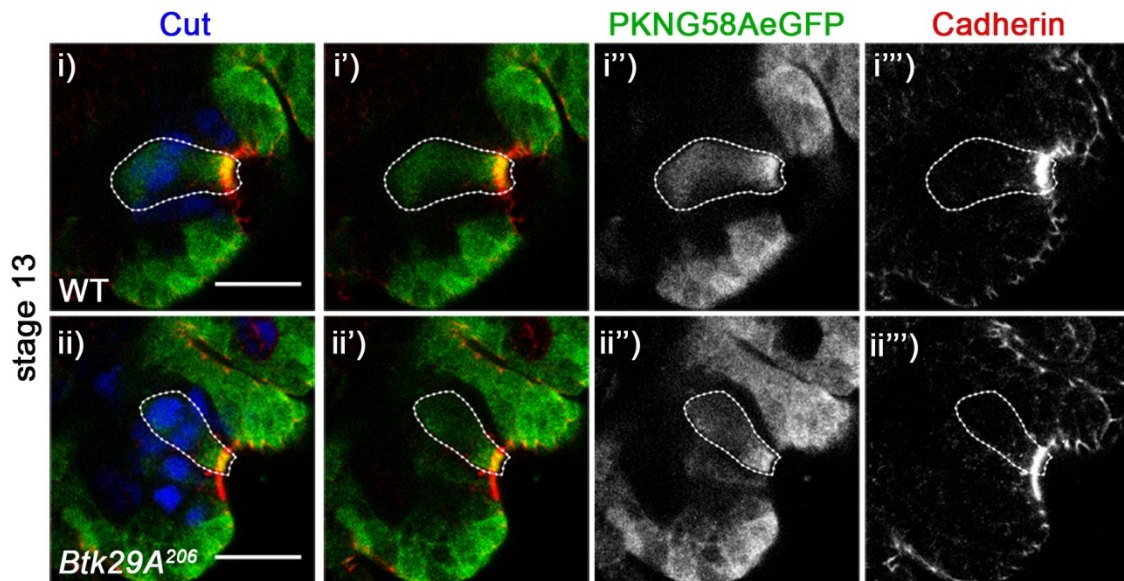


Figure 27: RhoGTPase activity is not affected in *Btk29A* mutants.

The GFP sensor of RhoGTPase activity (PKNG58AeGFP, green) accumulates at higher levels in the apical region of the bottle-shaped spiracular chamber cells (marked with DE-Cadherin, red), both in wild type and mutants (group of 3-4 cells outlined by dotted lines). The spiracular chamber cells were marked with anti-Cut (blue). (Scale bar: 15  $\mu$ m)

Rho1 GTPase activity can be monitored with the GFP-based probe PKNG58AeGFP, which recognizes the active, GTP-bound form of Rho1 (Simões et al., 2006). We expressed PKNG58AeGFP at the posterior spiracle cells (with both the *ems*-GAL4 and *sal*-GAL4 driver) and examined its localization in wild type and *Btk29A* mutant embryos. As shown in Figure 27, the reporter is apically enriched in the spiracular cells of *Btk29A* mutants (the invaginating and the non-invaginating ones), similarly to the wild type. This observation suggests that *Btk29A* is not affecting Rho1 GTPase activity.

### C.2.B.3e. Endoreplication

Endoreplication, a DNA replication process not followed by a subsequent phase of mitosis and/or cytokinesis, is the mechanism through which cells acquire elevated nuclear gene content and become polyploid.

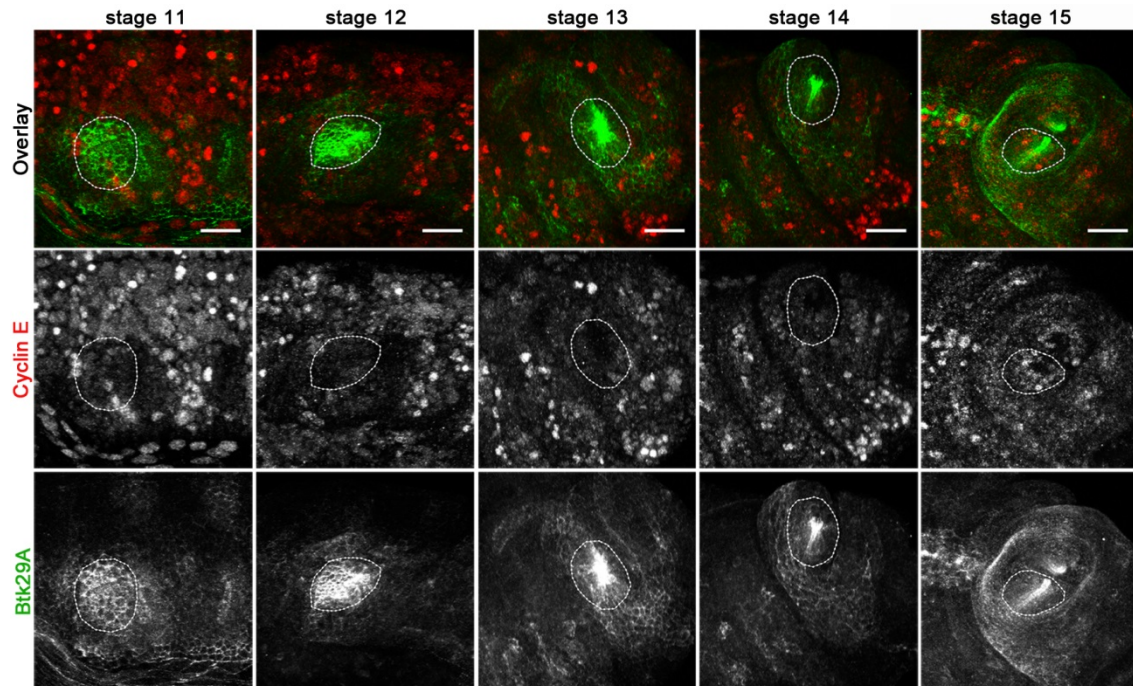


Figure 28: The spiracular cells do not undergo endoreplication.

Cyclin E staining (red) reveals that the posterior spiracle cells are not undergoing replication (or endoreplication) during the morphogenesis of the tissue (stage 11-15). Spiracular chamber cells expressing high levels of *Btk29A* (green) are outlined with dotted lines. (Scale bar: 20  $\mu$ m)

---

During *Drosophila* embryogenesis and subsequent larval life the salivary gland cells are the most characteristic endoreplicating cells. Through endoreplication these cells are establishing the characteristic polytene chromosome. A previous study by Chandrasekaran and Beckendorf, 2005 revealed that *Btk29A* is important for the temporal tuning of the salivary gland cell invagination in relation to the endoreplication process (see also Paragraph A5.B). For this reason, we wondered whether *Btk29A* has a similar function in the posterior spiracles. In order to examine this possibility, wild type embryos were stained with antibodies for Cyclin E (a marker of G1/S phase). We could not detect Cyclin E-positive cells in posterior spiracles from stage 11 to stage 15, suggesting that there is no significant endoreplication around the time of invagination (Figure 28 and (Smith and Orr-Weaver, 1991)).

The results presented in this Paragraph (C.2.B.3) suggest that none of the common features involved in spiracular invagination is affected in *Btk29A* mutants: apical constriction and cell shape changes are normally performed and the apical enrichment of the actomyosin and preferential apical activation of Rho1 GTPase. Additionally, the cells do not seem to undergo endoreplication, a mechanism that could connect the phenotype to the previously described role of *Btk29A* in the salivary gland invagination.

It is thus likely that *Btk29A* is affecting the spiracular chamber invagination process by regulating other, maybe not known parameters in the spiracular chamber cells. Another possibility could be that loss of *Btk29A* function in cells other than the spiracular chamber might interfere, in a non-cell autonomous manner.

---

### C.2.C. Rescue experiments

Spiracular chamber cell invagination is clearly affected in *Btk29* mutants. Yet the mechanism through which Btk29A is regulating this process is not clear, since none of the examined molecular and cellular parameters known to play a role in the invagination of other tissues seems to be affected in the spiracular chamber cells of our mutants (Paragraph C.2.B). For this reason, we wondered whether we could learn something from the results of tissue-specific rescue experiments. Specifically, we aimed to rescue the invagination phenotype of *Btk29A* mutants by driving expression of Btk29 with different GAL4 drivers. Six different drivers were selected (Figure 29) for the expression of the short isoform of Btk29A: Btk29A-C (which is the one expressed by the posterior spiracle cells in wild type - Paragraph C.1.A).

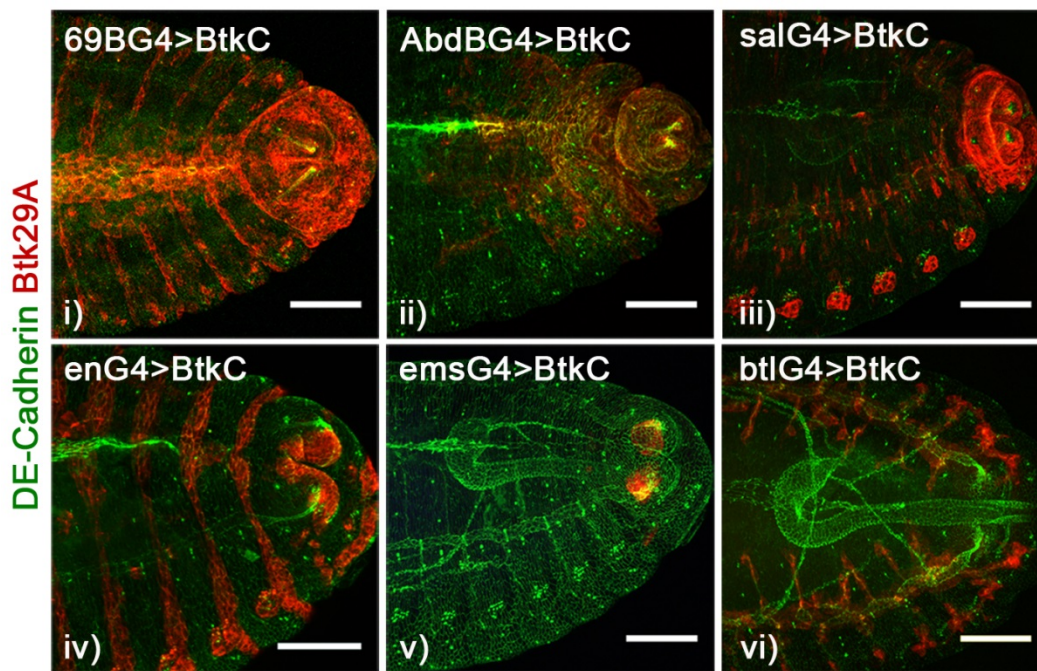


Figure 29: Rescue experiment using selected GAL4 drivers

The expression patterns of six different GAL4 drivers in embryonic stage 15: i) the 69B-GAL4 driver expressed in all the ectodermal cells, ii) the AbdB-GAL4 expressed in the cells of the A8-A11 abdominal embryonic segments, iii) the sal-GAL4 expressed among others by the stigmatophore and the tracheal (and very few of the spiracular chamber) cells, iv) the en-GAL4 expressed among others by some of the stigmatophore cells, v) the ems-GAL4 expressed by most of the spiracular chamber cells and the btl-GAL4 driver expressed by the trachea cells. (Scale bar: 50 μm)

Initially, we used the 69B-GAL4 driver, which drives expression in all the ectoderm-derived cells (central nervous system, epidermis, posterior spiracle cells, trachea, etc). Expression of Btk29A-C in all the ectodermal cells of *Btk29A* mutants rescued the posterior spiracle phenotype



---

(Figure 31iii). The phenotype was similarly rescued with AbdB-GAL4 (driving expression in the cells of abdominal embryonic segments A8 to A11), suggesting a requirement of the kinase in the most posterior embryonic segments (Figure 31iv).

Subsequently, we used the spiracular chamber specific *ems*-GAL4 driver. Phenotypic rescue with *Btk29A-C* expression in the invaginating spiracular chamber cells would suggest a cell autonomous requirement of *Btk29A* in these cells. *ems*-GAL4 failed to rescue the spiracular morphogenesis (Figure 31viii and 32). The spiracular chamber cells failed to invaginate, like in the *Btk29A* mutants.

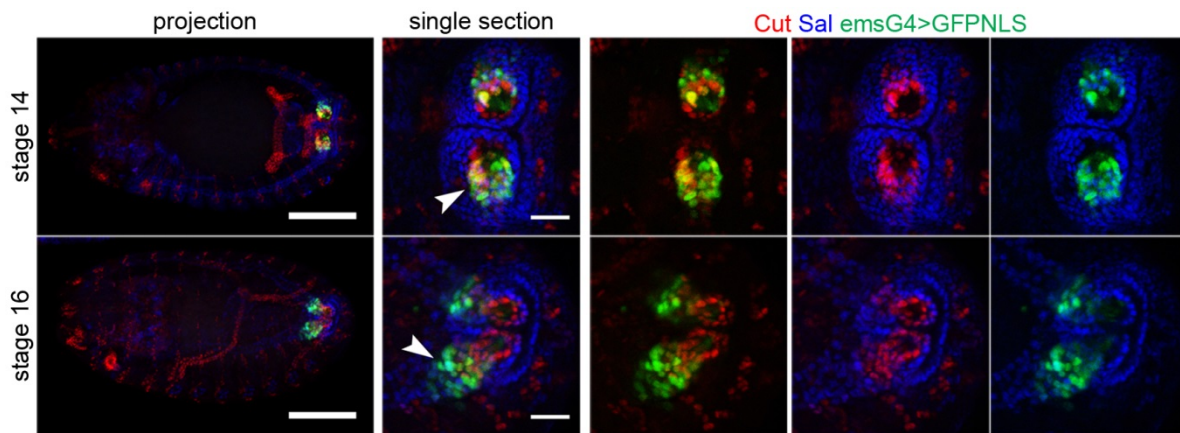
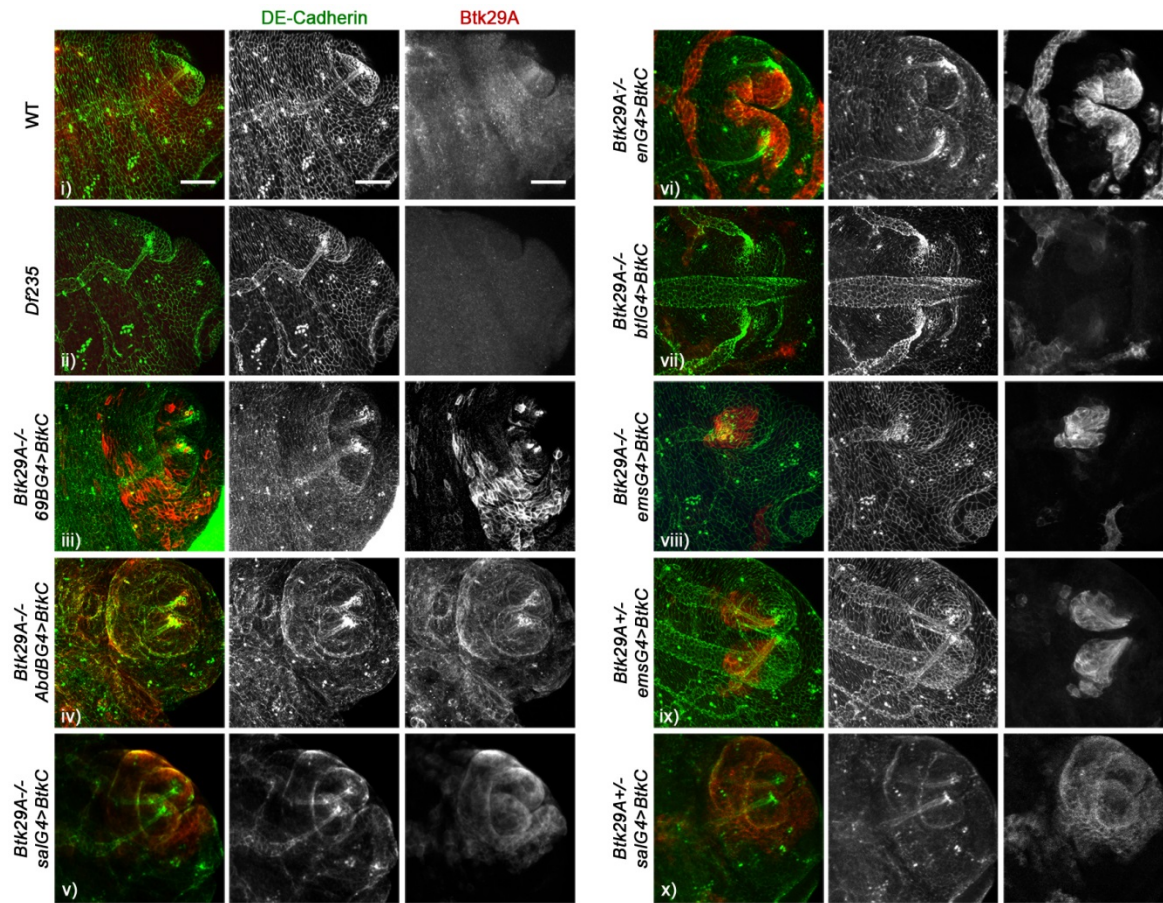


Figure 30: *ems*-GAL4 driver

The expression pattern of *ems*-GAL4 in relation to the stigmatophore (*Sal*<sup>+</sup>, blue) and spiracular chamber (*Cut*<sup>+</sup>, red) cells. Arrowheads point to the spiracular chamber cells. (Scale bar: 100  $\mu$ m for low and 20  $\mu$ m for high magnification)

Since *Btk29A* is also expressed by the neighbouring tissues (trachea and stigmatophore cells), we wondered if the invagination defect in *Btk29A* mutants is a result of the lack of the kinase from these tissues. For this reason, we used the trachea-specific driver *breathless*-GAL4 (*btl*-GAL4) (Shiga et al., 1996) and the *sal*-GAL4 driver which drives expression in the stigmatophore cells (among other tissues). The trachea driver *btl*-GAL4 failed to rescue the phenotype (Figure 31vii).

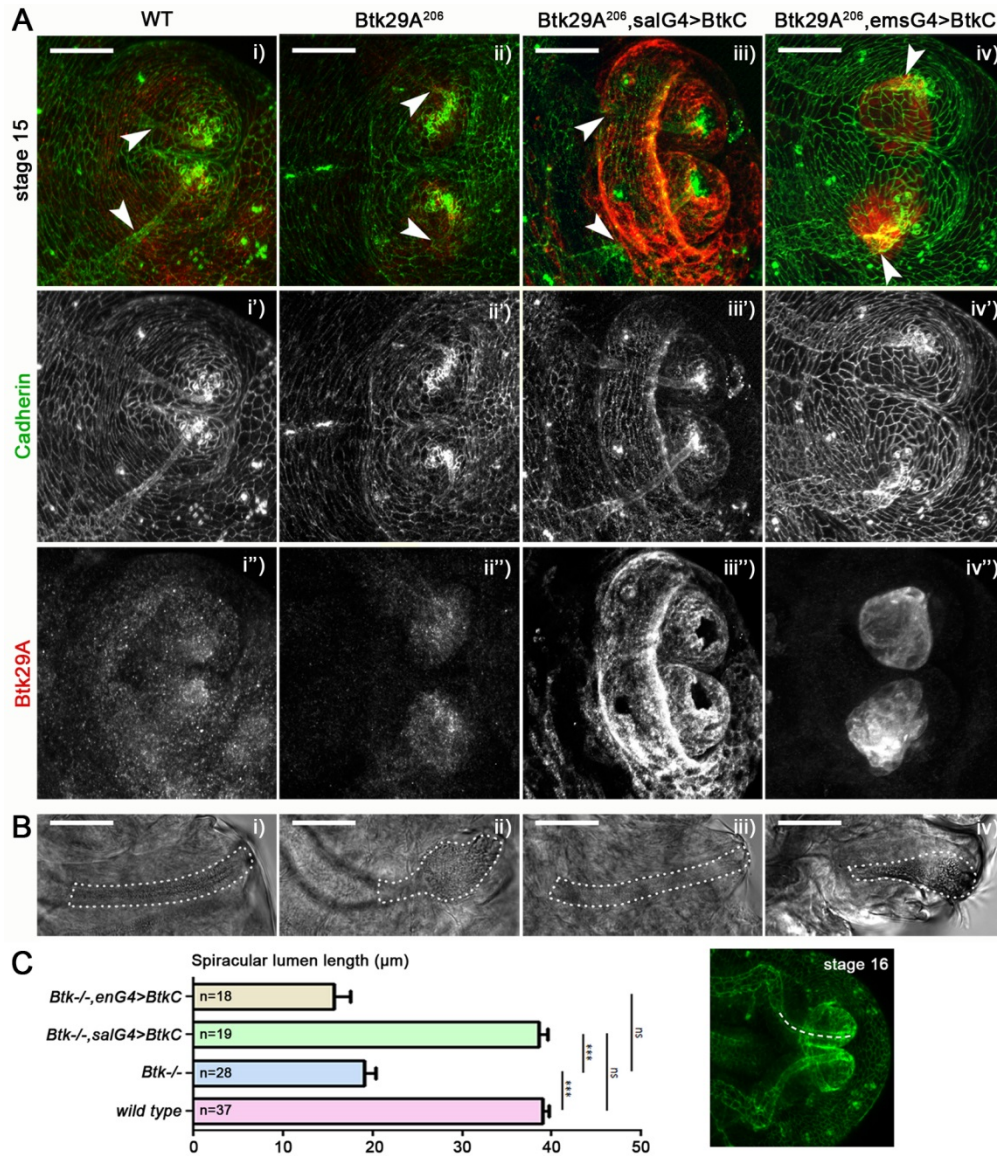


**Figure 31: Rescue experiments**

The spiracular chamber invagination phenotype observed in *Btk29A* mutants was rescued by tissue specific expression of Btk29A-C with three different GAL4 drivers: the ectodermal 69B-GAL4 (iii), the AbdB-GAL4 (iv) and the sal-GAL4 (v). The phenotype could not be rescued with the en-GAL4 (vi), the trachea specific btl-GAL4 (vii) and the ems-GAL4 driver (viii). The overexpression of Btk29-C in wild type embryos with ems-GAL4 or sal-GAL4 did not cause any spiracle phenotype (viii and x respectively). All the embryos are stage 15. Btk29A is depicted in red and DE-Cadherin in green. (Scale bar: 20  $\mu$ m)

Strikingly, the phenotype was rescued by the expression of Btk29A-C under the sal-GAL4 driver (Figure 31v and 32). sal-GAL4 is expressed in several embryonic tissues (subset of trachea, central nervous system, epidermis, etc) (Kuhnlein and Schuh, 1996). At the posterior spiracles it is known to be expressed by the stigmatophore cells (Castelli-Gair Hombría et al., 2009). The mutant embryos expressing Btk29A-C under the sal-GAL4 driver, acquire posterior spiracles similar to wild type: the spiracular lumen has normal length (Figure 32) and the cuticular lining is rescued.





**Figure 32: Rescue of the posterior spiracle morphology**

**A:** The spiracular lumen is shorter in *Btk29A*<sup>206</sup> homozygous mutant embryos compared to the heterozygous ones (i and ii). The phenotype is rescued when we use sal-GAL4 driver to express Btk29A-C in the stigmatophore cells of *Btk29A*<sup>206</sup> mutants (iii), but not when we use the ems-GAL4 driver which is spiracular chamber cell specific (iv).

**B:** Cuticle is deposited inside the lumen of the spiracular chamber of WT embryos at the end of embryogenesis, forming the filzkörper (i). In *Btk29A* mutants the cuticle is still secreted on the apical surface of the non invaginated cells, forming a cuticular layer on the epidermal surface of the abnormally shaped filzkörper (ii). In the sal-GAL4 rescue (iii) the filzkörper (shape and cuticle) is similar to WT (i), while Btk29A expression with ems-GAL4 does not rescue the phenotype (iv, similar to ii). Filzkörper outlined with dotted lines.

**C:** Quantification of spiracular lumen length (outlined with dashed line in the figure on the right; DE-Cad in green) in WT, *Btk29A* mutants and rescued embryos expressing the Btk29A-C in all (sal-GAL4) or some of the stigmatophore cells (en-GAL4). The luminal length is significantly reduced in *Btk29A* mutants ( $P < 0.0001$ ), gets back to normal length with Btk29A-C expression driven by sal-GAL4, but not with en-GAL4. All the embryos are stage 15. Btk29A is depicted in red and DE-Cadherin in green. Arrowheads indicate the meeting point of the trachea and spiracle. (Scale bar: 20 µm)

---

The above suggests that the spiracular chamber invagination defect in *Btk29A* mutants could be due to a non-cell autonomous function of the protein in the stigmatophore cells.

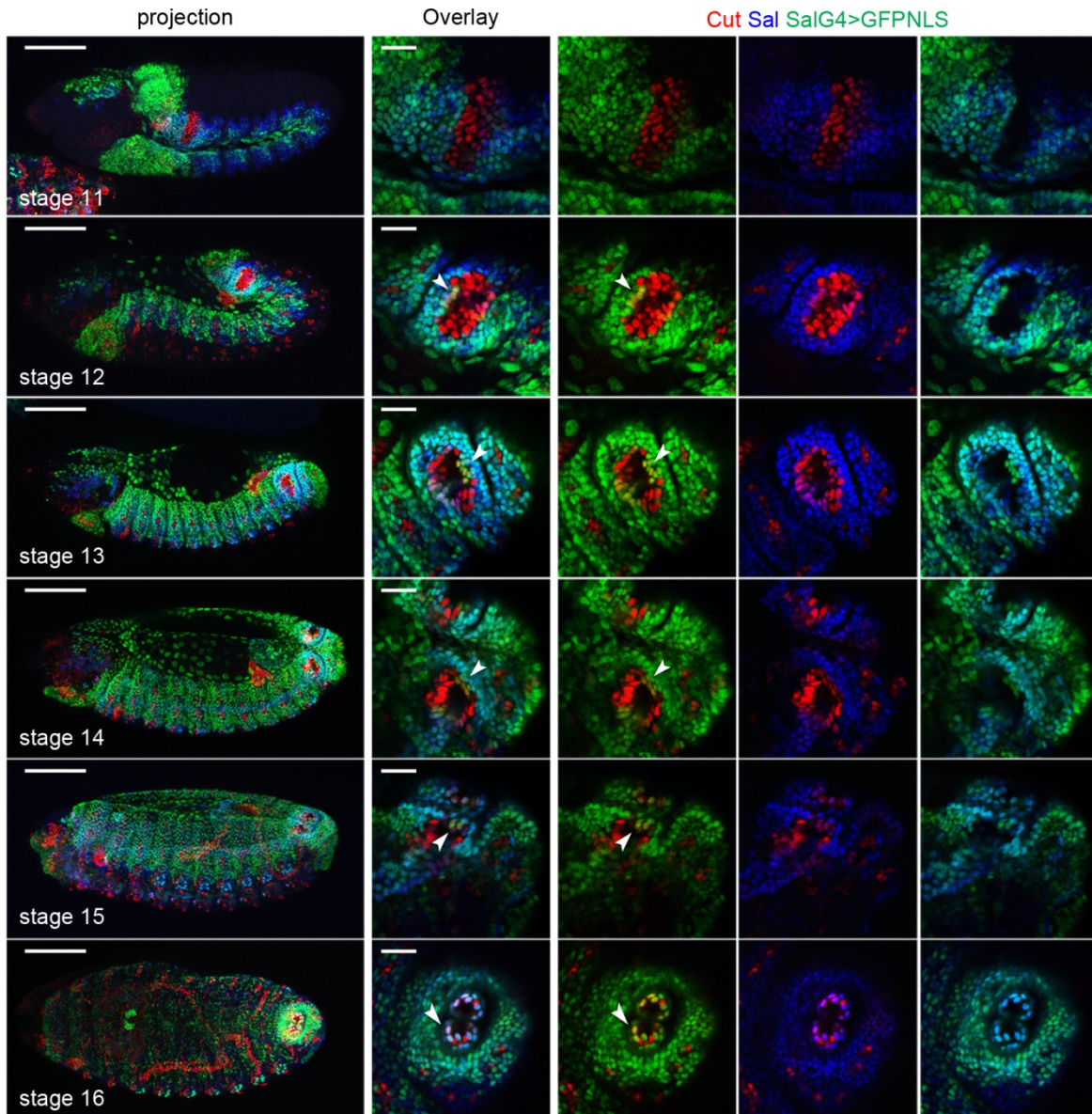
sal-GAL4 is considered as a stigmatophore-specific driver, not expressed in the spiracular chamber. Antibody staining of wild type embryos expressing UAS-GFP.NLS (Green Fluorescent Protein that carries a signal for nuclear tagging) under the sal-GAL4 driver revealed very few distal Cut-positive spiracular chamber cells that co-express, at low levels, sal-GAL4 driven GFP.NLS (Cut+, GFP+ cells in Figure 33). It should also be noted that *ems-GAL4* is not expressed in all of the Cut+ spiracular chamber cells: it is absent from very few among the most distal Cut-positive cells and in particular from the future spiracular hairs (Figure 20 and 30).

The expression of sal-GAL4 by some distal spiracular chamber cells, in combination with the fact that *ems-GAL4* driver is not expressed by some of the distal-most spiracular chamber cells (Figure 30) suggests that *Btk29A* expression in these very few distal cells is necessary (and sufficient) to complete the invagination of spiracular chamber.

In order to exclude this possibility, we performed one more rescue experiment using the engrailed-GAL4 (*en-GAL4*) driver. *en-GAL4* is expressed in a subset of Spalt-positive cells in the stigmatophore (Figure 34) (Hu and Castelli-Gair, 1999). It is also expressed in the same few cells of the distal spiracular chamber that express Cut and low levels of Spalt, like sal-GAL4. If expression of *Btk29A* in such cells is necessary and sufficient for the invagination of the spiracular chamber, we would achieve rescue of the invagination defects in *en-GAL4* rescue experiments.

As shown in Figures 31 and 32, *Btk29A* expression under the *en-GAL4* driver failed to rescue the spiracular phenotype in *Btk29A* mutants. Thus we can conclude that the recovery in the spiracular chamber cell invagination observed in sal-GAL4 rescued embryos is not due to the cell autonomous function of *Btk29* in the few “Cut+, Sal+, *en-GAL4*+” cells. Instead, it seems to depend on the expression of *Btk29A* by the Sal+ stigmatophore cells. Moreover the expression of the protein in only some of the stigmatophore cells (those that are both Sal+, *en-GAL4*+) is not sufficient to rescue the phenotype. But what is the role of *Btk29A* in the stigmatophore cells? And how can the kinase affect spiracular chamber invagination through the regulation of neighbouring structures?





**Figure 33: sal-GAL4 driver expression pattern**

Sal-GAL4 (green) driver expression in relation to the stigmatophore (Sal+, blue) and spiracular chamber (Cut+, red) cells from stage 11 till the end of the embryogenesis. Sal-GAL4 expression is highly overlapping with the Sal protein expression in the stigmatophore and trachea. It is also expressed by the epidermal cells and cells of the CNS. We observed that sal-GAL4 is also expressed by two distinct, very small groups of spiracular chamber cells (Cut+): one group close to the trachea (at the meeting point of the two tissues) and one group at the distal most part of the spiracular chamber (cells marked with arrowheads). Number of distal “Cut+, sal-GAL4+” cells from stage 11 to 16: 0, 4, 6, 7, 8, 10 respectively. (Scale bar: 100  $\mu$ m for low and 20  $\mu$ m for high magnification)

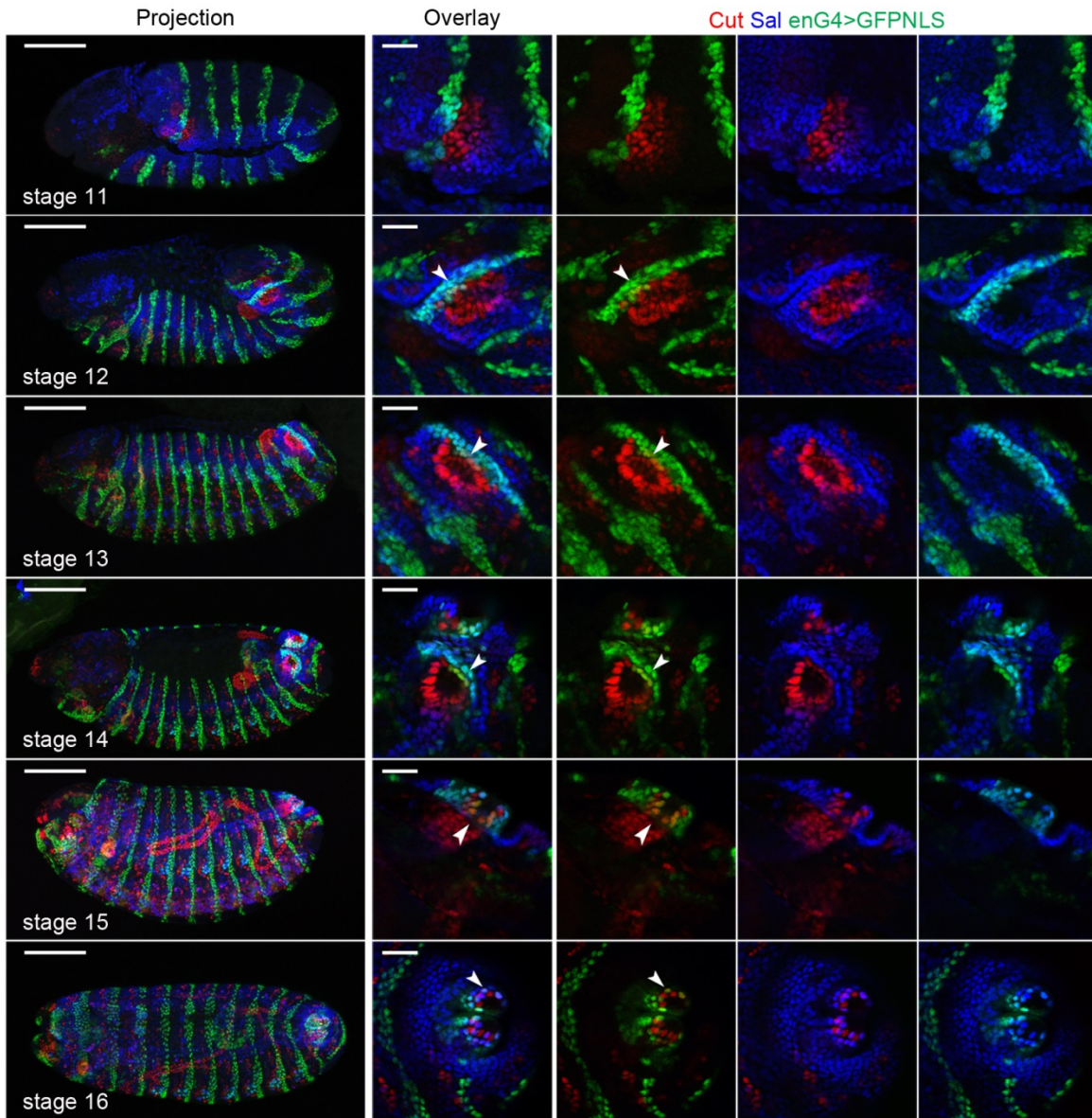


Figure 34: en-GAL4 driver expression pattern

Expression pattern of en-GAL4 (green) in relation to the stigmatophore (Sal+, blue) and spiracular chamber (Cut+, red) cells from stage 11 till the end of the embryogenesis. en-GAL4 is expressed in segmental stripes. We analyzed the expression of the driver in the posterior spiracles. One of the abdominal stripes of the GAL4 is overlapping with some of the Sal+ cells of the stigmatophore (“en-GAL4+, Sal+” cells). We also observed that en-GAL4 is expressed in few of the distal Cut+ cells of the spiracular chamber (cells marked with arrowheads). Number of “Cut+, en-GAL4+” cells from stage 11 to 16: 1, 4, 6, 6, 9, 9 respectively. (Scale bar: 100  $\mu$ m for low and 20  $\mu$ m for high magnification)



---

### C.2.D. Stigmatophore cell rearrangements

The stigmatophore, the external part of the posterior spiracles, is a protruding structure that surrounds the spiracular chamber and supports the overall organ. Its development depends on the spatial re-arrangements of the cells of its anlagen, which is regulated by the transcription factors Spalt and Grain (Grn) (Brown and Castelli-Gair Hombria, 2000) (see also Paragraph A.2.B.2).

The previous results (Paragraph C.2.C) suggest that *Btk29A* regulates the invagination of the spiracular chamber cells of the posterior spiracles non-cell autonomously, via its function in the neighbouring stigmatophore cells. In order to examine this hypothesis, we tried to analyse if and how *Btk29A* affects stigmatophore development.

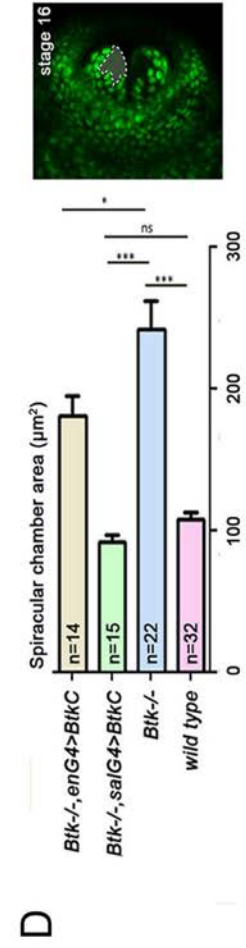
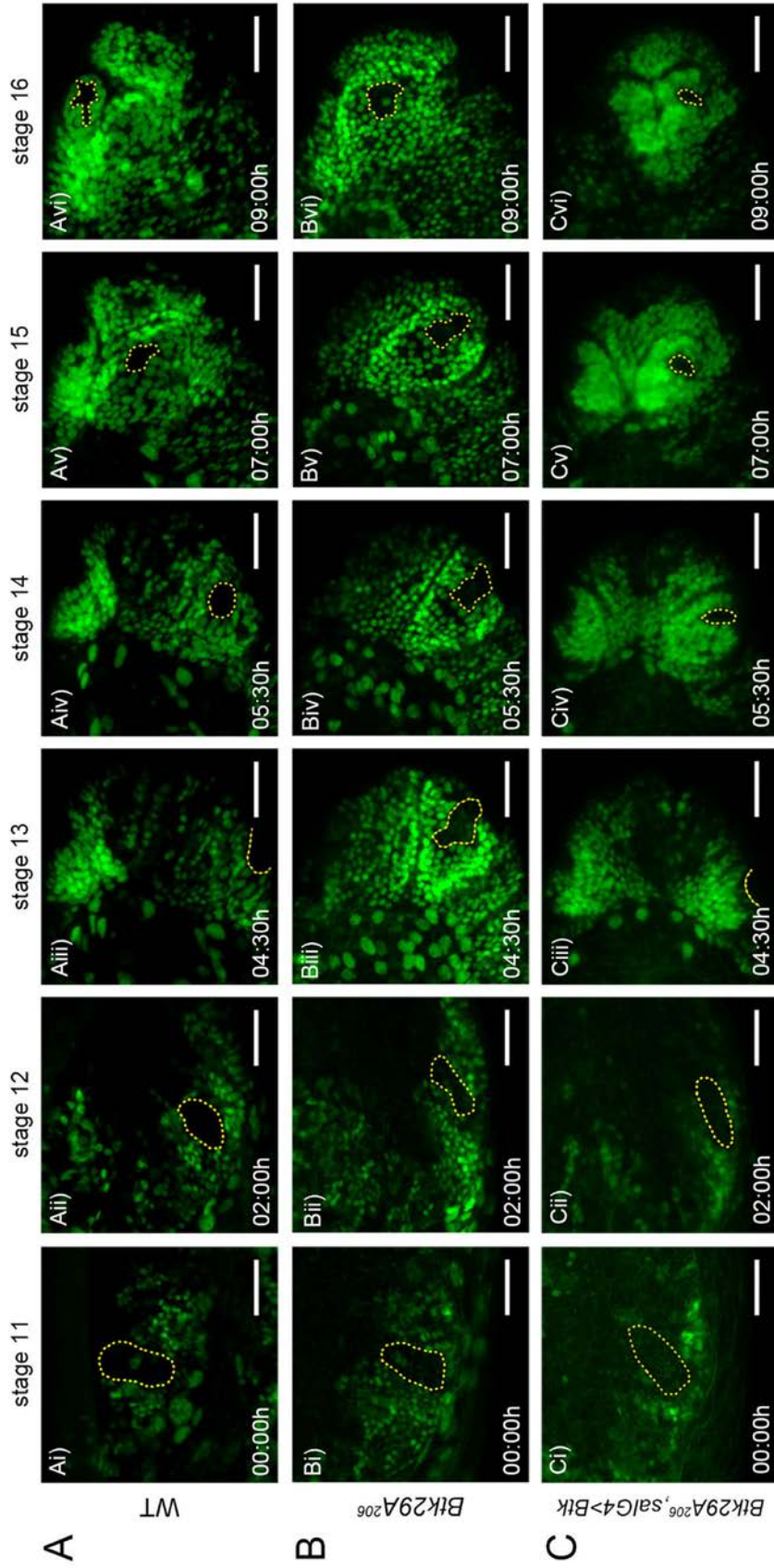
#### C.2.D.1. Defective cell rearrangements during stigmatophore morphogenesis in *Btk29A* mutants

For the analysis of the role of *Btk29A* in stigmatophore morphogenesis, the stigmatophore cells of fixed or live wild type and *Btk29A* mutant embryos were followed, with antibody staining and in vivo imaging respectively. The stigmatophore cells were marked either with anti-Sal or with the expression of nuclear GFP under the sal-GAL4 driver (sal-GAL4>UAS-GFP.NLS).

As shown in Figure 35A, the stigmatophore cells are initially specified in early stage 11, next to the Cut<sup>+</sup> spiracular chamber cells (located in the region outlined with yellow dotted line). During embryonic development these cells undergo convergent extension movements that contribute to the elongation of the stigmatophore; concomitantly, Cut<sup>+</sup> cells of the spiracular chamber invaginate (Figure 35A, also (Brown and Castelli-Gair Hombria (2000); Hu and Castelli-Gair (1999)) and Paragraph A.2.B.2). By the end of embryogenesis, the cells have completed the rearrangements and, at the surface of the embryos, the inner “Cut<sup>+</sup> cell area” has been restricted to a smaller area.

In *Btk29A* mutant embryos, the cells are correctly specified in early stage 11, but the subsequent cell arrangements are abnormal: although the cells undergo some movements to completely surround the spiracular chamber cells, they fail to restrict the “Cut<sup>+</sup> cell area”. More specifically, the spiracular area is restricted to around 106.8  $\mu\text{m}^2$  in wild type embryos, while in *Btk29A* mutants it occupies around 240.6  $\mu\text{m}^2$  (Figure 35).





---

### Figure 35: Abnormal cell rearrangements in *Btk29A* mutants

The spatial rearrangements of the stigmatophore cells (expressing sal-GAL4, UAS-GFP.NLS) were monitored with in vivo imaging in different genetic backgrounds.

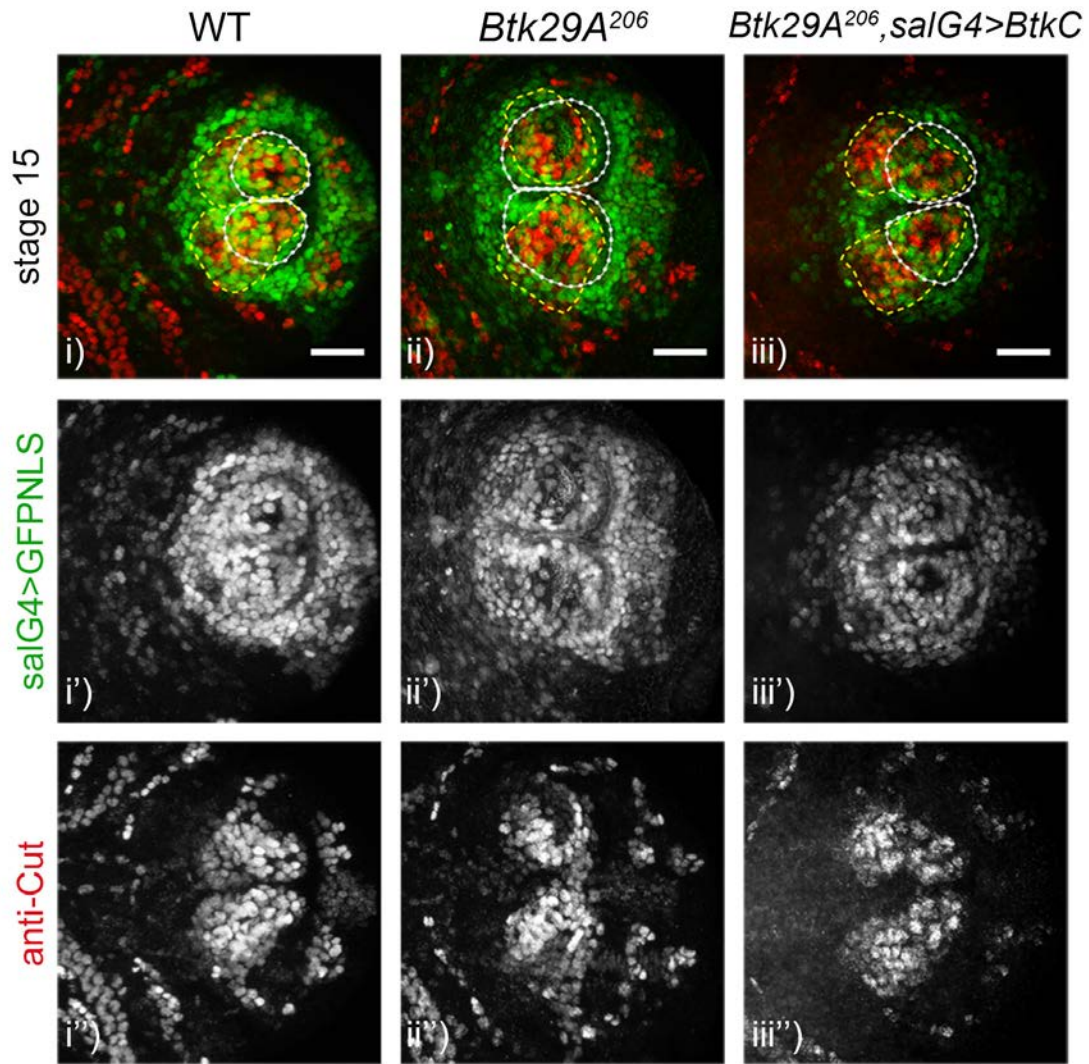
A. In WT embryos (Ai-Avi), stigmatophore cells rearrange their positions in the plane of the epidermis, starting at stage 11 (beginning of posterior spiracle morphogenesis) and reaching their final position by the end of embryogenesis. These rearrangements (convergent extension) lead to the apparent restriction of the area occupied by the unmarked (GFP-negative) spiracular chamber cells (outlined in yellow) and the increase of the width of the stigmatophore (Brown and Castelli-Gair Hombria, 2000).

B. In *Btk29A* homozygous mutants (Bi-Bvi) the stigmatophore cells do not perform such cell rearrangements so they fail to properly shape the stigmatophore. Additionally, the black area of the unmarked spiracular chamber cells never reaches the narrow asterisk like shape seen in stage 16 WT embryos (Avi).

C. In *Btk29A* homozygous mutants that express Btk29A in the stigmatophore cells under control of sal-GAL4 (Ci-Cvi), the GFP+ cells are rearranging their positions and come in closer proximity to each other. The area of the spiracular chamber is becoming narrow similarly to the WT and in some cases even more (Civ-Cvi). ubiCadherinGFP was recombined with *Btk29A*<sup>206</sup> and used for selection of homozygous mutant embryos in B and C. In stage 13 (iii) the spiracular chamber cannot be visualised completely due to embryo movements at germ-band retraction. (Scale bar: 30  $\mu\text{m}$ )

D. Quantification of the spiracular chamber area (outlined with dashed lines in the figure on the right) in WT, *Btk29A* mutants and embryos expressing Btk29A in all (sal-GAL4) or some of the stigmatophore cells (en-GAL4). The spiracular area is significantly wider in *Btk29A* mutants ( $240.6 \pm 20.89 \mu\text{m}^2$ , N=22) than in WT ( $106.8 \pm 5.622 \mu\text{m}^2$ , N=32) ( $P < 0.0001$ ). The size of the spiracular area is fully rescued in mutant embryos expressing Btk29A in all the (stigmatophore cells (with sal-GAL4) ( $90.72 \pm 5.231 \mu\text{m}^2$ , N=15). The spiracular area phenotype is only partially rescued in embryos expressing Btk29A in some of the stigmatophore cells (with en-GAL4) ( $179.8 \pm 14.38 \mu\text{m}^2$ , N=14) (difference from WT  $P < 0.0001$ , difference from *Btk29A* homozygous mutants  $P = 0,0413$ ). Unpaired t test was used for the data analysis.

Antibody staining with anti-Cut of wild type and mutant embryos expressing GFP.NLS under the sal-GAL4 driver allows us to visualize both stigmatophore and chamber cells. This revealed that the GFP+ (= Sal+) stigmatophore cells only partially surround the defective spiracle opening in *Btk29A* mutants. Interestingly both the Sal+ stigmatophore and the Cut+ spiracular chamber nuclei appear to have a more medial localization compared to the wild type (Figure 36).



**Figure 36: *Btk29A* affects the posterior spiracle cell positioning**

By stage 15, the Cut<sup>+</sup> (red) cells of the spiracular chamber have acquired their final position, forming a pear-shaped spiracular chamber (i'' and outlined in yellow in i), while the Sal<sup>+</sup> (green) cells have rearranged, enwrapping the Cut<sup>+</sup> cells and forming the protruding stigmatophore (i' and outlined in white in i). In *Btk29A* mutants, the positioning of the posterior spiracle cells is affected, with both the Cut<sup>+</sup> and Sal<sup>+</sup> nuclei preferentially localized at the medial side of the spiracle. This leads to a shorter and thicker spiracular chamber (ii'' and outlined in yellow in ii) and an increase in the area occupied by the stigmatophore cells (ii' and outlined in white in ii) compared to WT (i' and outlined in white in i). The arrangement of the spiracle cells is highly restored in homozygous mutants expressing *Btk29A* in Sal<sup>+</sup> cells (iii-iii''). (Scale bar: 20  $\mu$ m)

---

### **C.2.D.2. Btk-dependent cell rearrangements in the stigmatophore contribute to the invagination of the spiracular chamber**

The above observations show that the stigmatophore cells do not perform the necessary rearrangements in *Btk29A* mutants. Together with the rescue obtained with sal-GAL4 driven expression of *Btk29A*, this suggests that abnormal convergent extension movements of stigmatophore cells in the mutant lead to the impairment of the Cut<sup>+</sup> spiracular chamber cell morphogenesis. For this reason, we examined the convergent extension of stigmatophore cells after restoration of *Btk29A* expression in the stigmatophore by the sal-GAL4 driver and compared it to wild type and mutant embryos.

We wondered if we could detect a correlation between rescue of the stigmatophore cell rearrangements and of chamber invagination. Interestingly, the positioning of both spiracular chamber and stigmatophore cells was restored (Figure 36). Additionally, live imaging showed that, in the rescue experiments, the stigmatophore cells underwent the necessary convergent extension movements thus restricting the spiracular chamber cell area (around 91  $\mu\text{m}^2$ ) similarly to wild type spiracles (Figure 35D). In some cases, the area was restricted to an even smaller size.

We conclude that *Btk29A* is required cell autonomously in stigmatophore cells to perform the planar cell rearrangements that are necessary for stigmatophore morphogenesis. Moreover, these rearrangements are affecting non cell-autonomously the invagination of the nearby spiracular chamber cells.

### **C.2.D.3. Grain affects the stigmatophore cell rearrangements**

As described in Paragraph A.2.B.2, little information is available about the cell rearrangements that lead to proper stigmatophore formation. Stigmatophore cells are specified by the homeotic gene *AbdB* in the framework of the posterior spiracle developmental program. They express the transcription factors *Sal* (see Paragraph A.2.B.3) and *Grain* (Figure 37 and Brown and Castelli-Gair Hombria (2000)). More specifically, *Grn* expression in the spiracles begins at stage 11 in a group of stigmatophore cells (Figure 37i). During stage 13 all stigmatophore cells express *Grn*. This expression remains at high levels throughout posterior spiracle morphogenesis (Figure 37iii). *Grn* is described as a stigmatophore transcription factor, yet, there are references for *Grn* expression by the spiracular chamber cells (Brown and Castelli-Gair Hombria, 2000). Our analysis did not reveal expression of *Grn* in the spiracular chamber cells (Figure 37).



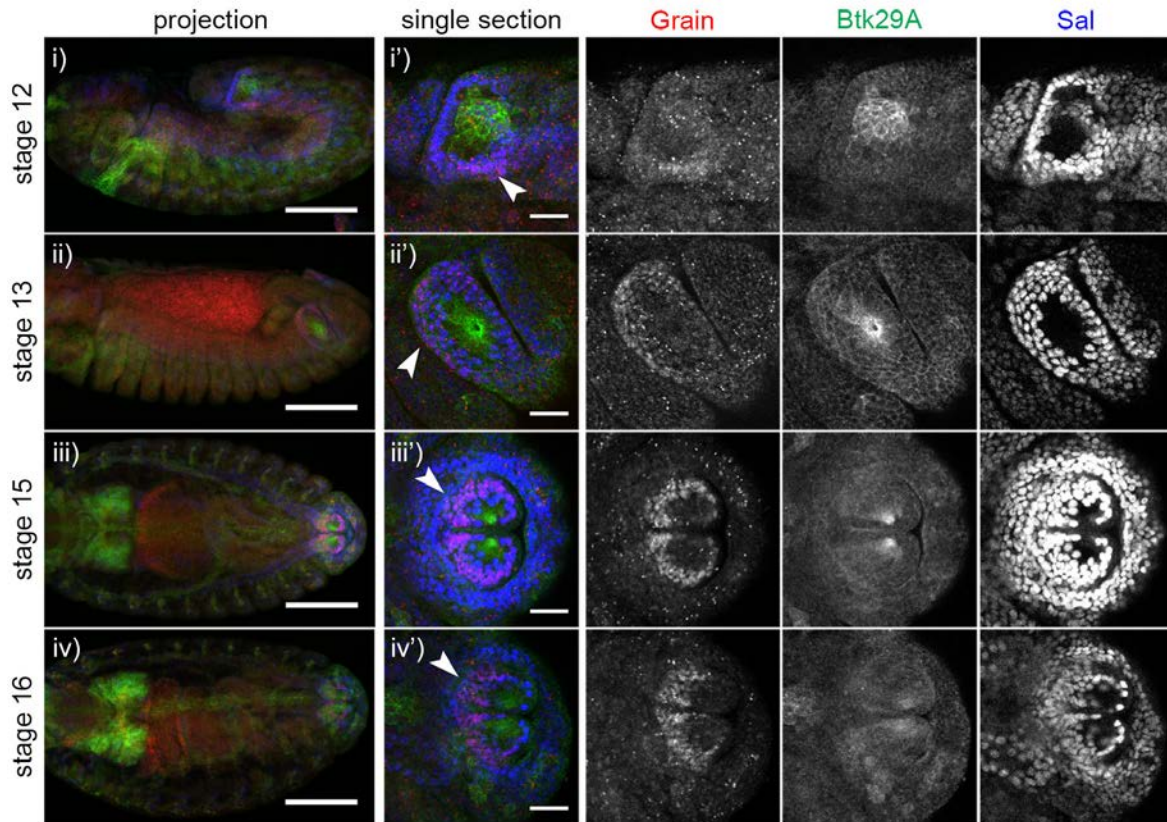


Figure 37: Expression of Grain at the posterior spiracles

Grain expression is initially detected at stage 11 of embryogenesis. It gets stronger and persists till the end of the morphogenesis. (Scale bar: 100  $\mu\text{m}$  for low and 20  $\mu\text{m}$  for high magnification)

In homozygous mutant embryos for *grain* stigmatophore cell rearrangements are impaired. According to Brown and Castelli-Gair Hombria (2000), *grn* mutant embryos display abnormally formed stigmatophores as well as shorter spiracular chamber lumen. In order to check if there is a correlation of *grain* function with the role of *Btk29A* in the posterior spiracle morphogenesis, we performed antibody stainings in *grn*<sup>7L</sup> homozygous mutant embryos and compared the phenotypes to the ones observed in *Btk29A* mutants.

*grn*<sup>7L</sup> mutants exhibit a severely impaired arrangement of both the stigmatophore and the spiracular chamber cells (Figure 38A). Additionally, the spiracular lumen length is significantly shorter compared to wild type (Figure 38B) and the cuticle deposition is abnormal (Figure 38C). The overall defects of the tissue are rather similar to those of *Btk29A* mutants, albeit more severe (compare Figure 36, 32A and 32B to Figure 38A, 38B and 38C respectively).

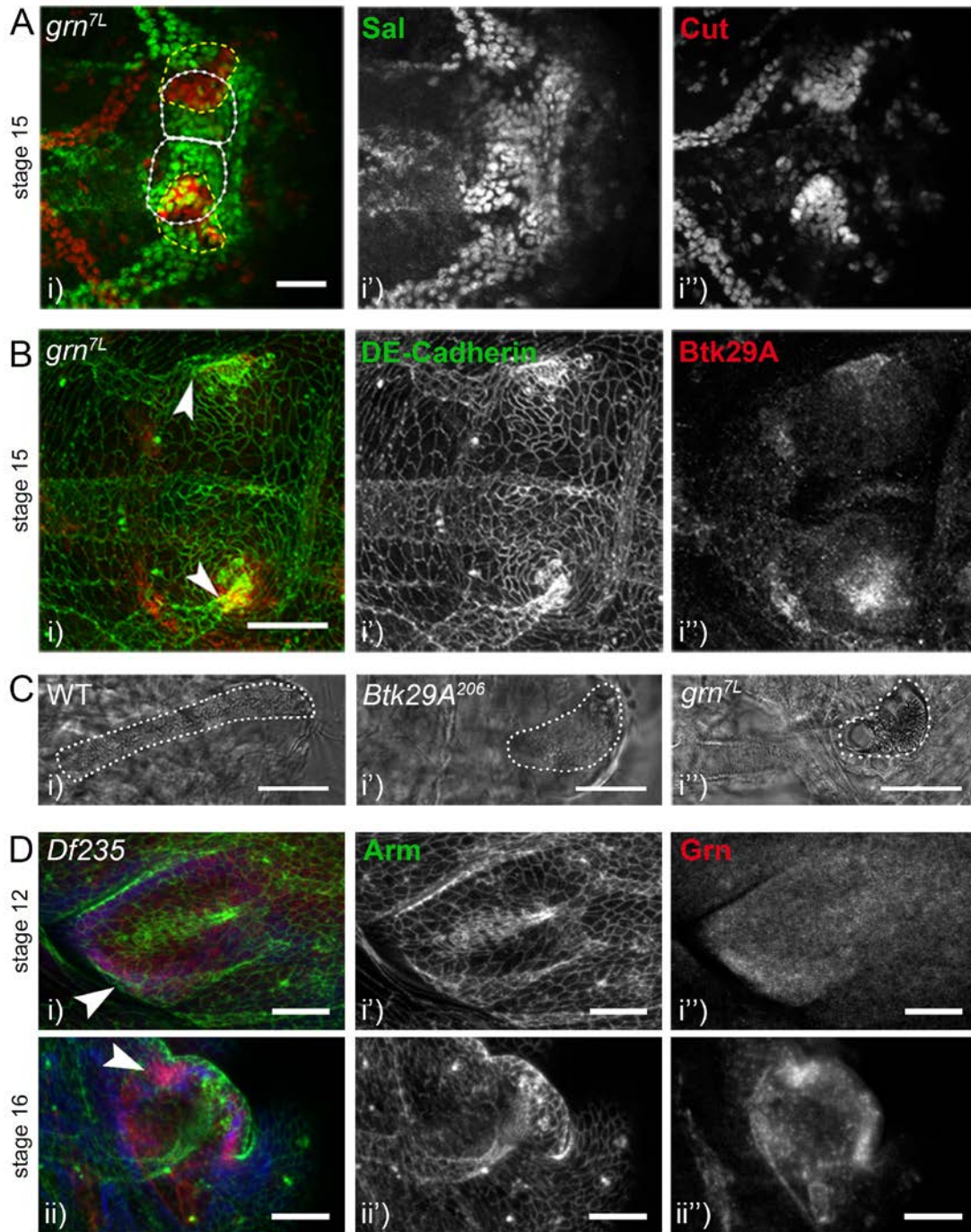


Figure 38: The posterior spiracle morphogenesis is impaired in *grain* mutants.

A. In *gm<sup>7L</sup>* homozygous mutants, both spiracular chamber (*Cut*+, red) and stigmatophore (*Sal*+, green) cells show a severely deranged spatial arrangement. B. The lumen of the spiracular chamber (outlined with *DE-Cadherin*, green) is shorter compared to the WT, and the shape of the stigmatophore is abnormal, but the expression of *Btk29A* (red) is not affected. Arrowheads indicate the meeting point of the trachea and spiracle. C. The shape and cuticle of the filzkörper are similarly abnormal in *Btk29A<sup>206</sup>* and *gm<sup>7L</sup>* homozygous embryos. Filzkörper outlined with dotted lines. D. The expression of *Grn* (red) is not affected in *Df235* mutants. (*Armadillo* in green) (Scale bar: 20 μm)



---

Stainings with anti-Btk29A revealed that the Btk29A expression is not affected in the abnormally shaped posterior spiracles of *grn*<sup>7L</sup> mutants (Figure 22iv and 37B). Additionally, Grn expression is not affected in *Btk2A* mutants (Figure 38D). Thus, we can conclude that the expression of *Btk29A* is not regulated by Grn and Btk29A does not affect *Grn* expression. However, the phenotypic similarities displayed in mutants for the two genes suggest a possible action of *Btk29A* and *grain* in the same or in parallel pathways to properly organise stigmatophore cell rearrangements.

### C.2.E. Btk29A in convergent extension-like movements

The above described experiments unravelled that stigmatophore cell rearrangements are disrupted in *Btk29A* mutants. But what is the involvement of the kinase in the regulation of such morphogenetic changes?

There is no previous analysis on the molecular-cellular mechanisms that drive the stigmatophore movements. However, they are described to resemble the convergent extension movements (Brown and Castelli-Gair Hombria, 2000) observed during development of several organisms (Keller et al., 2000).

Convergent extension is the process through which tissues are restructured to narrow along one axes and elongate towards the perpendicular axis. In *Drosophila*, such movements are known to take place during gastrulation, in order to facilitate the accompanying embryonic germ band extension along the anterior - posterior (A - P axis), with concurrent narrowing of the dorsal - ventral (D - V) axis. Convergent extension movements are directed by the establishment of planar cell polarity within the rearranging cells (Zallen and Wieschaus, 2004). More specifically, the A - P cell borders of these cells are enriched in actin and myosin cables (AJ destabilizing factors), while the D - V cell borders are enriched in AJ components like Bazooka and Par3 (stabilizing AJs).

In order to understand the molecular bases of the stigmatophore cell convergent extension like movements, we decided to examine the subcellular distribution of AJ components, non-muscle myosin-II heavy chain (Zipper) (Jordan and Karess, 1997) and filamentous actin (F-actin) in the stigmatophore cells of wild type embryos. Differential subcellular distribution of any of these factors would suggest a molecular similarity to the well-studied germ band extension movements. The distribution of this/ these factors would then be examined in *Btk29A* mutants. Preliminary analysis of the subcellular localization of DE-Cadherin, Zipper and F-actin, with antibody staining

---

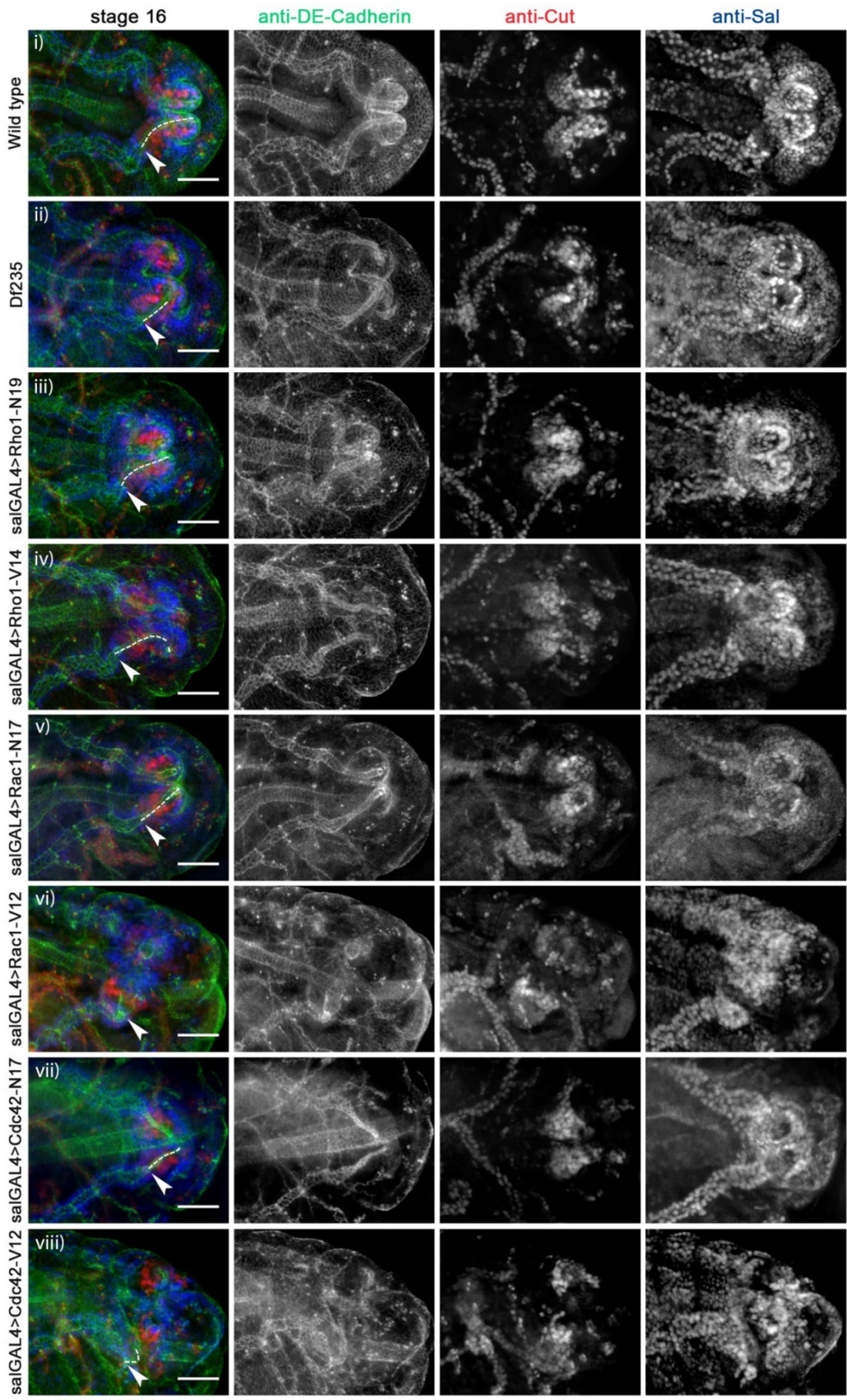
of fixed wild type embryos did not reveal a polarized subcellular localization: they were observed around the cell periphery of the stigmatophore cells (data not shown). These results suggest that the convergent extension movements of the stigmatophore cells are not regulated by the polarized localization of these factors. However, it is likely that our approach did not enable the detection of such polarized localization, since this process could be extremely dynamic. A more thorough *in vivo* analysis of the distribution of fluorescently tagged forms of the above molecules in live embryos would give a more accurate view.

In a different attempt to identify the molecular basis of the stigmatophore cell arrangements, we examined the effect of the small RhoGTPases: Rho1, Rac1 and Cdc42 in the process. These molecules have been previously implicated in convergent extension movements in *Drosophila* and *Xenopus* (Choi and Han, 2002; Simões et al., 2006; Tahinci and Symes, 2003).

Dominant negative (DN) and constitutively active (CA) forms of the three GTPases were expressed in the stigmatophore cells of wild type embryos, under the Sal-GAL4 driver. Stage 16 embryos were subsequently stained with anti-Cut and anti-Sal (in order to distinguish the stigmatophore and spiracular chamber cells), and anti-DE-Cadherin (in order to observe the cell profiles). The morphology of the posterior spiracles was examined.

As shown in Figure 39, the overexpression of all DN forms of Rho1 (Rho1-N19, Figure 39iii), Rac1 (Rac1-N17, Figure 39v) and Cdc42 (Cdc42-N17, Figure 39vii) did not affect the posterior spiracle morphology: the distribution of the stigmatophore and spiracular chamber cells was similar to wild type (Figure 39i) and the spiracular lumen acquired the normal length. Contrary to this, the overexpression of the CA forms of the RhoGTPases lead to strong impairment of posterior spiracle morphogenesis: Rho1-V14 (Figure 39iv) overexpressing embryos acquire an irregular stigmatophore and slightly elongated spiracular chamber lumen, while Rac1-V12 (Figure 39vi) and Cdc42-V12 (Figure 39viii) display completely impaired stigmatophore and they lack a spiracular chamber.

However, none of the observed embryos (expressing the different forms of RhoGTPases) showed posterior spiracle phenotype similar to that of *Btk29A* mutants (Figure 39ii for *Df235*). Further analysis (that exceeds the scope of the current study) is necessary in order to unravel the role of these molecules in posterior spiracle morphogenesis.



---

Figure 39: RhoGTPases in posterior spiracle morphogenesis

Constitutively active and dominant negative forms of the RhoGTPases: Rho1, Rac1 and Cdc42 were expressed in the stigmatophore cells of wild type embryos and the posterior spiracle morphology was examined. The above panels show the arrangement of the spiracular chamber (Cut+, in red) and stigmatophore (Sal+, in blue) cells of the posterior spiracles, while DE-Cadherin (green) marks the cell profiles. i) wild type, ii) of *Df235* homozygous mutant embryo, iii-viii) embryos expressing different forms of RhoGTPases. (Scale bar: 20  $\mu$ m)

---

### C.3. Btk29A in tracheal system development and function

---

As mentioned in the Paragraph A.4 we identified *Btk29A* as a gene whose mutations affect the morphogenesis of posterior spiracles (Paragraph C.2) and also disrupt the tracheal epithelial permeability barrier. *Btk29A* mutant embryos have a leaky tracheal epithelium: rhodamine-tagged dextran molecules injected in the hemocoel of the embryo are able to diffuse into the tracheal lumen.

The development of the *Drosophila* tracheal system is a multi-step procedure that requires the proper specification, invagination, migration and fusion of the tracheal cells, in order to form a complex tubular network (Paragraph A.3.A). This tubular network will gradually develop to acquire its final size: during the maturation phase, rounds of secretion and endocytosis control the attainment of the proper tube diameter and the final clearance of the lumen; luminal liquid clearance and air filling conclude trachea maturation just before hatching (Tsarouhas et al., 2007). Impairment of any of the above steps leads to the failure of the following steps and eventually to a non-functional respiratory system.

Epithelia surround the body of organisms and separate organs and organ compartments. One of their key functions is to act as permeability barriers, thus limiting and controlling the free diffusion of solutes across the two sides of the epithelium. In *Drosophila*, epithelial permeability barriers are dependent on Septate Junctions (SJs) (see Paragraph A.3.B). SJs consist of highly conserved protein complexes that facilitate the connection of the cells and the assembly of the structure. Mutations in most of the SJ components lead to the disruption of SJ complex integrity and thus to defective permeability barrier (Genova and Fehon, 2003). They also affect tracheal morphology (Paul et al., 2003; Wu et al., 2004; Wu and Beitel, 2004), epithelial polarity (Lecuit and Wieschaus, 2002), luminal secretion and organization (Nelson et al., 2010; Wang et al., 2006) and tracheal system maturation (Tsarouhas et al., 2007).

A series of experiments were performed in an attempt to identify which processes are perturbed in tracheal development and maturation in *Btk29* mutants and at what stage. Initially, the trachea system was observed for gross morphological defects (Paragraph C.3.A1 and C.3.A.2). Then, cell polarity (Paragraph C.3.B.1) and SJ organization (Paragraph C.3.B.1 and C.3.B.2) were examined, as well as luminal deposition of chitin and chitin-modifying enzymes (Paragraph C.3.B.3). Next the relationship between the tracheal and spiracular phenotypes were investigated and a phenotypic



rescue of the tracheal phenotype was attempted by driving UAS-Btk29A with different tissue/region specific GAL4 drivers (Paragraph C.3.B.4). Attempts to further characterize the dye penetration phenotypes are briefly reported in Paragraph C.3.B.5).

### C.3.A. Tracheal morphogenesis

#### C.3.A.1. Tracheal morphology

In the first part of the analysis, the overall shape of the trachea was examined. Wild type and *Btk29A* mutant embryos were stained for the luminal markers 2A12 and a FITC-conjugated Chitin Binding Probe (CBP). The embryos were examined for i) gross morphological differences in the development of the main tracheal tube (dorsal trunk, DT), the lateral (LB) and dorsal branches (DB), ii) breaks and gaps between the different parts of the system and iii) defects in the secretion of the two antigens, recognized by CBP and 2A12, in the lumen.

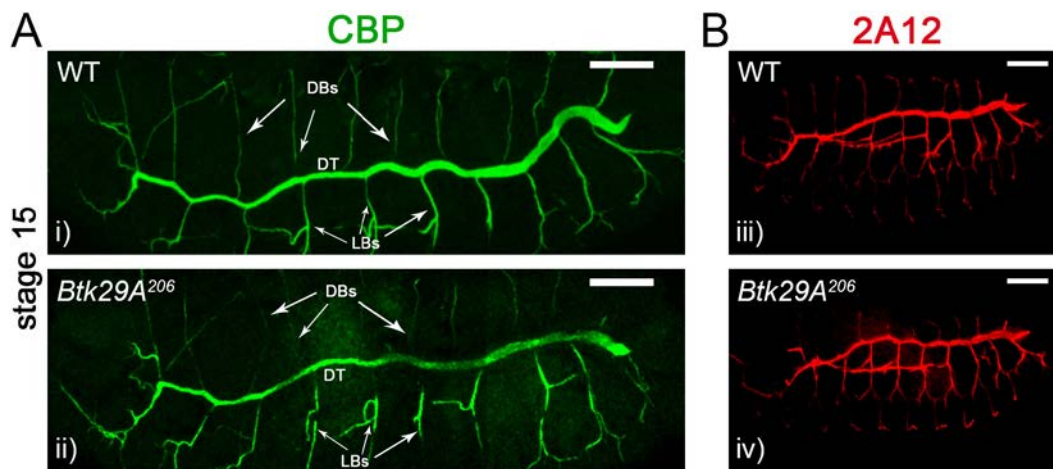


Figure 40: Tracheal morphology is not affected in *Btk29A* mutants

Antibody staining for the luminal markers Chitin Binding Probe (CBP) - green (A) and 2A12 - red (B) reveals that the morphology of the trachea is not affected in *Btk29A* mutants. DT: dorsal trunk, BD: dorsal branches and LB: lateral branches. (Scale bar: 50  $\mu$ m)

As shown in Figure 40, both antigens were detected inside the tracheal lumen and no morphological defects were observed in *Btk29A* mutants. The trachea develops normally and no gaps or breaks were detected in the dorsal trunk. The number as well as the spatial arrangement of the DB and LB was the same as in wild type.

---

### C.3.A.2. Tracheal length

Previous work from our group and in others has clearly shown that several proteins essential for a functional permeability barrier of the trachea system (in particular septate junctions components and associated proteins) affect tracheal size (Bätz et al., 2014; Behr et al., 2003; Llimargas et al., 2004; Nelson et al., 2010; Paul et al., 2003; Wu and Beitel, 2004). Additionally, recent studies by Nelson et al., 2012 and Forster et al., 2012 revealed that the tyrosine kinase Src42, which displays high similarity and functional redundancy with Btk29A in several systems (Matusek et al., 2006; Tateno et al., 2000), is involved in the regulation of the size of the tracheal tube through the regulation of the apical surface growth in the tracheal cells. For the above reasons, we decided to measure the tracheal length in *Btk29A* mutants and to compare it to wild type.

Stage 15 *Btk29A* homozygous mutant embryos were stained with anti-DE-Cadherin and the length of the trachea was calculated. That was done through the measurement of the length of the “tracheal metamere” that lies between the 7<sup>th</sup> (F7) and 8<sup>th</sup> (F8) fusion points (referred to as Tr8).

As shown in Figure 41, the tracheal length of *Btk29A* mutants is similar to the wild type. On the contrary, Tr8 length in *Src42A* mutant embryos appears decreased, a result which is consistent with published data (Forster and Luschnig, 2012; Nelson et al., 2012). Interestingly, the lack of both kinases enhanced the phenotype of *Src42* single mutants. Moreover, the length of the tracheal lumen is increased in wild type embryos overexpressing *Btk29A* in the trachea, similarly to what happens when Src42 is overexpressed in the trachea (data not shown). It is thus likely that there is a functional redundancy between the two kinases.

From the above observations, it becomes clear that *Btk29A* does not affect the overall tracheal morphology: continuous trachea system forms, with normal size, arrangement and patterning of the main and the smaller branches when the fly Tec kinase is not functional. Therefore the dye penetration phenotype observed in *Btk29A* mutants is not a secondary effect of an incomplete tracheal development.

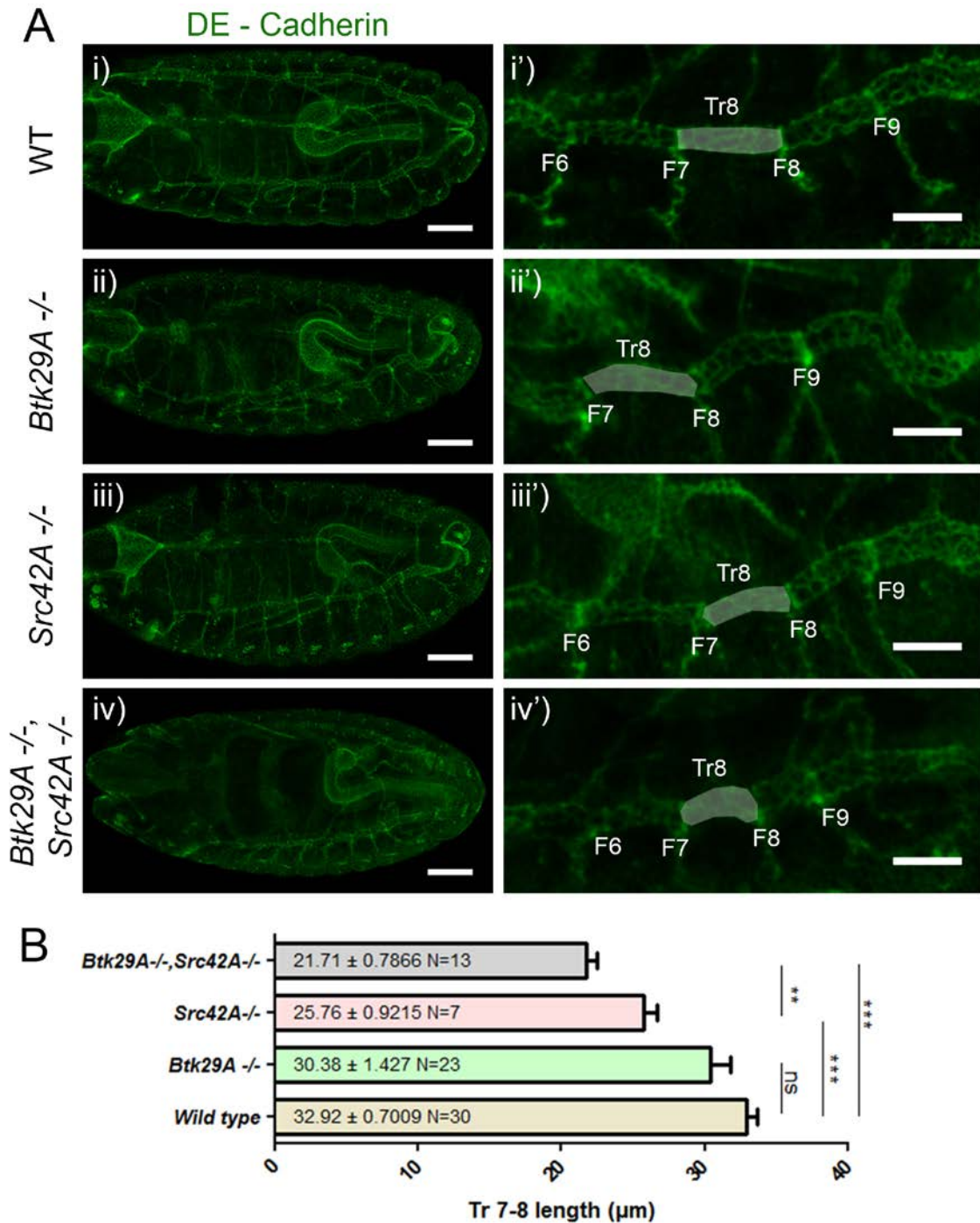


Figure 41: Tracheal length is normal in *Btk29A* mutants

A. The morphology of the trachea of wild type, *Btk29A* mutants, *Src42A* mutants and double mutants for both kinases was examined with DE-Cadherin staining. The length of a clearly defined part of the trachea system, referred to as Tr8 (distance between the 7<sup>th</sup> and 8<sup>th</sup> fusion point / region marked with grey), was measured and compared among different genotypes. Note the impaired posterior spiracle morphology in ii, iii and iv. (Scale bar 50µm for i-iv and 20µm for i'-iv') B. *Btk29A* mutants have regular Tr8 length (non-significant length difference compared to the WT,  $P = 0,0915$ ), while *Src42A* mutants show decreased Tr8 length when compared to WT ( $P < 0.0001$ ) (consistent with the previous studies (Forster and Luschnig, 2012; Nelson et al., 2012)). The phenotype is more prominent in double mutants for the two kinases (compare *Src42A*<sup>-/-</sup> to *Btk29A*<sup>-/-</sup>, *Src42A*<sup>-/-</sup>,  $P = 0.0051$ ). Unpaired t test was used for the data analysis.

---

### C.3.B. Dye penetration phenotype

In a first attempt to examine the role of *Btk29A* in the formation of the permeability barrier of the tracheal system, we focused on the Septate Junctions (SJs): important cellular junctions for the formation of a diffusion barrier that prevents water and solute exchange across epithelia (view Paragraph A.3.B). Mutations affecting SJs components result in disrupted subcellular localization of other SJ components and impaired permeability barrier (Hijazi et al., 2009). The molecular and ultrastructural organization of the SJs was examined in *Btk29A* mutants (Paragraph C.3.B.1). Additionally we tested the chitin deposition and organization inside the tracheal lumen, since these two parameters are known to be affected in several mutants that display epithelial barrier defects (Nelson et al., 2010; Wu et al., 2007).

#### C.3.B.1. Septate junctions

The localization of the SJ proteins: Coracle (Cora), Fasciclin III (Fas III), Gliotactin (Gli), Neurexin IV (NrxIV) and Discs large (Dlg) (see Paragraph A.3.B) was examined in the tracheal cells of wild type and *Btk29A* mutants. As shown in Figure 42 (and data not shown), the proteins are expressed and normally localized at the basolateral region of the epithelial cells both in wild type and *Btk29A* mutants.

Similarly, the localization of the polarity marker Crumbs (Knust et al., 1987; Tepass et al., 1990) and the AJ proteins Cadherin (Oda et al., 1994) (Figure 42) and Armadillo (Oda et al., 1994; Pai et al., 1996) (data not shown) is not affected. The above indicate that *Btk29A* is not disrupting the organization of the SJs or the general polarity of the tracheal cells.

Additionally, analysis of other epithelial tissues, including posterior spiracles (Figure 25), epidermis, salivary glands (data not shown), in *Btk29A* mutants also showed normal localization of the above mentioned polarity markers.

The SJs are characterized by a ladder-like ultrastructural organization called *septa* (Figure 9). In mutants for proteins affecting these junctions (and thus the epithelial permeability barrier), the ladder-like arrangement is impaired or lost (Genova and Fehon, 2003) (see also Paragraph A.3.B). Is this the case for *Btk29A* mutants? As shown in Figure 43, ultrastructural analysis of wild type and *Btk29A* mutants with Transmission Electron Microscopy (TEM) enabled the detection of the ladder-like SJs. The more apically localized AJs were also visible in both wild type and mutant tracheal cells.



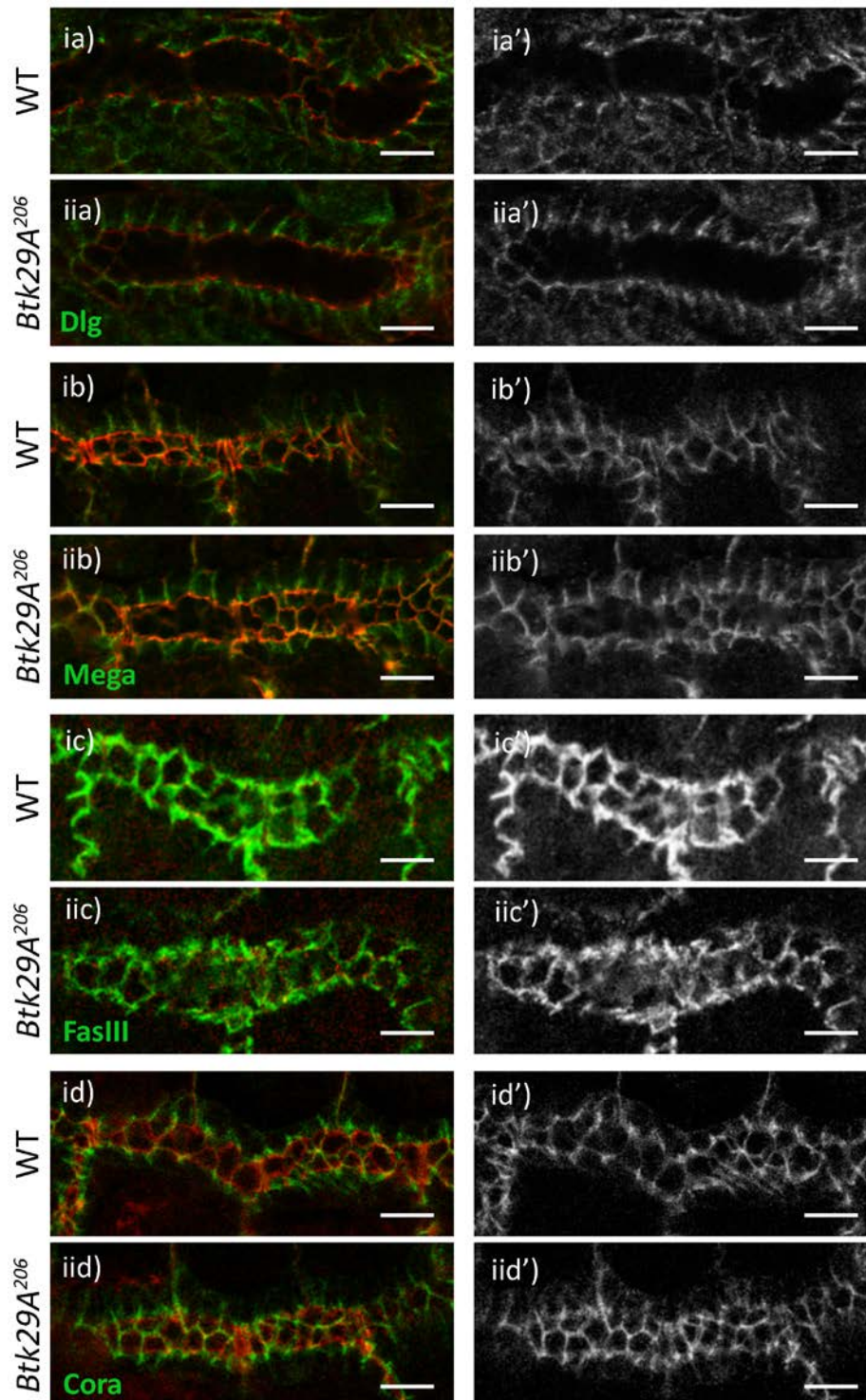


Figure 42: The subcellular localization of the SJ components is not affected in *Btk29A* mutants

Antibody staining for several SJ proteins (green):Dlg (ia-*iia*), Mega (*ib-*iib**), Fas III (*ic-*iic**), Cora (*id-*iid**) and DE-Cadherin (red) reveals that the lack of *Btk29A* is not disturbing the localization of these proteins to the junctional region. Additionally, the cell polarity is not affected: DE-Cadherin is localized at the apical and the SJ proteins the basolateral region of the membrane, like in WTs. (Scale bar: 5  $\mu$ m)



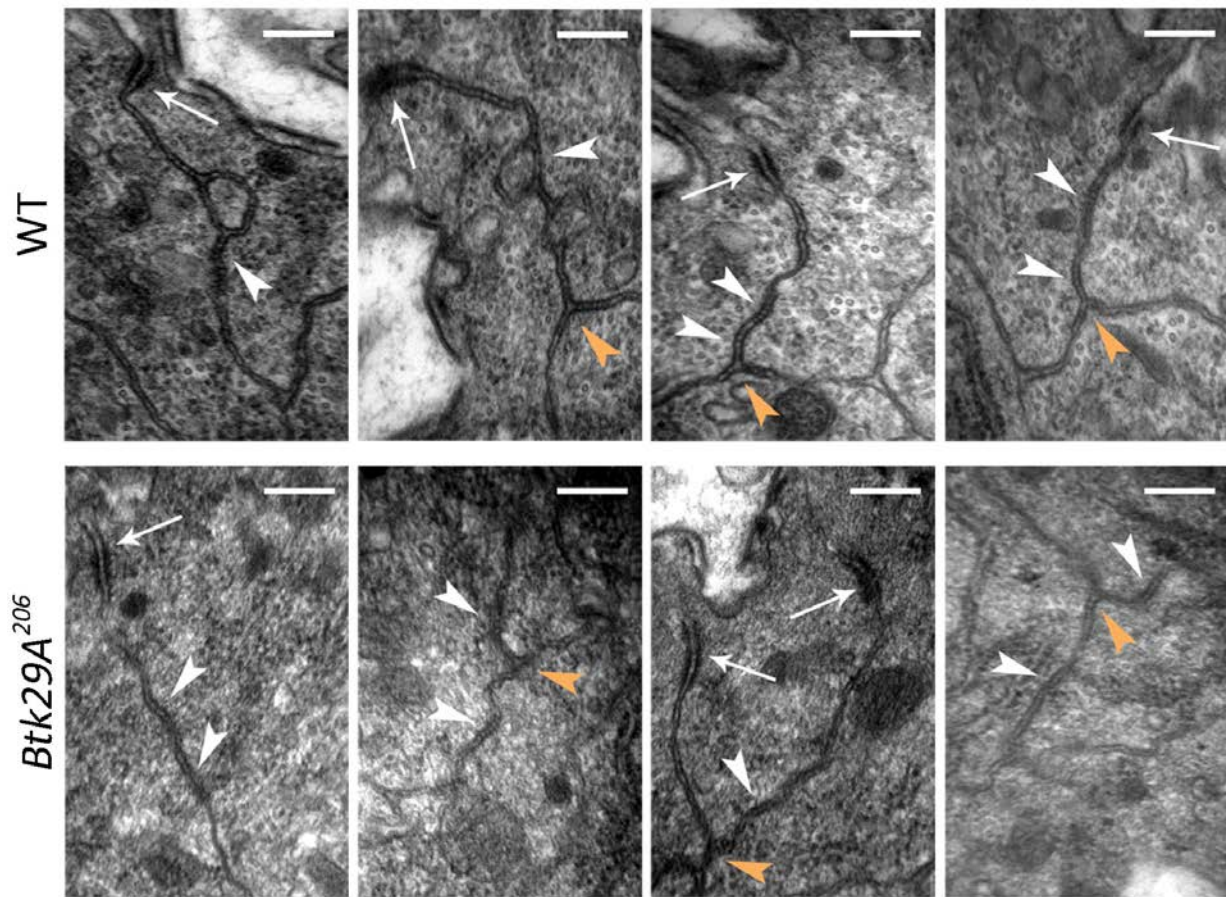


Figure 43: Septate junctions are detected in *Btk29A* mutants

Ultrastructural analysis of the SJs of the tracheal cells (with Transmission Electron Microscope) in WT and *Btk29A*<sup>206</sup> embryos showed that *Btk29A*<sup>206</sup> tracheal epithelial cells form SJs with the characteristic ladder-like arrangements (arrowheads). The arrows point to the AJs. Orange arrowheads point to the tricellular junctions (Scale bar: 200 nm)

Although septa are forming between the tracheal epithelial cells in *Btk29A* mutants, we cannot exclude, on the basis of the available data, that the number of septa per junction and/or the distance between the junctions and between the membranes of the adjacent cells are abnormal. Additionally, thorough analysis of the properties of the tricellular junctions (see next Paragraph) could not be performed on the collected EM images.

Overall, the above observations (normal SJ protein expression and localization and normal ultrastructure of the SJs) suggest that the SJs are not affected in *Btk29A* mutants. However, it cannot be refuted that subtle defects in SJ organization exist, whose identification would require a more extensive data collection and thorough quantitative analysis.

---

### C.3.B.2. Gliotactin and the Tricellular Septate Junctions

Gliotactin is a special SJ component, as it is the only protein known to localize specifically at the SJs formed at the meeting points between three epithelial cells, the tricellular corners (Tricellular Septate Junctions, TCJ) (Auld et al., 1995) (Figure 44A - compare the localization of Gli to Neurexin IV in wild type). It is involved in the maintenance of the epithelial permeability barrier, and its localization and function is regulated by tyrosine phosphorylation at two conserved residues (Padash-Barmchi et al., 2010). Tyrosine phosphorylation is important for the endocytosis and degradation of Gli and thus the regulation of its levels at the membrane of the epithelial cells of the wing discs. The kinase responsible for this phosphorylation is unknown but, at least *in vitro*, Src kinase can phosphorylate Gli at one or both tyrosine residues (Padash-Barmchi et al., 2010).

The Src-like Btk29A tyrosine kinase affects the permeability barrier of the tracheal epithelium without impairing the ultrastructural organization and molecular composition of the SJs. Could Btk29A selectively affect the organization of the TCJs formed between the tracheal cells? Could this function be mediated by tyrosine phosphorylation of the TCJ component Gliotactin, triggering Gli endocytosis and subsequent degradation?

A preliminary ultrastructural analysis of the TCJ of the tracheal cells in *Btk29A* mutants revealed that the septa are forming at the tricellular corners (orange arrowhead in Figure 43). However it is unclear if the number and organization of the tricellular septa are similar to wild type with the available EM data.

I then conducted immunostainings in order to test if Btk29A kinase modulates Gliotactin levels. *Btk29A* gain-of-function and loss-of-function experiments were performed and the levels of Gliotactin were examined. Initially, Gli levels were examined in the same paradigm as Padash-Barmchi et al., 2010: TCJ of the wing disc epithelium. Wild type wing discs and discs overexpressing *Btk29A* in the dorsal compartment of the wing disc epithelium only, with the apterous-GAL4 driver, were dissected and stained for anti-Gli. As shown in Figure 44, Btk29A overexpression completely distorts the morphology of the disc: some of the overexpressing cells appear enlarged, while others lose their epithelial polarity (DE-Cadherin, Coracle and Gliotactin expression are abnormal) and delaminate.

The levels of Gli were assessed in *Btk29A*-overexpressing cells that retain their epithelial properties (arrowheads in Figure 44Bib - ib'). Gli expression seems decreased and its localization at the SJ region is not so prominent. It should be noted though that since *Btk29A* overexpression in the wing disc leads to the reduction of other junctional proteins like Cadherin (at AJs) and Coracle (at

SJs) and loss of the polarity of the cells, the impairment of Gli levels could be a secondary effect to an overall impairment of the epithelial identity of the cells.

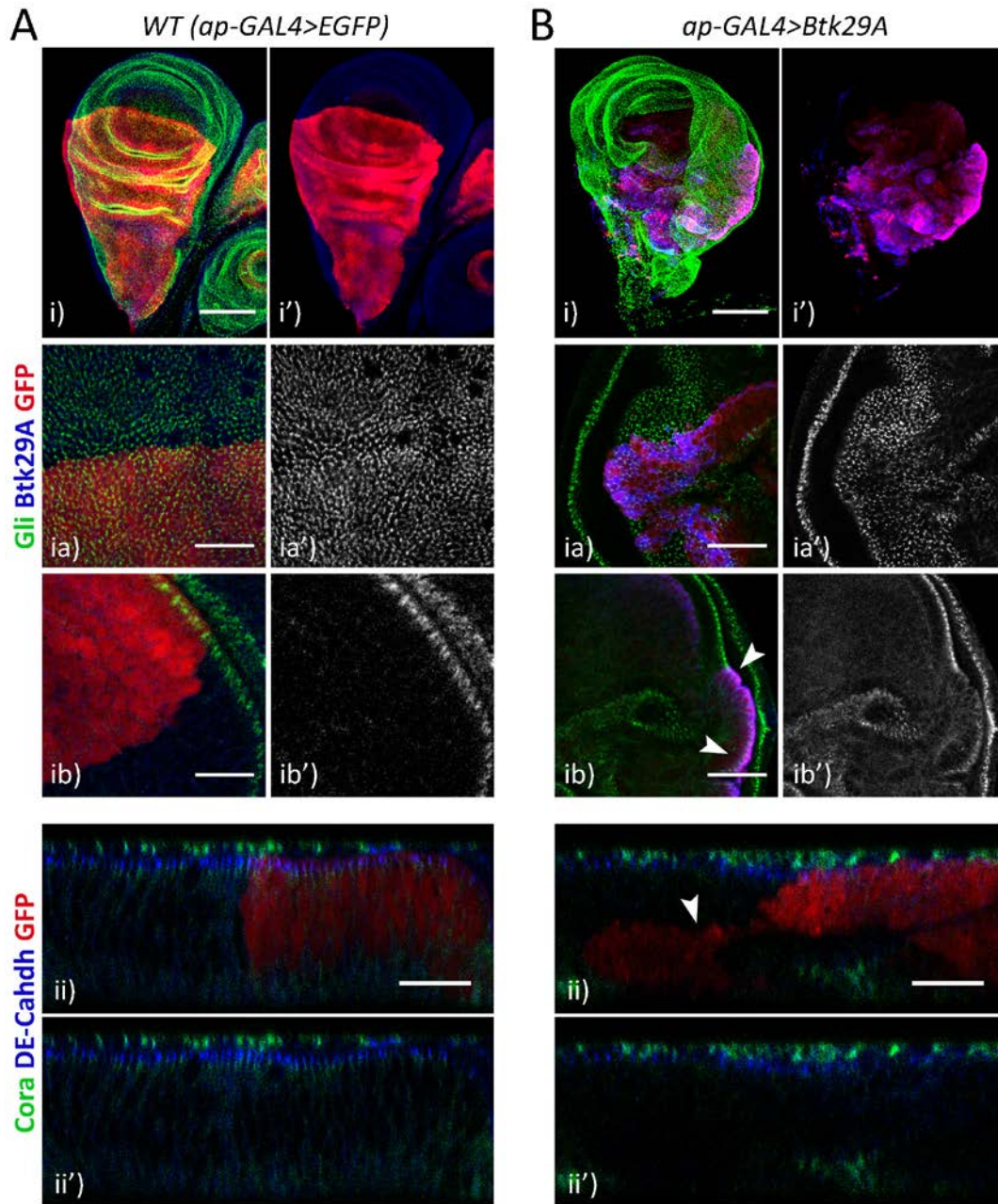


Figure 44: Overexpression of Btk29A by the apterous-GAL4 driver at the wing discs.

The overexpressing discs are abnormally shaped (compare Bi-i' to Ai-i'). The overexpressing cells appear enlarged and the levels of Gliotactin (green) in them seem decreased (compare Bia-ia' to Aia-ia' and the cells marked with the arrowheads in Bib-ib' to the nearby non-overexpressing cells and to Aib-ib'). In the most severe cases, the overexpressing cells lose their epithelial polarity: cells marked with the arrowhead in Bii-ii' do not show expression of the polarity markers DE-Cadherin (blue) and Coracle (green) (compare to Aii-ii') and delaminate. (Scale bar: for Ai-i' and Bi-i' 100 μm, for all the rest 20 μm)



Subsequently, Gliotactin levels were examined in wild type, *Btk29A* mutant and overexpressing cells in embryonic epithelia. Figure 45A, shows the localization of Gli at the TCJs of wild type, *Btk29A* mutant and *Btk29A* overexpressing cells. In the trachea, the distribution of the protein is not very easy to assess due to the tubular arrangement of the cells. It seems though, that the tracheal cells of the three different genotypes are forming clusters of Gli at the TCJs and the levels of the protein are not affected.

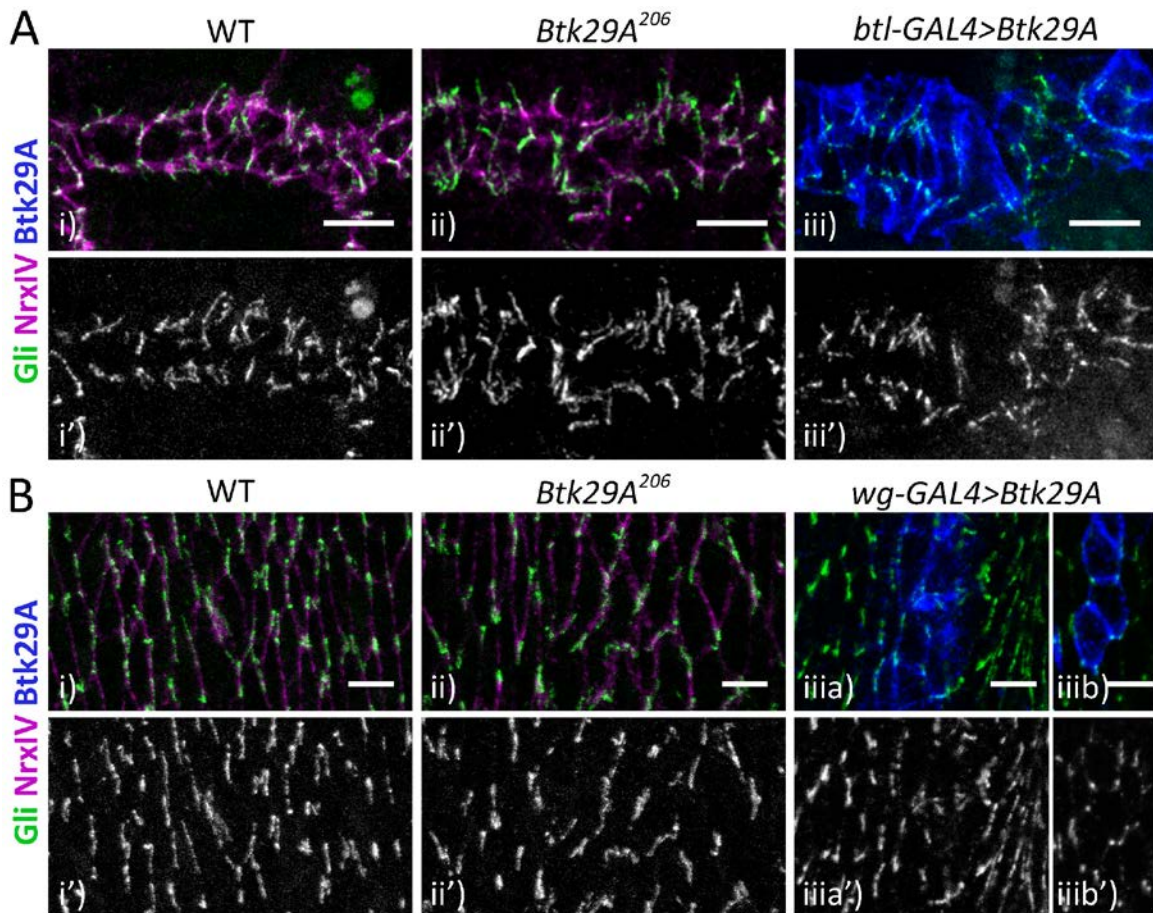


Figure 45: Gliotactin expression in the embryo

A. The expression of Gliotactin (green) was assessed in the trachea in WT (i-i'), *Btk29A*<sup>206</sup> mutants (ii-ii') and embryos overexpressing *Btk29A* by the tracheal cells (iii-iii'). The levels and the subcellular localization of the protein at the TCJ region do not seem affected. Neurexin IV (magenta), Btk29A (blue) (Scale bar: 10  $\mu$ m) lower panels show the green channel (Gliotactin)

B. The expression of Gliotactin (green) was assessed) in WT (i-i'), *Btk29A*<sup>206</sup> mutants (ii-ii') and embryos overexpressing *Btk29A* in epidermal stripes under the *wg*-GAL4 (iii-iii'). The levels and the subcellular localization of the protein at the TCJ region do not seem affected. Neurexin IV (magenta), Btk29A (blue) (Scale bar: 5  $\mu$ m)

---

Gli was also examined in the epidermis of wild type and *Btk29A* mutants (Figure 45B). The levels of Gli do not seem significantly changed in the mutants. In parallel, *Btk29A* was overexpressed in stripes of cells in the epidermis with patched-GAL4 (data not shown) and wingless-GAL4 drivers. Both drivers display a stripy pattern of expression and thus enable the comparison of the overexpressing groups of cells with the neighboring non-overexpressing ones (Figure 45Biii). If *Btk29A* regulates the levels of Gli at the cell membrane, one would expect to observe decreased Gli expression by the *Btk29A* overexpressing cells compared to the neighboring non-expressing ones. This does not seem to be the case though, as the levels of Gli seem similar in both cell groups.

The above results are favoring the conclusion that *Btk29A* does not affect the levels of Gliotactin in the TCJs formed between the cells of the tracheal and epidermal embryonic epithelia. Thus it is likely that *Btk29A* is not the (or the only) tyrosine kinase mediating Gli phosphorylation. Furthermore, the decrease of Gli in *Btk29A*-overexpressing wing disc cells is likely to be related to an overall impairment of the epithelial polarity of these cells, rather than to *Btk29A* mediated Gli phosphorylation and degradation. Our limited ultrastructural analysis of the TCJ would support this notion.

In conclusion, the dye penetration phenotype observed in *Btk29A* mutants is unlikely to be related to the regulation of Gliotactin by *Btk29A*-dependent phosphorylation.

### **C.3.B.3. Chitin deposition and organization**

Another feature known to be impaired in mutants affecting the tracheal permeability barrier is the organization of the chitin inside the tracheal lumen (Hijazi et al., 2009; Luschnig et al., 2006; Nelson et al., 2010; Tonning et al., 2005; Wang et al., 2006) (see also Paragraph intro 3.A.3). As shown in Figure 40, chitin is deposited inside the tracheal lumen in *Btk29A* mutants.

Chitin lining is known to be regulated by chitin modifying proteins. Some of the best studied are the *Obst-A* and *Gasp* (Tiklová et al., 2013) and the chitin deacetylases *Serpentine* (*Serp*) and *Vermiform* (*Verm*) (Luschnig et al., 2006; Wang et al., 2006). The expression of *Verm* and *Serp* in tracheal cells was examined in *Btk29A* mutants. The luminal secretion of both of these proteins, which is known to be disrupted in mutants for SJ components (for example Nelson et al. (2010)), is not affected in *Btk29A* mutants (Figure 46).



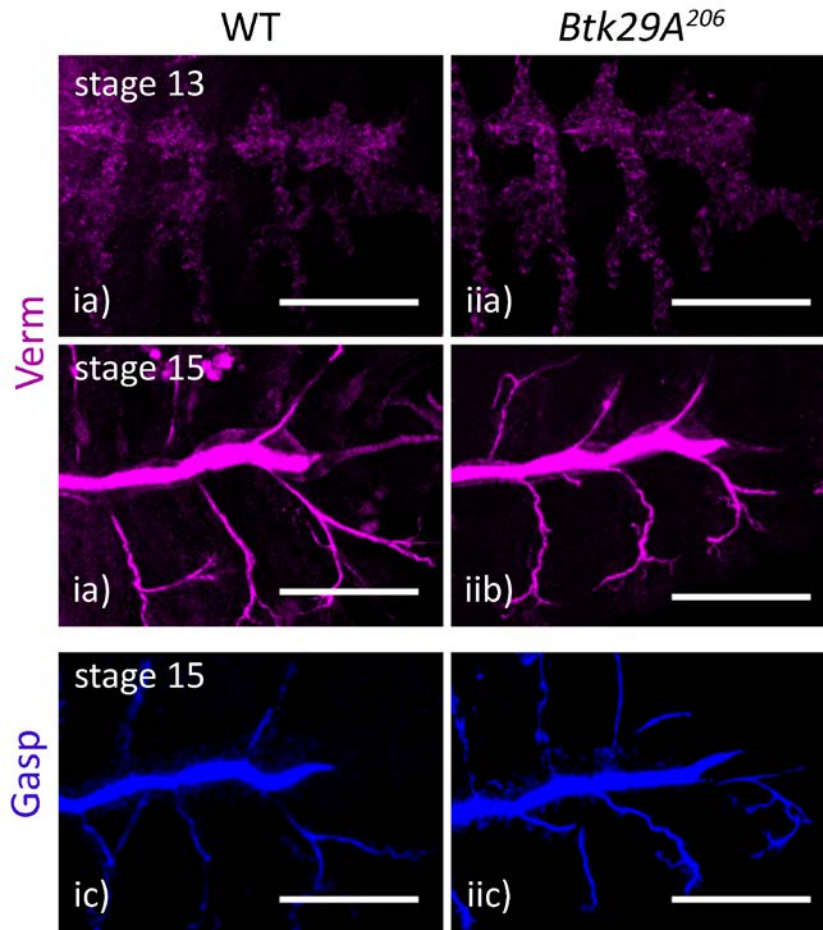


Figure 46: Luminal deposition of chitin modifying proteins is intact in *Btk29A* mutants

Antibody stainings with anti-Gasp (blue), anti-Vermiform (magenta) and anti-Serpentine (not shown) reveal that the expression of the proteins by the tracheal cells, as well as their secretion into the lumen is not affected in *Btk29A* mutants. (Scale bar: 50 nm)

2A12 antibody recognises the luminal protein Gasp which is known to participate in the assembly of the chitin filaments and the establishment of the taenidial fold integrity (Tiklová et al., 2013). Gasp mutants show impaired chitin organization but they acquire normal tracheal length in late stages and Verm is secreted in the trachea. As shown in Figure 40, the levels of Gasp were similar in the lumen of both wild type and *Btk29A* mutants, proposing that the secretion of Gasp is not affected in the absence of Btk29A. The same result was observed with anti-Gasp antibody staining (Figure 46).

The above results suggest that the dye penetration phenotype observed in *Btk29A* mutants is not linked to a defect in the chitin deposition and modification.

---

### C.3.B.4. Dye permeability and posterior spiracle morphogenesis

As described in the Paragraph C.2, *Btk29A* mutants develop irregularly shaped posterior spiracles. The posterior spiracles develop in the abdominal segment A8 and, importantly, the lumen of the spiracular chamber is continuous with that of the tracheal system. The functional correlation and the juxtaposition of these two components of the respiratory system suggest that the failure in the tracheal permeability barrier (witnessed by the dye penetration phenotype) could be a secondary effect of the impaired morphogenesis of posterior spiracles. Specifically an abnormal spiracle morphogenesis could lead to a discontinuity between the epithelia lining of the tracheal and spiracular lumens in *Btk29* mutants, thus creating breaks/ruptures in the tracheal epithelial barrier. In order to test this possibility, two different approaches were followed: i) the *Btk29A*-related dye penetration phenotype was examined in embryos lacking posterior spiracles (Paragraph C.3.B.4.a) and ii) rescue experiments were designed in order to attempt tissue specific phenotypic rescue of the phenotype (Paragraph C.3.B.4.b).

#### C.3.B.4a. Is dye penetration phenotype “posterior spiracle-dependent”?

As described in Paragraph A.2.A., the transcription factor *Ems* is important for posterior spiracle morphogenesis. In *ems* homozygous mutant embryos posterior spiracles are virtually absent: most of the spiracular chamber cells fail to invaginate, thus the chamber lumen and, later, the filzkörper do not form and the embryos lack a “trachea - posterior spiracle” connection (Castelli-Gair Hombría et al., 2009) (Figure 47B). The “posterior spiracle-isolated” trachea system of the *ems* mutants was used in order to test *Btk29A* tracheal function.

First, the integrity of the trachea permeability barrier in *ems* mutants was examined with the dye penetration assay. As shown in Figure 47Biii, *ems* mutants display normal tracheal barrier: no dye penetration phenotype.

But, what is happening in embryos that carry mutations in both *ems* and *Btk29A*? It is important to stress that similarly to *ems* mutants, *Btk29A*; *ems* double mutants embryos essentially do not have posterior spiracles. Thus lack of a dye penetration phenotype in double mutants would imply that the *Btk29A* permeability defect is secondary to the posterior spiracles morphogenetic defects observed in *Btk29A* mutants. Contrary to this, dye penetration phenotype in double mutants would rather suggest that *Btk29A* has a “trachea-autonomous” function for the establishment of the permeability barrier.

Recombinant flies with mutations in both *Btk29A* and *ems* were generated and the dye penetration assay was performed. The double mutant embryos display a defective tracheal permeability barrier, with rhodamine-dextran diffusing into the tracheal lumen (Figure 47Biii).

On the basis of the above results, we would tentatively suggest that *Btk29A* is not secondary to the spiracle defects and that *Btk29A* might be required by the tracheal cells in a “tissue-autonomous” manner in order for the tracheal permeability barrier to be functional.

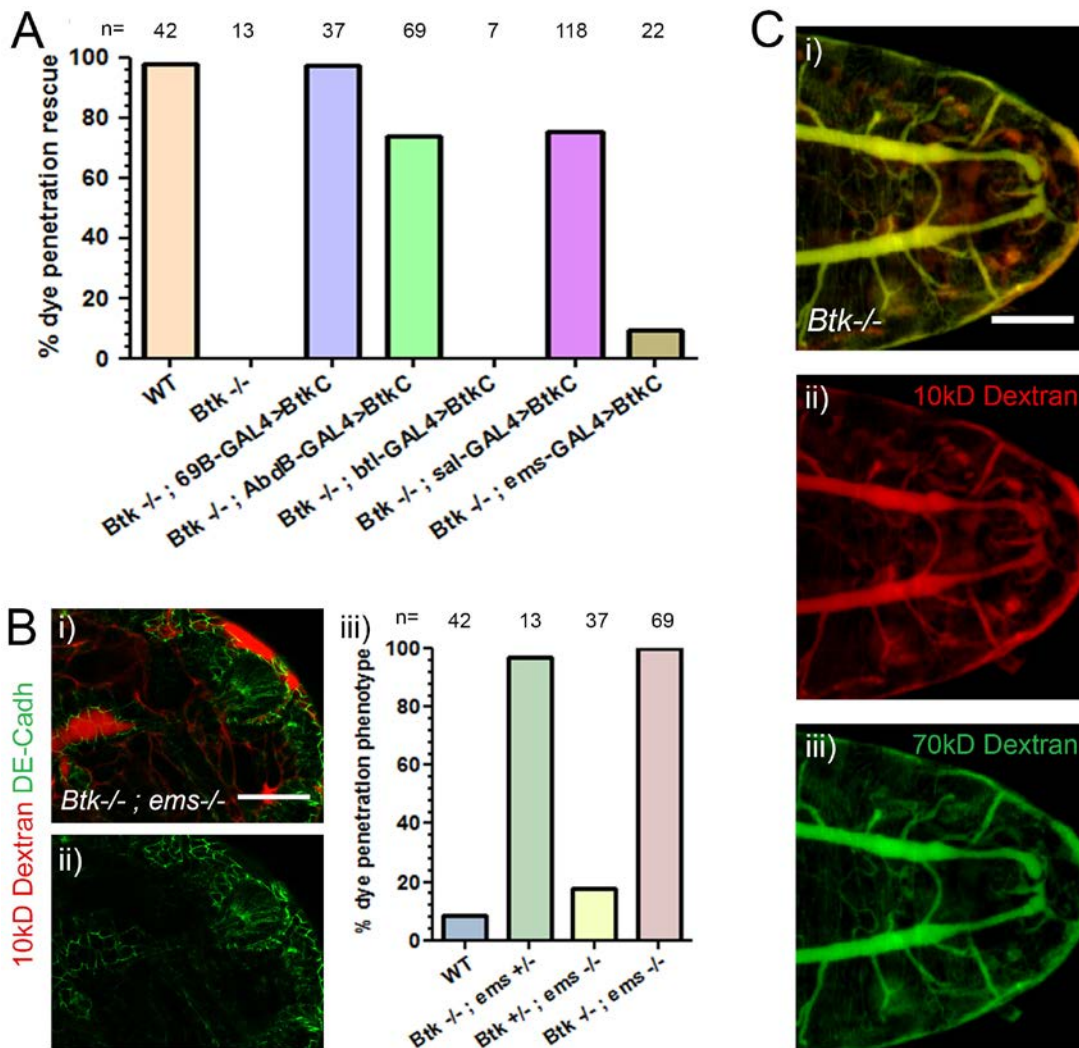


Figure 47: Dye penetration assay

A. Tissue-specific recovery of *Btk29A* expression was attempted with the use of 5 different GAL4 drivers. Dye penetration assay was performed and the number of embryos showing phenotypic rescue of the dye penetration phenotype was scored. The phenotype was almost completely rescued in the case of 69B-GAL4, while sal-GAL4 and Abd-B-GAL4 embryos showed a significant rescue. The trachea specific btl-GAL4 and the spiracular *ems*-GAL4 driver did not rescue the phenotype. The total number of embryos examined for each genotype is reported.

B. The tracheal permeability barrier is affected in double mutants for *Btk29A* and *ems*, as shown by dye penetration assay experiments. The phenotype is ascribed to the lack of *Btk29A*, since single mutants for *ems* do not have an

---

impaired permeability barrier. The total number of the embryos examined for each genotype is reported. (Scale bar: 20  $\mu\text{m}$ )

C. The permeability phenotype of *Btk29A* mutants was tested by different sizes of rhodamine dextran: 10kDa rhodamine dextran (in red) and 70kDa FITC-dextran (in green). Both types of dextran were able to penetrate the tracheal lumen. (Scale bar: 50  $\mu\text{m}$ )

#### **C.3.B.4b. Phenotypic rescue of the dye penetration phenotype**

A second approach to investigate the cellular basis of the tracheal permeability defect involves phenotypic rescue experiments using different GAL4 drivers. More specifically, 5 different drivers were selected (Figure 29) for the expression of *Btk29A* in different tissues in *Btk29A* homozygous mutant embryos: i) ectodermal expression with 69B-GAL4 (Figure 29i), ii) tracheal expression with *btl*-GAL4 (Figure 29vi), iii) spiracular chamber expression with *ems*-GAL4 (Figure 29v), iv) expression in the posterior segments (A8-A9) with *AbdB*-GAL4 (Figure 29ii) and v) expression in the stigmatophore cells and trachea with the *sal*-GAL4 (Figure 29iii). Incidentally, among the above drivers, only 69B-GAL4, *sal*-GAL4 and *AbdB*-GAL4 rescued the posterior spiracle phenotypes in the corresponding experiments (Paragraph C.2.C and Figures 30 and 31). Rescue of the dye penetration phenotype with the same three drivers would suggest a link between the two phenotypes. Rescue with *btl*-GAL4 would suggest a requirement for *Btk29A* throughout the trachea.

Stage 16 embryos of the desired genotypes were injected with 10kDa rhodamine-dextran and the embryos were observed under the microscope after 30 minutes. Figure 47A summarizes the results of the experiment. The dye penetration phenotype was rescued with 69B-GAL4 induced *Btk29A* expression. Additionally, it was significantly rescued with “*sal*-GAL4 driven” as well as “*AbdB*-GAL4 driven” *Btk29A* expression, but not with *btl*-GAL4. These results suggest that the impairment of the permeability barrier observed in *Btk29A* mutants is secondary effect of the abnormal posterior spiracle morphogenesis. The spiracular chamber specific *ems*-GAL4 driver gave only a minor (non-significant) rescue of the phenotype.

Obviously these results are in agreement with those reported in the previous Paragraph (C.3.B.4a) and remain at present unresolved.

---

### C.3.B.5. Permeability in time and space

The analysis of several parameters that could affect the tracheal permeability barrier (Paragraphs C.3.B.1 – C.3.B.4) revealed that the SJs are properly forming between the tracheal cells of *Btk29A* mutants. However, the trachea system is permeable to the injected 10kDa fluorescent dye.

In order to obtain a better understanding of the permeability defect observed in *Btk29A* mutants, the temporal and the spatial features of the dye penetration phenotype were assessed. More specifically, live *Btk29A* mutant embryos were monitored under the confocal microscope after the dye injection aiming to identify: i) the time requirement for the trachea to fill with dye and ii) the position (if a single one exists) from which the dye is penetrating the trachea lumen. Both the spatial and temporal definition of the dye insertion in the trachea lumen were impossible.



---

## **D. DISCUSSION**

---

In this study, we examined the role of the non-receptor tyrosine kinase in the development of the *Drosophila* respiratory system, consisting of the trachea and posterior spiracles. Both tissues show phenotypes when *Btk29A* is mutated: the tracheal system develops defective epithelial permeability barrier and does not complete airway maturation and the posterior spiracles appear shorter, with irregular shape.

### **D.1. *Btk29A* expression pattern**

Prior to the investigation of the phenotypes, the expression of *Btk29A* in these tissues was assessed. We decided to perform a thorough expression analysis using *in situ* hybridization and antibody staining, in order to solve issues with older data and taking into account up-to-date genome and transcript annotations. In addition, given that the published monoclonal antibody for *Btk29A* is now only available in very limited amount, we embarked in the generation of a new rat polyclonal anti-*Btk29A* antibody.

Our results showed that *Btk29A* has a quite abundant expression during embryogenesis. In early stages, maternally supplied *Btk29A* mRNA is detected, while gradually, as zygotic expression initiates, *Btk29A* mRNA and protein is spotted in the newly forming cellular blastoderm and during germ band elongation, in a stripy pattern (consistent with Vincent et al., 1987). In later stages, *Btk29A* expression is observed in the salivary glands, epidermis, gonads, central and peripheral nervous system, dorsal vessel and leading edge cells and in the cells of the respiratory system. These results are consistent with mRNA expression analysis from previous studies (Katzen et al., 1990; Wadsworth et al., 1990; Vincent et al., 1987, Chandrasekaran and Beckendorf, 2005) and from BDGP (<http://insitu.fruitfly.org/cgi-bin/ex/report.pl?ftype=3&ftext=RE17878>).

Moreover, distinct examination of the expression of the different *Btk29A* isoforms (with RNA probes that recognise different *Btk29A* transcripts), revealed that the Short Isoform is the most abundant, while the Long one is expressed only by the cells of the central nervous system.

In the respiratory system, only the Short *Btk29A* isoform is detected. This informed our phenotypic rescue experiments (see below), that we performed with the UAS-GAL4 system using a UAS-*Btk29A-C* transgene, encoding for the Short isoform of *Btk29A*.

The Short isoform of *Btk29A* displays a subcellular localization at the cell periphery of the respiratory system cells. However it lacks the PH domain that mediates such localization in the Long isoform, while it maintains the SH2, SH3, TH and kinase domains. In the *Drosophila* ovaries, the SH2 and SH3 domains together are sufficient to direct the subcellular localisation of the Short isoform of *Btk29A* to the ring canals, possibly through the interaction of the SH2 with other

---

molecules (Lu et al., 2004). It is likely that a similar mechanism is employed in the cells of the respiratory system.

*Btk29A* expression was examined in the mutant alleles used in the current study: the P-element insertions *Btk29A*<sup>206</sup> and *Btk29*<sup>5610</sup> and the small chromosomal deletion *Df235*. All the alleles show the same phenotypic expressivity and penetration. Contrary to the previous studies that described the two P-element insertion alleles as molecular null mutations (Chandrashekar and Beckendorf, 2005), we found residual expression of *Btk29A* in the trachea and spiracular chamber cells. This is likely to be due to the expression of a smaller truncated (and non-functional) form of the protein.

The possibility of the involvement of other genes (and not *Btk29A*) in the respiratory phenotypes observed in *Btk29A* mutants was excluded, as the phenotypes are reverted with UAS-*Btk29A* rescue experiments. Therefore we continued our analysis in order to clarify the role of *Btk29A* in the development of the respiratory system.

---

## D.2. Posterior Spiracle morphogenesis

*Btk29A* falls into the genetic cascade that controls posterior spiracle morphogenesis downstream of Abdominal B. *Drosophila* posterior spiracles are formed in a region adjacent and posterior to the tracheal system and consist of two separate compartments: the stigmatophore and the spiracular chamber. The morphogenesis of the internal part, the spiracular chamber, is based on the invagination of the cells to form a 3D tubular structure from a 2D epithelial sheet. That of the external part, the stigmatophore, depends on convergent extension-like cellular rearrangements of the cells. The developmental processes that establish the two parts are thought to be completely independent of each other (Hu and Castelli, 1999).

We show here for the first time that the processes are interdependent. In particular we show that the non-receptor tyrosine kinase Btk29A, expressed in both compartments, regulates the invagination of the spiracular chamber cells through the organization of the stigmatophore cell rearrangements. On the other hand, no dramatic cell-autonomous role of the kinase in the spiracular chamber invagination has been observed.

### D.2.A. Btk-dependent epithelial cell rearrangements contribute to the invagination of nearby tubular structures in the posterior spiracles of *Drosophila*

*Btk29A* mutants display shorter and abnormally shaped posterior spiracles. Spiracle morphogenesis was monitored with *in vivo* imaging of live *Btk29A* mutant embryos. The analysis showed that the phenotype results from a failure of the spiracular chamber cells to complete the invagination process necessary for their morphogenesis. This result, together with the observation that *Btk29A* is expressed in high levels in the spiracular chamber cells, made us initially favour the hypothesis of a cell-autonomous function of the kinase in these cells to regulate their invagination. Examination of parameters known to affect epithelial invagination, cell polarity, cell shape changes (apical constriction and basolateral elongation), cytoskeletal organisation and Rho1 GTPase activation in the cells of the spiracular chamber, did not reveal any relevant defects.

Restoration of Btk29A expression in the spiracular chamber cells with the spiracular chamber-specific *ems-GAL4* driver didn't rescue the phenotype. However, driving Btk29A expression in the surrounding non-invaginating cells of the developing stigmatophore, using *sal-GAL4* driver, rescued spiracular chamber invagination. The above results proposed that Btk29A might regulate the spiracular chamber cell invagination in a non-cell autonomous manner through the stigmatophore cells.

But is *Btk29A* important for proper stigmatophore development? *In vivo* imaging of the morphogenetic movements of the stigmatophore cells showed that *Btk29A* mutants fail to execute

---

the spatial cell rearrangements that pattern the stigmatophore. At the same time, antibody staining analysis of the relative positions of the stigmatophore and spiracular chamber cells revealed that the positioning of the spiracular chamber cells and the execution of their invagination is highly dependent on the extent of stigmatophore cell rearrangements.

Is there an additional cell-autonomous function of *Btk29A* in the spiracular chamber cells? The unsuccessful rescue of the invagination phenotype with the *ems-GAL4* driver argues against this hypothesis. However, the fact that the *emsGAL4* driver misses some of the distal-most cells of the spiracle could imply a cell autonomous *Btk29A* function in these few “Cut +, *emsGAL4* -” cells. Thorough analysis of the *sal-GAL4* and *en-GAL4* drivers revealed that they are expressed in few distal Cut+ spiracular chamber cells, as well as in some (in the case of *en-GAL4*) or all (in the case of *sal-GAL4*) of the stigmatophore cells. Comparison of the rescue effect of *Btk29A* expression under those two drivers revealed that although both mediate *Btk29A* restoration in the distal spiracular chamber cells, only *salGAL4* can rescue the invagination phenotype. This result is not consistent with a cell autonomous function of *Btk9A* in the distal spiracular chamber cells. Moreover, it reveals that restoration of *Btk29A* in some of the stigmatophore cells can only partially restore the stigmatophore arrangements in *Btk29A* mutants.

Are there other stigmatophore mutants that affect spiracular chamber invagination non cell-autonomously? According to the older studies, the morphogenesis of the two spiracle compartments are forming independently of each other (and of the neighbouring tracheal system) (Hu and Castelli-Gair, 1999). Additionally, although previous studies have revealed that mutants of *spalt* and *grain* display phenotypes both in the spiracular chamber and the stigmatophore, their interdependence was not specifically addressed (Brown and Castelli-Gair Hombria, 2000; Hu and Castelli-Gair, 1999). Similarly, the likelihood of a reciprocal effect of chamber invagination on the rearrangement of stigmatophore cells has been discussed, but remains untested (Castelli-Gair Hombría et al., 2009; Lovegrove et al., 2006).

### **D.2.B. Convergent extension of stigmatophore cells**

The convergent extension movements of the stigmatophore cells are impaired in *Btk29A* mutants and can be rescued with *sal-GAL4* driven expression of *Btk29A*. Previous studies have shown that this cell repositioning also requires *grain*, a gene encoding a GATA-transcription factor and itself a target of the Zn-finger transcription factor *Spalt*. The phenotypic similarity of *grain* and *Btk29A* mutants suggests that *Btk29A* is required cell-autonomously for stigmatophore cell rearrangements in parallel or downstream of *grain*. The two genes do not appear to regulate each



---

other at the transcriptional level, since Btk29A expression is not *grain* dependent, nor is Grain expression *Btk29A* dependent.

But which are the mechanisms that regulate the intercalation of the stigmatophore cells and what is the role of Btk29A in this process? Mechanisms of Grain function (that would give us a hint on how Btk29A might be acting for regulation of stigmatophore cell rearrangements) are not known. Thus in an attempt to examine possible mechanisms of Btk29A action we examined parameters known to regulate convergent extension in other systems: polarity, actomyosin network, RhoGTPase function. We could not detect any abnormality in the parameters examined. Nevertheless, these features can be extremely dynamic or subtle and thus difficult to pinpoint. *In vivo* imaging of fluorescently tagged forms of these factors could give an insight into the molecular basis of the stigmatophore cell rearrangements.

### **D.2.C. Spiracular chamber invagination**

Invagination is one of the key morphogenetic events that contribute to development. Several morphogenetic actions such as apical constriction, cell-shape changes and junctional repositioning are important for the efficient epithelial invagination (Sawyer et al., 2010; Schöck and Perrimon, 2002; Wang et al., 2012). Moreover, additional cellular processes can accompany apical constriction to ensure robust invagination (Llimargas and Casanova, 2010), for example in the case of the invagination of the tracheal placides.

The invagination process could also be coupled to other cellular events for the proper establishment of the tissue development. For example, proper morphogenesis of the salivary glands involves the synchronization of the apical constriction (and cytoskeletal organization) to the regulation of the endocycle of these cells (Chandrasekaran and Beckendorf, 2005). Interestingly, Btk29A has been shown to affect both of these processes in the salivary gland cells, likely in a cell-autonomous manner (Chandrasekaran and Beckendorf, 2005).

Spiracular chamber cell invagination is important for the proper formation of the posterior spiracle. The molecular and cellular basis of this morphogenetic action has been studied in the past and several polarity, cytoskeletal and cell adhesion related molecules have been implicated (Simões et al., 2006; Lovegrove et al., 2006). Apical constriction and cell elongation are important for the efficient spiracular chamber invagination, as mutants affecting these processes display abnormal morphogenesis of the tissue (reviewed in Castelli-Gair Hombría et al., 2009).

We show here for the first time that the non-receptor tyrosine kinase Btk29A regulates the spiracular chamber invagination in a non-cell autonomous manner by influencing the spatial arrangements of nearby epithelial cells.

---

Given the strong expression of *Btk29A* mRNA and protein in the spiracular chamber, *Btk29A* was expected to be required cell-autonomously by the spiracular chamber cells for their invagination. However our analysis did not reveal any relevant cell polarity, cell shape and cytoskeletal defects there. Rescue experiments with *sal-GAL4* and *ems-GAL4* strengthened the view that the gene does not have a dramatic cell-autonomous role in spiracular chamber cells.

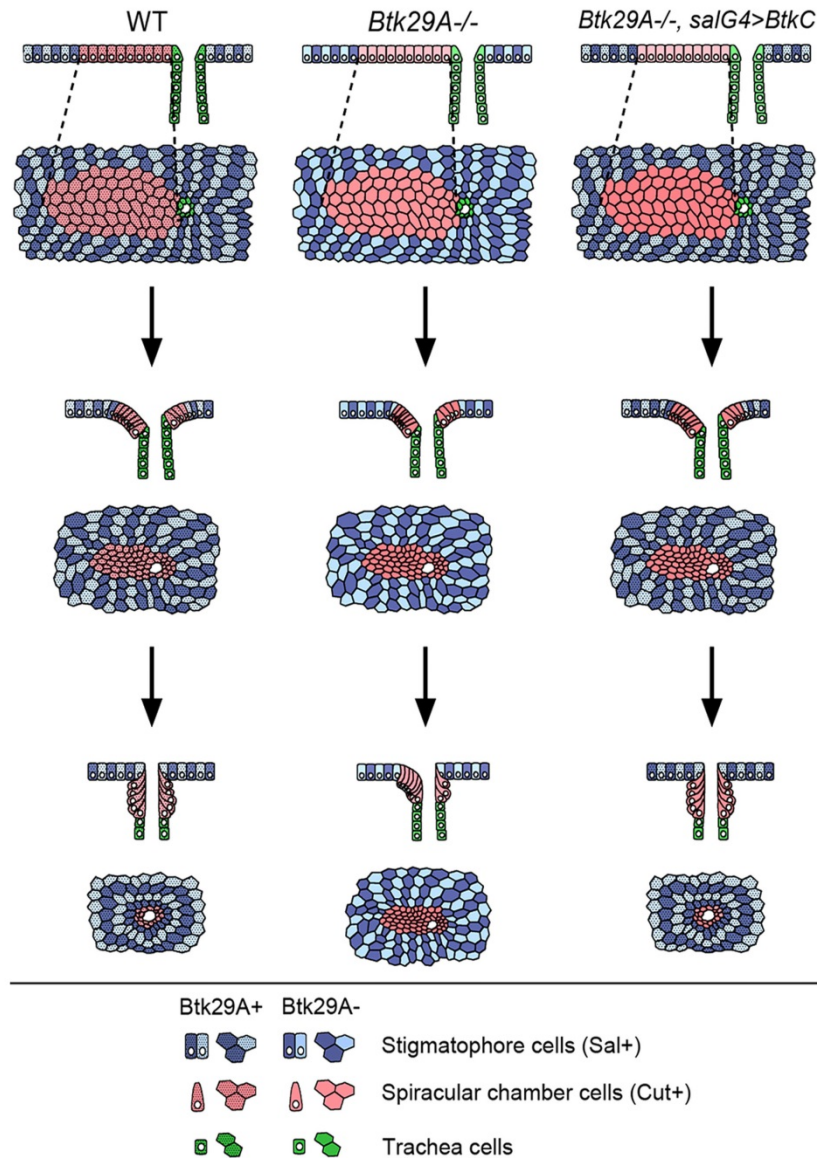
Then what is the role of *Btk29A* in the spiracular chamber cells? Although all the known aspects important for the morphogenesis of these cells do not seem to be affected, other yet unknown factors significant for their function might be disrupted.

#### **D.2.D. Contribution of convergent extension to invagination**

Analysis of both of these morphogenetic processes in *Btk29A* mutants showed that the kinase is necessary for the regulation of the special rearrangement of the stigmatophore and through this for the efficient invagination of the spiracular chamber cells.

Early in posterior spiracle morphogenesis, the stigmatophore cell rearrange their positions and surround the spiracular chamber cells. Subsequently and while the spiracular chamber cells undergoes apical constriction and cell shape changes, stigmatophore cells undergo convergent extension like movements and decrease the circumference of the area that they occupy. Through these rearrangements the stigmatophore cells could generate compression to the spiracular chamber cells and confer an extra push to the invagination (Figure 48). Impairment of the stigmatophore rearrangements in *Btk29A* mutants leads to abnormally formed stigmatophore, invagination defects at the spiracular chamber and an overall impaired morphology of the spiracle morphology.

Convergent extension/intercalation movements have been linked to remodelling of adhesion junctions (reviewed in (Munjal and Lecuit, 2014; Wirtz-Peitz and Zallen, 2009)). It remains to be tested (through modelling and direct measurements of the involved mechanical forces) whether they could also generate equivalent compression onto nearby tissues in some contexts. An analysis of the cell biological basis of stigmatophore morphogenesis coupled to modelling of the cell and tissue interactions during spiracle morphogenesis will provide further clues as to the similarities among mechanisms of invagination.



**Figure 48: Stigmatophore cell rearrangements mediate the invagination of the neighboring spiracular chamber cells**

Physical interactions among organ components drive posterior spiracle morphogenesis. Spiracle development relies on the concurrent movements of two different cell populations: Cut<sup>+</sup> spiracular chamber cells (reddish colour) constrict apically and invaginate, while the surrounding Sal<sup>+</sup> stigmatophore cells (bluish colour) perform convergent extension-like movements and rearrange in the plane of the epidermis. In *Btk29A* mutants, the Cut<sup>+</sup> cells constrict apically and elongate, but they fail to complete the invagination process. Additionally, the morphogenetic movements of the Sal<sup>+</sup> cells are impaired. Driving expression of *Btk29A* in the stigmatophore cells rescues both morphogenetic events, while expressing the kinase in the spiracular chamber does not rescue any of the two. This suggests that the execution of the *Btk29A*-dependent convergent extension movements in the stigmatophore is required for the nearby chamber cells to complete their invagination.

---

### D.2.E. Btk29A as a “member” of the AbdB regulatory cascade

The genetic cascade that controls posterior spiracle morphogenesis has been extensively studied. The Hox gene *Abdominal-B* (*AbdB*) is necessary and sufficient to drive posterior spiracle development and thus lays on top of this cascade (Hu and Castelli., 1999; Lovegrove et al., 2006; Castelli-Gair, 2009). During embryogenesis *AbdB* is expressed in the most abdominal segments of the embryo (A8 and A9). *AbdB* mutants completely lack posterior spiracle formation, while ectopic expression of *AbdB* in more anterior embryonic segments leads to the formation of ectopic anterior spiracles.

Our analysis revealed that *Btk29A* falls into the genetic cascade that regulates posterior spiracle morphogenesis. *Btk29A* protein is detected in both spiracular chamber (in high levels) and stigmatophore cells (in moderate levels). In *AbdB* mutants, the relevant *Btk29A* expression in the abdominal segment A8 is completely lost, while all the ectopic anterior segments formed following *AbdB* ectopic expression acquire higher levels of *Btk29A* protein, in a fashion similar to the wild type.

But where does *Btk29A* stand in the *AbdB* morphogenetic cascade? Several factors lay downstream of *AbdB* in the posterior spiracle cascade: transcription factors and signalling molecules (primary and secondary targets of *AbdB*) and proteins involved in cell adhesion, cytoskeleton organization and cell polarity (realisator genes) (Lovegrove et al., 2006). Analysis of *Btk29A* expression in stage 11 mutant embryos for primary and secondary *AbdB* target genes (*cut*, *ems*, *spalt*, *grn*, *trh*, *grh*) showed normal levels of *Btk29A* expression in both spiracular chamber and stigmatophore cells. Is stage 11 late enough to see effects of loss-of-function of these genes? It is, because for example upregulation of *Crb* is lost in *upd* mutants already at stage 11 (Lovegrove et al., 2006).

Thus, since none of these factors seems to regulate *Btk29A* expression in the posterior spiracles, we assume that the expression of the kinase is a direct target of *AbdB*. Of course the possibility that the *Btk29A* expression is regulated by more than one of the downstream targets or by a yet unknown *AbdB* target cannot be excluded.

Analysis of *Btk29A* function in other systems (Guarnieri et al., 1998; Matusek et al., 2006; Roulier et al., 1998; Tateno et al., 2000) has shown that the kinase is involved in the organization of the actin cytoskeleton in different tissues. This would suggest a similar function of *Btk29A* in the posterior spiracles, putting the kinase in the “group” of *AbdB* realisator genes. In our system such scenario though is not substantiated by our results: *Btk29A* mutants display high levels of actin on the apical side of the spiracular chamber cells, like in wild type.

---

The role of the kinase in the stigmatophore remains to be identified. The only realisor gene known to be expressed in the stigmatophore cells is Cad86C (Lovegrove et al., 2006), but its role in the morphogenesis of the tissue has not been examined. Analysis of the role of Btk29A together with Cad86C will give information about the mechanisms regulating stigmatophore morphogenesis.

#### **D.2. F. Conclusion and perspectives**

Altogether our data uncover the interaction between the morphogenetic processes occurring in the two adjacent epithelial primordia that make up the spiracles. Specifically, it is shown for the first time that proper cell intercalation in the stigmatophore is required for the complete invagination of the spiracular chamber.

Of note, all cells of the spiracular chamber undergo apical constriction in *Btk29A* mutants as in the wild type. This shows that apical constriction per se is not enough to ensure the invagination of all chamber cells in the spiracle and that somehow the planar cell rearrangements of the surrounding cells ensure that the spiracular chamber invagination programme is fully accomplished.

Now that such relationship has been uncovered, it will be interesting to identify and measure the forces mediating this interaction and to reveal its cellular and molecular mediators in this context.



---

### D.3.Trachea system

The interest of our group in the *Btk29A* gene followed its identification in a screen for mutations that impair the *Drosophila* respiratory system and in particular the permeability barrier of the tracheal epithelium. *Btk29A* mutant embryos have a leaky tracheal epithelium: rhodamine tagged dextran molecules injected in the hemocoel of the embryo are able to diffuse into the tracheal lumen. Part of the work undertaken during my doctoral studies was aimed at the identification of the cellular and molecular bases for the dye penetration phenotype observed in *Btk29A* mutants. In particular I set out to identify possible developmental, differentiation and maturation defects in the trachea.

First, I examined the general tracheal morphology at different embryonic stages and found no defects: tracheal size and branching pattern are normal in the mutant and no convolutions, distortions or breaks in the tubes could be detected. This would suggest that early embryonic development of the tissue is not affected by *Btk29A* loss of function.

Second, I assessed several cell biological parameters of the tracheal cells, including cell polarity and cell adhesion. Importantly my analysis revealed that the Septate Junctions (SJs), found among epithelial cells in *Drosophila* and known to be important for the establishment of the permeability barrier, are not affected in *Btk29A* mutants. Specifically, SJ components localize normally (as assessed by immunostaining and confocal imaging) and SJ can be clearly seen in transmission electron micrographs of both control and mutant trachea.

I next tried to pinpoint the cellular basis of the tracheal permeability defects through tissue-specific rescue experiments. The phenotype can be rescued when *Btk29A* expression is restored in all ectoderm-derived tissues, confirming that loss of *Btk29A* is responsible for the defect. Contrary to our expectations, pan-tracheal expression with the *btl-GAL4* driver could not restore an impermeable tracheal epithelium. This could be explained by a requirement for *Btk29A* outside of the *btl-GAL* spatial and/or temporal domains, or insufficient expression levels. The results of these and other rescue experiments also suggested an alternative interpretation, pointing to a function for *Btk29A* in the most posterior part of the respiratory system. In particular, could the dye phenotype be a secondary effect of the impaired posterior spiracle morphogenesis characteristic of *Btk29A* mutants? Some of these points are discussed in more detail in the paragraphs below.

---

### D.3.A. Is the Btk29A kinase a regulator of tissue insulation?

The establishment of epithelial permeability barriers is crucial for the maintenance of tissue integrity and the functionality of the organs. In the vertebrate nervous system, specialized intercellular junctions, the Paranodal Junctions, are formed between the axons and glial cells. They ensure the formation of a diffusion barrier which is critical for the efficient insulation of the nervous system and thus crucial for the conduction of the neural signal. Several pathological conditions have been linked to impaired Paranodal Junction (PJs) formation.

In *Drosophila*, the formation of epithelial diffusion barriers depends on the SJs formed between the neighboring epithelial cells. In addition to their functional similarities *Drosophila* SJs and vertebrate PJs share common features in their molecular composition and ultrastructure. They display highly conserved protein complexes containing Neurexins and membrane cell adhesion molecules. They also share a similar ultrastructural organization: they both display a characteristic ladder-like ultrastructure (Banerjee et al., 2006; Hortsch and Margolis, 2003). In recent years fruit fly SJs have been developed as a useful model for the analysis of the formation and function of diffusion barriers, as well as for the identification of new components and regulators of adhesion structures.

Impairment of the formation or maintenance of the SJ leads to defective permeability barriers. In the *Drosophila* tracheal epithelium the barrier impairments can be monitored by the well-established dye penetration phenotype: the diffusion of dextran molecules in the tracheal lumen. Observation of such phenotype in the tracheal system of *Btk29A* mutants led to the initial hypothesis that the SJs are affected in the absence of the Tec kinase. We started our analysis with this hypothesis, aiming to understand the role of Btk29A in the SJ formation. At a basic research level and in the long term, this project fitted well with the main interests of the host group in the molecular mechanisms of nervous system insulation and Paranodal Junctions.

Analysis of several parameters related to efficient SJ development and function in *Drosophila* were examined in *Btk29A* mutants. The localization of the known SJ components was not impaired and the characteristic ladder-like ultrastructural morphology of the junctions was not affected. Moreover, additional tracheal features known to be dependent on SJ function, like the deposition of chitin modifying molecules and the establishment of a proper tracheal size, appeared normal. As mentioned earlier in the Results section, I cannot exclude that more subtle SJ phenotypes exist. In particular, future work might try to expand the mutant analysis at the ultrastructural level and to assess the phenotypes in a more quantitative manner. In addition, the issue of selectivity of the tracheal barrier could be explored more systematically.

---

Mammalian Tec kinases are primarily expressed in the immune system, but some family members are also expressed in other tissues, including epithelia. In at least one in vitro system of epithelial culture cells Tek kinases regulate the phosphorylation of the tight-junction component occluding (Hamm-Alvarez et al., 2001). Leda Zoupi in the Karagogeos lab conducted preliminary experiments with samples from the paranodal region of the mouse nervous system with RT-PCR. Her analysis of Btk kinase expression showed no detectable expression. The expression and function of other Tec kinases in the glial permeability barrier has not been investigated.

#### D.3.B. The “yet unknown” cellular basis for Btk29A function in the tracheal system

Permeability of the tracheal epithelium can be rescued in Btk29A mutants if gene expression is restored in all epidermal derivatives, (with 69B-GAL4) in posterior segments (with AbdB-GAL4), in subsets of trachea and in spiracles (with sal-GAL4). Efficient rescue of the phenotype with the sal-GAL4 and AbdB-GAL4 drivers points towards the posterior region of the respiratory system as the site where the kinase is required. Specifically, these tissues include the posterior part of the trachea system and the stigmatophore cells of the posterior spiracle. Having uncovered that Btk29A affects stigmatophore formation, we wondered if the trachea dye phenotype is a secondary effect to the impaired posterior spiracle morphogenesis?

In order to test this hypothesis, double mutants for *Btk29A* and *ems* were injected with rhodamine dextran. *ems* mutant embryos essentially lack the spiracles and the trachea-spiracle connection but they do not show dye penetration phenotype. On the contrary trachea become dye-permeable when both *ems* and *Btk29A* are missing. These results suggest that the phenotype might be “tissue autonomous” and not secondary to the posterior spiracle phenotype.

Our analysis of the tracheal dye penetration phenotype has led to the exclusion of several scenarios and has narrowed down the region where Btk29A function is required for a proper tracheal diffusion barrier to the posterior most region of the embryo. Exclusion of the involvement of the posterior spiracles would suggest that the phenotype is mostly linked to the posterior part of the trachea. But what is special with this part? Further analysis is required to answer this point.

---

## CONCLUSION

---

My PhD project belonged to an ongoing effort in the host laboratory aimed at the identification and characterization of novel genes involved in the development and maturation of the tubular respiratory system of *Drosophila*. In particular the overarching aim of my work was to explain the role of the Btk29A kinase. I developed several tools to tackle this question with a combination of molecular, genetic and imaging (including live-imaging) analysis. Specifically I generated probes, a polyclonal antibody, transgenic lines, and imaging protocols to study Btk29A in the trachea and spiracles of the fruit fly.

I attempted to understand the involvement of Btk29A in the integrity of the tracheal system. I combined functional assays (dye penetration assay, observation of air-filling) and electron-microscopy to the above mentioned approaches to investigate this point. My analysis led to the exclusion of what we initially thought would be the most likely some molecular-cellular scenarios to explain the failure of the permeability barrier in the airways of *Btk29A* mutants, namely a disruption of SJ assembly. It has not yet been possible to identify the mechanisms linking the loss of Btk29A to the phenotype.

Significant results were obtained for the role of the kinase in the developing posterior spiracles. An unexpected connection between the morphogenesis of the inner part of the system, the invaginating spiracular chamber, and the Btk29A-dependent cell rearrangements of the adjacent outer stigmatophore was proven for the first time. This intriguing observation opens up new perspectives on the morphogenesis of this and other tissues.

To conclude, this study points out the importance of the physical interactions occurring among nearby tissues during morphogenesis that have an impact on organ development and, possibly, physiology.

---

## REFERENCES

---

- Anderson, J.M. (2001). Molecular Structure of Tight Junctions and Their Role in Epithelial Transport. *Physiology* 16, 126-130.
- Araújo, S.J., Aslam, H., Tear, G., and Casanova, J. (2005). *mummy/cystic* encodes an enzyme required for chitin and glycan synthesis, involved in trachea, embryonic cuticle and CNS development--Analysis of its role in *Drosophila* tracheal morphogenesis. *Developmental Biology* 288, 179-193.
- Asztalos, Z., Baba, K., Yamamoto, D., and Tully, T. (2007). The fickle mutation of a cytoplasmic tyrosine kinase effects sensitization but not dishabituation in *Drosophila melanogaster*. *Journal of Neurogenetics* 21, 59-71.
- Auld, V.J., Fetter, R.D., Broadie, K., and Goodman, C.S. (1995). Gliotactin, a novel transmembrane protein on peripheral glia, is required to form the blood-nerve barrier in *drosophila*. *Cell* 81, 757-767.
- Baba, K., Takeshita, A., Majima, K., Ueda, R., Kondo, S., Juni, N., and Yamamoto, D. (1999). The *Drosophila* Bruton's Tyrosine Kinase (Btk) Homolog Is Required for Adult Survival and Male Genital Formation. *Mol Cell Biol* 19, 4405-4413.
- Bachmann, A., Draga, M., Grawe, F., and Knust, E. (2008). On the role of the MAGUK proteins encoded by *Drosophila varicose* during embryonic and postembryonic development. *BMC Developmental Biology* 8, 55.
- Banerjee, S., Sousa, A., and Bhat, M. (2006). Organization and function of septate junctions. *Cell Biochemistry and Biophysics* 46, 65-77.
- Bätz, T., Förster, D., and Luschnig, S. (2014). The transmembrane protein Macroglobulin complement-related is essential for septate junction formation and epithelial barrier function in *Drosophila*. *Development* 141, 899-908.
- Baumgartner, S., Littleton, J., Broadie, K., Bhat, M., Harbecke, R., Lengyel, J., Chiquet-Ehrismann, R., Prokop, A., and Bellen, H. (1996). A *Drosophila* neurexin is required for septate junction and blood-nerve barrier formation and function. *Cell* 87, 1059 - 1068.
- Beckett, K., and Baylies, M.K. (2006). *Parcas*, a regulator of non-receptor tyrosine kinase signaling, acts during anterior-posterior patterning and somatic muscle development in *Drosophila melanogaster*. *Developmental Biology* 299, 176-192.
- Behr, M., Riedel, D., and Schuh, R. (2003). The Claudin-like *Megatrachea* is essential in septate junctions for the epithelial barrier function in *Drosophila*. *Dev Cell* 5, 611 - 620.
- Beitel, G., and Krasnow, M. (2000). Genetic control of epithelial tube size in the *Drosophila* tracheal system. *Development* 127, 3271 - 3282.
- Boulet, A.M., Lloyd, A., and Sakonju, S. (1991). Molecular definition of the morphogenetic and regulatory functions and the cis-regulatory elements of the *Drosophila* *Abd-B* homeotic gene. *Development* 111, 393-405.
- Bradley, P.L., and Andrew, D.J. (2001). *ribbon* encodes a novel BTB/POZ protein required for directed cell migration in *Drosophila melanogaster*. *Development* 128, 3001-3015.
- Brand, A.H., and Perrimon, N. (1993). Targeted gene expression as a means of altering cell fates and generating dominant phenotypes. *Development* 118, 401-415.
- Bray, S.J., and Kafatos, F.C. (1991). Developmental function of *Elf-1*: an essential transcription factor during embryogenesis in *Drosophila*. *Genes & Development* 5, 1672-1683.
- Brodu, V., and Casanova, J. (2006). The RhoGAP *crossveinless-c* links *trachealess* and EGFR signaling to cell shape remodeling in *Drosophila* tracheal invagination. *Genes & Development* 20, 1817-1828.
- Brown, S., and Castelli-Gair Hombria, J. (2000). *Drosophila* *grain* encodes a GATA transcription factor required for cell rearrangement during morphogenesis. *Development* 127, 4867-4876.
- Brown, S., Hu, N., and Castelli-Gair Hombria, J. (2001). Identification of the first invertebrate interleukin JAK/STAT receptor, the *Drosophila* gene *domeless*. *Current Biology* 11, 1700-1705.



- 
- Brown, S., Hu, N., and Hombría, J.C.-G. (2003). Novel level of signalling control in the JAK/STAT pathway revealed by in situ visualisation of protein-protein interaction during *Drosophila* development. *Development* *130*, 3077-3084.
  - Casanova, J., Sánchez-Herrero, E., and Morata, G. (1986). Identification and characterization of a parasegment specific regulatory element of the abdominal-B gene of *Drosophila*. *Cell* *47*, 627-636.
  - Castelli-Gair Hombría, J., Rivas, M.L., and Sotillos, S. (2009). Genetic control of morphogenesis - Hox induced organogenesis of the posterior spiracles. *The International Journal of Developmental Biology* *53*, 1349 - 1358.
  - Castelli-Gair, J. (1998). Implications of the spatial and temporal regulation of Hox genes on development and evolution, pp. 437-444.
  - Castelli-Gair, J., Greig, S., Micklem, G., and Akam, M. (1994). Dissecting the temporal requirements for homeotic gene function. *Development* *120*, 1983-1995.
  - Caviglia, S., and Luschnig, S. (2014). Tube fusion: Making connections in branched tubular networks. *Seminars in Cell & Developmental Biology* *31*, 82-90.
  - Centanin, L., Dekanty, A., Romero, N., Irisarri, M., Gorr, T.A., and Wappner, P. (2008). Cell Autonomy of HIF Effects in *Drosophila*: Tracheal Cells Sense Hypoxia and Induce Terminal Branch Sprouting. *Developmental Cell* *14*, 547-558.
  - Centanin, L., Gorr, T.A., and Wappner, P. (2010). Tracheal remodelling in response to hypoxia. *Journal of Insect Physiology* *56*, 447-454.
  - Chandran, R.R., Iordanou, E., Ajja, C., Wille, M., and Jiang, L. (2014). Gene expression profiling of *Drosophila* tracheal fusion cells. *Gene Expression Patterns* *15*, 112-123.
  - Chandrasekaran, V., and Beckendorf, S.K. (2005). Tec29 controls actin remodeling and endoreplication during invagination of the *Drosophila* embryonic salivary glands. *Development* *132*, 3515-3524.
  - Chen, C.K., Kuhnlein, R.P., Eulenberg, K.G., Vincent, S., Affolter, M., and Schuh, R. (1998). The transcription factors KNIRPS and KNIRPS RELATED control cell migration and branch morphogenesis during *Drosophila* tracheal development. *Development* *125*, 4959-4968.
  - Choi, S.-C., and Han, J.-K. (2002). *Xenopus* Cdc42 Regulates Convergent Extension Movements during Gastrulation through Wnt/Ca2+ Signaling Pathway. *Developmental Biology* *244*, 342-357.
  - Chung, S., Chavez, C., and Andrew, D.J. (2011). Trachealess (Trh) regulates all tracheal genes during *Drosophila* embryogenesis. *Developmental Biology* *360*, 160-172.
  - Chung, S., Vining, M.S., Bradley, P.L., Chan, C.-C., Wharton, K.A., Jr., and Andrew, D.J. (2009). Serrano (Sano) Functions with the Planar Cell Polarity Genes to Control Tracheal Tube Length. *PLoS Genet* *5*, e1000746.
  - Dalton, D., Chadwick, R., and McGinnis, W. (1989). Expression and embryonic function of empty spiracles: a *Drosophila* homeo box gene with two patterning functions on the anterior-posterior axis of the embryo. *Genes & Development* *3*, 1940-1956.
  - de Celis, J.F., Barrio, R., and Kafatos, F.C. (1996). A gene complex acting downstream of dpp in *Drosophila* wing morphogenesis. *Nature* *381*, 421-424.
  - de Celis, J.F., Barrio, R., and Kafatos, F.C. (1999). Regulation of the spalt/spalt-related gene complex and its function during sensory organ development in the *Drosophila* thorax. *Development* *126*, 2653-2662.
  - de Celis, J.F., Llimargas, M., and Casanova, J. (1995). Ventral veinless, the gene encoding the Cf1a transcription factor, links positional information and cell differentiation during embryonic and imaginal development in *Drosophila melanogaster*. *Development* *121*, 3405-3416.
  - de Navas, L., Foronda, D., Suzanne, M., and Sánchez-Herrero, E. (2006). A simple and efficient method to identify replacements of P-lacZ by P-Gal4 lines allows obtaining Gal4 insertions in the bithorax complex of *Drosophila*. *Mechanisms of Development* *123*, 860-867.
  - Devine, W.P., Lubarsky, B., Shaw, K., Luschnig, S., Messina, L., and Krasnow, M.A. (2005). Requirement for chitin biosynthesis in epithelial tube morphogenesis. *Proceedings of the National Academy of Sciences of the United States of America* *102*, 17014-17019.
-

- 
- Faivre-Sarrailh, C., Banerjee, S., Li, J., Hortsch, M., Laval, M., and Bhat, M. (2004). Drosophila contactin, a homolog of vertebrate contactin, is required for septate junction organization and paracellular barrier function. *Development* *131*, 4931 - 4942.
  - Faulkner, D.L., Dockendorff, T.C., and Jongens, T.A. (1998). Clonal analysis of *cmp44E*, which encodes a conserved putative transmembrane protein, indicates a requirement for cell viability in Drosophila. *Developmental Genetics* *23*, 264-274.
  - Fehon, R., Dawson, I., and Artavanis, T. (1994). A Drosophila homologue of membrane-skeleton protein 4.1 is associated with septate junctions and is encoded by the *coracle* gene. *Development* *120*, 545 - 557.
  - Förster, D., Armbruster, K., and Luschnig, S. (2010). Sec24-Dependent Secretion Drives Cell-Autonomous Expansion of Tracheal Tubes in Drosophila. *Current Biology* *20*, 62-68.
  - Forster, D., and Luschnig, S. (2012). Src42A-dependent polarized cell shape changes mediate epithelial tube elongation in Drosophila. *Nat Cell Biol* *14*, 526–534.
  - Fung, S., Wang, F., Chase, M., Godt, D., and Hartenstein, V. (2008). Expression profile of the cadherin family in the developing Drosophila brain. *The Journal of Comparative Neurology* *506*, 469-488.
  - Gallio, M., Englund, C., Kylsten, P., and Samakovlis, C. (2004). Rhomboid 3 orchestrates Slit-independent repulsion of tracheal branches at the CNS midline. *Development* *131*, 3605-3614.
  - Garces, A., and Thor, S. (2006). Specification of Drosophila aCC motoneuron identity by a genetic cascade involving even-skipped, grain and *zfh1*. *Development* *133*, 1445-1455.
  - Garcia-Bellido, A. (1975). Genetic control of wing disc development in Drosophila. In *Cell Patterning Ciba Found Symp* *29*, 161-178.
  - Genova, J., and Fehon, R. (2003). Neuroglian, Gliotactin, and the Na<sup>+</sup>/K<sup>+</sup> ATPase are essential for septate junction function in Drosophila. *J Cell Biol* *161*, 979 - 989.
  - Gervais, L., and Casanova, J. (2010). In Vivo Coupling of Cell Elongation and Lumen Formation in a Single Cell. *Current Biology* *20*, 359-366.
  - Ghabrial, A., Luschnig, S., Metzstein, M.M., and Krasnow, M.A. (2003). Branching morphogenesis of the Drosophila tracheal system. *Annual Review of Cell and Developmental Biology* *19*, 623-647.
  - Grawe, F., Wodarz, A., Lee, B., Knust, E., and Skaer, H. (1996). The Drosophila genes *crumbs* and *stardust* are involved in the biogenesis of adherens junctions. *Development* *122*, 951-959.
  - Gregory, R.J., Kammermeyer, K.L., Vincent, W.S., and Wadsworth, S.G. (1987). Primary sequence and developmental expression of a novel Drosophila melanogaster *src* gene. *Molecular and Cellular Biology* *7*, 2119-2127.
  - Guarnieri, D.J., Dodson, G.S., and Simon, M.A. (1998). SRC64 Regulates the Localization of a Tec-Family Kinase Required for Drosophila Ring Canal Growth. *Molecular cell* *1*, 831-840.
  - Hamada-Kawaguchi, N., Nore, B.F., Kuwada, Y., Smith, C.I.E., and Yamamoto, D. (2014). Btk29A Promotes Wnt4 Signaling in the Niche to Terminate Germ Cell Proliferation in Drosophila. *Science* *343*, 294-297.
  - Hamada, N., Bäckesjö, C.-M., Smith, C.I.E., and Yamamoto, D. (2005). Functional replacement of Drosophila Btk29A with human Btk in male genital development and survival. *FEBS Letters* *579*, 4131-4137.
  - Hamm-Alvarez, S.F., Chang, A., Wang, Y., Jerdeva, G., Lin, H.H., Kim, K.-J., and Ann, D.K. (2001). Etk/Bmx activation modulates barrier function in epithelial cells. *American Journal of Physiology - Cell Physiology* *280*, C1657-C1668.
  - Heymann, N., and Lehmann, F.-O. (2006). The significance of spiracle conductance and spatial arrangement for flight muscle function and aerodynamic performance in flying Drosophila. *Journal of Experimental Biology* *209*, 1662-1677.
  - Hijazi, A., Masson, W., Augé, B., Waltzer, L., Haenlin, M., and Roch, F. (2009). *boudin* is required for septate junction organisation in Drosophila and codes for a diffusible protein of the Ly6 superfamily. *Development* *136*, 2199-2209.
  - Hill, E., Broadbent, I.D., Chothia, C., and Pettitt, J. (2001). Cadherin superfamily proteins in *Caenorhabditis elegans* and *Drosophila melanogaster*. *Journal of Molecular Biology* *305*, 1011-1024.
-

- 
- Hortsch, M., and Margolis, B. (2003). Septate and paranodal junctions: kissing cousins. *Trends Cell Biol* *13*, 557 - 561.
  - Hu, N., and Castelli-Gair, J. (1999). Study of the Posterior Spiracles of *Drosophila* as a Model to Understand the Genetic and Cellular Mechanisms Controlling Morphogenesis. *Developmental Biology* *214*, 197-210.
  - Huang, F.D., Matthies, H.J., Speese, S.D., Smith, M.A., and Broadie, K. (2004). Rolling blackout, a newly identified PIP2-DAG pathway lipase required for *Drosophila* phototransduction. *Nature Neuroscience* *7*, 1070-1078.
  - Huang, F.D., Woodruff, E., Mohrmann, R., and Broadie, K. (2006). Rolling blackout is required for synaptic vesicle exocytosis. *Journal of Neuroscience* *26*, 2369-2379.
  - Ile, K.E., Tripathy, R., Goldfinger, V., and Renault, A.D. (2012). Wunen, a *Drosophila* lipid phosphate phosphatase, is required for septate junction-mediated barrier function. *Development* *139*, 2535-2546.
  - Ingley, E. (2008). Src family kinases: Regulation of their activities, levels and identification of new pathways. *Biochimica et Biophysica Acta (BBA) - Proteins and Proteomics* *1784*, 56-65.
  - Isaac, D.D., and Andrew, D.J. (1996). Tubulogenesis in *Drosophila*: a requirement for the tracheless gene product. *Genes & Development* *10*, 103-117.
  - Jayaram, S.A., Senti, K.-A., Tiklová, K., Tsarouhas, V., Hemphälä, J., and Samakovlis, C. (2008). COPI Vesicle Transport Is a Common Requirement for Tube Expansion in *Drosophila*. *PLoS ONE* *3*, e1964.
  - Johnson, T.K., and Judd, B.H. (1979). Analysis of the cut locus of *Drosophila melanogaster*. *Genetics* *92*, 485-502.
  - Jones, B., and McGinnis, W. (1993). The regulation of empty spiracles by Abdominal-B mediates an abdominal segment identity function. *Genes & Development* *7*, 229-240.
  - Jordan, P., and Karess, R. (1997). Myosin Light Chain-activating Phosphorylation Sites Are Required for Oogenesis in *Drosophila*. *The Journal of Cell Biology* *139*, 1805-1819.
  - Katzen, A.L., Kornberg, T., and Bishop, J.M. (1990). Diverse expression of *Dsrc29A*, a gene related to *src*, during the life cycle of *Drosophila melanogaster*. *Development* *110*, 1169-1183.
  - Keller, R., Davidson, L., Edlund, A., Elul, T., Ezin, M., Shook, D., and Skoglund, P. (2000). Mechanisms of convergence and extension by cell intercalation. *Philosophical Transactions of the Royal Society B: Biological Sciences* *355*, 897-922.
  - Kerman, B.E., Cheshire, A.M., and Andrew, D.J. (2006). From fate to function: the *Drosophila* trachea and salivary gland as models for tubulogenesis. *Differentiation* *74*, 326-348.
  - Klämbt, C., Glazer, L., and Shilo, B.Z. (1992). *breathless*, a *Drosophila* FGF receptor homolog, is essential for migration of tracheal and specific midline glial cells. *Genes & Development* *6*, 1668-1678.
  - Klebes, A., and Knust, E. (2000). A conserved motif in *Crumbs* is required for E-cadherin localisation and zonula adherens formation in *Drosophila*. *Curr Biol* *10*, 76 - 85.
  - Knust, E., Dietrich, U., Tepass, U., Bremer, K.A., Weigel, D., Vässin, H., and Campos-Ortega, J.A. (1987). EGF homologous sequences encoded in the genome of *Drosophila melanogaster*, and their relation to neurogenic genes. *The EMBO Journal* *6*, 761-766.
  - Koerner, T.J., Hill, J.E., Myers, A.M., and Tzagoloff, A. (1991). [33] High-expression vectors with multiple cloning sites for construction of *trpE* fusion genes: *pATH* vectors. In *Methods in enzymology*, G.R.F. Christine Guthrie, ed. (Academic Press), pp. 477-490.
  - Kondo, T., and Hayashi, S. (2013). Mitotic cell rounding accelerates epithelial invagination. *Nature* *494*, 125-129.
  - Krattinger, A., Gendre, N., Ramaekers, A., Grillenzoni, N., and Stocker, R. (2007). *DmOAZ*, the unique *Drosophila melanogaster* OAZ homologue is involved in posterior spiracle development. *Development Genes and Evolution* *217*, 197-208.
  - Kuhnlein, R.P., Frommer, G., Friedrich, M., Gonzalez-Gaitan, M., Weber, A., Wagner-Bernholz, J.F., Gehring, W.J., Jackle, H., and Schuh, R. (1994). *spalt* encodes an evolutionarily conserved zinc finger
-

---

protein of novel structure which provides homeotic gene function in the head and tail region of the *Drosophila* embryo. *The EMBO Journal* 13, 168-179.

- Kuhnlein, R.P., and Schuh, R. (1996). Dual function of the region-specific homeotic gene *spalt* during *Drosophila* tracheal system development. *Development* 122, 2215-2223.
- Kumar, M., Joseph, M., and Chandrashekar, S. (2001). Effects of mutations at the *stambh A* locus of *Drosophila melanogaster*. *Journal of Genetics* 80, 83-95.
- Lamb, R., Ward, R., Schweizer, L., and Fehon, R. (1998). *Drosophila* *coracle*, a member of the protein 4.1 superfamily, has essential structural functions in the septate junctions and developmental functions in embryonic and adult epithelial cells. *Mol Biol Cell* 9, 3505 - 3519.
- Lamka, M.L., Boulet, A.M., and Sakonju, S. (1992). Ectopic expression of *UBX* and *ABD-B* proteins during *Drosophila* embryogenesis: competition, not a functional hierarchy, explains phenotypic suppression. *Development* 116, 841-854.
- Laprise, P., Paul, S.M., Boulanger, J., Robbins, R.M., Beitel, G.J., and Tepass, U. (2010). Epithelial Polarity Proteins Regulate *Drosophila* Tracheal Tube Size in Parallel to the Luminal Matrix Pathway. *Current Biology* 20, 55-61.
- Laval, M., Bel, C., and Faivre-Sarrailh, C. (2008). The lateral mobility of cell adhesion molecules is highly restricted at septate junctions in *Drosophila*. *BMC Cell Biol* 9, 38.
- Lebreton, G., and Casanova, J. (2014). Specification of leading and trailing cell features during collective migration in the *Drosophila* trachea. *Journal of Cell Science* 127, 465-474.
- Lecuit, T., and Wieschaus, E. (2002). Junctions as Organizing Centers in Epithelial Cells? A Fly Perspective. *Traffic* 3, 92-97.
- Lee, S., and Kolodziej, P.A. (2002). The plakin *Short Stop* and the *RhoA* GTPase are required for E-cadherin-dependent apical surface remodeling during tracheal tube fusion. *Development* 129, 1509-1520.
- Li, W., Noll, E., and Perrimon, N. (2000). Identification of Autosomal Regions Involved in *Drosophila* *Raf* Function. *Genetics* 156, 763-774.
- Liu, R., Woolner, S., Johndrow, J.E., Metzger, D., Flores, A., and Parkhurst, S.M. (2008). *Sisyphus*, the *Drosophila* myosin XV homolog, traffics within filopodia transporting key sensory and adhesion cargos. *Development* 135, 53-63.
- Llimargas, M. (1999). The Notch pathway helps to pattern the tips of the *Drosophila* tracheal branches by selecting cell fates. *Development* 126, 2355-2364.
- Llimargas, M., and Casanova, J. (2010). Apical constriction and invagination: A very self-reliant couple. *Developmental Biology* 344, 4-6.
- Llimargas, M., Strigini, M., Katidou, M., Karagogeos, D., and Casanova, J. (2004). *Lachesin* is a component of a septate junction-based mechanism that controls tube size and epithelial integrity in the *Drosophila* tracheal system. *Development* 131, 181-190.
- Lovegrove, B., Simões, S., Rivas, M.L., Sotillos, S., Johnson, K., Knust, E., Jacinto, A., and Hombría, J.C.-G. (2006). Coordinated Control of Cell Adhesion, Polarity, and Cytoskeleton Underlies Hox-Induced Organogenesis in *Drosophila*. 16, 2206-2216.
- Lu, N., Guarnieri, D.J., and Simon, M.A. (2004). Localization of *Tec29* to ring canals is mediated by *Src64* and *PtdIns(3,4,5)P3*-dependent mechanisms. *EMBO J* 23, 1089-1100.
- Lundström, A., Gallio, M., Englund, C., Steneberg, P., Hemphälä, J., Aspenström, P., Keleman, K., Falileeva, L., Dickson, B.J., and Samakovlis, C. (2004). *Vilse*, a conserved *Rac/Cdc42* GAP mediating *Robo* repulsion in tracheal cells and axons. *Genes & Development* 18, 2161-2171.
- Luschnig, S., Batz, T., Armbruster, K., and Krasnow, M. (2006). *serpentine* and *vermiform* encode matrix proteins with chitin binding and deacetylation domains that limit tracheal tube length in *Drosophila*. *Curr Biol* 16, 186 - 194.
- Manning, G., and Krasnow, M.A. (1993). Development of the *Drosophila* tracheal system. In *The Development of Drosophila* (ed. A. Martinez-Arias and M. Bate) (Cold Spring Harbor, New York: Cold Spring Harbor Laboratory Press), pp. 609-685.



- 
- Mano, H. (1999). Tec family of protein-tyrosine kinases: an overview of their structure and function. *Cytokine & Growth Factor Reviews* 10, 267-280.
  - Martin, A.C., Gelbart, M., Fernandez-Gonzalez, R., Kaschube, M., and Wieschaus, E.F. (2010). Integration of contractile forces during tissue invagination. *The Journal of Cell Biology* 188, 735-749.
  - Massarwa, R.a., Schejter, E.D., and Shilo, B.-Z. (2009). Apical Secretion in Epithelial Tubes of the *Drosophila* Embryo Is Directed by the Formin-Family Protein Diaphanous. *Developmental Cell* 16, 877-888.
  - Matusek, T., Djiane, A., Jankovics, F., Brunner, D., Mlodzik, M., and Mihály, J. (2006). The *Drosophila* formin DAAM regulates the tracheal cuticle pattern through organizing the actin cytoskeleton. *Development* 133, 957-966.
  - Maurel-Zaffran, C., Pradel, J., and Graba, Y. (2010). Reiterative use of signalling pathways controls multiple cellular events during *Drosophila* posterior spiracle organogenesis. *Developmental Biology* 343, 18-27.
  - Maybeck, V., and Roper, K. (2009). A Targeted Gain-of-Function Screen Identifies Genes Affecting Salivary Gland Morphogenesis/Tubulogenesis in *Drosophila*. *Genetics* 181, 543-565.
  - Merabet, S., Catala, F., Pradel, J., and Graba, Y. (2002). A Green Fluorescent Protein Reporter Genetic Screen That Identifies Modifiers of Hox Gene Function in the *Drosophila* Embryo. *Genetics* 162, 189-202.
  - Merabet, S., Hombria, J.C.-G., Hu, N., Pradel, J., and Graba, Y. (2005). Hox-controlled reorganisation of intrasegmental patterning cues underlies *Drosophila* posterior spiracle organogenesis. *Development* 132, 3093-3102.
  - Moussian, B. (2010). Recent advances in understanding mechanisms of insect cuticle differentiation. *Insect Biochemistry and Molecular Biology* 40, 363-375.
  - Moussian, B., Schwarz, H., Bartoszewski, S., and Nüsslein-Volhard, C. (2005a). Involvement of chitin in exoskeleton morphogenesis in *Drosophila melanogaster*. *J Morphol* 264, 117 - 130.
  - Moussian, B., Söding, J., Schwarz, H., and Nüsslein-Volhard, C. (2005b). Retroactive, a membrane-anchored extracellular protein related to vertebrate snake neurotoxin-like proteins, is required for cuticle organization in the larva of *Drosophila melanogaster*. *Developmental Dynamics* 233, 1056-1063.
  - Moussian, B., Tång, E., Tønning, A., Helms, S., Schwarz, H., Nüsslein-Volhard, C., and Uv, A.E. (2006). *Drosophila* Knickkopf and Retroactive are needed for epithelial tube growth and cuticle differentiation through their specific requirement for chitin filament organization. *Development* 133, 163-171.
  - Munjal, A., and Lecuit, T. (2014). Actomyosin networks and tissue morphogenesis. *Development* 141, 1789-1793.
  - Nelson, K.S., Furuse, M., and Beitel, G.J. (2010). The *Drosophila* Claudin Kune-kune Is Required for Septate Junction Organization and Tracheal Tube Size Control. *Genetics* 185, 831-839.
  - Nelson, K.S., Khan, Z., Molnar, I., Mihaly, J., Kaschube, M., and Beitel, G.J. (2012). *Drosophila* Src regulates anisotropic apical surface growth to control epithelial tube size. *Nat Cell Biol* 14, 518-525.
  - Nilton, A., Oshima, K., Zare, F., Byri, S., Nannmark, U., Nyberg, K.G., Fehon, R.G., and Uv, A.E. (2010). Crooked, Coiled and Crimped are three Ly6-like proteins required for proper localization of septate junction components. *Development* 137, 2427-2437.
  - Nishimura, M., Inoue, Y., and Hayashi, S. (2007). A wave of EGFR signaling determines cell alignment and intercalation in the *Drosophila* tracheal placode. *Development* 134, 4273-4282.
  - Oda, H., and Tsukita, S. (2001). Real-time imaging of cell-cell adherens junctions reveals that *Drosophila* mesoderm invagination begins with two phases of apical constriction of cells. *J Cell Sci* 114, 493-501.
  - Oda, H., Uemura, T., Harada, Y., Iwai, Y., and Takeichi, M. (1994). A *Drosophila* Homolog of Cadherin Associated with Armadillo and Essential for Embryonic Cell-Cell Adhesion. *Developmental Biology* 165, 716-726.
  - Oshima, K., and Fehon, R.G. (2011). Analysis of protein dynamics within the septate junction reveals a highly stable core protein complex that does not include the basolateral polarity protein Discs large. *Journal of Cell Science* 124, 2861-2871.
-



- 
- Padash-Barmchi, M., Browne, K., Sturgeon, K., Jusiak, B., and Auld, V.J. (2010). Control of Gliotactin localization and levels by tyrosine phosphorylation and endocytosis is necessary for survival of polarized epithelia. *J Cell Sci* *123*, 4052-4062.
  - Pai, L.-M., Kirkpatrick, C., Blanton, J., Oda, H., Takeichi, M., and Peifer, M. (1996). Drosophila  $\alpha$ -Catenin and E-cadherin Bind to Distinct Regions of Drosophila Armadillo. *Journal of Biological Chemistry* *271*, 32411-32420.
  - Parsons, S.J., and Parsons, J.T. (2004). Src family kinases, key regulators of signal transduction. *Oncogene* *23*, 7906-7909.
  - Paul, S.M., Palladino, M.J., and Beitel, G.J. (2007). A pump-independent function of the Na,K-ATPase is required for epithelial junction function and tracheal tube-size control. *Development* *134*, 147-155.
  - Paul, S.M., Ternet, M., Salvaterra, P.M., and Beitel, G.J. (2003). The Na<sup>+</sup>/K<sup>+</sup> ATPase is required for septate junction function and epithelial tube-size control in the Drosophila tracheal system. *Development* *130*, 4963-4974.
  - Ribeiro, C., Neumann, M., and Affolter, M. (2004). Genetic Control of Cell Intercalation during Tracheal Morphogenesis in Drosophila. *Current Biology* *14*, 2197-2207.
  - Richardson, H., O'Keefe, L.V., Marty, T., and Saint, R. (1995). Ectopic cyclin E expression induces premature entry into S phase and disrupts pattern formation in the Drosophila eye imaginal disc. *Development* *121*, 3371-3379.
  - Rivas, M.L., Espinosa-Vázquez, J.M., Sambrani, N., Greig, S., Merabet, S., Graba, Y., and Castelli-Gair Hombría, J. (2013). Antagonism Versus Cooperativity with TALE Cofactors at the Base of the Functional Diversification of Hox Protein Function. *PLoS Genet* *9*, e1003252.
  - Roegiers, F., Kavalier, J., Tolwinski, N., Chou, Y.-T., Duan, H., Bejarano, F., Zitserman, D., and Lai, E.C. (2009). Frequent Unanticipated Alleles of lethal giant larvae in Drosophila Second Chromosome Stocks. *Genetics* *182*, 407-410.
  - Roulier, E.M., Panzer, S., and Beckendorf, S.K. (1998). The Tec29 Tyrosine Kinase Is Required during Drosophila Embryogenesis and Interacts with Src64 in Ring Canal Development. *Molecular cell* *1*, 819-829.
  - Royou, A., Sullivan, W., and Karess, R. (2002). Cortical recruitment of nonmuscle myosin II in early syncytial Drosophila embryos: its role in nuclear axial expansion and its regulation by Cdc2 activity. *The Journal of Cell Biology* *158*, 127-137.
  - Samakovlis, C., Hacohen, N., Manning, G., Sutherland, D.C., Guillemin, K., and Krasnow, M.A. (1996a). Development of the Drosophila tracheal system occurs by a series of morphologically distinct but genetically coupled branching events. *Development* *122*, 1395-1407.
  - Samakovlis, C., Manning, G., Steneberg, P., Hacohen, N., Cantera, R., and Krasnow, M.A. (1996b). Genetic control of epithelial tube fusion during Drosophila tracheal development. *Development* *122*, 3531-3536.
  - Sanchez-Herrero, E., Vernos, I., Marco, R., and Morata, G. (1985). Genetic organization of Drosophila bithorax complex. *Nature* *313*, 108-113.
  - Sanson, B. (2001). Generating patterns from fields of cells: Examples from Drosophila segmentation. *EMBO Reports* *2*, 1083-1088.
  - Sawyer, J.M., Harrell, J.R., Shemer, G., Sullivan-Brown, J., Roh-Johnson, M., and Goldstein, B. (2010). Apical constriction: A cell shape change that can drive morphogenesis. *Developmental Biology* *341*, 5-19.
  - Schejter, E.D., and Wieschaus, E. (1993). bottleneck acts as a regulator of the microfilament network governing cellularization of the Drosophila embryo. *Cell* *75*, 373-385.
  - Schöck, F., and Perrimon, N. (2002). Molecular mechanisms of epithelial morphogenesis. *Annual Review of Cell and Developmental Biology* *18*, 463-493.
  - Schulte, J., Tepass, U., and Auld, V. (2003). Gliotactin, a novel marker of tricellular junctions, is necessary for septate junction development in Drosophila. *J Cell Biol* *161*, 991 - 1000.
  - Shiga, Y., Tanaka-Matakatsu, M., and Hayashi, S. (1996). A nuclear GFP/ $\beta$ -galactosidase fusion protein as a marker for morphogenesis in living Drosophila. *Development, Growth & Differentiation* *38*, 99-106.
-

- 
- Simões, S., Denholm, B., Azevedo, D., Sotillos, S., Martin, P., Skaer, H., Hombría, J.C.-G., and Jacinto, A. (2006). Compartmentalisation of Rho regulators directs cell invagination during tissue morphogenesis. *Development* *133*, 4257-4267.
  - Sinka, R., Jankovics, F., Somogyi, K., Szlanka, T., Lukácsovich, T., and Erdélyi, M. (2002). *poirot*, a new regulatory gene of *Drosophila oskar* acts at the level of the short Oskar protein isoform. *Development* *129*, 3469-3478.
  - Smith, A.V., and Orr-Weaver, T.L. (1991). The regulation of the cell cycle during *Drosophila* embryogenesis: the transition to polyteny. *Development* *112*, 997-1008.
  - Smith, C.I.E., Islam, T.C., Mattsson, P.T., Mohamed, A.J., Nore, B.F., and Vihinen, M. (2001). The Tec family of cytoplasmic tyrosine kinases: mammalian Btk, Bmx, Itk, Tec, Txk and homologs in other species. *Bioessays* *23*, 436-446.
  - Sotillos, S., Espinosa-Vázquez, J.M., Foglia, F., Hu, N., and Hombría, J.C.-G. (2010). An efficient approach to isolate STAT regulated enhancers uncovers STAT92E fundamental role in *Drosophila* tracheal development. *Developmental Biology* *340*, 571-582.
  - Stork, T., Engelen, D., Krudewig, A., Slies, M., Bainton, R., and Klambt, C. (2008). Organization and function of the blood-brain barrier in *Drosophila*. *J Neurosci* *28*, 587 - 597.
  - Strigini, M., Cantera, R., Morin, X., Bastiani, M.J., Bate, M., and Karagogeos, D. (2006). The IgLON protein Lachesin is required for the blood-brain barrier in *Drosophila*. *Molecular and Cellular Neuroscience* *32*, 91-101.
  - Struhl, G., and White, R.A.H. (1985). Regulation of the Ultrabithorax gene of *Drosophila* by other bithorax complex genes. *Cell* *43*, 507-519.
  - Superti-Furga, G., and Courtneidge, S.A. (1995). Structure-function relationships in Src family and related protein tyrosine kinases. *BioEssays* *17*, 321-330.
  - Sutherland, D., Samakovlis, C., and Krasnow, M.A. (1996). *branchless* Encodes a *Drosophila* FGF Homolog That Controls Tracheal Cell Migration and the Pattern of Branching. *Cell* *87*, 1091-1101.
  - Swanson, L.E., Yu, M., Nelson, K.S., Laprise, P., Tepass, U., and Beitel, G.J. (2009). *Drosophila* convoluted/dALS Is an Essential Gene Required for Tracheal Tube Morphogenesis and Apical Matrix Organization. *Genetics* *181*, 1281-1290.
  - Tahinci, E., and Symes, K. (2003). Distinct functions of Rho and Rac are required for convergent extension during *Xenopus* gastrulation. *Developmental Biology* *259*, 318-335.
  - Tatenno, M., Nishida, Y., and Adachi-Yamada, T. (2000). Regulation of JNK by Src During *Drosophila* Development. *Science* *287*, 324-327.
  - Tepass, U., Tanentzapf, G., Ward, R., Fehon, and Richard (2001). Epithelial cell polarity and cell junctions in *Drosophila*. *Annual Review of Genetics* *35*, 747-784.
  - Tepass, U., Theres, C., and Knust, E. (1990). *crumbs* encodes an EGF-like protein expressed on apical membranes of *Drosophila* epithelial cells and required for organization of epithelia. *Cell* *61*, 787-799.
  - Theroux, S.J., and Wadsworth, S.C. (1992). Protein-tyrosine kinase activity of alternate protein products of the *Drosophila* Dsrc28C locus. *FEBS Letters* *311*, 1-6.
  - Thomas, J.H., and Wieschaus, E. (2004). *src64* and *tec29* are required for microfilament contraction during *Drosophila* cellularization. *Development* *131*, 863-871.
  - Tiklová, K., Tsarouhas, V., and Samakovlis, C. (2013). Control of Airway Tube Diameter and Integrity by Secreted Chitin-Binding Proteins in *Drosophila*. *PLoS ONE* *8*, e67415.
  - Tonning, A., Hemphälä, J., Tång, E., Nannmark, U., Samakovlis, C., and Uv, A. (2005). A Transient Luminal Chitinous Matrix Is Required to Model Epithelial Tube Diameter in the *Drosophila* Trachea. *J Biol Chem* *280*, 423-430.
  - Tsarouhas, V., Senti, K.-A., Jayaram, S.A., Tiklová, K., Hemphälä, J., Adler, J., and Samakovlis, C. (2007). Sequential Pulses of Apical Epithelial Secretion and Endocytosis Drive Airway Maturation in *Drosophila*. *J Biol Chem* *282*, 214-225.
-

- 
- Tsarouhas, V., Yao, L., and Samakovlis, C. (2014). Src kinases and ERK activate distinct responses to Stitcher receptor tyrosine kinase signaling during wound healing in *Drosophila*. *Journal of Cell Science* *127*, 1829-1839.
  - Tsukita, S., Furuse, M., and Itoh, M. (2001). Multifunctional strands in tight junctions. *Nat Rev Mol Cell Biol* *2*, 285 - 293.
  - Uv, A., Cantera, R., and Samakovlis, C. (2003). *Drosophila* tracheal morphogenesis: intricate cellular solutions to basic plumbing problems. *Trends in Cell Biology* *13*, 301-309.
  - Vincent, W.S., Gregory, R.J., and Wadsworth, S.C. (1989). Embryonic expression of a *Drosophila* src gene: alternate forms of the protein are expressed in segmental stripes and in the nervous system. *Genes & Development* *3*, 334-347.
  - Wadsworth, S.C., Madhavan, K., and Bilodeau-Wentworth, D. (1985). Maternal inheritance of transcripts from three *Drosophila* src-related genes. *Nucleic Acids Research* *13*, 2153-2170.
  - Wadsworth, S.C., Muckenthaler, F.A., and Vincent Iii, W.S. (1990). Differential expression of alternate forms of a *Drosophila* src protein during embryonic and larval tissue differentiation. *Developmental Biology* *138*, 296-312.
  - Wang, S., Jayaram, S., Hemphala, J., Senti, K., Tsarouhas, V., Jin, H., and Samakovlis, C. (2006). Septate-junction-dependent luminal deposition of chitin deacetylases restricts tube elongation in the *Drosophila* trachea. *Curr Biol* *16*, 180 - 185.
  - Wang, W., and Struhl, G. (2005). Distinct roles for Mind bomb, Neuralized and Epsin in mediating DSL endocytosis and signaling in *Drosophila*. *Development* *132*, 2883-2894.
  - Wang, Y.-C., Khan, Z., Kaschube, M., and Wieschaus, E.F. (2012). Differential positioning of adherens junctions is associated with initiation of epithelial folding. *Nature* *484*, 390-393.
  - Ward, R.E., Lamb, R.S., and Fehon, R.G. (1998). A Conserved Functional Domain of *Drosophila* Coracle Is Required for Localization at the Septate Junction and Has Membrane-organizing Activity. *The Journal of Cell Biology* *140*, 1463-1473.
  - Wilk, R., Weizman, I., and Shilo, B.Z. (1996). trachealess encodes a bHLH-PAS protein that is an inducer of tracheal cell fates in *Drosophila*. *Genes & Development* *10*, 93-102.
  - Wirtz-Peitz, F., and Zallen, J.A. (2009). Junctional trafficking and epithelial morphogenesis. *Current Opinion in Genetics & Development* *19*, 350-356.
  - Woods, D., Hough, C., Peel, D., Callaini, G., and Bryant, P. (1996). Dlg protein is required for junction structure, cell polarity, and proliferation control in *Drosophila* epithelia. *J Cell Biol* *134*, 1469 - 1482.
  - Wu, V., Schulte, J., Hirschi, A., Tepass, U., and Beitel, G. (2004). Sinuous is a *Drosophila* claudin required for septate junction organization and epithelial tube size control. *J Cell Biol* *164*, 313 - 323.
  - Wu, V.M., and Beitel, G.J. (2004). A junctional problem of apical proportions: epithelial tube-size control by septate junctions in the *Drosophila* tracheal system. *Current Opinion in Cell Biology* *16*, 493-499.
  - Wu, V.M., Yu, M.H., Paik, R., Banerjee, S., Liang, Z., Paul, S.M., Bhat, M.A., and Beitel, G.J. (2007). *Drosophila* Varicose, a member of a new subgroup of basolateral MAGUKs, is required for septate junctions and tracheal morphogenesis. *Development* *134*, 999-1009.
  - Xu, N., Pirraglia, C., Patel, U., and Myat, M.M. (2012). Mechanisms of Lumen Development in *Drosophila* Tubular Organs, Embryogenesis. Dr Ken-Ichi Sato (Ed).
  - Zallen, J.A., and Wieschaus, E. (2004). Patterned Gene Expression Directs Bipolar Planar Polarity in *Drosophila*. *Developmental Cell* *6*, 343-355.